

Chapter 6 Criticality Evaluation

TABLE OF CONTENTS

6.1	Description of the Criticality Design.....	6-1
6.1.1	Design Features.....	6-1
6.1.2	Summary Table of Criticality Evaluation.....	6-1
6.1.3	Criticality Safety Index.....	6-2
6.2	Fissile Material Contents.....	6-3
6.3	General Considerations.....	6-4
6.3.1	Model Configuration.....	6-4
6.3.2	Material properties.....	6-4
6.3.3	Computer Codes and Cross Section Libraries.....	6-4
6.3.4	Demonstration of Maximum Reactivity.....	6-4
6.4	Single Package Evaluation.....	6-5
6.5	Evaluation of Package Arrays under Normal Conditions of Transport.....	6-6
6.6	Package Arrays under Hypothetical Accident Conditions.....	6-7
6.7	Fissile Material Packages for Air Transport.....	6-8
6.8	Benchmark Evaluations.....	6-9
6.9	References.....	6-10
6.10	Appendices.....	6-11
6.10.1	TN-LC-MTR Basket Criticality Evaluation.....	6-11
6.10.2	TN-LC-NRUX Basket Criticality Evaluation.....	6-11
6.10.3	TN-LC-TRIGA Basket Criticality Evaluation.....	6-11
6.10.4	TN-LC-1FA Basket Criticality Evaluation.....	6-11

LIST OF TABLES

Table 6-1	Summary of Criticality Evaluations.....	6-12
-----------	---	------

Chapter 6

Criticality Evaluation

NOTE: References in this Chapter are shown as [1], [2], etc. and refer to the reference list in Section 6.9.

A separate criticality evaluation is performed for the four basket types. Information common to all analyses are summarized in the main body of this Chapter. The details for each analysis are contained in a separate appendix. The list of appendices is as follows:

TN-LC-MTR Basket: Appendix 6.10.1.

TN-LC-NRUX Basket: Appendix 6.10.2.

TN-LC-TRIGA Basket: Appendix 6.10.3.

TN-LC-1FA Basket: Appendix 6.10.4.

6.1 Description of the Criticality Design

6.1.1 Design Features

Criticality control is provided primarily by the baskets. The description of the criticality design for the four basket types are contained in the individual appendices for each basket. The cask provides separation between the baskets in the array evaluations. The inner diameter of the cask is 18 in., and the cask consists of 1.0 in. steel, 3.50 in. lead, and 1.5 in. steel in the radial direction. The neutron shield is conservatively omitted in all criticality models because it contains poison. Impact limiters are omitted in all criticality models, although credit is taken for the distance provided by the impact limiters in the NCT array analysis for the MTR basket.

6.1.2 Summary Table of Criticality Evaluation

MCNP5 V1.4 [1] is used for the criticality analyses for the TN-LC-MTR, TN-LC-NRUX, and TN-LC-TRIGA baskets, and SCALE6 [2] is used for the criticality analysis for the TN-LC-1FA basket. Because each fuel type is unique, separate benchmarking is performed for each fuel type. Hence, a different upper subcritical limit (USL) is utilized for each analysis.

The package is considered to be acceptably subcritical if the computed k_{safe} (k_s), which is defined as $k_{\text{effective}}$ (k_{eff}) plus twice the statistical uncertainty (σ), is less than or equal to the USL, or:

$$k_s = k_{\text{eff}} + 2\sigma \leq \text{USL}$$

The packaging design is shown to meet the requirements of 10CFR71.55(b). No credit is taken for fuel element burnup in any models. In both the normal conditions of transport (NCT) and hypothetical accident condition (HAC) models, water is conservatively modeled in all cavities at the most reactive density. In all single package evaluation models, 12 in. of water reflection is utilized (12 feet were used in the TN-LC-1FA model).

In the NCT array models, an array of three packages is utilized. The entire array is reflected with 12 in. of water.

The maximum results of the criticality calculations are summarized in Table 6-1. No HAC array models are developed. Therefore, the HAC array results listed in this table are simply the same as the HAC single package maximum results. The results listed for the TN-LC-1FA basket are for a single pressurized water reactor (PWR) fuel assembly, which bounds a single boiling water reactor (BWR) fuel assembly, and individual PWR, BWR, EPR or MOX fuel rods.

In the TN-LC-MTR, TN-LC-NRUX, and TN-LC-TRIGA basket analyses, fuel damage is conservatively modeled in both the NCT and HAC models for convenience. Therefore, for these baskets, the most reactive case is the NCT array. In the TN-LC-1FA basket analysis, fuel is modeled as undamaged in the NCT cases and damaged in the HAC cases. Therefore, the HAC single package case is limiting in the TN-LC-1FA basket analysis.

6.1.3 Criticality Safety Index

Per 10CFR71.59, the criticality safety index (CSI) is determined by dividing the number 50 by the value of "N" that is derived based on the criticality evaluations performed on package arrays. Since no HAC array calculations are performed, the maximum number of damaged packages per 10CFR71.59(a)(2) is 1 (two times "N" = 1) ensuring that the value of "N" = 0.5. This is consistent with the minimum value of "N" per 10CFR71.59(a)(3). An array of three undamaged packages is conservatively evaluated to comply with 10CFR71.59(a)(1), limit of 2.5 (five times "N") packages.

Therefore, the CSI for the TN-LC package is 100.

6.2 Fissile Material Contents

The TN-LC-MTR basket may transport up to 54 MTR fuel elements. The TN-LC-NRUX basket may transport up to 26 NRU or NRX fuel elements. The TN-LC-TRIGA basket may transport up to 180 TRIGA fuel elements. The TN-LC-1FA basket may transport either 1 PWR fuel assembly, 1 BWR fuel assembly, or up to 25 individual PWR, BWR, EPR or MOX fuel rods. Additional information about the fissile material contents is included in the individual appendices and in Chapter 1.

6.3 General Considerations

6.3.1 Model Configuration

The model configuration is different for each of the basket types and is described in the individual appendices.

6.3.2 Material properties

The material properties for each model are described in the individual appendices.

6.3.3 Computer Codes and Cross Section Libraries

MCNP5 V1.4 [1] is used for the criticality analyses for the TN-LC-MTR, TN-LC-NRUX, and TN-LC-TRIGA baskets, and SCALE6 [2] is used for the criticality analysis for the TN-LC-1FA basket. In the MCNP models, continuous energy ENDF/B-V and ENDF/B-VI cross-sections are utilized at room temperature (293 K). In the SCALE6 models, 44 group ENDF/B-V cross-sections are utilized at room temperature (293 K) in conjunction with NITAWL for treatment of resonances. The cross-sections utilized are consistent with the individual benchmarking for each basket type. Additional information about the cross-sections utilized is included in the individual appendices.

6.3.4 Demonstration of Maximum Reactivity

In all models, fuel is modeled as fresh, although the TN-LC is a spent fuel package and fuel will typically be much less reactive due to U-235 depletion and fission product buildup. Full flooding is modeled in all NCT and HAC cases, although the package is leak tight and water intrusion during NCT and HAC is not credible. Fuel is modeled in the most reactive configuration within the baskets, including postulated fuel damage as a result of an accident. Additional information about the conservative assumptions utilized in the criticality analyses is included in the individual appendices.

6.4 Single Package Evaluation

In the single package evaluation, fuel is modeled in the most reactive damaged condition with water present at the density at which the reactivity is maximized. The details for each analysis are included in the individual appendices.

6.5 Evaluation of Package Arrays under Normal Conditions of Transport

In the NCT array configuration, three packages are modeled, and the water density is varied both within and between the packages to determine the maximum reactivity. The details for each analysis are included in the individual appendices.

6.6 Package Arrays under Hypothetical Accident Conditions

Because the CSI = 100, no HAC array cases are performed.

6.7 Fissile Material Packages for Air Transport

This section does not apply.

6.8 Benchmark Evaluations

A separate benchmark evaluation is performed for each fuel type. The USL for each of the four analyses is as follows:

- TN-LC-MTR USL = 0.9213
- TN-LC-NRUX USL = 0.9227
- TN-LC-TRIGA USL = 0.9297
- TN-LC-1FA USL = 0.9420

The details of the USL determination are included in the individual appendices.

6.9 References

1. MCNP5, "MCNP – A General Monte Carlo N-Particle Transport Code, Version 5; Volume II: User's Guide," LA-CP-03-0245, Los Alamos National Laboratory, April 2003.
2. SCALE: A Modular Code System for Performing Standardized Computer Analyses for Licensing Evaluations, ORNL/TM-2005/39, Version 6, Vols. I-III, January 2009.

6.10 Appendices

6.10.1 TN-LC-MTR Basket Criticality Evaluation

6.10.2 TN-LC-NRUX Basket Criticality Evaluation

6.10.3 TN-LC-TRIGA Basket Criticality Evaluation

6.10.4 TN-LC-1FA Basket Criticality Evaluation

Table 6-1
Summary of Criticality Evaluations

	MTR Payload	NRUX Payload	TRIGA Payload	1FA Payload
Normal Conditions of Transport (NCT)				
Case	k_s	k_s	k_s	k_s
Single Package Maximum	≤ 0.918	0.872	0.887	0.8895
Array Maximum (3 packages)	0.918	0.874	0.896	0.9047
Hypothetical Accident Conditions (HAC)				
Case	k_s	k_s	k_s	k_s
Single Package Maximum	≤ 0.918	0.872	0.887	0.9351
Array Maximum (1 package)	≤ 0.918	0.872	0.887	0.9351
USL	0.9213	0.9227	0.9297	0.9420

Appendix 6.10.1
TN-LC-MTR Basket Criticality Evaluation

TABLE OF CONTENTS

6.10.1.1	Description of the Criticality Design.....	6.10.1-1
6.10.1.1.1	Design Features.....	6.10.1-1
6.10.1.1.2	Summary Table of Criticality Evaluation.....	6.10.1-1
6.10.1.1.3	Criticality Safety Index.....	6.10.1-2
6.10.1.2	Fissile Material Contents.....	6.10.1-3
6.10.1.3	General Considerations.....	6.10.1-5
6.10.1.3.1	Model Configuration.....	6.10.1-5
6.10.1.3.2	Material properties.....	6.10.1-7
6.10.1.3.3	Computer Codes and Cross Section Libraries.....	6.10.1-7
6.10.1.3.4	Demonstration of Maximum Reactivity.....	6.10.1-7
6.10.1.4	Single Package Evaluation.....	6.10.1-9
6.10.1.4.1	Configuration.....	6.10.1-9
6.10.1.4.2	Results.....	6.10.1-13
6.10.1.5	Evaluation of Package Arrays under Normal Conditions of Transport.....	6.10.1-14
6.10.1.5.1	Configuration.....	6.10.1-14
6.10.1.5.2	Results.....	6.10.1-15
6.10.1.6	Package Arrays under Hypothetical Accident Conditions.....	6.10.1-16
6.10.1.7	Fissile Material Packages for Air Transport.....	6.10.1-17
6.10.1.8	Benchmark Evaluations.....	6.10.1-18
6.10.1.8.1	Applicability of Benchmark Experiments.....	6.10.1-18
6.10.1.8.2	Bias Determination.....	6.10.1-19
6.10.1.9	Appendix.....	6.10.1-22
6.10.1.9.1	References.....	6.10.1-22
	Proprietary Information Withheld Pursuant to 10 CFR 2.390.	
6.10.1.9.3	Parametric Evaluations.....	6.10.1-32

LIST OF TABLES

Table 6.10.1-1	Summary of TN-LC-MTR Criticality Evaluations	6.10.1-34
Table 6.10.1-2	MTR HEU Fuel Element Specifications	6.10.1-35
Table 6.10.1-3	MTR LEU and MEU Fuel Element Specifications.....	6.10.1-36
Table 6.10.1-4	Allowable MTR Fuel Elements.....	6.10.1-36
Table 6.10.1-5	Example Fuel Composition for Limiting LEU and HEU Fuel	6.10.1-37
Table 6.10.1-6	Stock Tolerances per ASTM A480	6.10.1-37
Table 6.10.1-7	TN-LC-MTR Fuel Bucket Dimensions, Nominal and Bounding	6.10.1-37
Table 6.10.1-8	TN-LC-MTR Weldment Dimensions, Nominal and Bounding.....	6.10.1-38
Table 6.10.1-9	TN-LC Cask Dimensions, Nominal and Bounding.....	6.10.1-38
Table 6.10.1-10	Composition of Stainless Steel.....	6.10.1-39
Table 6.10.1-11	Cross Section Libraries Utilized.....	6.10.1-39
Table 6.10.1-12	TN-LC-MTR Single Package Fuel Movement Results	6.10.1-40
Table 6.10.1-13	TN-LC-MTR Single Package Manufacturing Tolerance Results	6.10.1-41
Table 6.10.1-14	TN-LC-MTR Single Package Moderator Density Results.....	6.10.1-41
Table 6.10.1-15	MTR Single Package Bounding Element Characteristic Results.....	6.10.1-42
Table 6.10.1-16	Initial Bounding Assembly Characteristics.....	6.10.1-43
Table 6.10.1-17	Summary of NCT Array Calculations.....	6.10.1-44
Table 6.10.1-18	NCT Array Results.....	6.10.1-46
Table 6.10.1-19	Benchmark Experiments Utilized	6.10.1-47
Table 6.10.1-20	USL Results.....	6.10.1-47
Table 6.10.1-21	Benchmark Experiment Data	6.10.1-48
Table 6.10.1-22	Summary of Limiting Element Selection k_{eff} Results	6.10.1-49
Table 6.10.1-23	Limiting Elements in HAC Configuration	6.10.1-49

LIST OF FIGURES

Figure 6.10.1-1	HFBR MTR Fuel Element	6.10.1-50
Figure 6.10.1-2	TN-LC-MTR Single Package Model, planar view	6.10.1-51
Figure 6.10.1-3	TN-LC-MTR Weldment and Fuel Buckets (planar view)	6.10.1-52
Figure 6.10.1-4	Potential Axial Element Spacing (MCT1, MCT2, MCT3).....	6.10.1-53
Figure 6.10.1-5	Potential Horizontal Element Spacing (MCT4, MCT5, MCT6, MCT21).....	6.10.1-54
Figure 6.10.1-6	Five- and Four- Bucket TN-LC-MTR Basket Configurations (MCT17, MCT19).....	6.10.1-55
Figure 6.10.1-7	Elements Moved Uniformly Toward Axial Center.....	6.10.1-56
Figure 6.10.1-8	Limiting Fuel Location in the Radial and Axial Plane.....	6.10.1-57
Figure 6.10.1-9	Summary of TN-LC-MTR Basket Tolerance Results.....	6.10.1-58
Figure 6.10.1-10	Summary of MTR Uranium Loading in Fuel Results.....	6.10.1-59
Figure 6.10.1-11	Summary of MTR Active Fuel Height Results.....	6.10.1-60
Figure 6.10.1-12	TN-LC-MTR NCT Array Configuration with Flooded Casks.....	6.10.1-61
Figure 6.10.1-13	Reactivity Change with Varying Water Density Between Casks	6.10.1-62
Figure 6.10.1-14	MCNP Model Used to Determine Bounding MTR Assembly.....	6.10.1-63

Appendix 6.10.1 TN-LC-MTR Basket Criticality Evaluation

NOTE: References in this Appendix are shown as [1], [2], etc. and refer to the reference list in Appendix 6.10.1.9.1.

This Appendix presents the criticality evaluation of the TN-LC-MTR basket with a payload of up to 54 MTR fuel elements. In this evaluation, MTR is used to denote a range of uranium-aluminum plate fuels that are physically similar to the Materials Test Reactor fuel. The following analyses demonstrate that the TN-LC package complies with the requirements of 10CFR71.55 and 71.59. The Criticality Safety Index (CSI), per 10CFR71.59, is 100.

6.10.1.1 Description of the Criticality Design

6.10.1.1.1 Design Features

Criticality control is provided primarily by the TN-LC-MTR basket. The basket contains up to six interlocking layers. Each layer may contain up to nine MTR fuel elements.

Proprietary Information Withheld Pursuant to 10 CFR 2.390.

No poisons are utilized in the package. The separation provided by the cask and basket is sufficient to maintain criticality safety.

6.10.1.1.2 Summary Table of Criticality Evaluation

The upper subcritical limit (USL) for ensuring that the package is acceptably subcritical, as determined in Section 6.10.1.8 is:

$$\text{USL} = 0.9213$$

The package is considered to be acceptably subcritical if the computed k_{safe} (k_s), which is defined as $k_{\text{effective}}$ (k_{eff}) plus twice the statistical uncertainty (σ), is less than or equal to the USL, or:

$$k_s = k_{\text{eff}} + 2\sigma \leq \text{USL}$$

The USL is determined on the basis of a benchmark analysis and incorporates the combined effects of code computational bias, the uncertainty in the bias based on both benchmark-model and computational uncertainties, and an administrative margin. The results of the benchmark analysis indicate that the USL is adequate to ensure subcriticality of the package.

The packaging design is shown to meet the requirements of 10CFR71.55(b). Moderation by water in the most reactive credible extent is utilized in both the normal conditions of transport (NCT) and

hypothetical accident conditions of transport (HAC) analyses. In both the NCT and HAC models, full-density water fills all cavities. Sensitivity cases are run to ensure that full-density water is most reactive. In the fuel element models, the most reactive credible configuration is utilized by maximizing the gap between the fuel plates. Maximizing this gap simulates fuel damaged under HAC and maximizes the moderation and hence the reactivity because the system is undermoderated. In all single package models, 12 in. of water reflection is utilized.

A triangular array of three packages is used in the NCT array cases and partial moderation is considered between the packages to maximize array interaction effects.

The maximum results of the criticality calculations are summarized in Table 6.10.1-1. The maximum calculated k_s is 0.918 which occurs for the optimally moderated NCT array case. Both the NCT and HAC single package cases are flooded and fuel damage is conservatively allowed in all models. No HAC array cases are developed, so the HAC array results in Table 6.10.1-1 are the same as the HAC single package results. Both low- and full-density water are modeled between the casks in the NCT array calculations; therefore, the single package is bounded by the array calculation.

6.10.1.1.3 Criticality Safety Index

No HAC array models are developed ($2N=1$). Therefore, per 10CFR71.59, $N=0.5$, and the criticality safety index (CSI) is $50/N = 100$. In the NCT array cases, $5N=2.5$, so that 3 packages are modeled.

6.10.1.2 Fissile Material Contents

The TN-LC cask loaded with the TN-LC-MTR basket can hold between 36 and 54 MTR fuel assemblies or elements. Each element is composed of between 10 and 23 fuel plates held in place by two parallel aluminum side plates. The fuel plates are compacts composed of aluminum cladding surrounding uranium-aluminum fuel meat. The fuel meat can have one of several chemical compositions: U_3O_8 -Al, U-Al, or U_3Si_2 -Al.

An example fuel element, the HFBR, is shown in Figure 6.10.1-1. The HFBR element shown in Figure 6.10.1-1 features 18 fueled plates and two outer aluminum plates. The outer aluminum plates are not typical but do appear in a few of the MTR elements.

The U-235 loading per fuel plate is also used as a figure of merit in this study. This represents the total number of grams of U-235 in an individual fuel plate. Plates in a given element contain equal U-235 loadings. The total fissile (U-235) loading of a fuel element is the product of the U-235 loading per plate and the number of fuel plates.

Proprietary Information Withheld Pursuant to 10 CFR 2.390.

Proprietary Information Withheld Pursuant to 10 CFR 2.390.

6.10.1.3 General Considerations

6.10.1.3.1 Model Configuration

The fuel, basket, and packaging are modeled explicitly in the MCNP5 V1.4 computer program [1]. The waste package consists of several components. The outer containment is the TN-LC cask which is modeled in the radial direction as concentric layers of stainless steel and lead. The top and bottom of the cask is composed of layered stainless steel and lead. Before shipping MTR fuel, the TN-LC cask will be outfitted with the TN-LC-MTR basket. This basket is comprised of three components: outer aluminum rails, a stainless steel weldment, and three sets of fuel buckets. Each bucket features three compartments for MTR fuel. Between four and six fuel buckets are stacked along the length of the cask. Therefore, the total cask capacity is between 36 and 54 MTR fuel elements. Each bucket cavity is intended to hold one MTR fuel element.

Figure 6.10.1-2 shows a planar view of the TN-LC-MTR cask loaded with MTR fuel elements. The cask is surrounded by a 12 in. layer of full-density water to provide reflection.

In both the NCT and HAC models, water is modeled inside the package at the density that maximizes reactivity. Because the cask is designed for wet loading, water drains freely inside the basket, and preferential flooding scenarios are not credible. However, the cavity could be partially flooded. Because the baskets drain freely, if the TN-LC cavity is partially flooded, the only credible scenario is that some fuel would be submerged in water, and the remaining fuel would remain unsubmerged. Therefore, any partial flooding scenarios would result in unmoderated fuel. It is demonstrated that MTR fuels have very low reactivity in the absence of moderation. Therefore, any partial flooding would uncover fuel and decrease the reactivity. It is demonstrated explicitly in Section 6.10.2.4 for HEU NRU fuel that a partially flooded cavity results in lower reactivities, and MTR fuel will behave in a similar manner. For these reasons, cases are not developed for partial and/or preferential flooding. Water is always modeled at the same density in all basket regions of the model.

Effect of Manufacturing Tolerances on Reactivity:

The manufacturing tolerances of the basket components are modeled in order to maximize the reactivity. In these calculations, the HFBR fuel element is used as a representative fuel element as the HFBR fuel element is the most reactive fuel element listed in Table 6.10.1-2 and Table 6.10.1-3, as demonstrated in Section 6.10.1.9.3.

The tolerances for the TN-LC, basket, and bucket are given in accordance with ASME Y14.5M-1994 [2] with the exception of components manufactured from stock material. For decimal values quoted to the hundredth of an inch, the tolerances are ± 0.05 in. For decimal values quoted to the thousand of an inch, the tolerances are ± 0.015 in. Angles are quoted to within ± 1 degree.

For stock materials, tolerances are given by ASTM A480 [6]. The TN-LC-MTR bucket contains three sizes of stock plate with the tolerances given in Table 6.10.1-6. The tolerance values are taken from Tables A2.13 and A2.17 of ASTM A480. Maximum values are used to define the largest possible range and produce the most conservative results.

For the fuel bucket, the thickness of the stainless steel plates is decreased according to the values in Table 6.10.1-6. The fuel bucket compartment plates are thinned on both sides. The plates that comprise the side walls of the buckets are also thinned. This reduces neutron absorption in the stainless steel and increases reactivity. Bucket dimensions are summarized in Table 6.10.1-7.

Proprietary Information Withheld Pursuant to 10 CFR 2.390.0

Proprietary Information Withheld Pursuant to 10 CFR 2.390. Increasing the thickness of the outer plates causes increased reflection and produces a higher calculated k_{eff} . Altering the

thickness of the compartment plates increases reactivity very slightly. Weldment dimensions are summarized in Table 6.10.1-8.

Proprietary Information Withheld Pursuant to 10 CFR 2.390.

A closer view of the weldment region and buckets, with the fuel removed, is given in Figure 6.10.1-3. This shows the nine available regions for MTR fuel elements. The surrounding rail and part of the cask model are also visible.

The cask dimensional tolerances are assumed to have a negligible impact. Thus, the cask is modeled at nominal conditions for simplicity. This assumption is supported by the analysis of a single cask and an array of casks. Since there is little change in k_{eff} between the single cask and the array, any neutrons streaming through the cask are unlikely to affect reactivity in another fuel region. The cask material dimensions are summarized in Table 6.10.1-9.

Effect of Fuel Movement on Reactivity:

The TN-LC-MTR fuel bucket design allows for movement of the fuel elements within the bucket. Several studies are performed to find the most reactive configuration of the fuel elements. The results presented in Section 6.10.1.4 show that reactivity is maximized when the fuel is clustered together in the axial plane and moved toward the center of the cask in the radial plane. This configuration is depicted in the central illustration of Figure 6.10.1-4 and in the bottom-left illustration of Figure 6.10.1-5.

The TN-LC-MTR fuel buckets can assume three different configurations: 30-70-S, 30-70-I, and 30-70-L. This allows the cask to transport fuels of varying length without having to reconfigure the cask. Calculations show that reactivity is driven by the fuel in two sections moving together to form a cluster; thus, the limiting reactivity is roughly equal for all three configurations. The six-section configuration is used for all final cases to maximize the fissile mass in the cask.

Effect of Moderator Density on Reactivity:

The cask is assumed to be flooded for all HAC and NCT cases. This assumption is checked in Section 6.10.1.4 to ensure that flooding with full-density water is the most conservative. These cases reduced the moderator (light water) density from 1.0 g/cc to 0.90, 0.75, 0.50, 0.25, and 0.01 g/cc, respectively. Reactivity is shown to decrease with decreasing water density, confirming that flooding the cask with full-density water is conservative.

Effect of MTR Fuel Element Characteristics on Reactivity:

The sensitivity of calculated reactivity to various fuel element characteristics is explored in Section 6.10.1.4. This will allow for the construction of a single, most-limiting fuel element.

6.10.1.3.2 Material properties

The methodology for computing the fuel compositions is provided in Section 6.10.1.2. The material properties of the remaining packaging and moderating materials are described in the following paragraphs.

The TN-LC-MTR basket and bucket, along with sections of the TN-LC cask, are constructed from stainless steel 304. Although MCNP is used in the calculations, the standard compositions for stainless steel 304 are obtained from the SCALE material library which is a standard set accepted for use in criticality analyses [3]. The stainless steel composition and density utilized in the MCNP models are provided in Table 6.10.1-10.

Some cask materials may be constructed of XM-19 rather than stainless steel 304. XM-19 features increased levels of chromium and nickel compared to SS304. The difference in chemical composition would not increase system reactivity, and these materials are assumed to be interchangeable for criticality purposes.

Cask lead is modeled as pure with a density of 11.35 g/cm^3 , and aluminum is modeled as pure with a density of 2.702 g/cm^3 .

Water is modeled with a density ranging up to 1.0 g/cm^3 and the chemical formula H_2O . The $S(\alpha,\beta)$ card LWTR.60T is used to simulate hydrogen bound to oxygen in water.

6.10.1.3.3 Computer Codes and Cross Section Libraries

MCNP5 v1.40 is used for the criticality analysis [1]. All cross-sections utilized are at room temperature (293 K). The uranium isotopes utilize preliminary ENDF/B-VII cross-section data that are considered by Los Alamos National Laboratory to be more accurate than ENDF/B-VI cross sections. ENDF/B-V cross-sections are utilized for chromium, nickel, iron, and lead because natural composition ENDF/B-VI cross-sections are not available for these elements. The remaining isotopes utilize ENDF/B-VI cross-sections. Titles of the cross-sections utilized in the models have been extracted from the MCNP output (when available) and provided in Table 6.10.1-11. The $S(\alpha,\beta)$ card LWTR.60T is used to simulate hydrogen bound to water in all models.

All cases are run with 5000 neutrons per generation for 250 generations, skipping the first 50. The 1-sigma uncertainty is less than 0.001 for all cases. These values were occasionally increased as necessary for increased precision or convergence.

6.10.1.3.4 Demonstration of Maximum Reactivity

No credit is taken for fuel element burnup. Full-water moderation and postulated HAC damage to the fuel is modeled for both the NCT and HAC cases. The postulated fuel damage is fuel plate pitch expansion which increases the moderation. These assumptions are conservative but not credible for NCT analysis, since the package is leak tight and fuel would not be damaged during NCT. The NCT single package is identical to the HAC single package; thus, the reactivities are equal. The NCT array produces the limiting reactivity.

Dimensions of both the fuel element and basket are chosen to maximize reactivity. The fuel is modeled in a generalized manner to bound most MTR-type fuel elements. Parameters varied

include the number of fuel plates, the U-235 loading per plate, active fuel width, active fuel length, and U-235 enrichment. For all cases, the cask is fully flooded and the elements are located to maximize reactivity. The cask and basket maintain their dimensions during accident conditions.

The most reactive allowable configuration (MAB7_1) produces a k_s of 0.91783 (rounded to 0.918) which is less than the USL of 0.9213.

6.10.1.4 Single Package Evaluation

During HAC and NCT, the cask is assumed to be flooded with full-density water. The bounding fuel and cask geometry is determined using the HAC single package model, but the results are identical to NCT single package model as the cask and basket are undamaged under HAC. The fuel element used for the initial calculations is the HFBR as discussed in Section 6.10.1.9.3. However, this element is used only as a placeholder during initial sensitivity studies. The purpose of this section is to define the limiting single package configuration. The generalized fuel element used in the NCT array analysis presented in Section 6.10.1.5 bounds the single package results; thus, no final results are presented in this section.

6.10.1.4.1 Configuration

The bounding characteristics for MTR fuel elements will be found using the HAC single package model. Four different criteria are evaluated and the limiting values and characteristics are found for the following: fuel movement, manufacturing tolerances, moderator density, and fuel element physical characteristics.

Unless otherwise noted, the calculations in this section are performed using damaged HFBR fuel as discussed in Section 6.10.1.9.3. Under HAC, it is assumed that there will be no damage to the basket. Any cask damage will not significantly change the dimensions of the shielding materials.

Identifying Bounding MTR Fuel Movement within the TN-LC Package:

The purpose of these calculations is to specify limiting fuel element locations. All fuel movement results are provided in Table 6.10.1-12.

The initial model, MCT1, features the HFBR fuel element with expanded fuel plates and nominal cask/bucket/basket dimensions. Figure 6.10.1-4 shows the three vertical spacing options explored in cases MCT1, MCT2, and MCT3. The calculated reactivity is nearly identical between cases MCT2 and MCT3. Case MCT2 (three clusters of fuel elements) is used for subsequent calculations as it produces the maximum k_s .

Cases MCT4, MCT5, and MCT6 show that pushing the fuel elements as close together as possible in the horizontal plane increases reactivity. These configurations are shown in Figure 6.10.1-5. MCT4 is shown to the top-left, MCT5 is shown to the top-right, MCT6 is shown to the bottom-left, and MCT21 is shown to the bottom-right.

Note that fuel movement calculations MCT1 through MCT6 use nominal dimensions. Cases MCT7 through MCT15 convert the model to the limiting manufacturing tolerances as discussed in the following sub-section "Identifying Bounding MTR Manufacturing Tolerances." MCT15 is repeated in Table 6.10.1-12 for easier comparisons as cases MCT16 to MCT22 and MCT28 through MCT34 return to examining fuel movement.

The initial models feature six fuel buckets stacked axially. Cases MCT15, MCT17, and MCT19 compare the reactivity of the six-bucket case to the five-bucket and four-bucket cases, respectively (see Figure 6.10.1-6 for the five- and four-bucket cases). As the differences between the cases are not significant, three additional cases (MCT16, MCT18, and MCT20) are run with more neutrons. These cases also show very small changes in reactivity when the

number of fuel buckets is reduced. This behavior is somewhat counterintuitive as a reduction in fissile mass appears to have no impact on system reactivity. It is apparent that a cluster of the layers of fuel elements is essentially isolated from the rest of the problem and is driving reactivity. Thus no reactivity differences are anticipated between the configurations. The six-bucket configuration is used for subsequent analysis to maximize the fissile loading in the cask.

Cases MCT21 and MCT22 test some further refinement of case MCT15. In case MCT21, the fuel elements in the central row are shifted in the +y direction with no increase in reactivity (see Figure 6.10.1-5, bottom-right). To simulate the non-fuel material that is present above and below the active fuel region, but is not included in other models, case MCT22 adds a slab of aluminum above and below the fuel. This case also shows a decrease in reactivity, indicating that modeling only the active fuel is conservative.

Cases MCT28 through MCT34 are illustrated in Figure 6.10.1-7. For the first four of these cases, equal water gaps are maintained axially between the fuel elements in each model as the elements are moved closer together. While reactivity does generally increase (MCT29 to MCT32), the magnitude is small. When the constant gap is abandoned and the center two elements are brought into a "cluster," the calculated reactivity increases significantly, approaching the previously-limiting value. These cases are further proof that two layers of elements clustered together axially will dominate system reactivity.

While several sets of fuel movement are explored, the only significant effects are seen in cases MCT1 through MCT6. Case MCT6, shown in Figure 6.10.1-8, represents the most limiting physical movement of the MTR fuel elements. A single cluster of fuel elements is also shown to drive system reactivity.

Identifying Bounding TN-LC-MTR Manufacturing Tolerances:

Manufacturing tolerances are discussed at length in Section 6.10.1.3.1. This section provides some discussion of the specific calculations performed and the calculated changes in reactivity. The purpose of these calculations is to specify a limiting TN-LC and TN-LC-MTR basket and bucket model. All manufacturing tolerance results are provided in Table 6.10.1-13.

Cases MCT7 through MCT10 change the thickness of the bucket walls. As is expected, minimizing the bucket thickness (and thus the neutron absorption in the steel) increases reactivity. For all final cases, the minimal bucket thickness is used.

A similar study is performed with cases MCT11 through MCT14. Thinning of the inner compartment plate, which is located between the buckets, increases reactivity. Conversely, increasing the thickness of the outer plates proves to be more reactive. This is likely due to increased reflection as the outer plates are located beyond the fuel region. Furthering the argument for reflection, case MCT15 shows that filling the region around the tie plates with steel is more reactive than leaving the region as water. This is a modeling approximation. The actual tie plate volume is less than the modeled volume of steel which introduces some additional conservatism to the model.

The results shown in Figure 6.10.1-9 lead to the following conclusions: Minimizing the thickness of steel in the bucket walls is the most reactive. The tube cap thickness has a relatively

small impact on reactivity. The final cases will model a minimum thickness of the tube cap for consistency with the other bucket dimensions. Thinning the basket compartment plate reduces absorption and increases moderation between the fuel elements, thus increasing reactivity. The basket outer plates and tie plate regions serve as reflectors and maximizing the steel thickness is most conservative.

In general, reducing the volume of stainless steel in the TN-LC-MTR basket reduces neutron absorption and increases reactivity. Increasing the thickness of the outer plates is shown to increase reactivity, likely due to increased neutron reflection.

Identifying Bounding Moderator Density within the Cask:

The moderator density sensitivity results – cases MCT23 through MCT27 – are shown in Table 6.10.1-14. These cases incrementally reduce the moderator (light water) density in the cask from 1.0 g/cc to 0.001 g/cc. The reactivity decreases significantly as the water density decreases. The full-density case (MCT15) exhibits the greatest reactivity; thus, full-density water is used in the cask for all subsequent calculations.

Identifying Bounding MTR Fuel Element Characteristics:

This section will define the most limiting combination of MTR fuel element characteristics. The intention is to define an envelope of parameters used to identify fuel in licensing documentation, such as a Certificate of Compliance. While the specific fuel designs given in Table 6.10.1-2 and Table 6.10.1-3 can be shown to be sufficiently subcritical, it is desired to define fuel elements by their key physical characteristics so that fuel elements not explicitly analyzed may be shipped.

The limiting configurations from the previous three sub-sections are carried forward into this analysis.

The following discussion pertains to the cases summarized in Table 6.10.1-15. The conclusions from this section form the basis for Table 6.10.1-16.

There are several variables that may affect reactivity. The first is the chemical composition of the fuel material. Cases MCT15, MCT35, and MCT36 in Table 6.10.1-15 show the variation in k_{eff} for the three possible fuel forms. There are no significant differences in reactivity between the fuel forms, so $\text{U}_3\text{O}_8\text{-Al}$ fuel will be used for all subsequent analysis.

Case MCT37 replaces the aluminum side plate with water. The side plate is a block of aluminum located perpendicular to the fuel plates and is used to hold the fuel plates in position. As expected, reactivity increases. This is used to confirm the assumption used throughout the document that replacing aluminum by water is conservative.

Consistent with the results of case MCT37, MCT38 shows that compressing the fuel element by removing the aluminum between the fuel and side plate such that the active fuel nearly touches the side plate is conservative. Thus the bounding model will include a minimal length of aluminum between the active fuel and the inner edge of the side plate.

In cases MCT39 through MCT41, the mass of U-235 is held constant, while the mass of the non-uranium fuel matrix materials (O, Si, Al) is allowed to vary. The mass of non-uranium materials

in the fuel matrix has a negligible impact on reactivity, as shown in Figure 6.10.1-10. The error bars are shown at two-sigma. As the results show, there is no clear correlation between the mass of non-uranium fuel matrix materials and reactivity. The average value for HEU (case MCT39) will be used as the starting point for the analysis in Section 6.10.1.5.

In cases MCT42 and MCT43 a reduction in the active fuel height is shown to increase reactivity for a fixed fissile loading per fuel plate. The trend is shown in Figure 6.10.1-11. This is likely due to the increasing fissile density (in mass per volume) of the shorter fuel elements. A 56 cm active fuel height will be used as the bounding value. Note that no structural materials are included above or below the active fuel in the MCNP model. The bottom of the bucket is modeled at the minimum thickness per quoted tolerances.

The active fuel width is varied (for a fixed fissile loading) in cases MCT44 and MCT45. These cases show that a wider active fuel region is more reactive, likely due to increased radial interaction. The final two cases, MCT46 and MCT47, show that minimizing fuel thickness will produce the maximum reactivity due to decreased self-absorption.

Cases MCT35 through MCT47 are reduced to the following conclusions for maximizing reactivity:

1. Minimize structural material outside of the fueled region
 - Cladding and side plate volume
2. Maximize active fuel width
3. Minimize active fuel height
4. Minimize fuel thickness

One additional conclusion is based on results presented in Section 6.10.1.9.3, and confirmed by the NCT array results presented in Section 6.10.1.5: maximizing the number of fuel plates for a given fissile mass per plate will increase reactivity.

Two parameters – fuel material chemical composition and the uranium loading in the fuel – are shown to be insignificant. Here uranium loading is the percentage of the fuel that is uranium. In all cases, the total mass of uranium is held constant.

From the parameters given in Table 6.10.1-2 and Table 6.10.1-3, a first guess is taken for the bounding fuel element parameters. For this analysis, the MEU fuel is grouped with the HEU fuel. The LEU fuel is analyzed separately when necessary. Table 6.10.1-16 summarizes the expected bounding values for HEU and LEU. The listed tolerances are taken from the values for Comision Nacional De Energia Atomica (CNEA) fuel elements listed in Table 6.10.1-2. The table also includes a first guess at a bounding element description which is composed of the most limiting values accounting for the stated tolerances.

Some assumptions are embedded in the initial bounding characteristics. The element width is assumed to be equal to the active fuel width plus twice the side plate thickness. This ignored some aluminum fuel plate cladding between the active fuel and the side plate (based on case MCT38). The water channel thickness is calculated assuming the plates separate to the maximum extent possible. Increasing plate separation is shown to increase reactivity.

Table 6.10.1-16 gives a listing of the element characteristics that describe a given MTR element. Characteristics that will be calculated are noted in the table. Several parameters are calculated based on other parameters. The required input data is listed below.

- Element depth
- Side plate thickness
- No. of plates
- Plate thickness
- Active fuel length
- Active fuel width
- Clad thickness
- Wt percent U-235
- U-235 per plate
- U in fuel composition

The remaining values are calculated as follows. The constants used are 8.8392 cm as the width of the fuel bucket and 15.24 cm (6 in.) as the focal length of the curved fuel plates.

- Element width = $2 * \text{side plate thickness} + \text{active fuel width}$
- Active fuel thickness = $\text{plate thickness} - 2 * \text{clad thickness}$
- Arc length = $2 * \arcsin(\text{active fuel width} / 2 / 15.24) * 15.24$
- Water channel thickness $\approx (8.8392 - \text{no. of plates} * \text{plate thickness}) / (\text{no. of plates} - 1)$
- U-235 per fuel element = $\text{no. of plates} * \text{U-235 per plate}$
- U density = $(\text{U-235 per plate} / \text{wt\% U-235}) / (\text{active fuel length} * \text{active fuel thickness} * \text{arc length})$
- Fuel density = $\text{U density} / \text{U in fuel composition}$

The results for cases MCT35 through MCT47 inform the selection of the bounding characteristics shown in Table 6.10.1-16. These bounding values will be used as a starting point for the analysis in Section 6.10.1.5 which defines the allowable fuel characteristics for shipment. The NCT array cases bound the single package cases because the same fuel geometry and moderation assumptions are utilized in both analyses. Therefore, single package calculations using the final bounding characteristics are not performed.

6.10.1.4.2 Results

The single package results are summarized in Table 6.10.1-12 through Table 6.10.1-15.

6.10.1.5 Evaluation of Package Arrays under Normal Conditions of Transport

6.10.1.5.1 Configuration

This section is used to confirm that the NCT array – three casks in a triangular arrangement – will remain subcritical for various limiting configurations. This array geometry is illustrated in Figure 6.10.1-12. The three casks are separated by 36 in. which is the minimum length permitted by the impact limiters. The outer ring depicted in the figure is a layer of full-density water to provide neutron reflection. Water is assumed to fill the space between the casks.

The most limiting manufacturing tolerances, fuel position in the cask, water density in the cask, and fuel element characteristics were found in Section 6.10.1.4. These worst-case parameters are used to build the initial NCT array model, case MAB1. The characteristics of the bounding MTR fuel element are shown in Table 6.10.1-17, case MAB1. Starting from this worst-case model, a range of allowable configurations is found that bound the fuel elements described in Table 6.10.1-2 and Table 6.10.1-3.

Two further changes are made between cases MAB1 and MAB2. The dimensions of the TN-LC-MTR bucket tube cap are changed to reflect the tolerances for stock plate and the thickness is reduced by a factor of 0.88 to account for the drainage holes. The thickness of the TN-LC-MTR bucket compartment wall is also decreased to match the appropriate stock tolerances. Both changes should cause a very slight increase in reactivity.

The space between casks is filled with water. Cases MAD1 through MAD5 vary the water density between the casks from 1.0 or 0.001 g/cc. These cases run ten times the typical number of neutrons in an attempt to resolve the small changes in reactivity. The lowest and highest water densities produce the highest reactivity, suggesting that either reflection back into the cask or streaming between casks is most limiting. The uncertainty in the Monte Carlo calculation is approximately equal to any changes in reactivity as shown by cases MAB1 and MAD1 (the only difference is the number of neutrons simulated). The MCNP-calculated k_{eff} values and standard error (at two-sigma) are presented in Figure 6.10.1-13. Based on these results, subsequent cases are run with both low and high water densities between casks.

Two cases (MAB2 and MAB3) are considered to allow the widest possible range of cask operations. In these calculations, the central stack of fuel elements is partially or fully empty. MAB2 removes three fuel elements from the TN-LC package. For the central stack, every other element is removed. Case MAB3 removes all six elements from the central stack. While this case is not ideal from an operations perspective, it is provided in the event that future MTR fuel elements are not bound by those considered in this analysis. Case MAB3 produces column H of Table 6.10.1-4.

The remaining groups of cases are fairly straightforward. For a given number of fuel plates per element, the maximum fissile loading (expressed as grams of U-235 per plate) for an element is determined. This process yields cases MAB7, MAB11, MAB14, MAB18, and MAB21. These five cases represent columns A through E in Table 6.10.1-4.

Case MAB15 is a test for an element approximating the LEU BSR to ensure that LEU fuel is not more reactive than HEU fuel. The results in Table 6.10.1-18 show a decrease in reactivity, confirming previous conclusions that HEU analysis is bounding of LEU fuels.

After the general bounding cases are found, two elements lie outside the allowable configurations: HFBR and NISTR. The especially short active fuel for NISTR is analyzed in case MAB22 and found to be allowable and represents column G in Table 6.10.1-4. The HFBR requires a few changes to the allowable dimensions to accommodate 20.5 g of U-235 per plate. An explicit case is run for 18 fuel plates and the active fuel width is limited to 5.85 cm. Given these constraints, the HFBR fuel is found to be allowable and represents column F in Table 6.10.1-4.

After the eight limiting fuel elements are found, each case is re-run with the water density between the casks reduced to 0.001 g/cc. This should ensure that the final k_s is correct given the inconclusive results presented in Figure 6.10.1-13. These cases are denoted with “_1” (underscore one) and the relevant details and results are presented in Table 6.10.1-17 and Table 6.10.1-18.

Case MAB7_1 produces the highest reactivity with $k_s = 0.91783$ which is less than the USL of 0.9213. This case bounds a single package reflected with water.

6.10.1.5.2 Results

The NCT array calculations are summarized in Table 6.10.1-17 and Table 6.10.1-18.

6.10.1.6 Package Arrays under Hypothetical Accident Conditions

Because the CSI = 100, no HAC array cases are performed.

6.10.1.7 Fissile Material Packages for Air Transport

This section does not apply.

6.10.1.8 Benchmark Evaluations

The Monte Carlo computer program MCNP5 v1.40 is utilized for this benchmark analysis [1]. MCNP has been used extensively in criticality evaluations for several decades and is considered a standard in the industry.

A listing of the cross-section libraries used in the analysis is provided in Table 6.10.1-11. These cross-sections are consistent with the cross-sections utilized in the benchmarks.

The ORNL USLSTATS computer program [4] is used to establish a USL for the analysis. USLSTATS provides a simple means of evaluating and combining the statistical error of the calculation, code biases, and benchmark uncertainties. The USLSTATS calculation uses the combined uncertainties and data to provide a linear trend and an overall uncertainty. Computed multiplication factors, k_{eff} , for the package are deemed to be adequately subcritical if the computed value of k_s is less than or equal to the USL as follows:

$$k_s = k_{\text{eff}} + 2\sigma \leq \text{USL}$$

The USL is determined on the basis of a benchmark analysis and incorporates the combined effects of code computational bias, the uncertainty in the bias based on both benchmark-model and computational uncertainties, and an administrative margin. This methodology has accepted precedence in establishing criticality safety limits for transportation packages complying with 10CFR71.

6.10.1.8.1 Applicability of Benchmark Experiments

The critical experiment benchmarks are selected from the “International Handbook of Evaluated Criticality Safety Benchmark Experiments” based upon their similarity to the TN-LC-MTR basket and contents [5]. The important selection parameters are high-enriched uranium plate-type fuel with a thermal spectrum. Thirty-five (35) benchmarks that meet these criteria are selected from the Handbook. The titles for all utilized experiments are listed in Table 6.10.1-19.

Ideally, benchmarks would be limited to those with a fuel matrix of UAl_x and aluminum, aluminum cladding, and no absorbers, consistent with the MTR criticality models. Experiment set HEU-MET-THERM-006 consists of 23 benchmark experiments. The first 16 experiments are directly applicable, although experiments 17 and 18 utilize thin cadmium sheets, and experiments 19 through 23 utilize uranium in solution in addition to the fuel plates. Experiment set HEU-COMP-THERM-022 consists of 11 benchmark experiments that utilize UO_2 powder sintered with stainless steel, and stainless steel cladding. Experiments 1 through 5 do not utilize control rods, while experiments 6 through 11 utilize boron control rods. HEU-MET-THERM-022 is a detailed model of the Advanced Test Reactor (ATR) core using explicit ATR fuel elements. However, this full-core model necessarily contains absorber materials.

Therefore, of these 35 benchmarks, 17 benchmarks are directly applicable, while 18 benchmarks are applicable to a lesser degree. To compensate for the benchmarks that are not directly applicable, trending will be performed both on all 35 benchmark experiments and on the subset of 17 directly applicable benchmark experiments. The USL selected is the minimum of both experimental sets.

6.10.1.8.2 Bias Determination

The USL is calculated by application of the USLSTATS computer program [4]. USLSTATS receives as input the k_{eff} as calculated by MCNP, the total 1- σ uncertainty (combined benchmark and MCNP uncertainties), and a trending parameter. Five trending parameters have been selected: (1) Energy of the Average neutron Lethargy causing Fission (EALF), (2) U-235 number density, (3) channel width, (4) ratio of the number of hydrogen atoms in a unit cell to the number of U-235 atoms in a unit cell (H/U-235), and (5) plate pitch.

The uncertainty value, σ_{total} , assigned to each case is a combination of the benchmark uncertainty for each experiment, σ_{bench} , and the Monte Carlo uncertainty associated with the particular computational evaluation of the case, σ_{MCNP} , or:

$$\sigma_{\text{total}} = \left(\sigma_{\text{bench}}^2 + \sigma_{\text{MCNP}}^2 \right)^{1/2}$$

These values are input into the USLSTATS program in addition to the following parameters, which are the values recommended by the USLSTATS user's manual [4]:

- P, proportion of population falling above lower tolerance level = 0.995 (note that this parameter is required input but is not utilized in the calculation of USL Method 1)
- $1-\gamma$, confidence on fit = 0.95
- α , confidence on proportion P = 0.95 (note that this parameter is required input but is not utilized in the calculation of USL Method 1)
- Δk_m , administrative margin used to ensure subcriticality = 0.05.

These data are followed by triplets of trending parameter value, computed k_{eff} , and uncertainty for each case. A confidence band analysis is performed on the data for each trending parameter using USL Method 1. The USL generated for each of the trending parameters utilized is provided in Table 6.10.1-20. All benchmark data used as input to USLSTATS are reported in Table 6.10.1-21.

Energy of the Average Neutron Lethargy causing Fission (EALF):

The EALF is used as the first trending parameter for the benchmark cases. The EALF comparison provides a means to observe neutron spectral dependencies or trends. Over the range of applicability, the minimum USL is 0.9256 for the full benchmark set, and 0.9217 for the subset of directly applicable benchmarks.

All of the models fall within the range of applicability. The EALF of the most reactive model (case MAB7_1) is 8.65E-08 MeV. The range of applicability is between 5.23E-08 and 1.59E-07 MeV.

U-235 Number Density:

The U-235 number density is used as the second trending parameter for the benchmark cases. Over the range of applicability, the minimum USL is 0.9242 for the full benchmark set, and 0.9213 for the subset of directly applicable benchmarks.

For the limited element cases, the U-235 number density generally falls below the benchmark range of 1.85E-03 to 3.93E-03 atom/b-cm. However, the highest-reactivity elements (HBFR, NISTR, BSR LEU) fall within the acceptable range. For the limiting fuel compositions used in the NCT array cases, the number density fluctuates between approximately 1.70E-03 and 1.90E-03 atom/b-cm. While this value occasionally falls outside the benchmark range, it only deviates slightly and is acceptable for this analysis.

Channel Width:

The channel width is used as the third trending parameter for the benchmark cases. Over the range of applicability, the minimum USL is 0.9227 for the full benchmark set, and 0.9213 for the subset of directly applicable benchmarks.

The MTR elements generally fall outside the maximum channel width of 0.2 cm. Typical MTR values are between 0.2 and 0.4 cm. These values are further increased in order to maximize reactivity. The main function of the water gap is to thermalize neutrons which, given the EALF results, is being handled consistently between benchmark cases. This gives confidence that the benchmark set is valid even if the typical channel widths differ.

H/U-235 Atom Ratio:

The H/U-235 atom ratio is used as the fourth trending parameter for the benchmark cases. The H/U-235 atom ratio is defined here as the ratio of hydrogen atoms to U-235 atoms in a unit cell. This parameter is computed by the following equation:

$$NH * C / (NU235 * M)$$

Where:

NH is the hydrogen number density

C is the channel width

NU235 is the U-235 number density

M is the fuel meat width

Over the range of applicability, the minimum USL is 0.9258 for the full benchmark set, and 0.9213 for the subset of directly applicable benchmarks.

Using the maximum MTR plate U-235 number density for the optimized fuel element model, the H/U-235 value may be computed as:

$$6.74E-02 * 0.1114 / (2.08E-03 * 0.0291) = 124.0$$

The H/U-235 of the limiting model is slightly above the maximum benchmark range of 116.5. This is a relatively small difference and is acceptable for the limiting configuration.

Pitch:

The fuel plate pitch is used as the fifth trending parameter for the benchmark cases. Over the range of applicability, the minimum USL is 0.9227 for the full benchmark set, and 0.9213 for the subset of directly applicable benchmarks.

The fuel plate pitch is consistent with the benchmark cases for the limiting elements. For the bounding cases, the fuel plates are expanded to fill the TN-LC-MTR fuel bucket which increases the pitch to beyond the benchmark basis. This is considered acceptable for the limiting case.

6.10.1.9 Appendix

6.10.1.9.1 References

1. MCNP5, "MCNP – A General Monte Carlo N-Particle Transport Code, Version 5; Volume II: User's Guide," LA-CP-03-0245, Los Alamos National Laboratory, April 2003.
2. ASME Y14.5M – 1994 Dimensioning and Tolerancing.
3. SCALE: A Modular Code System for Performing Standardized Computer Analyses for Licensing Evaluations, ORNL/TM-2005/39, Version 6, Vols. I-III, January 2009.
4. USLSTATS, "USLSTATS: A Utility To Calculate Upper Subcritical Limits For Criticality Safety Applications," Version 1.4.2, Oak Ridge National Laboratory, April 23, 2003. Note: USLSTATS is described in Appendix C, User's Manual for USLSTATS V1.0, in NUREG/CR-6361 Criticality Benchmark Guide for Light-Water-Reactor Fuel in Transportation and Storage Packages, March 1997.
5. International Handbook of Evaluated Criticality Safety Benchmark Experiments, Nuclear Energy Agency, NEA/NSC/DOC(95)03, September 2009.
6. ASTM A 480/A 480M-03c, Standard Specification for General Requirements for Flat-Rolled Stainless and Heat-Resisting Steel Plate, Sheet, and Strip, Oct. 1, 2003.

**Proprietary Information on Pages 6.10.1-23 through 6.10.1-31
Withheld Pursuant to 10 CFR 2.390.**

Proprietary Information Withheld Pursuant to 10 CFR 2.390.

6.10.1.9.3 Parametric Evaluations

MTR fuel encompasses many different uranium plate fuels of varying enrichment. Since the fuel types can vary, the first step in this analysis is to determine the limiting (most reactive) fuel type of the known types. The limiting fuel element is used in the models that determine the most reactive fuel position and basket tolerances.

Proprietary Information Withheld Pursuant to 10 CFR 2.390.

Starting with the HFBR and BSR LEU elements, the plate pitch is reduced by 50 percent (cases MLE24 and MLE28) and then increased twice (cases MLE25, MLE26, MLE29, and MLE30). The first increase will occupy roughly half of the available space in the basket. The second increase will expand the plates equally to fill the cavity. As a check, two fuel plates are removed from the most reactive case and the pitch is increased further (MLE27). Two additional high-reactivity elements are tested in the maximally-expanded condition: ORR#2 (MLE32) and ASTRA MEU (MLE33). The results of the sensitivity studies are shown in Table 6.10.1-23.

The results in Table 6.10.1-23 show that fuel element one, case MLE1 or HFBR HEU fuel, is the most reactive when the plates are free to expand to the most reactive configuration. HFBR fuel elements also contain the highest loading of U-235 per element. Increased plate pitch, facilitated by removing fuel plates, is shown to be less reactive than the 18-fuel-plate configuration.

A second conclusion is that HEU, MEU, and LEU fuel elements are all more reactive when the plates are allowed to expand to the maximum possible plate pitch. This is demonstrated with cases MLE26, MLE30, MLE32, and MLE33. This indicates that using the maximum pitch will be conservative for all fuel elements.

Thus far, the element calculations have been done with flat fuel plates. Case MLE31 tests the change in reactivity due to modeling the fuel plates with some curvature (consistent with their actual construction). In the MCNP models, fuel density is reduced slightly to account for the increased volume of the curve plate with a six in. radius of curvature. The curved plates reduce reactivity by 0.008 because this curvature will slightly limit the expansion of the element in the TN-LC-MTR basket. In spite of this slight non-conservatism, subsequent models will feature curved plates to better reflect their actual construction.

For all HFBR fuel element cases, the two solid aluminum plates are assumed to be absent. Since the HFBR fuel element exhibits the peak reactivity in the damaged fuel configuration (maximum plate pitch, MLE26) and features the maximum fissile loading, it will be used in the initial HAC and NCT calculations. The HFBR fuel element will be modeled in the damaged configuration to provide the maximum reactivity. The selection of an individual element is done only for convenience – the final calculations will be done using the characteristics of several generic fuel elements.

Table 6.10.1-1
 Summary of TN-LC-MTR Criticality Evaluations

Normal Conditions of Transport (NCT)	
Case	k_s
Single Unit Maximum	≤ 0.918
Array Maximum (3 packages)	0.918
Hypothetical Accident Conditions (HAC)	
Case	k_s
Single Unit Maximum	≤ 0.918
Array Maximum (1 package)	≤ 0.918
USL = 0.9213	

Table 6.10.1-2
MTR HEU Fuel Element Specifications

Proprietary Information Withheld Pursuant to 10 CFR 2.390.

Table 6.10.1-3
MTR LEU and MEU Fuel Element Specifications

Proprietary Information Withheld Pursuant to 10 CFR 2.390.

Table 6.10.1-4
Allowable MTR Fuel Elements

		A	B	C	D	E	F	G	H ⁽¹⁾
No. of Fuel Plates		≤23	≤21	≤19	≤17	≤10	≤18	≤17	≤23
²³⁵ U per Plate	grams	≤16	≤16.5	≤17.5	≤19	≤22	≤20.5	≤11.5	≤22
Active Fuel Width	cm	≤6.62					≤5.85	≤6.62	≤6.62
Active Fuel Length	cm	≥56						≥27.5	≥56
wt% ²³⁵ U	%	≤94							
Plate Thickness	cm	≥0.114							
Clad Thickness	cm	≥0.020							
Element Depth	cm	≥7.5							
Side Plate Thickness	cm	≥0.40							

Notes:

1. Configuration H requires that the central stack of fuel elements remain empty.

Table 6.10.1-5
Example Fuel Composition for Limiting LEU and HEU Fuel

	20 wt% U-235			94 wt% U-235		
	U-Al	U ₃ O ₈ -Al	U ₃ Si ₂ -Al	U-Al	U ₃ O ₈ -Al	U ₃ Si ₂ -Al
U-234	0.113%	0.113%	0.113%	0.157%	0.157%	0.157%
U-235	14.800%	14.800%	14.800%	20.680%	20.680%	20.680%
U-238	59.087%	59.087%	59.087%	1.163%	1.163%	1.163%
Al-27	12.736%	26.000%	20.179%	74.057%	78.000%	76.269%
O-16	13.264%			3.943%		
Si			5.821%			1.731%

Table 6.10.1-6
Stock Tolerances per ASTM A480

Stock Thickness [in.]	Tolerance	
	Over [in.]	Under [in.]
1/8 (0.125)	0.085	0.013
3/16 (0.1875)	0.085	0.014
1/4 (0.25)	0.085	0.015

Table 6.10.1-7
TN-LC-MTR Fuel Bucket Dimensions, Nominal and Bounding

Proprietary Information Withheld Pursuant to 10 CFR 2.390.

Table 6.10.1-8
TN-LC-MTR Weldment Dimensions, Nominal and Bounding

Proprietary Information Withheld Pursuant to 10 CFR 2.390.

Table 6.10.1-9
TN-LC Cask Dimensions, Nominal and Bounding

Proprietary Information Withheld Pursuant to 10 CFR 2.390.

Table 6.10.1-10
Composition of Stainless Steel

Component	Wt. %
C	0.08
Si	1.0
P	0.045
Cr	19.0
Mn	2.0
Fe	68.375
Ni	9.5
Density = 7.94 g/cm ³	

Table 6.10.1-11
Cross Section Libraries Utilized

Isotope/Element	Cross Section Label (from MCNP output)
1001.62c	1-h-1 at 293.6K from endf-vi.8 njoy99.50
8016.62c	8-o-16 at 293.6K from endf-vi.8 njoy99.50
13027.62c	13-al-27 at 293.6K from endf-vi.8 njoy99.50
25055.62c	25-mn-55 at 293.6K from endf/b-vi.8 njoy99.50
6000.60c	6-c-nat from endf-vi.1
14000.60c	14-si-nat from endf/b-vi
15031.66c	15-p-31 at 293.6K from endf-vi.6 njoy99.50
24000.50c	njoy
26000.55c	njoy
28000.50c	njoy
82000.50c	njoy
92234.69c	92-u-234 at 293.6K from t16 u234la4 njoy99.50
92235.69c	92-u-235 at 293.6K from t16 u235la9d njoy99.50
92238.69c	92-u-238 at 293.6K from t16 u238la8h njoy99.50
lwtr.60t	1-h-1 in h2o at 293.6k from endf-vi.5 njoy99.0

Table 6.10.1-12
 TN-LC-MTR Single Package Fuel Movement Results

Case	Parent	k_{eff}	σ	k_s	Description
		0.80672	0.00082	0.80836	starting point
		0.83792	0.00083	0.83958	elements shifted vertically - three clusters
		0.83644	0.00091	0.83826	elements shifted vertically - two clusters, two apart
		0.85420	0.00087	0.85594	elements shifted horizontally - together in y
		0.80770	0.00086	0.80942	elements shifted horizontally - apart in y
		0.86451	0.00080	0.86611	Fuel bucket shifted +/-y toward the cask center
		0.87569	0.00083	0.87735	Small fuel buckets - six stacked axially
		0.87569	0.00035	0.87639	longer run - previous case with ~4x more neutrons
		0.87555	0.00086	0.87727	Medium fuel buckets - five stacked axially
		0.87612	0.00037	0.87686	longer run - previous case with ~4x more neutrons
		0.87642	0.00085	0.87812	Large fuel buckets - four stacked axially
		0.87629	0.00037	0.87703	longer run - previous case with ~4x more neutrons
		0.86952	0.00082	0.87116	fuel in central bucket shifted to +y limit
		0.86322	0.00073	0.86468	Add Al plate above & below fuel (simulate non-fuel structure)
		0.84342	0.00079	0.84500	Fuel elements centered in buckets
		0.84445	0.00085	0.84615	Fuel elements moved toward center (+/-z) - 1 of 4
		0.84328	0.00084	0.84496	Fuel elements moved toward center (+/-z) - 2 of 4
		0.84414	0.00083	0.84580	Fuel elements moved toward center (+/-z) - 3 of 4
		0.84794	0.00088	0.84970	Fuel elements moved toward center (+/-z) - 4 of 4
		0.85213	0.00079	0.85371	Two middle elements moved together
		0.87324	0.00085	0.87494	Two middle elements touching

Proprietary Information Withheld Pursuant to 10 CFR 2.390.

Table 6.10.1-13
 TN-LC-MTR Single Package Manufacturing Tolerance Results

Case	Parent	k_{eff}	σ	k_s	Description
Proprietary Information Withheld Pursuant to 10 CFR 2.390.		0.86451	0.00080	0.86611	limiting fuel location
		0.84274	0.00081	0.84436	fuel bucket wall thickened to max tolerance
		0.86754	0.00079	0.86912	fuel bucket wall thinned to min tolerance
		0.86551	0.00086	0.86723	fuel bucket tube cap thickened to max tolerance
		0.86702	0.00085	0.86872	fuel bucket tube cap thinned to min tolerance
		0.87011	0.00084	0.87179	basket general assembly compartment plate thinned to min tolerance
		0.86304	0.00077	0.86458	basket general assembly compartment plate thickened to max tolerance
		0.86670	0.00083	0.86836	basket general assembly outer plates thinning to min tolerance
		0.87221	0.00088	0.87397	basket general assembly outer plates thickened to max tolerance
		0.87569	0.00083	0.87735	steel added to tie plate region

Table 6.10.1-14
 TN-LC-MTR Single Package Moderator Density Results

Case	Parent	k_{eff}	σ	k_s	Description
Proprietary Information Withheld Pursuant to 10 CFR 2.390.		0.87569	0.00083	0.87735	water density inside cask, $\rho = 1.00$ g/cc
		0.84759	0.00081	0.84921	water density inside cask, $\rho = 0.90$ g/cc
		0.79541	0.00082	0.79705	water density inside cask, $\rho = 0.75$ g/cc
		0.66936	0.00066	0.67068	water density inside cask, $\rho = 0.50$ g/cc
		0.45799	0.00062	0.45923	water density inside cask, $\rho = 0.25$ g/cc
		0.08742	0.00021	0.08784	water density inside cask, $\rho = 0.001$ g/cc

Table 6.10.1-15
MTR Single Package Bounding Element Characteristic Results

Case	Parent	k_{eff}	σ	k_s	Description
		0.87569	0.00083	0.87735	steel added to tie plate region
		0.87435	0.00083	0.87601	U-Al fuel material
		0.87573	0.00076	0.87725	U3Si2-Al fuel material
		0.87981	0.00081	0.88143	side plate replaced with water
		0.87665	0.00077	0.87819	no gap between fuel and side plate (fuel element size reduced +/-y)
		0.87810	0.00051	0.87912	U loading in fuel decreased from 30% to 10% - U mass constant
		0.87631	0.00083	0.87797	U loading in fuel increased from 30% to 50% - U mass constant
		0.87438	0.00078	0.87594	U loading in fuel increased from 30% to 75% - U mass constant
		0.86123	0.00081	0.86285	increase active fuel height by 5 cm
		0.88964	0.00085	0.89134	decrease active fuel height by 5 cm
		0.89197	0.00081	0.89359	increase active fuel width by 0.5 cm
		0.85875	0.00079	0.86033	decrease active fuel width by 0.5 cm
		0.86690	0.00083	0.86856	increase fuel thickness by 20% w/ constant clad thickness
		0.88333	0.00084	0.88501	decrease fuel thickness by 20% w/ constant clad thickness

Proprietary Information Withheld Pursuant to 10 CFR 2.390.

Table 6.10.1-16
Initial Bounding Assembly Characteristics

Proprietary Information Withheld Pursuant to 10 CFR 2.390.

Table 6.10.1-17
Summary of NCT Array Calculations

(Part 1 of 2)

Case	Parent	No. of Fuel Plates	Grams of U235 per Plate	Active Fuel Width [cm]	Active Fuel Length [cm]	wt% U235	Description
MAB1	-	23	22	6.62	56	94	Generic, bounding MTR fuel element in NCT Array configuration
MAD1	MAB1	"	"	"	"	"	MAB1, more neutrons, water density between casks = 1.0 g/cc
MAD2	MAB1	"	"	"	"	"	MAB1, more neutrons, water density between casks = 0.75 g/cc
MAD3	MAB1	"	"	"	"	"	MAB1, more neutrons, water density between casks = 0.5 g/cc
MAD4	MAB1	"	"	"	"	"	MAB1, more neutrons, water density between casks = 0.25 g/cc
MAD5	MAB1	"	"	"	"	"	MAB1, more neutrons, water density between casks = 0.001 g/cc
MAB2	MAB1	"	"	"	"	"	Removed 3 central elements
MAB3	MAB1	"	"	"	"	"	Removed 6 (all) central elements, central $\rho=1.0$ g/cc
MAB3 1	MAB1	"	"	"	"	"	Removed 6 (all) central elements, central $\rho=0.001$ g/cc
MAB4	MAB1	"	20	"	"	"	23 plates, fissile content = 20g/plate
MAB5	MAB1	"	18	"	"	"	23 plates, fissile content = 18g/plate
MAB6	MAB1	"	17	"	"	"	23 plates, fissile content = 17g/plate
MAB7	MAB1	"	16	"	"	"	23 plates, fissile content = 16g/plate, central $\rho=1.0$ g/cc
MAB7 1	MAB1	"	"	"	"	"	23 plates, fissile content = 16g/plate, central $\rho=0.001$ g/cc
MAB8	MAB1	21	22	6.62	56	94	21 plates, fissile content = 22g/plate
MAB9	MAB1	"	20	"	"	"	21 plates, fissile content = 20g/plate
MAB10	MAB1	"	18	"	"	"	21 plates, fissile content = 18g/plate
MAB11	MAB1	"	17	"	"	"	21 plates, fissile content = 17g/plate
MAB12	MAB1	"	16.5	"	"	"	21 plates, fissile content = 16.5g/plate, central $\rho=1.0$ g/cc
MAB12 1	MAB1	"	"	"	"	"	21 plates, fissile content = 16.5g/plate, central $\rho=0.001$ g/cc
MAB13	MAB1	19	22	6.62	56	94	19 plates, fissile content = 22g/plate
MAB14	MAB1	"	20	"	"	"	19 plates, fissile content = 20g/plate
MAB15	MAB1	"	18	"	"	"	19 plates, fissile content = 18g/plate
MAB16	MAB15	"	"	"	"	20	LEU configuration, approximate LEU BSR
MAB17	MAB1	"	17.5	"	"	94	19 plates, fissile content = 17.5g/plate, central $\rho=1.0$ g/cc
MAB17 1	MAB1	"	"	"	"	"	19 plates, fissile content = 17.5g/plate, central $\rho=0.001$ g/cc

Table 6.10.1-17
Summary of NCT Array Calculations
(Part 2 of 2)

Case	Parent	No. of Fuel Plates	Grams of U235 per Plate	Active Fuel Width [cm]	Active Fuel Length [cm]	wt% U235	Description
MAB18	MAB1	17	22	6.62	56	94	17 plates, fissile content = 22g/plate
MAB19	MAB1	"	20	"	"	"	17 plates, fissile content = 20g/plate
MAB20	MAB1	"	19	"	"	"	17 plates, fissile content = 19g/plate, central $\rho=1.0$ g/cc
MAB20 1	MAB1	"	"	"	"	"	17 plates, fissile content = 19g/plate, central $\rho=0.001$ g/cc
MAB21	MAB1	18	20.5	6.62	56	94	18 plates, approximate HFBR
MAB22	MAB21	"	"	5.85	"	"	18 plates, approximate HFBR, 5.85 cm active fuel width, central $\rho=1.0$ g/cc
MAB22 1	MAB21	"	"	"	"	"	18 plates, approximate HFBR, 5.85 cm active fuel width, central $\rho=0.001$ g/cc
MAB23	MAB1	10	22	6.62	56	94	10 plates, fissile content = 22g/plate, central $\rho=1.0$ g/cc
MAB23 1	MAB1	"	"	"	"	"	10 plates, fissile content = 22g/plate, central $\rho=0.001$ g/cc
MAB24	MAB18	17	11.5	6.62	27.5	94	17 plates, approximate NISTR, central $\rho=1.0$ g/cc
MAB24 1	MAB18	"	"	"	"	"	17 plates, approximate NISTR, central $\rho=0.001$ g/cc

Table 6.10.1-18
NCT Array Results

Case	Parent	k_{eff}	σ	k_s
		0.98025	0.00083	0.98191
		0.97978	0.00024	0.98026
		0.97959	0.00024	0.98007
		0.97929	0.00024	0.97977
		0.97964	0.00025	0.98014
		0.98024	0.00024	0.98072
		0.95345	0.00080	0.95505
		0.84866	0.00078	0.85022
		0.84974	0.00051	0.85076
		0.96366	0.00090	0.96546
		0.94334	0.00086	0.94506
		0.93023	0.00085	0.93193
		0.91475	0.00080	0.91635
		0.91681	0.00051	0.91783
		0.97459	0.00085	0.97629
		0.95442	0.00080	0.95602
		0.93241	0.00085	0.93411
		0.91735	0.00084	0.91903
		0.91097	0.00079	0.91255
		0.91181	0.00049	0.91279
		0.96226	0.00095	0.96416
		0.94122	0.00081	0.94284
		0.91785	0.00075	0.91935
		0.87563	0.00075	0.87713
		0.91082	0.00078	0.91238
		0.91107	0.00051	0.91209
		0.94567	0.00082	0.94731
		0.92214	0.00075	0.92364
		0.91111	0.00077	0.91265
		0.91072	0.00048	0.91168
		0.93699	0.00081	0.93861
		0.91603	0.00087	0.91777
		0.91412	0.00050	0.91512
		0.82074	0.00071	0.82216
		0.81989	0.00045	0.82079
		0.90076	0.00082	0.90240
		0.90091	0.00052	0.90195

Proprietary Information Withheld Pursuant to 10 CFR 2.390.

Table 6.10.1-19
Benchmark Experiments Utilized

Series	Title
HEU-COMP-THERM-022	SPERT III Stainless-Steel-Clad Plate-Type Fuel in Water
HEU-MET-THERM-006	SPERT-D Aluminum-Clad Plate-Type Fuel in Water, Dilute Uranyl Nitrate, or Borated Uranyl Nitrate
HEU-MET-THERM-022	Advanced Test Reactor: Serpentine Arrangement of Highly Enriched Water-Moderated Uranium-Aluminide Fuel Plates Reflected by Beryllium

Table 6.10.1-20
USL Results

Trending Parameter (X)	Filename	Minimum USL Over Range of Applicability	Range of Applicability
35 Experiment Set			
EALF [MeV]	EALF_35.i	0.9256	5.23E-8 <= X <= 1.59E-7
U-235 Number Density [atom/barn-cm]	NDEN_35.i	0.9242	1.85E-3 <= X <= 3.93E-3
Channel Width [in]	CHAN_35.i	0.9227	6.46E-2 <= X <= 7.80E-2
H/U-235	HX_35.i	0.9258	6.51E+1 <= X <= 1.16E+2
Pitch [in]	PIT_35.i	0.9227	1.25E-1 <= X <= 1.28E-1
17 Experiment Set			
EALF [MeV]	EALF_17.i	0.9217	5.23E-8 <= X <= 1.59E-7
U-235 Number Density [atom/barn-cm]	NDEN_17.i	0.9213	1.85E-3 <= X <= 3.93E-3
Channel Width [in]	CHAN_17.i	0.9213	6.46E-2 <= X <= 7.80E-2
H/U-235	HX_17.i	0.9213	6.51E+1 <= X <= 1.16E+2
Pitch [in]	PIT_17.i	0.9213	1.25E-1 <= X <= 1.28E-1

Table 6.10.1-21
Benchmark Experiment Data

No	Name	k	σ_{mcnp}	σ_{bench}	σ_{total}	EALF [MeV]	NDEN [a/b-cm]	CHAN [in]	H/X	PITCH [in]
1	HCT022_C01	0.98895	0.00060	0.00810	0.00812	9.53E-08	3.32E-03	6.46E-02	6.51E+01	1.25E-01
2	HCT022_C02	0.98980	0.00061	0.00810	0.00812	9.66E-08	3.32E-03	6.46E-02	6.51E+01	1.25E-01
3	HCT022_C03	0.98985	0.00063	0.00810	0.00812	9.81E-08	3.32E-03	6.46E-02	6.51E+01	1.25E-01
4	HCT022_C04	0.98856	0.00060	0.00810	0.00812	9.92E-08	3.32E-03	6.46E-02	6.51E+01	1.25E-01
5	HCT022_C05	0.98909	0.00063	0.00810	0.00812	9.59E-08	3.32E-03	6.46E-02	6.51E+01	1.25E-01
6	HCT022_C06	0.98902	0.00059	0.00810	0.00812	9.84E-08	3.32E-03	6.46E-02	6.51E+01	1.25E-01
7	HCT022_C07	0.98963	0.00056	0.00810	0.00812	9.89E-08	3.32E-03	6.46E-02	6.51E+01	1.25E-01
8	HCT022_C08	0.98908	0.00057	0.00810	0.00812	9.95E-08	3.32E-03	6.46E-02	6.51E+01	1.25E-01
9	HCT022_C09	0.98840	0.00056	0.00810	0.00812	9.59E-08	3.32E-03	6.46E-02	6.51E+01	1.25E-01
10	HCT022_C10	0.98845	0.00060	0.00810	0.00812	9.96E-08	3.32E-03	6.46E-02	6.51E+01	1.25E-01
11	HCT022_C11	0.98930	0.00060	0.00810	0.00812	1.00E-07	3.32E-03	6.46E-02	6.51E+01	1.25E-01
12	HMT006_C01	0.99240	0.00081	0.00440	0.00447	8.42E-08	1.85E-03	6.46E-02	1.17E+02	1.25E-01
13	HMT006_C02	0.99217	0.00085	0.00400	0.00409	7.03E-08	1.85E-03	6.46E-02	1.17E+02	1.25E-01
14	HMT006_C03	0.99645	0.00085	0.00400	0.00409	6.34E-08	1.85E-03	6.46E-02	1.17E+02	1.25E-01
15	HMT006_C04	0.99249	0.00076	0.00400	0.00407	6.17E-08	1.85E-03	6.46E-02	1.17E+02	1.25E-01
16	HMT006_C05	0.99026	0.00081	0.00400	0.00408	5.85E-08	1.85E-03	6.46E-02	1.17E+02	1.25E-01
17	HMT006_C06	0.98908	0.00077	0.00400	0.00407	5.61E-08	1.85E-03	6.46E-02	1.17E+02	1.25E-01
18	HMT006_C07	0.98702	0.00078	0.00400	0.00408	5.46E-08	1.85E-03	6.46E-02	1.17E+02	1.25E-01
19	HMT006_C08	0.98411	0.00074	0.00400	0.00407	5.24E-08	1.85E-03	6.46E-02	1.17E+02	1.25E-01
20	HMT006_C09	0.98652	0.00066	0.00400	0.00405	5.23E-08	1.85E-03	6.46E-02	1.17E+02	1.25E-01
21	HMT006_C10	0.99922	0.00080	0.00400	0.00408	8.23E-08	1.85E-03	6.46E-02	1.17E+02	1.25E-01
22	HMT006_C11	0.99201	0.00081	0.00400	0.00408	6.20E-08	1.85E-03	6.46E-02	1.17E+02	1.25E-01
23	HMT006_C12	0.99495	0.00074	0.00400	0.00407	5.43E-08	1.85E-03	6.46E-02	1.17E+02	1.25E-01
24	HMT006_C13	1.01212	0.00088	0.00400	0.00410	8.26E-08	1.85E-03	6.46E-02	1.17E+02	1.25E-01
25	HMT006_C14	0.98560	0.00073	0.00610	0.00614	5.73E-08	1.85E-03	6.46E-02	1.17E+02	1.25E-01
26	HMT006_C15	0.98278	0.00075	0.00400	0.00407	5.67E-08	1.85E-03	6.46E-02	1.17E+02	1.25E-01
27	HMT006_C16	0.99386	0.00079	0.00400	0.00408	6.35E-08	1.85E-03	6.46E-02	1.17E+02	1.25E-01
28	HMT006_C17	0.98926	0.00085	0.00400	0.00409	7.36E-08	1.85E-03	6.46E-02	1.17E+02	1.25E-01
29	HMT006_C18	0.99174	0.00088	0.00400	0.00410	8.00E-08	1.85E-03	6.46E-02	1.17E+02	1.25E-01
30	HMT006_C19	0.99312	0.00068	0.00400	0.00406	5.23E-08	1.85E-03	6.46E-02	1.14E+02	1.25E-01
31	HMT006_C20	0.99257	0.00080	0.00400	0.00408	6.44E-08	1.85E-03	6.46E-02	1.14E+02	1.25E-01
32	HMT006_C21	0.99815	0.00080	0.00400	0.00408	6.93E-08	1.85E-03	6.46E-02	1.14E+02	1.25E-01
33	HMT006_C22	0.99588	0.00078	0.00400	0.00408	7.37E-08	1.85E-03	6.46E-02	1.14E+02	1.25E-01
34	HMT006_C23	1.00023	0.00083	0.00400	0.00409	7.70E-08	1.85E-03	6.46E-02	1.14E+02	1.25E-01
35	HMT022_C01	0.99168	0.00012	0.00350	0.00350	1.59E-07	3.93E-03	7.80E-02	6.60E+01	1.28E-01

Table 6.10.1-22
Summary of Limiting Element Selection k_{eff} Results

Case	Reactor	k_{eff}	σ	k_s ($k_{eff}+2\sigma$)
	Proprietary Information Withheld Pursuant to 10 CFR 2.390.	1.16531	0.00104	1.16739
		1.08002	0.00094	1.08190
		1.18979	0.00092	1.19163
		1.10565	0.00091	1.10747
		1.11338	0.00109	1.11556
		1.06554	0.00111	1.06776
		0.89722	0.00089	0.89900
		1.03886	0.00089	1.04064
		1.05067	0.00094	1.05255
		1.02965	0.00095	1.03155
		1.17728	0.00152	1.18032
		1.17364	0.00095	1.17554
		1.17451	0.00081	1.17613
		1.11705	0.00104	1.11913
		1.14830	0.00088	1.15006
		0.96001	0.00090	0.96181
		1.06247	0.00100	1.06447
		1.18373	0.00096	1.18565
		1.02144	0.00098	1.02340
		1.01212	0.00109	1.01430
	1.15651	0.00098	1.15847	
	1.01655	0.00090	1.01835	
	1.18933	0.00094	1.19121	

Table 6.10.1-23
Limiting Elements in HAC Configuration

Case	Parent	k_{eff}	σ	k_s ($k_{eff}+2\sigma$)	Case Description
	Proprietary Information Withheld Pursuant to 10 CFR 2.390.	0.99628	0.00115	0.99858	HFBR, pitch reduced by 50%
		1.21351	0.00104	1.21559	HFBR, pitch increased by 25%
		1.24767	0.00103	1.24973	HFBR, maximum pitch
		1.21473	0.00094	1.21661	HFBR, maximum pitch, two plates removed
		1.02509	0.00102	1.02713	BSR LEU, pitch reduced by 50%
		1.20032	0.00092	1.20216	BSR LEU, pitch increased by 10%
		1.21090	0.00087	1.21264	BSR LEU, maximum pitch
		1.23944	0.00093	1.24130	HFBR, maximum pitch, curved plates
		1.21771	0.00100	1.21971	ORR#2, maximum pitch
		1.21618	0.00090	1.21798	ASTRA MEU, maximum pitch

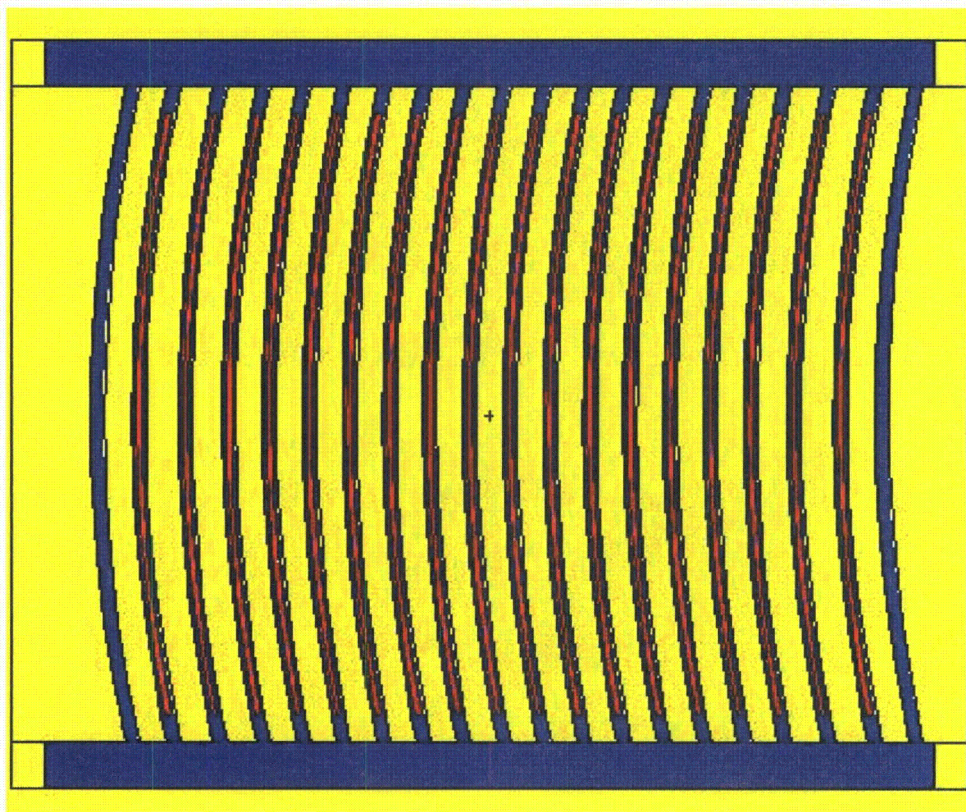


Figure 6.10.1-1
HFBR MTR Fuel Element

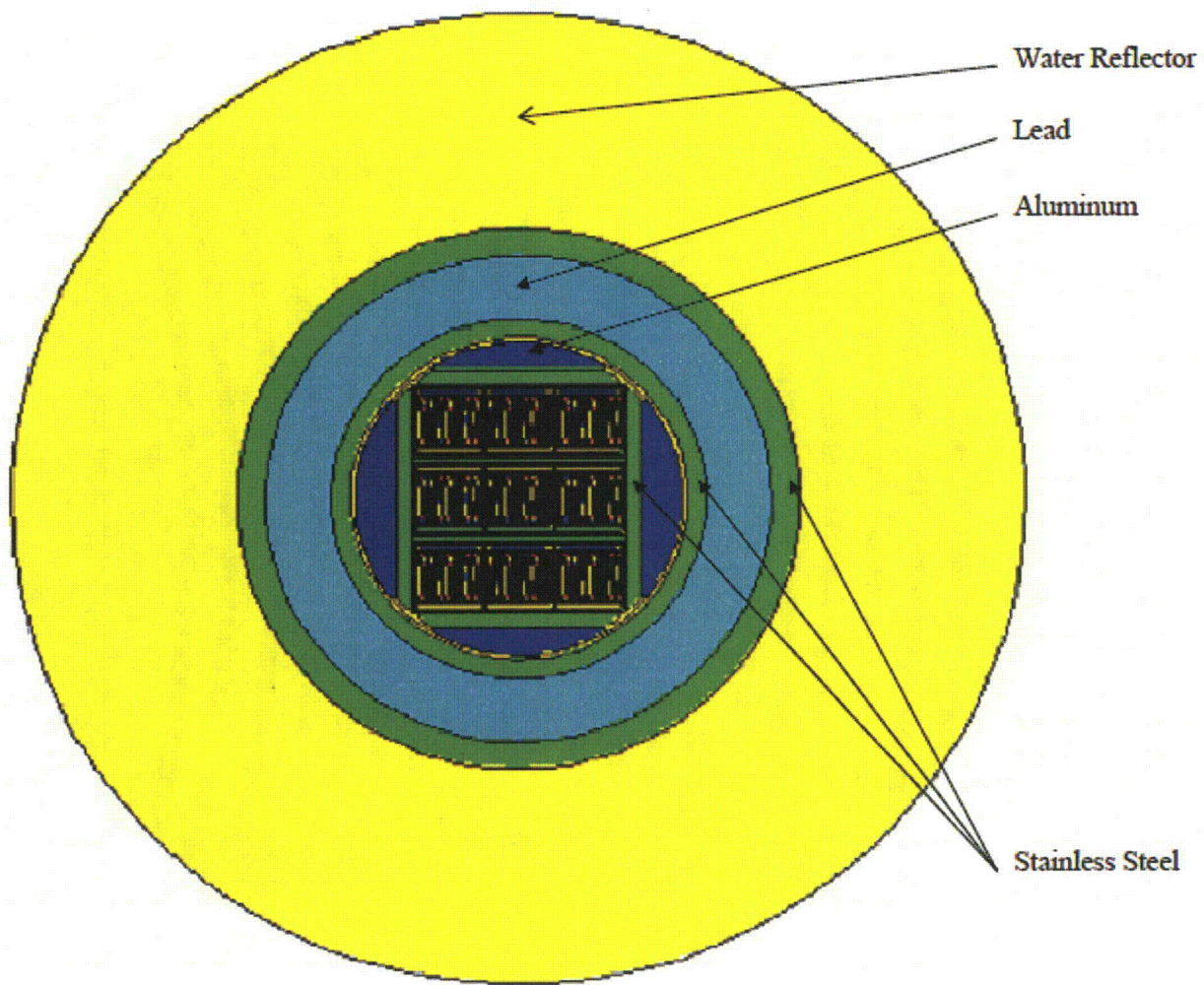


Figure 6.10.1-2
TN-LC-MTR Single Package Model, planar view

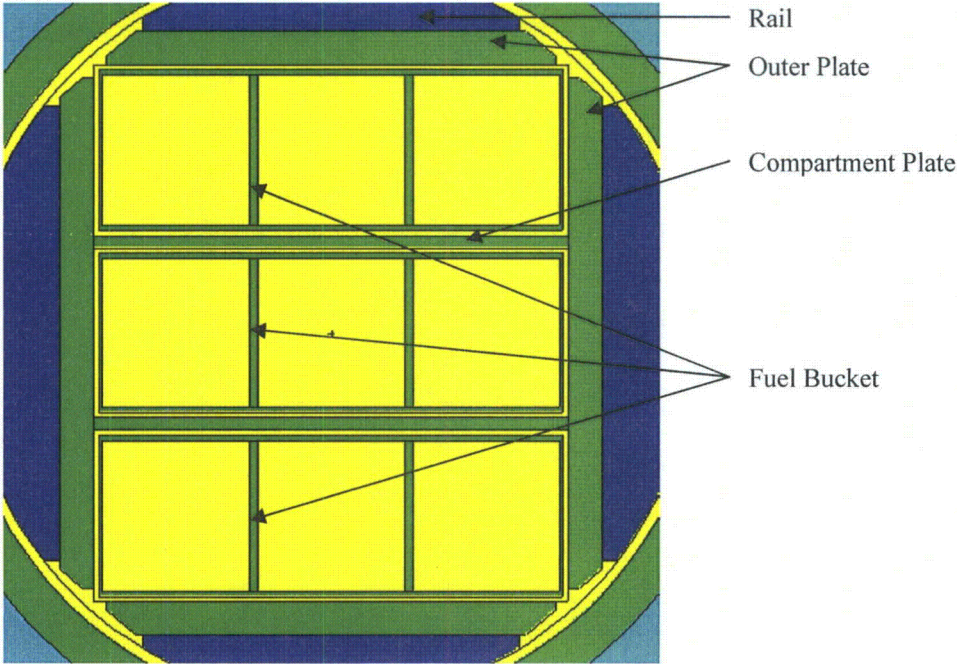


Figure 6.10.1-3
TN-LC-MTR Weldment and Fuel Buckets (planar view)

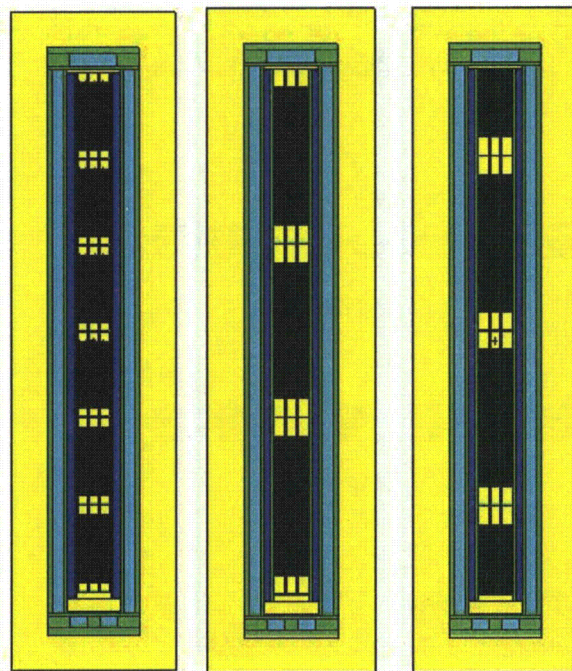


Figure 6.10.1-4
Potential Axial Element Spacing (MCT1, MCT2, MCT3)

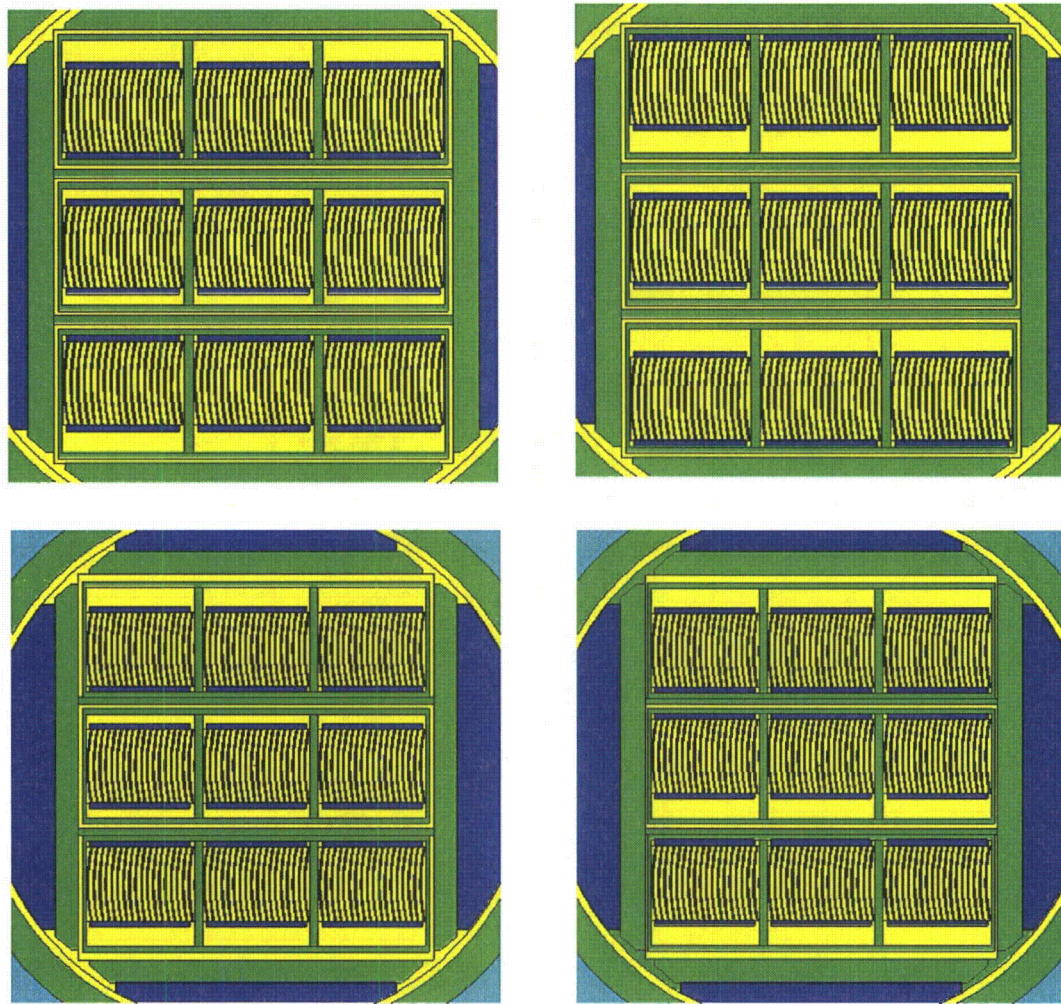


Figure 6.10.1-5
Potential Horizontal Element Spacing (MCT4, MCT5, MCT6, MCT21)

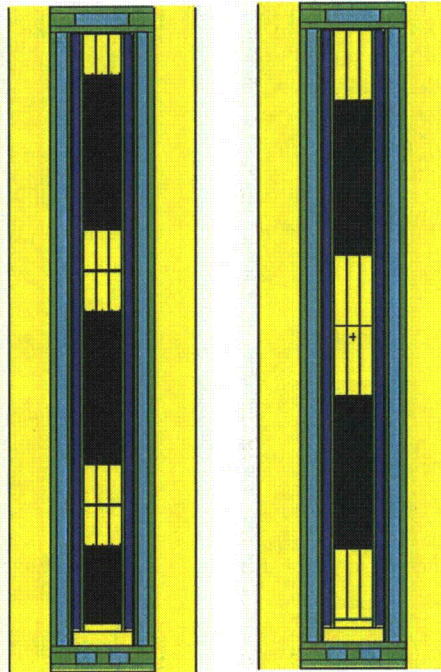


Figure 6.10.1-6
Five- and Four- Bucket TN-LC-MTR Basket Configurations (MCT17, MCT19)

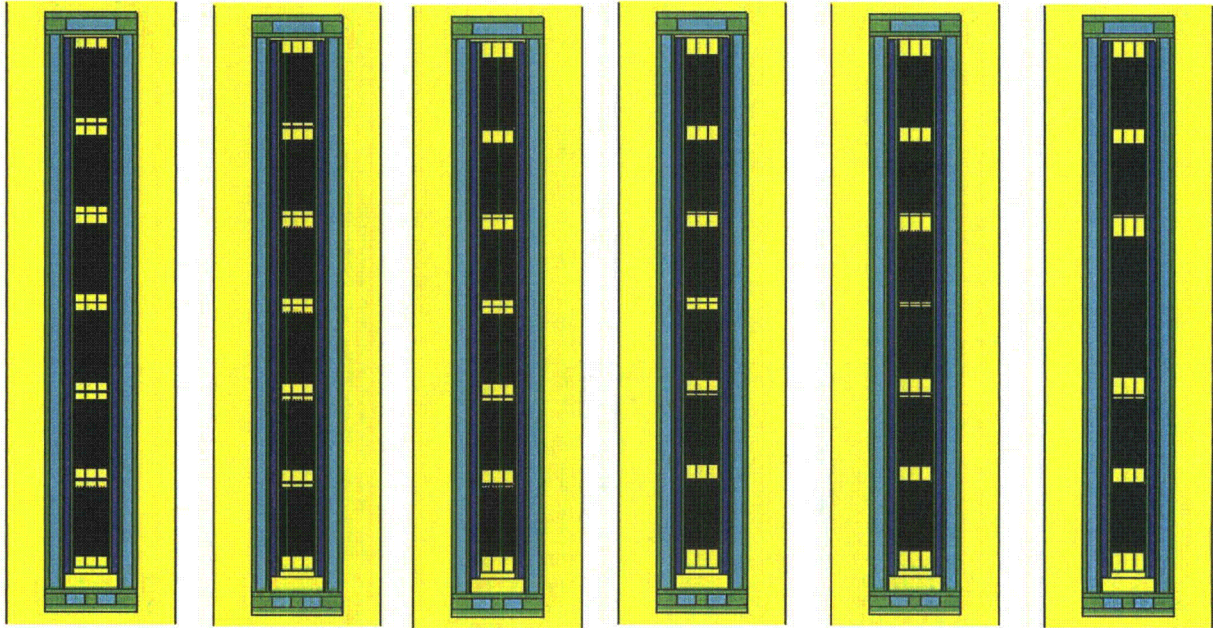


Figure 6.10.1-7
Elements Moved Uniformly Toward Axial Center

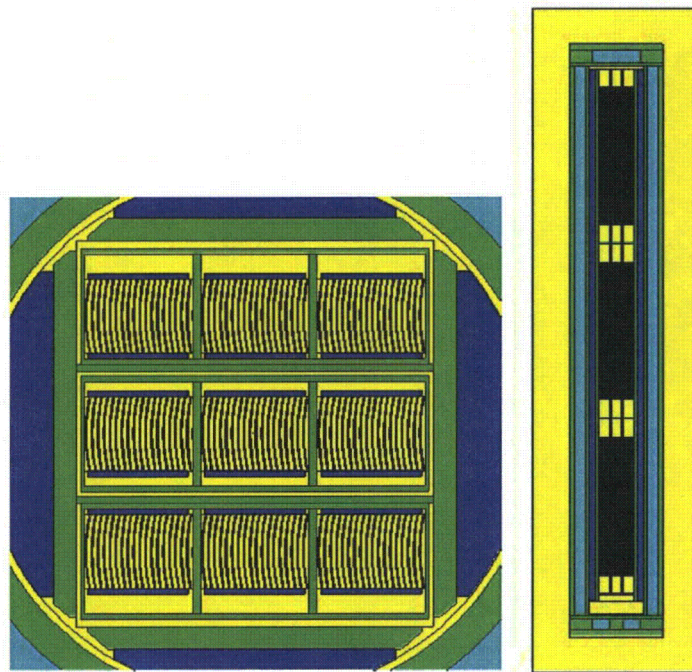


Figure 6.10.1-8
Limiting Fuel Location in the Radial and Axial Plane

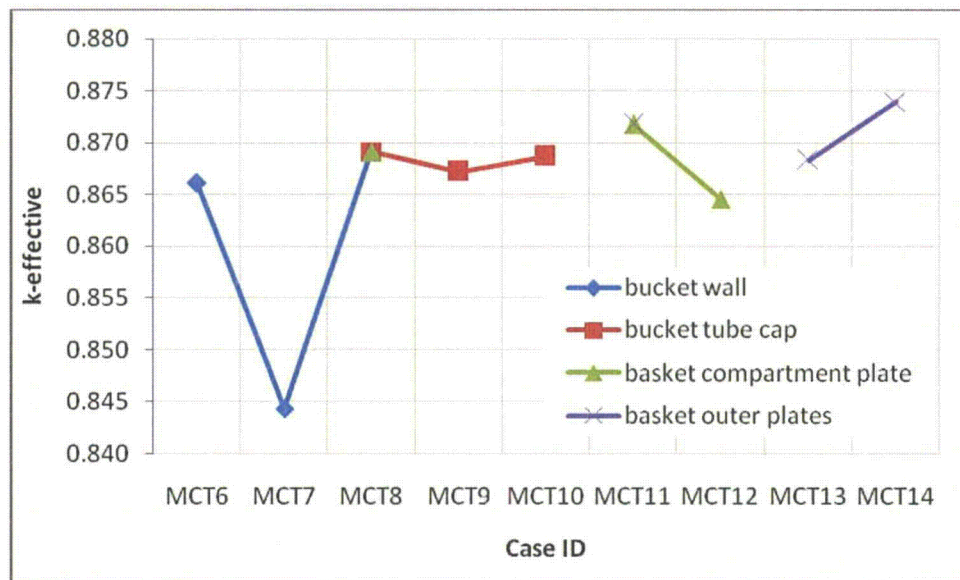


Figure 6.10.1-9
 Summary of TN-LC-MTR Basket Tolerance Results

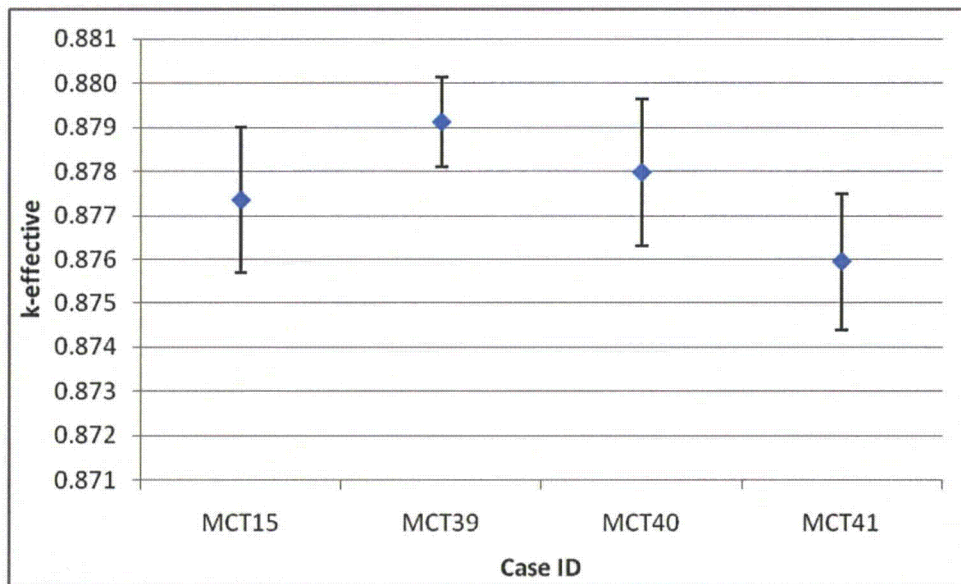


Figure 6.10.1-10
Summary of MTR Uranium Loading in Fuel Results

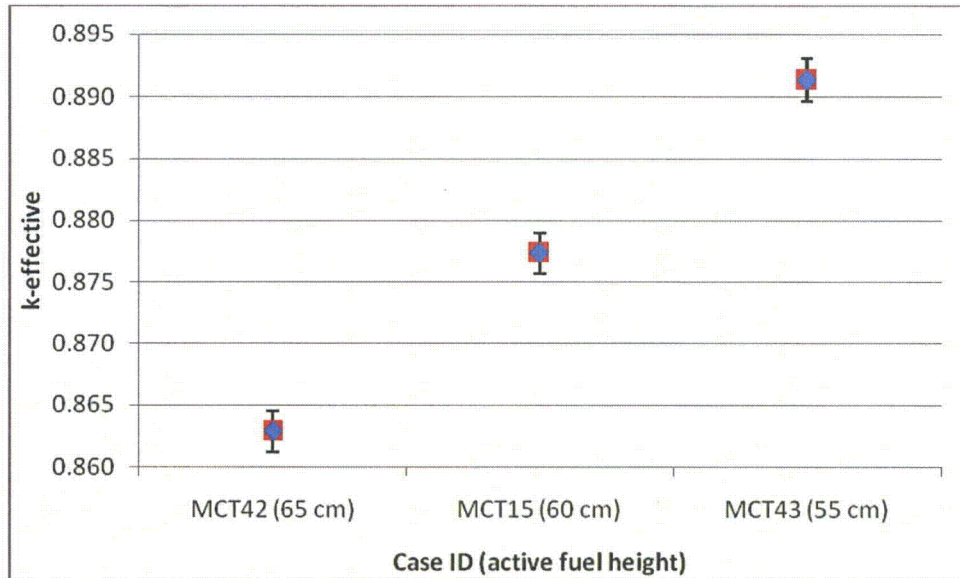


Figure 6.10.1-11
Summary of MTR Active Fuel Height Results

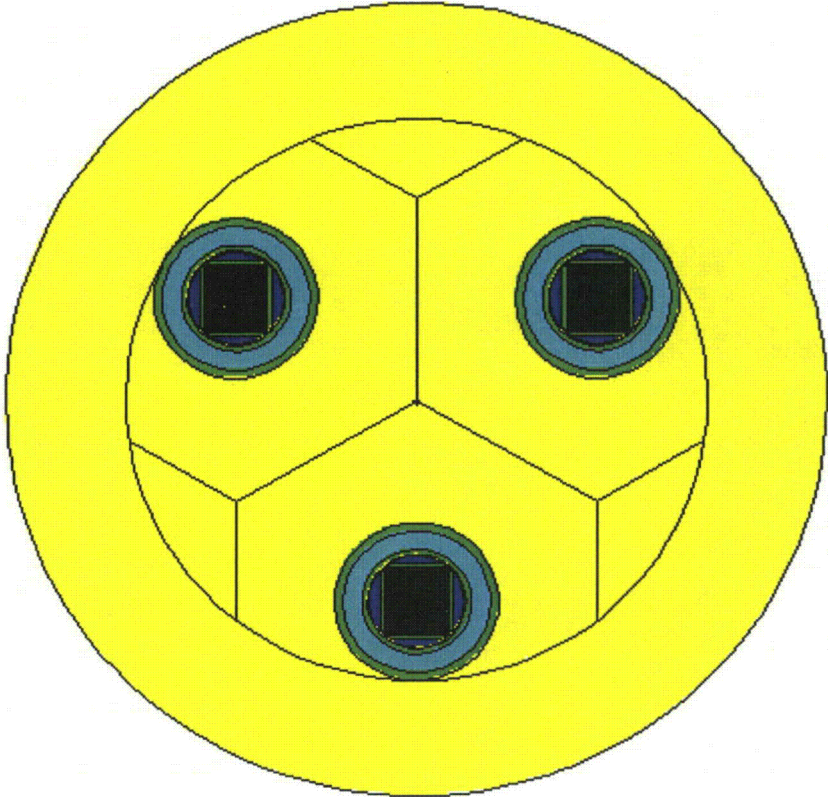


Figure 6.10.1-12
TN-LC-MTR NCT Array Configuration with Flooded Casks

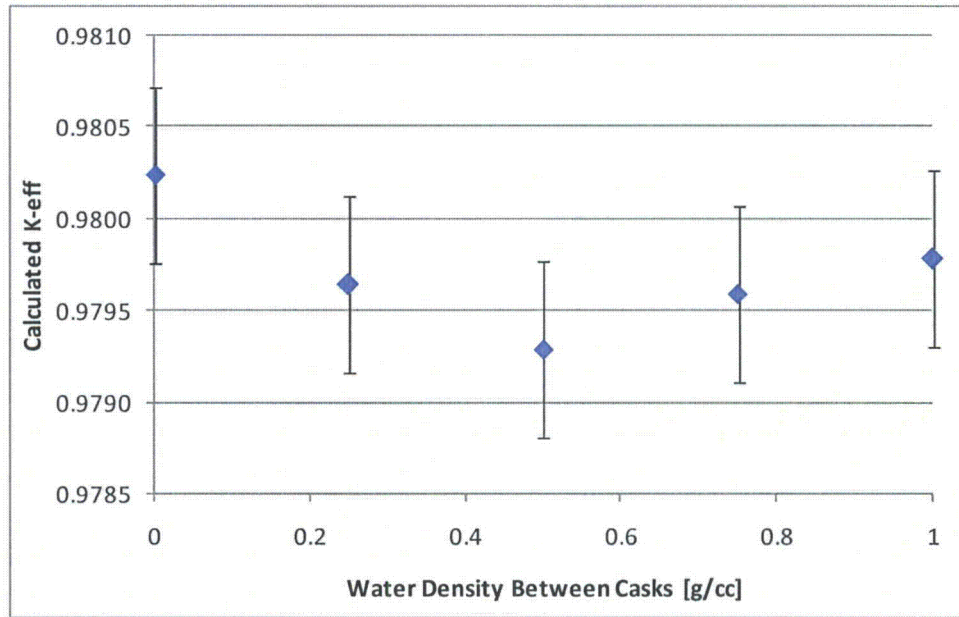


Figure 6.10.1-13
 Reactivity Change with Varying Water Density Between Casks

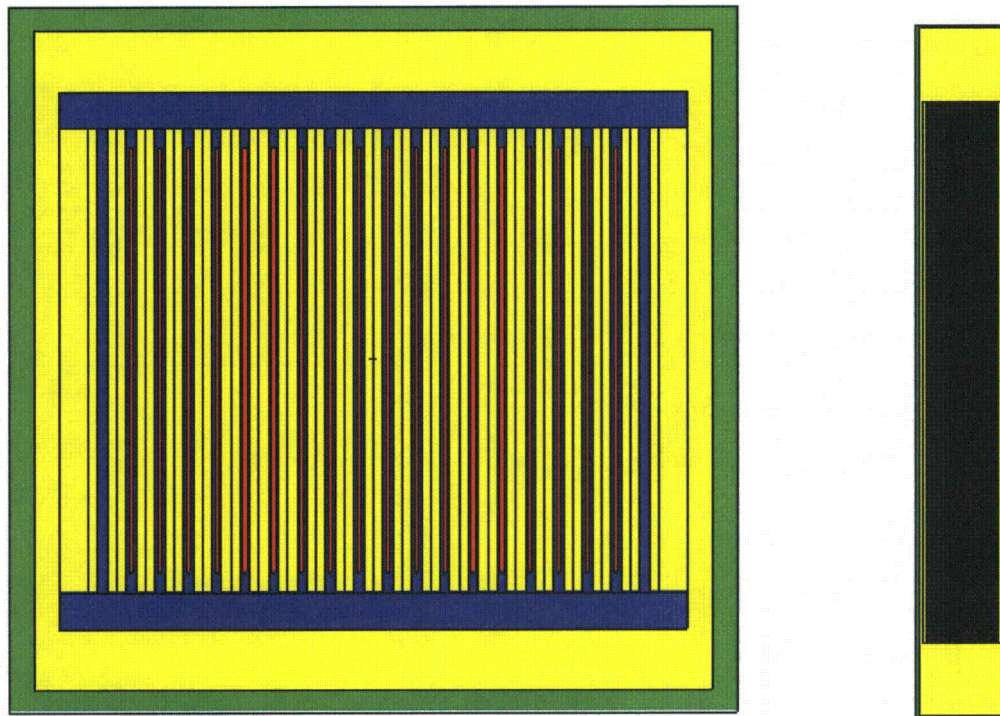


Figure 6.10.1-14
MCNP Model Used to Determine Bounding MTR Assembly

Appendix 6.10.2
TN-LC-NRUX Basket Criticality Evaluation

TABLE OF CONTENTS

6.10.2.1	Description of the Criticality Design	6.10.2-1
6.10.2.1.1	Design Features.....	6.10.2-1
6.10.2.1.2	Summary Table of Criticality Evaluation.....	6.10.2-1
6.10.2.1.3	Criticality Safety Index.....	6.10.2-2
6.10.2.2	Fissile Material Contents	6.10.2-3
6.10.2.3	General Considerations.....	6.10.2-4
6.10.2.3.1	Model Configuration.....	6.10.2-4
6.10.2.3.2	Material properties.....	6.10.2-5
6.10.2.3.3	Computer Codes and Cross-Section Libraries.....	6.10.2-5
6.10.2.3.4	Demonstration of Maximum Reactivity	6.10.2-5
6.10.2.4	Single Package Evaluation.....	6.10.2-7
6.10.2.4.1	Configuration.....	6.10.2-7
6.10.2.4.2	Results.....	6.10.2-8
6.10.2.5	Evaluation of Package Arrays under Normal Conditions of Transport.....	6.10.2-9
6.10.2.5.1	Configuration.....	6.10.2-9
6.10.2.5.2	Results.....	6.10.2-9
6.10.2.6	Package Arrays under Hypothetical Accident Conditions.....	6.10.2-10
6.10.2.7	Fissile Material Packages for Air Transport.....	6.10.2-11
6.10.2.8	Benchmark Evaluations	6.10.2-12
6.10.2.8.1	Applicability of Benchmark Experiments	6.10.2-12
6.10.2.8.2	Bias Determination	6.10.2-13
6.10.2.9	Appendix.....	6.10.2-15
6.10.2.9.1	References.....	6.10.2-15

Proprietary Information Withheld Pursuant to 10 CFR 2.390.

LIST OF TABLES

Table 6.10.2-1	Summary of TN-LC-NRUX Criticality Evaluations	6.10.2-21
Table 6.10.2-2	NRU Fuel Data	6.10.2-21
Table 6.10.2-3	NRX Fuel Data	6.10.2-22
Table 6.10.2-4	Packaging Model Dimensions	6.10.2-22
Table 6.10.2-5	TN-LC-NRUX Basket Nominal Model Dimensions.....	6.10.2-23
Table 6.10.2-6	Composition of Stainless Steel	6.10.2-23
Table 6.10.2-7	Cross-Section Libraries Utilized.....	6.10.2-24
Table 6.10.2-8	TN-LC-NRUX Single Package Results, Preliminary.....	6.10.2-25
Table 6.10.2-9	Single Package Results, Tolerance and Moderation Study	6.10.2-26
Table 6.10.2-10	TN-LC-NRUX NCT Array Results.....	6.10.2-26
Table 6.10.2-11	Benchmark Experiments Utilized.....	6.10.2-27
Table 6.10.2-12	USL Results	6.10.2-27
Table 6.10.2-13	Benchmark Experiment Data.....	6.10.2-28

LIST OF FIGURES

<i>Figure 6.10.2-1 MCNP NRU/NRX Fuel Element Models</i>	<i>6.10.2-30</i>
<i>Figure 6.10.2-2 MCNP TN-LC-NRUX Model, y-z View</i>	<i>6.10.2-31</i>
<i>Figure 6.10.2-3 MCNP TN-LC-NRUX Model, x-y View</i>	<i>6.10.2-32</i>
<i>Figure 6.10.2-4 MCNP TN-LC-NRUX Single Package Model with Tolerances.....</i>	<i>6.10.2-33</i>
<i>Figure 6.10.2-5 MCNP TN-LC-NRUX Array Model.....</i>	<i>6.10.2-34</i>
<i>Figure 6.10.2-6 Partially Filled Cavity.....</i>	<i>6.10.2-35</i>

Appendix 6.10.2 TN-LC-NRUX Basket Criticality Evaluation

NOTE: References in this Appendix are shown as [1], [2], etc. and refer to the reference list in Appendix 6.10.2.9.1.

The Appendix presents the criticality evaluation of the TN-LC-NRUX basket with a payload of either 26 NRU or NRX fuel assemblies. The following analyses demonstrate that the TN-LC package complies with the requirements of 10CFR71.55 and 71.59. The Criticality Safety Index (CSI), per 10CFR71.59, is 100.

6.10.2.1 Description of the Criticality Design

6.10.2.1.1 Design Features

Criticality control is provided primarily by the TN-LC-NRUX basket. The basket consists of two bundles of 13 tubes. **Proprietary Information Withheld Pursuant to 10 CFR 2.390.** No neutron poisons are required for criticality safety.

6.10.2.1.2 Summary Table of Criticality Evaluation

The upper subcritical limit (USL) for ensuring that the package is acceptably subcritical as determined in Section 6.10.2.8 is:

$$\text{USL} = 0.9227$$

The package is considered to be acceptably subcritical if the computed k_{safe} (k_s), which is defined as $k_{\text{effective}}$ (k_{eff}) plus twice the statistical uncertainty (σ), is less than or equal to the USL, or:

$$k_s = k_{\text{eff}} + 2\sigma \leq \text{USL}$$

The USL is determined on the basis of a benchmark analysis and incorporates the combined effects of code computational bias, the uncertainty in the bias based on both benchmark-model and computational uncertainties, and an administrative margin. The results of the benchmark analysis indicate that the USL is adequate to ensure subcriticality of the package.

The packaging design is shown to meet the requirements of 10CFR71.55(b). No credit is taken for fuel element burnup in any models. In both the normal conditions of transport (NCT) and hypothetical accident condition (HAC) models, water is conservatively modeled in all cavities at the most reactive density. Maximum allowable fuel element pitch expansion is modeled to simulate postulated fuel damage in both the NCT and HAC models. In all single package models, 12 in. of water reflection is utilized.

In the NCT array models, a close-packed array of three packages is utilized. The entire array is reflected with 12 in. of water. No HAC array models are developed. Therefore, the HAC array result is the same as the single package result.

The maximum results of the criticality calculations are summarized in Table 6.10.2-1. The maximum calculated k_s is 0.874 which occurs for the NCT array. The maximum reactivity is below the USL of 0.9227.

6.10.2.1.3 Criticality Safety Index

No HAC array models are developed ($2N=1$). Therefore, per 10CFR71.59, $N=0.5$, and the criticality safety index (CSI) is $50/N = 100$. In the NCT array cases, $5N=2.5$, so that 3 packages are modeled.

6.10.2.2 Fissile Material Contents

The fissile material contents consist of either 26 NRU or NRX fuel elements.

NRU fuel data used as input to MCNP is summarized in Table 6.10.2-2.

Proprietary Information Withheld Pursuant to 10 CFR 2.390.

The NRU fuel matrix is a mixture of aluminum and high-enriched uranium. All cladding and structural materials are fabricated from aluminum. NRU fuel elements may exist with up to 545 g U-235. Therefore, the 545 g U-235 per element is used in the models. An enrichment of 94 weight percent is utilized in the models, which bounds the actual enrichment of 93 weight percent. Figure 6.10.2-1 shows the MCNP NRU element geometry inside a basket tube.

NRX fuel data used as input to MCNP is summarized in Table 6.10.2-3.

Proprietary Information Withheld Pursuant to 10 CFR 2.390.

The NRX fuel matrix is a mixture of aluminum and high-enriched uranium. All cladding and structural materials are fabricated from aluminum. The uranium mass per rod is 75 ± 3.1 g which is bounded by modeling 80 g of uranium per rod (526.4 g U-235 per element). An enrichment of 94 weight percent is utilized in the models which bounds the actual enrichment of 93 weight percent. Figure 6.10.2-1 shows the MCNP NRX element geometry inside a basket tube.

6.10.2.3 General Considerations

6.10.2.3.1 Model Configuration

The fuel, basket, and packaging are modeled explicitly in the MCNP computer program [1]. The packaging is conservatively modeled without the neutron shield and impact limiters in both the NCT and HAC models. The key nominal dimensions are provided in Table 6.10.2-4 for the cask and Table 6.10.2-5 for the TN-LC-NRUX basket. The TN-LC cask and TN-LC-NRUX basket dimensions are obtained from the drawings in Chapter 1. The overall model geometry is illustrated in Figure 6.10.2-2. A view showing the basket is illustrated in Figure 6.10.2-3.

The cask body is modeled with nominal dimensions because the tolerances on the cask body dimensions would have little effect on the system reactivity. However, key basket dimensions are modeled considering tolerances in order to maximize the reactivity. The tolerance study is described in more detail in Section 6.10.2.4.

Several items are neglected for simplicity, including the tube cap, lid spacer plate, and lid spacer blocks. The bottom of the basket, as well as the bottom spacer, are also neglected. These items have little effect on the reactivity. Because the bottom spacer and basket bottom are not modeled, the active fuel length may contact the bottom of the cask in the models which maximizes neutron reflection from the bottom end of the cask.

Only the active fuel regions of the NRU or NRX elements are modeled, and it is assumed that any flow tubes are removed. The NRU and NRX fuel element dimensions are given in Table 6.10.2-2 and Table 6.10.2-3, respectively. The majority of the models are for NRU fuel only because it is demonstrated that NRU fuel is more reactive than NRX fuel.

In both the NCT and HAC models, water is modeled inside the package at the density that maximizes reactivity. *In the fully-flooded models*, water is always modeled at the same density in all basket regions of the model. Above the basket but inside the cavity, water is modeled at full density to maximize neutron reflection. All single package models are reflected with 12 in. of water.

Because the cask is designed for wet loading, water drains freely inside the basket, and *preferential flooding scenarios are not credible. However, the cavity could be partially flooded. Because the baskets drain freely, if the TN-LC cavity is partially flooded, the only credible scenario is that some fuel would be submerged in water, and the remaining fuel would remain unsubmerged. Therefore, any partial flooding scenarios would result in less moderation for the fuel. It is demonstrated that NRU/NRX fuels have very low reactivity in the absence of moderation. Therefore, any partial flooding would uncover fuel and decrease the reactivity. The effect of partial flooding is demonstrated explicitly.*

Under HAC, it is assumed that the fuel, which is loaded as undamaged, may become damaged. The fuel would not be damaged under NCT, but, to be conservative and simplify the modeling, fuel damage is also modeled under NCT. For modeling purposes, it is assumed that the fuel rod pitch may either contract until the rods touch or expand in a uniform manner until constrained by the basket tubes. Applying this penalizing damage assumption to every fuel element bounds all credible accident damage scenarios. Both minimum and maximum pitch HAC models are illustrated in Figure 6.10.2-3.

For the NCT array, an array of 3 packages is modeled to justify a CSI = 100. Water of variable density is placed between the packages. No HAC array cases are developed.

6.10.2.3.2 Material properties

The fuel pellet number densities for NRU and NRX fuel are provided in Table 6.10.2-2 and Table 6.10.2-3, respectively. NRU and NRX fuel have aluminum cladding which is modeled as pure.

Cask lead is modeled as pure with a density of 11.35 g/cm³.

The stainless steel composition is provided in Table 6.10.2-6. Although MCNP is used in the criticality analysis, the steel composition is the standard composition used for criticality analysis in SCALE6 [2]. Steel is used in the cask body as well as the basket. The XM-19 stainless steel that comprises the inner shell, outer shell, and top and bottom forgings is modeled as 304 stainless steel for simplicity.

6.10.2.3.3 Computer Codes and Cross-Section Libraries

MCNP5 v1.40 is used for the criticality analysis [1]. All cross-sections utilized are at room temperature (293 K). The uranium isotopes utilize preliminary ENDF/B-VII cross-section data that are considered by Los Alamos National Laboratory to be more accurate than ENDF/B-VI cross-sections. ENDF/B-V cross-sections are utilized for chromium, nickel, iron, and lead because natural composition ENDF/B-VI cross-sections are not available for these elements. The remaining isotopes utilize ENDF/B-VI cross-sections. Titles of the cross-sections utilized in the models have been extracted from the MCNP output (when available) and provided in Table 6.10.2-7. The S(α,β) card LWTR.60T is used to simulate hydrogen bound to water in all models.

Single package cases are run with 2500 neutrons per generation for 250 generations, skipping the first 50. NCT array cases are run with 5000 neutrons per generation for 250 generations, skipping the first 50. The 1-sigma uncertainty is approximately 0.001 for the single package cases and somewhat less for the NCT array cases.

6.10.2.3.4 Demonstration of Maximum Reactivity

No credit is taken for fuel element burnup. NRU and NRX fuel are modeled with U-235 fuel loadings and enrichment (94 weight percent) that bound the known values for these fuel types. A comparison is made between NRU and NRX fuel allowing pitch contraction and expansion until constrained by the basket tubes. The pitch variation simulates damage to a fuel element under HAC, although this degree of damage is not expected during HAC. Increasing the pitch increases the reactivity because the system is undermoderated at the nominal pitch. For both NRU and NRX fuel, the reactivity increases as the pitch increases. NRU fuel is more reactive than NRX fuel; thus, additional calculations are performed only for NRU fuel.

Using the NRU fuel, a tolerance study is performed on the basket material thicknesses. It is demonstrated that the reactivity increases if the tube wall thickness is reduced as the steel tube wall is acting as a poison. The reactivity also increases if the thickness of the steel plate between the basket tube assemblies is reduced and the baskets are moved to the closest proximity of each other. The reactivity also increases slightly if the tube wrap thickness is minimized between the bundles as this reduces the distance between the bundles. Reactivity increases slightly if the remaining tube wrap is modeled at the maximum thickness as the tube wrap in this location is acting as a

reflector. Beyond the tube wrap, the results are insensitive to small perturbations in the basket dimensions. Axial shifting of the fuel has little effect on the results, although the system reactivity is maximized with the active fuel touching the bottom end of the cask. A variable water density study within the basket indicates that reactivity is maximized with full-density water.

The NCT array uses the same cask and fuel geometry as the single package case, except with an array of 3 packages. The reactivity increases in the array configuration compared to the single package configuration, but only slightly.

Therefore, reactivity is maximized using NRU fuel with a high fissile loading in a flooded cask with maximum pitch expansion and basket tolerances chosen to maximize the reactivity. NCT array Case NC1 is the most reactive with $k_s = 0.874$.

6.10.2.4 Single Package Evaluation

6.10.2.4.1 Configuration

The geometry of the single package model is described in Section 6.10.2.3.1. Both the NCT and HAC single package cases use the same geometry and moderator assumptions. Initial calculations are performed for both NRU and NRX fuel. The basket is modeled with nominal dimensions with the bottom of the active fuel touching the bottom of the cavity. Cases are generated with a reduced pitch, until the fuel rods contact, and increased pitch, up to the maximum allowed by the basket tubes, see Figure 6.10.2-3. This pitch variation bounds all credible fuel damage during HAC.

The results are provided in Table 6.10.2-8. Cases NA1 through NA5 are for NRU fuel, and Cases NA10 through NA18 are for NRX fuel. For both fuel types, the reactivity increases as the pitch increases. Case NA5 for NRU fuel is the most reactive, with $k_s = 0.83965$. This case has the maximum NRU pitch. The NRX cases are less reactive than the NRU cases. Therefore, the remaining cases in this analysis are for NRU fuel only.

In Cases NB1 through NB8, the effects of basket tolerances are examined. The results are presented in Table 6.10.2-9. In Case NB1, the wall thickness of the tubes is reduced by increasing the inner diameter. Per ASTM A 312, Table 3, the permitted under tolerance for wall thickness is 12.5 percent [3]. Therefore, the tube thickness is reduced by this amount, and the fuel rod pitch is increased slightly to 1.65 cm to fill the additional space. Reactivity increases by ~17 mk (milli-k) compared to the parent case (Case NA5) due to the decreased parasitic absorption in the steel.

In Cases NB2 and NB3, Case NB1 is used as the parent case, and the 0.5-in. thick center member is modeled at the minimum (Case NB2) and maximum (Case NB3) tolerance. Per ASTM A 480, Table A2.13 for coil processed product, the tolerance is ± 0.02 in. while, for Table A2.17 for mill plate, the tolerance is $-0.01/+0.09$ in. [4]. Therefore, combining the worst possible tolerances, Case NB2 uses a tolerance of -0.02 in. while Case NB3 uses a tolerance of $+0.09$ in. In addition, the tube basket assemblies are moved toward the center to minimize the distance between the tube baskets. Reactivity increases for both cases compared to the parent case due to shifting of the baskets, although the increase (~11 mk) is larger for Case NB2.

In Cases NB4 and NB5, Case NB2 is used as the parent case, and the 0.25-in. thick tube wrap is modeled at the minimum (Case NB4) and maximum (Case NB5) tolerance. Per ASTM A 480, Table A2.13 for coil processed product, the tolerance is ± 0.015 in. while, for Table A2.17 for mill plate, the tolerance is $-0.01/+0.085$ in. [4]. Therefore, combining the worst possible tolerances, Case NB4 uses a tolerance of -0.015 in. while Case NB5 uses a tolerance of $+0.085$ in. In addition, the tube basket assemblies are moved toward the center to minimize the distance between the tube baskets. Because it is known from Cases NB2 and NB3 that moving the baskets closer increases the reactivity, the tube wrap that contacts the center member is modeled at the minimum thickness in Case NB5, and the remaining five sides are modeled at the maximum thickness. The reactivity changes little for either case. Case NB5 is slightly more reactive than the parent case, although the difference is within the statistical variation of the calculation.

In Case NB6, Case NB5 is used as the parent case, and the 0.25-in. side guide plates (guide plate A) are modeled only at the maximum thickness of $0.25+0.085 = 0.335$ in. since the results from Case NB5 imply that the reactivity may increase slightly due to increased reflection from the steel surrounding the basket tube assemblies. The reactivity increases by ~ 3 mk for this case compared to the parent case. Because this is the most reactive case, Figure 6.10.2-4 shows the model geometry for Case NB6. The input file for this case is also included in Section 6.10.2.9.2.

In Case NB7, Case NB6 is used as the parent case, and the 0.375-in. side guide plates are modeled at the maximum thickness per ASTM A 480 of $0.375+0.09 = 0.465$ to increase reflection. However, reactivity decreases by 1 mk, indicating the change is within the statistical variation of the calculation. Because the tolerance changes have little effect with increasing distance from the fuel, additional tolerance studies on the basket shell and cask are not performed.

In Case NB8, Case NB6 is used as the parent case, and the active fuel is shifted up 30 cm so that a layer of water exists between the bottom of the active fuel and the end of the cask. The reactivity change is within the uncertainty of the calculation.

In Cases NB20 through NB23, Case NB6 is used as the parent case, and it is assumed that the cavity is partially flooded so that the lower half of the active fuel is moderated with full-density water, while the voids above this height is filled with water of density 0, 0.25, 0.5, and 0.75 g/cm³. The geometry is shown in Figure 6.10.2-6. As expected, uncovering the fuel is less reactive than the fully flooded condition.

In Cases NB9 through NB12, Case NB6 is used as the parent case, and the density of water inside the basket region is reduced. The water density above the basket region is conservatively set at 1.0 g/cm³ to maximize reflection. Reactivity drops quickly with reduced water density, indicating that the system is most reactive with full-water moderation.

Therefore, Case NB6 is the most reactive, with $k_s = 0.87191$. This result is less than the USL of 0.9227.

6.10.2.4.2 Results

The single package results are summarized in Table 6.10.2-8 and Table 6.10.2-9. The most reactive configurations are listed in boldface.

6.10.2.5 Evaluation of Package Arrays under Normal Conditions of Transport

6.10.2.5.1 Configuration

For the package array under NCT, an array of three packages is modeled. The packages are modeled in a triangular array and reflected with 12 in. of water. No credit is taken for the separation provided by the impact limiters, although credit could be taken for this distance, if desired, because the impact limiters are attached during NCT. The NCT array model is shown in Figure 6.10.2-5.

The most reactive single package case is used as the basis for the NCT array model. Therefore, the package is flooded, and the basket tolerances are modeled at the most reactive values. Although there is no fuel damage under NCT, the fuel damage assumption from the single package models (i.e., maximum pitch expansion) is also conservatively employed.

Results are presented in Table 6.10.2-10. In Cases NC1 through NC5, the water density between the packages is varied while the water density inside the packages is 1.0 g/cm^3 . The reactivity of these cases is nearly identical, indicating that interaction between packages is small. Case NC1, with void between packages, has the highest k_s value. In Cases NC6 and NC7, void is modeled between packages while the water density inside the package is reduced. The reactivity quickly drops as water is removed from the package cavity.

Case NC1 is the most reactive, with $k_s = 0.87400$. This value is below the USL of 0.9227

6.10.2.5.2 Results

The NCT array results are summarized in Table 6.10.2-10. The most reactive configuration is listed in boldface.

6.10.2.6 Package Arrays under Hypothetical Accident Conditions

Because the CSI = 100, no HAC array cases are performed.

6.10.2.7 Fissile Material Packages for Air Transport

This section does not apply.

6.10.2.8 Benchmark Evaluations

The Monte Carlo computer program MCNP5 v1.40 is utilized for this benchmark analysis [1]. MCNP has been used extensively in criticality evaluations for several decades and is considered a standard in the industry.

A listing of the cross-section libraries used in the analysis is provided in Table 6.10.2-7. These cross-sections are consistent with the cross-sections utilized in the benchmarks.

The ORNL USLSTATS computer program [5] is used to establish a USL for the analysis. USLSTATS provides a simple means of evaluating and combining the statistical error of the calculation, code biases, and benchmark uncertainties. The USLSTATS calculation uses the combined uncertainties and data to provide a linear trend and an overall uncertainty. Computed multiplication factors, k_{eff} , for the package are deemed to be adequately subcritical if the computed value of k_s is less than or equal to the USL as follows:

$$k_s = k_{\text{eff}} + 2\sigma \leq \text{USL}$$

The USL is determined on the basis of a benchmark analysis and incorporates the combined effects of code computational bias, the uncertainty in the bias based on both benchmark-model and computational uncertainties, and an administrative margin. This methodology has accepted precedence in establishing criticality safety limits for transportation packages complying with 10CFR71.

6.10.2.8.1 Applicability of Benchmark Experiments

The critical experiment benchmarks are selected from the “International Handbook of Evaluated Criticality Safety Benchmark Experiments” [6] based upon their similarity to the TN-LC packaging and contents. The important selection parameters are high-enriched uranium fuel with a uranium aluminide fuel matrix, aluminum cladding, and a thermal spectrum. Sixty-four (64) benchmarks that meet some or all of these criteria are selected from the Handbook. The titles for all utilized experiments are listed in Table 6.10.2-11.

Ideally, benchmarks would be limited to those with a fuel matrix of UAl_x and aluminum, aluminum cladding, and no absorbers, consistent with the NRU and NRX criticality models. However, NRU and NRX fuels are unique, so identical benchmarks are not available. Experiment set HEU-MET-THERM-006 consists of 23 benchmark experiments. The first 16 experiments are similar to NRU and NRX fuel (except for the shape of the fuel plates, which are flat), although experiments 17 and 18 utilize thin cadmium sheets, and experiments 19 through 23 utilize uranium in solution in addition to the fuel plates. Experiment set HEU-COMP-THERM-022 consists of 11 benchmark experiments using flat plates that utilize UO_2 powder sintered with stainless steel, and stainless steel cladding. Experiments 1 through 5 do not utilize control rods, while experiments 6 through 11 utilize boron control rods. HEU-MET-THERM-022 is a detailed model of the Advance Test Reactor core and therefore utilizes flat plates and absorber materials. Experiment set HEU-COMP-THERM-021 consists of 29 experiments with high-enriched uranium and thorium oxide in cylindrical fuel elements, aluminum cladding, without absorbers.

Trending is performed separately on the flat plate and cylindrical fuel element benchmarks, in addition to a combined set of all benchmark experiments. The USL selected is the minimum of all experimental sets.

6.10.2.8.2 Bias Determination

The USL is calculated by application of the USLSTATS computer program [5]. USLSTATS receives as input the k_{eff} as calculated by MCNP, the total 1- σ uncertainty (combined benchmark and MCNP uncertainties), and a trending parameter. Three trending parameters have been selected: (1) Energy of the Average neutron Lethargy causing Fission (EALF), (2) ratio of the number of hydrogen atoms in a unit cell to the number of U-235 atoms in a unit cell (H/U-235), and (3) moderator to fuel ratio (V_M/V_F).

The uncertainty value, σ_{total} , assigned to each case is a combination of the benchmark uncertainty for each experiment, σ_{bench} , and the Monte Carlo uncertainty associated with the particular computational evaluation of the case, σ_{MCNP} , or:

$$\sigma_{\text{total}} = (\sigma_{\text{bench}}^2 + \sigma_{\text{MCNP}}^2)^{1/2}$$

These values are input into the USLSTATS program in addition to the following parameters, which are the values recommended by the USLSTATS user's manual [5]:

- P, proportion of population falling above lower tolerance level = 0.995 (note that this parameter is required input but is not utilized in the calculation of USL Method 1)
- $1-\gamma$, confidence on fit = 0.95
- α , confidence on proportion P = 0.95 (note that this parameter is required input but is not utilized in the calculation of USL Method 1)
- Δk_m , administrative margin used to ensure subcriticality = 0.05.

These data are followed by triplets of trending parameter value, computed k_{eff} , and uncertainty for each case. A confidence band analysis is performed on the data for each trending parameter using USL Method 1. The USL generated for each of the trending parameters utilized is provided in Table 6.10.2-12. Trending is performed over the entire benchmark set, the subset of plate fuel benchmarks, and the subset of fuel rod benchmarks. All benchmark data used as input to USLSTATS are reported in Table 6.10.2-13.

Energy of the Average neutron Lethargy causing Fission (EALF)

The EALF is used as the first trending parameter. The EALF comparison provides a means to observe neutron spectral dependencies or trends. Over the range of applicability, the minimum USL is 0.9255 for the three benchmark sets.

The EALF of the fully-flooded models are within the range of acceptability, and the EALF of the most reactive case (Case NC1) is 6.89E-08 MeV.

H/U-235 Atom Ratio

The H/U-235 atom ratio is used as the second trending parameter. The H/U-235 atom ratio is defined here as the ratio of hydrogen atoms to U-235 atoms in a unit cell and is an indication of the degree of moderation of the system. This parameter is computed by the following equation:

$$NH*V_M/(NU235*V_F)$$

Where:

NH is the hydrogen number density in a unit cell

V_M is the fuel volume in a unit cell

NU235 is the U-235 number density in a unit cell

V_F is the fuel meat volume in a unit cell

Over the range of applicability, the minimum USL is 0.9259 for the three benchmark sets.

For the most reactive models, this parameter is within the range of applicability, and the H/U-235 atom ratio for the most reactive case (Case NC1) is 311.

Moderator to Fuel Ratio (V_M/V_F)

The moderator to fuel ratio (V_M/V_F) is used as the third trending parameter. Over the range of applicability, the minimum USL is 0.9227 for the three benchmark sets. This parameter is out of the range of applicability for the most reactive models. The most reactive models have a V_M/V_F = 8.3 while the maximum range of applicability is 5.8. However, the USL for this parameter is trending upward with increasing V_M/V_F so that it is conservative to use a USL based on smaller values of this parameter. Also, this parameter is similar to the H/U-235 parameter, which is within the range of applicability for the most reactive models. Therefore, this parameter is considered to be acceptable.

Recommended USL

The minimum USL for the three parameters and three different groupings of benchmarks is 0.9227. This USL occurs for the flat plate benchmarks as the fuel rod benchmarks result in a higher USL. The lowest USL of 0.9227 is conservatively selected for this analysis.

6.10.2.9 Appendix

6.10.2.9.1 References

1. MCNP5, "MCNP – A General Monte Carlo N-Particle Transport Code, Version 5; Volume II: User's Guide," LA-CP-03-0245, Los Alamos National Laboratory, April 2003.
2. SCALE: A Modular Code System for Performing Standardized Computer Analyses for Licensing Evaluations, ORNL/TM-2005/39, Version 6, Vols. I-III, January 2009.
3. ASTM A 312/A 312M – 03c, Standard Specification for Seamless and Welded Austenitic Stainless Steel Pipes.
4. ASTM A 480/A 480M – 03c, Standard Specification for General Requirements for Flat-Rolled Stainless and Heat-Resisting Plate, Sheet, and Strip.
5. USLSTATS, "USLSTATS: A Utility To Calculate Upper Subcritical Limits For Criticality Safety Applications," Version 1.4.2, Oak Ridge National Laboratory, April 23, 2003. Note: USLSTATS is described in Appendix C, User's Manual for USLSTATS V1.0, in NUREG/CR-6361 Criticality Benchmark Guide for Light-Water-Reactor Fuel in Transportation and Storage Packages, March 1997.
6. International Handbook of Evaluated Criticality Safety Benchmark Experiments, Nuclear Energy Agency, NEA/NSC/DOC(95)03, September 2009.

**Proprietary Information on Pages 6.10.2-16 through 6.10.2-20
Withheld Pursuant to 10 CFR 2.390.**

Table 6.10.2-1
Summary of TN-LC-NRUX Criticality Evaluations

Normal Conditions of Transport (NCT)	
Case	k_s
Single Unit Maximum	0.872
Array Maximum (3 packages)	0.874
Hypothetical Accident Conditions (HAC)	
Case	k_s
Single Unit Maximum	0.872
Array Maximum (1 package)	0.872
USL = 0.9227	

Table 6.10.2-2
NRU Fuel Data

Proprietary Information Withheld Pursuant to 10 CFR 2.390.

Table 6.10.2-3
NRX Fuel Data

Proprietary Information Withheld Pursuant to 10 CFR 2.390.

Table 6.10.2-4
Packaging Model Dimensions

Proprietary Information Withheld Pursuant to 10 CFR 2.390.

Table 6.10.2-5
TN-LC-NRUX Basket Nominal Model Dimensions

Proprietary Information Withheld Pursuant to 10 CFR 2.390.

Table 6.10.2-6
Composition of Stainless Steel

Component	Wt.%
C	0.08
Si	1.0
P	0.045
Cr	19.0
Mn	2.0
Fe	68.375
Ni	9.5
Density = 7.94 g/cm ³	

Table 6.10.2-7
Cross-Section Libraries Utilized

Isotope/Element	Cross-Section Label (from MCNP output)
1001.62c	1-h-1 at 293.6K from endf-vi.8 njoy99.50
6000.66c	6-c-0 at 293.6K from endf-vi.6 njoy99.50
8016.62c	8-o-16 at 293.6K from endf-vi.8 njoy99.50
13027.62c	13-al-27 at 293.6K from endf-vi.8 njoy99.50
14000.60c	14-si-nat from endf/b-vi
15031.66c	15-p-31 at 293.6K from endf-vi.6 njoy99.50
24000.50c	njoy
25055.62c	25-mn-55 at 293.6K from endf/b-vi.8 njoy99.50
26000.55c	njoy
28000.50c	njoy
82000.50c	njoy
92235.69c	92-u-235 at 293.6K from t16 u235la9d njoy99.50
92238.69c	92-u-238 at 293.6K from t16 u238la8h njoy99.50

Table 6.10.2-8
 TN-LC-NRUX Single Package Results, Preliminary

Proprietary Information Withheld Pursuant to
 10 CFR 2.390.

Pitch (cm)	k_{eff}	σ	k_s ($k_{eff}+2\sigma$)
0.702	0.64421	0.00106	0.64633
1.012	0.75486	0.00100	0.75686
1.323	0.81884	0.00111	0.82106
1.480	0.83528	0.00108	0.83744
1.630	0.83769	0.00098	0.83965
NRX			
0.864	0.61138	0.00109	0.61356
1.039	0.66052	0.00113	0.66278
1.213	0.70162	0.00104	0.70370
1.400	0.73718	0.00119	0.73956
1.600	0.77036	0.00107	0.77250
1.800	0.79185	0.00108	0.79401
2.000	0.80657	0.00103	0.80863
2.200	0.81172	0.00099	0.81370
2.400	0.80899	0.00102	0.81103

Table 6.10.2-9
Single Package Results, Tolerance and Moderation Study

Proprietary Information Withheld Pursuant to 10 CFR 2.390.

Pitch (cm)	Water Density (g/cm ³)	k _{eff}	σ	k _s (k _{eff} +2σ)
1.650	1.0	0.85441	0.00094	0.85629
1.650	1.0	0.86509	0.00114	0.86737
1.650	1.0	0.86276	0.00099	0.86474
1.650	1.0	0.86305	0.00091	0.86487
1.650	1.0	0.86626	0.00109	0.86844
1.650	1.0	0.86991	0.00100	0.87191
1.650	1.0	0.86841	0.00103	0.87047
1.650	1.0	0.86971	0.00097	0.87165
1.650	0.25	0.49884	0.00089	0.50062
1.650	0.5	0.69583	0.00108	0.69799
1.650	0.75	0.80678	0.00109	0.80896
1.650	0.9	0.85075	0.00106	0.85287
<i>Cavity Half-filled with Water</i>				
Pitch (cm)	Water Density (g/cm ³)	k _{eff}	σ	k _s (k _{eff} +2σ)
1.650	0	0.86199	0.00094	0.86387
1.650	0.25	0.86151	0.00108	0.86367
1.650	0.5	0.86071	0.00108	0.86287
1.650	0.75	0.86154	0.00107	0.86368

Table 6.10.2-10
TN-LC-NRUX NCT Array Results

Proprietary Information Withheld Pursuant to 10 CFR 2.390.

Water Density Between Packages (g/cm ³)	Water Density Inside Packages (g/cm ³)	k _{eff}	σ	k _s (k _{eff} +2σ)
0	1.0	0.87264	0.00068	0.87400
0.25	1.0	0.87194	0.00067	0.87328
0.5	1.0	0.87137	0.00075	0.87287
0.75	1.0	0.87157	0.00075	0.87307
1.0	1.0	0.87250	0.00071	0.87392
0	0.75	0.81432	0.00071	0.81574
0	0.9	0.85424	0.00072	0.85568

Table 6.10.2-11
Benchmark Experiments Utilized

Series	Title
HEU-COMP-THERM-022	SPERT III Stainless-Steel-Clad Plate-Type Fuel in Water
HEU-MET-THERM-006	SPERT-D Aluminum-Clad Plate-Type Fuel in Water, Dilute Uranyl Nitrate, or Borated Uranyl Nitrate
HEU-MET-THERM-022	Advanced Test Reactor: Serpentine Arrangement of Highly Enriched Water-Moderated Uranium-Aluminide Fuel Plates Reflected by Beryllium
HEU-COMP-THERM-021	Water Reflected and Moderated Uniform Lattice Cores of Aluminum Clad Uranium Oxide and Thorium Oxide With and Without Boron Poison

Table 6.10.2-12
USL Results

Trending Parameter (X)	Filename	Minimum USL Over Range of Applicability	Range of Applicability
All Benchmarks Proprietary Information Withheld Pursuant to 10 CFR 2.390.			
EALF (MeV)	Proprietary Information Withheld Pursuant to 10 CFR 2.390.	0.9256	$5.22220E-08 \leq X \leq 2.89770E-07$
H/U-235		0.9281	$65.052 \leq X \leq 531.02$
V_M/V_F		0.9256	$1.3790 \leq X \leq 5.7950$
Flat Plate Benchmarks Proprietary Information Withheld Pursuant to 10 CFR 2.390.			
EALF (MeV)	Proprietary Information Withheld Pursuant to 10 CFR 2.390.	0.9255	$5.22220E-08 \leq X \leq 1.58530E-07$
H/U-235		0.9259	$65.052 \leq X \leq 116.53$
V_M/V_F		0.9227	$3.2290 \leq X \leq 3.9000$
Fuel Rod Benchmarks Proprietary Information Withheld Pursuant to 10 CFR 2.390.			
EALF (MeV)	Proprietary Information Withheld Pursuant to 10 CFR 2.390.	0.9302	$5.29600E-08 \leq X \leq 2.89770E-07$
H/U-235		0.9328	$77.985 \leq X \leq 531.02$
V_M/V_F		0.9327	$1.3790 \leq X \leq 5.7950$

Table 6.10.2-13
 Benchmark Experiment Data
 (Part 1 of 2)

Proprietary Information Withheld Pursuant to 10 CFR 2.390.

k_{eff}	σ_{mcnp}	σ_{bench}	σ_{total}	EALF (MeV)	H/U-235	V_M/V_F
0.98895	0.00060	0.0081	0.0081	9.528E-08	65.1	3.229
0.98980	0.00061	0.0081	0.0081	9.665E-08	65.1	3.229
0.98985	0.00063	0.0081	0.0081	9.809E-08	65.1	3.229
0.98856	0.00060	0.0081	0.0081	9.917E-08	65.1	3.229
0.98909	0.00063	0.0081	0.0081	9.587E-08	65.1	3.229
0.98902	0.00059	0.0081	0.0081	9.840E-08	65.1	3.229
0.98963	0.00056	0.0081	0.0081	9.890E-08	65.1	3.229
0.98908	0.00057	0.0081	0.0081	9.951E-08	65.1	3.229
0.98840	0.00056	0.0081	0.0081	9.589E-08	65.1	3.229
0.98845	0.00060	0.0081	0.0081	9.963E-08	65.1	3.229
0.98930	0.00060	0.0081	0.0081	1.001E-07	65.1	3.229
0.99200	0.00087	0.0044	0.0045	8.475E-08	116.5	3.229
0.99292	0.00076	0.0040	0.0041	7.029E-08	116.5	3.229
0.99841	0.00083	0.0040	0.0041	6.318E-08	116.5	3.229
0.99087	0.00078	0.0040	0.0041	6.162E-08	116.5	3.229
0.98917	0.00080	0.0040	0.0041	5.855E-08	116.5	3.229
0.98954	0.00077	0.0040	0.0041	5.592E-08	116.5	3.229
0.98773	0.00073	0.0040	0.0041	5.452E-08	116.5	3.229
0.98393	0.00071	0.0040	0.0041	5.266E-08	116.5	3.229
0.98713	0.00072	0.0040	0.0041	5.222E-08	116.5	3.229
0.99821	0.00081	0.0040	0.0041	8.196E-08	116.5	3.229
0.99105	0.00077	0.0040	0.0041	6.217E-08	116.5	3.229
0.99490	0.00072	0.0040	0.0041	5.442E-08	116.5	3.229
1.01246	0.00087	0.0040	0.0041	8.261E-08	116.5	3.229
0.98556	0.00079	0.0061	0.0062	5.720E-08	116.5	3.229
0.98232	0.00076	0.0040	0.0041	5.671E-08	116.5	3.229
0.99327	0.00080	0.0040	0.0041	6.328E-08	116.5	3.229
0.98924	0.00085	0.0040	0.0041	7.347E-08	116.5	3.229
0.99068	0.00084	0.0040	0.0041	8.053E-08	116.5	3.229
0.99293	0.00071	0.0040	0.0041	5.225E-08	113.9	3.229
0.99215	0.00077	0.0040	0.0041	6.449E-08	113.7	3.229
0.99492	0.00084	0.0040	0.0041	6.942E-08	113.7	3.229
0.99569	0.00078	0.0040	0.0041	7.395E-08	113.6	3.229
0.99798	0.00084	0.0040	0.0041	7.678E-08	113.5	3.229
0.99199	0.00013	0.0035	0.0035	1.585E-07	66.0	3.900
0.99004	0.00063	0.0029	0.0030	2.373E-07	78.0	1.379
0.98905	0.00061	0.0024	0.0025	1.855E-07	92.8	1.642

Table 6.10.2-13
 Benchmark Experiment Data
 (Part 2 of 2)

Proprietary Information Withheld Pursuant to 10 CFR 2.390.

k_{eff}	σ_{mcnp}	σ_{bench}	σ_{total}	EALF (MeV)	H/U-235	V_M/V_F
0.99847	0.00060	0.0018	0.0019	9.980E-08	166.5	2.945
1.00026	0.00052	0.0016	0.0017	6.698E-08	333.2	3.636
1.00179	0.00044	0.0014	0.0015	5.296E-08	531.0	5.795
0.99183	0.00064	0.0029	0.0030	2.898E-07	78.0	1.379
0.99143	0.00065	0.0029	0.0030	2.672E-07	78.0	1.379
0.99106	0.00064	0.0029	0.0030	2.617E-07	78.0	1.379
0.98912	0.00064	0.0029	0.0030	2.541E-07	78.0	1.379
0.98618	0.00063	0.0029	0.0030	2.474E-07	78.0	1.379
0.98654	0.00063	0.0029	0.0030	2.430E-07	78.0	1.379
0.98504	0.00061	0.0029	0.0030	2.421E-07	78.0	1.379
0.98749	0.00064	0.0029	0.0030	2.382E-07	78.0	1.379
1.00267	0.00065	0.0018	0.0019	1.084E-07	166.5	2.945
1.00265	0.00063	0.0018	0.0019	1.082E-07	166.5	2.945
1.00263	0.00063	0.0018	0.0019	1.064E-07	166.5	2.945
1.00117	0.00064	0.0018	0.0019	1.050E-07	166.5	2.945
1.00118	0.00062	0.0018	0.0019	1.035E-07	166.5	2.945
0.99969	0.00064	0.0018	0.0019	1.021E-07	166.5	2.945
0.99980	0.00063	0.0018	0.0019	1.014E-07	166.5	2.945
1.00072	0.00062	0.0018	0.0019	1.008E-07	166.5	2.945
1.00133	0.00064	0.0018	0.0019	1.008E-07	166.5	2.945
0.99998	0.00053	0.0016	0.0017	6.881E-08	333.2	3.636
0.99916	0.00052	0.0016	0.0017	6.844E-08	333.2	3.636
1.00024	0.00050	0.0016	0.0017	6.805E-08	333.2	3.636
1.00063	0.00051	0.0016	0.0017	6.777E-08	333.2	3.636
1.00057	0.00050	0.0016	0.0017	6.721E-08	333.2	3.636
1.00223	0.00050	0.0016	0.0017	6.713E-08	333.2	3.636
1.00102	0.00051	0.0016	0.0017	6.678E-08	333.2	3.636

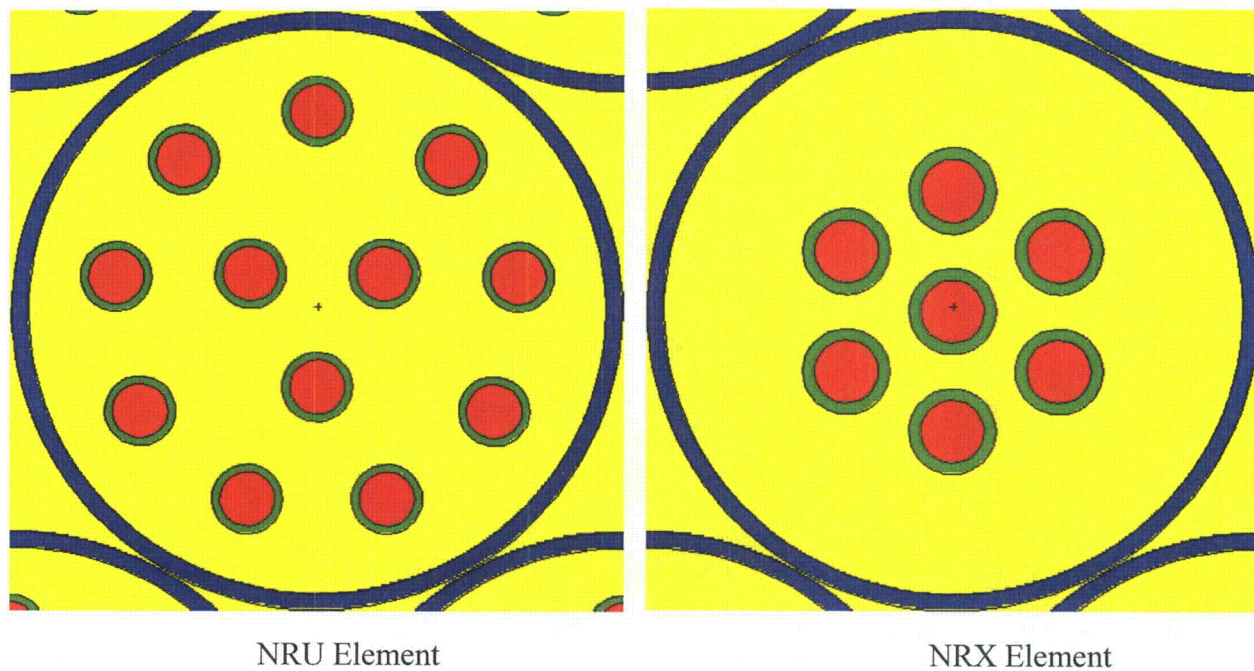


Figure 6.10.2-1
MCNP NRU/NRX Fuel Element Models

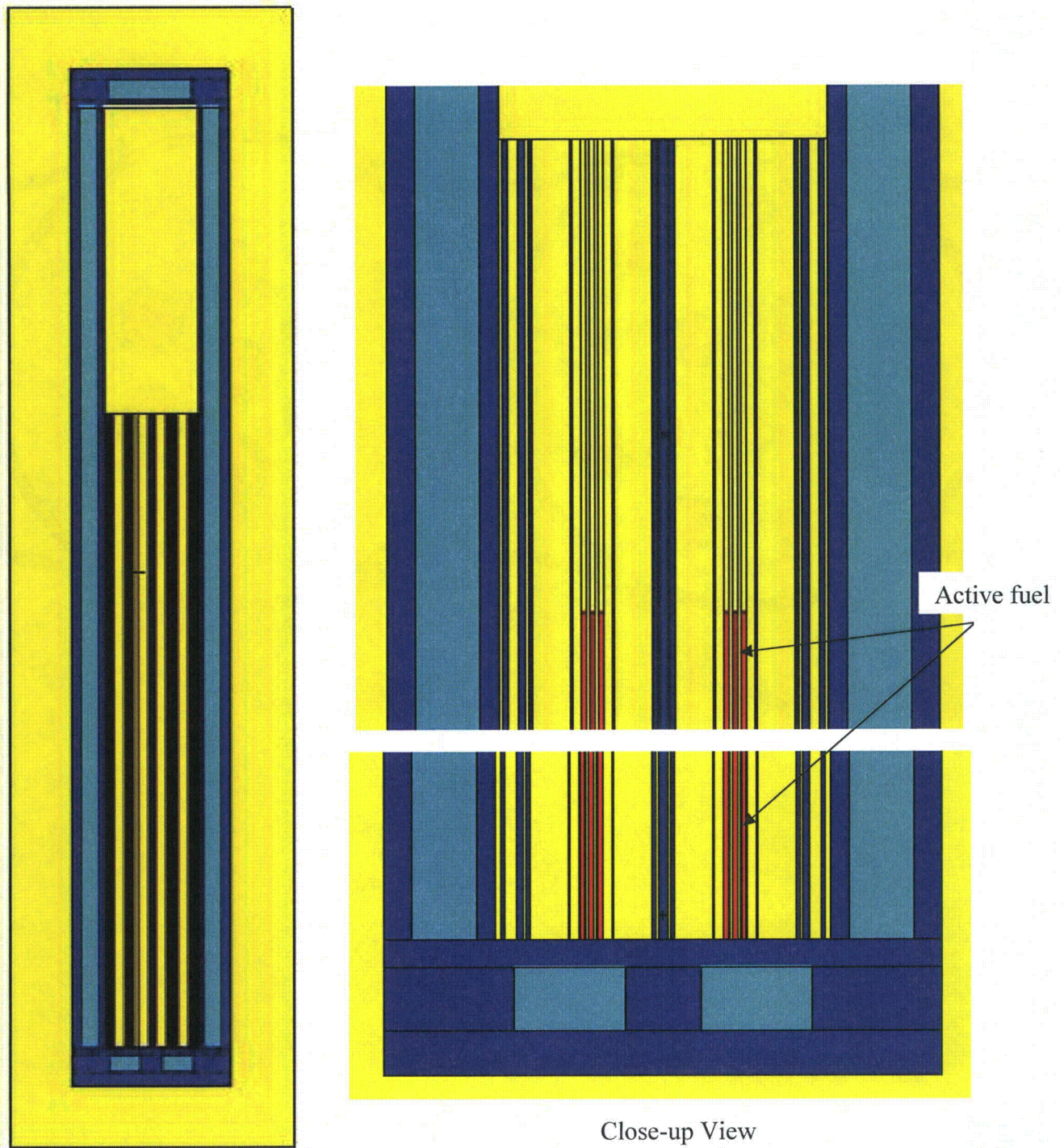
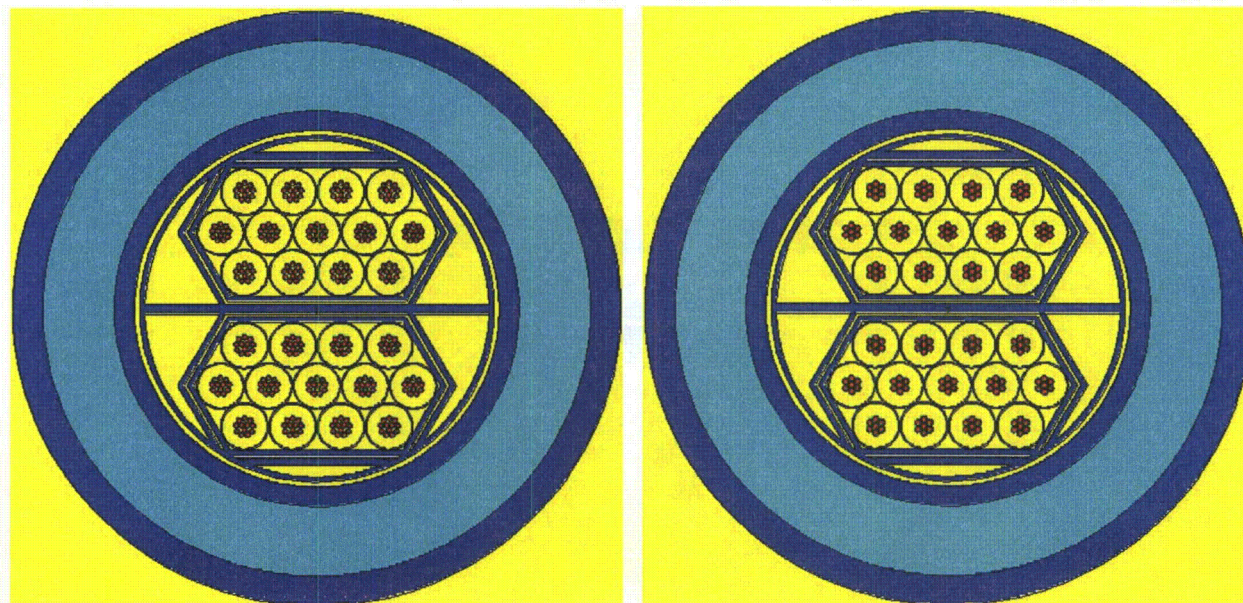
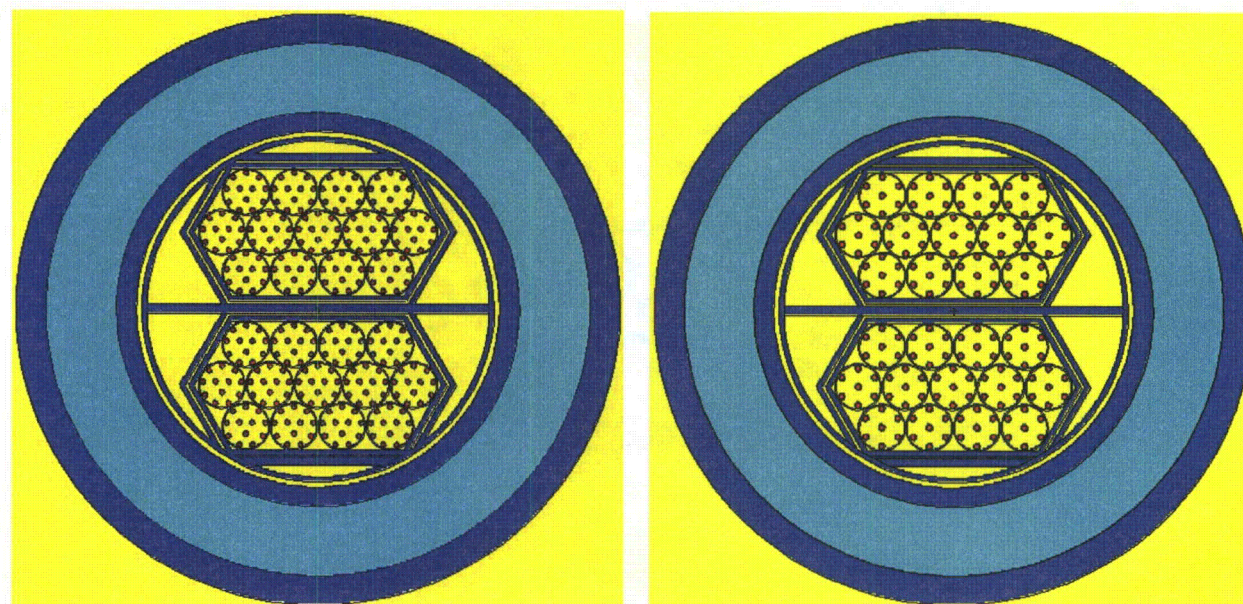


Figure 6.10.2-2
MCNP TN-LC-NRUX Model, y-z View



NRU, Minimum Pitch

NRX, Minimum Pitch



NRU, Maximum Pitch

NRX, Maximum Pitch

Figure 6.10.2-3
MCNP TN-LC-NRUX Model, x-y View

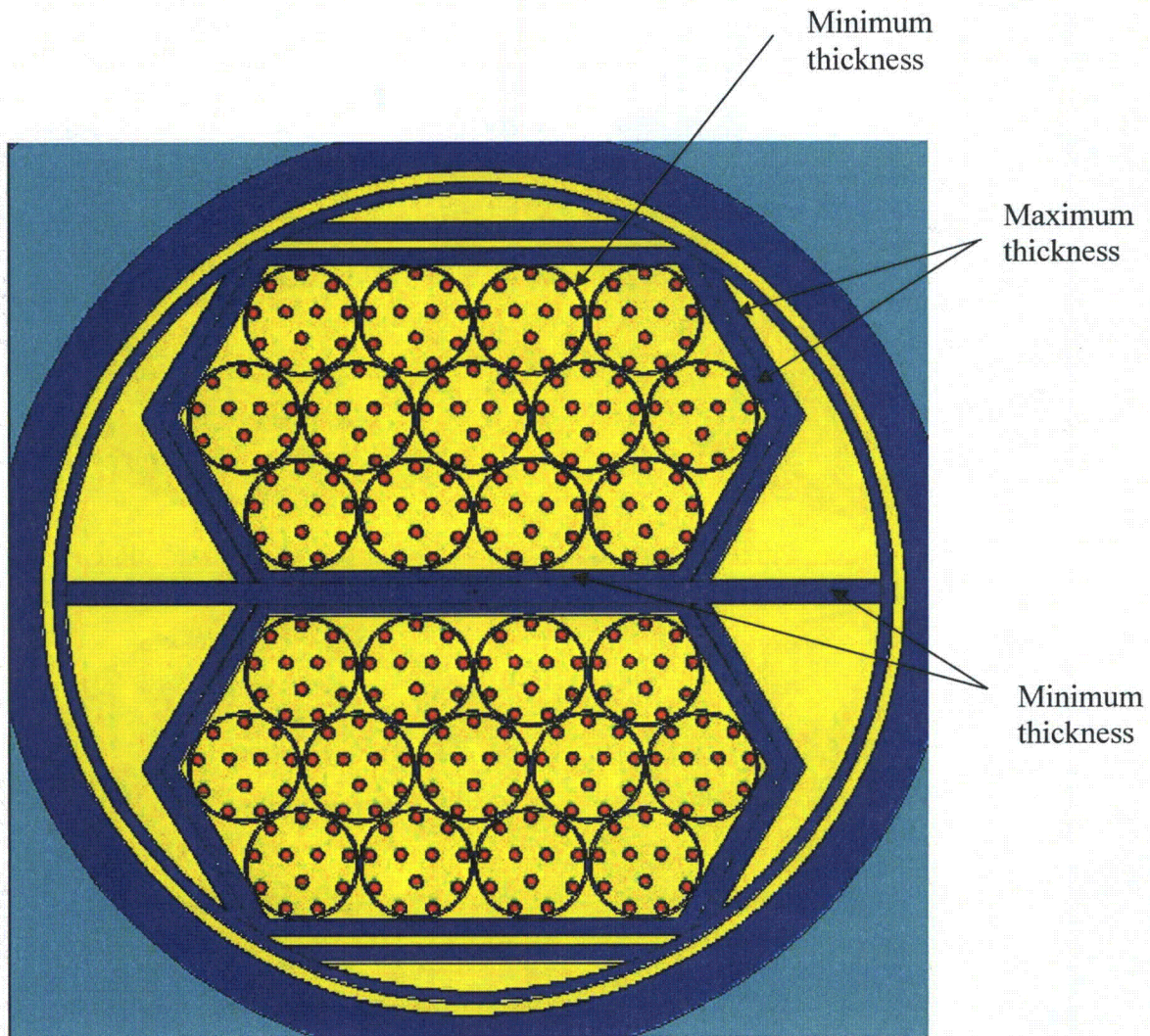


Figure 6.10.2-4
MCNP TN-LC-NRUX Single Package Model with Tolerances

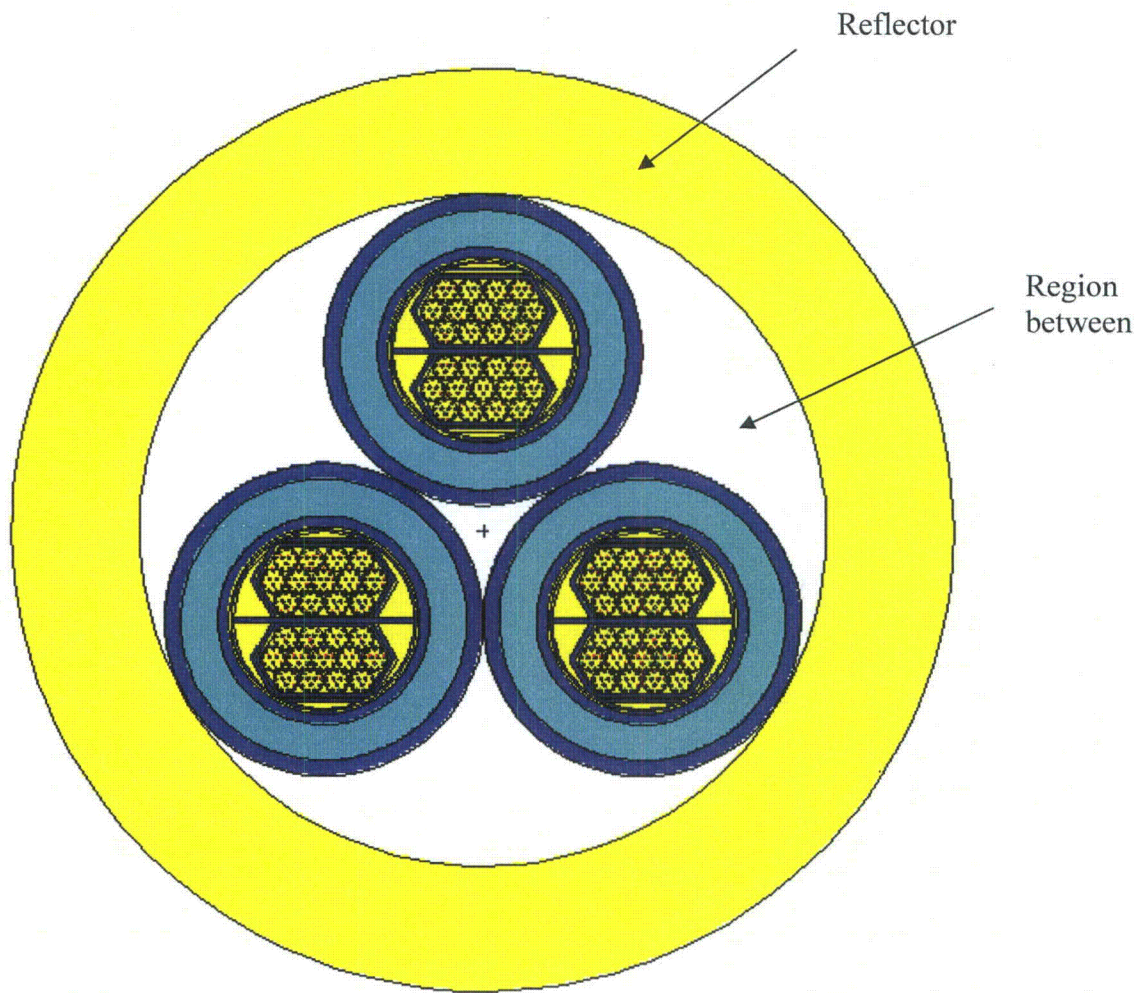
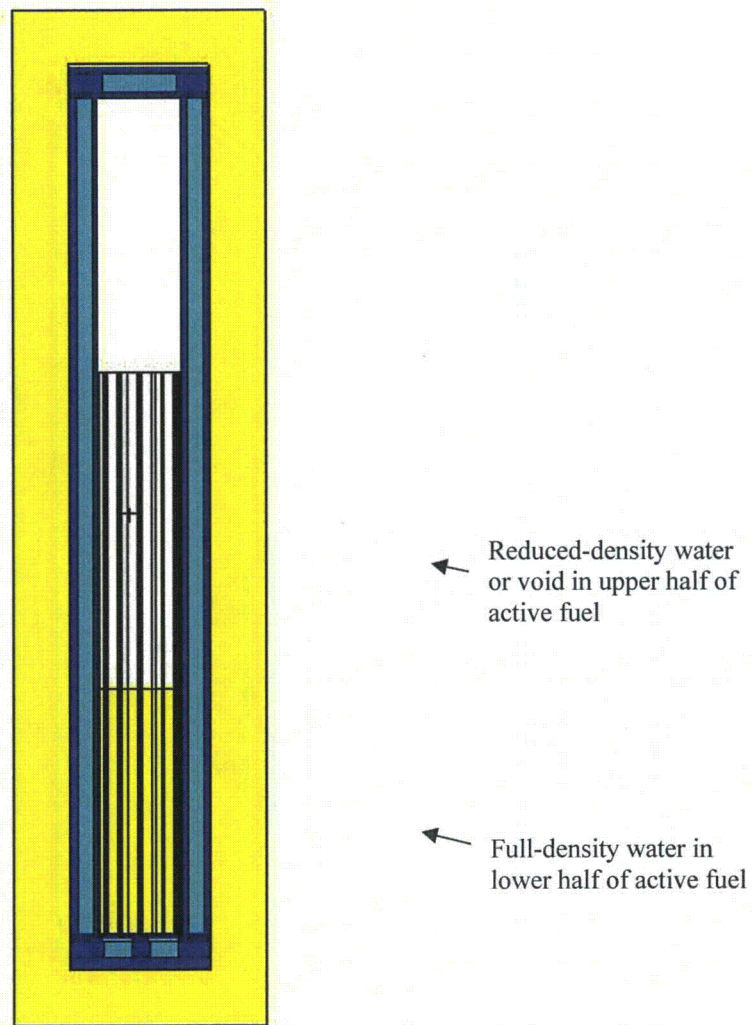


Figure 6.10.2-5
MCNP TN-LC-NRUX Array Model



*Figure 6.10.2-6
Partially Filled Cavity*

Appendix 6.10.3 TN-LC-TRIGA Basket Criticality Evaluation

TABLE OF CONTENTS

6.10.3.1	Description of the Criticality Design	6.10.3-1
6.10.3.1.1	Design Features.....	6.10.3-1
6.10.3.1.2	Summary Table of Criticality Evaluation	6.10.3-1
6.10.3.1.3	Criticality Safety Index.....	6.10.3-2
6.10.3.2	Fissile Material Contents	6.10.3-3
6.10.3.3	General Considerations.....	6.10.3-5
6.10.3.3.1	Model Configuration.....	6.10.3-5
6.10.3.3.2	Material Properties.....	6.10.3-5
6.10.3.3.3	Computer Codes and Cross-Section Libraries	6.10.3-6
6.10.3.3.4	Demonstration of Maximum Reactivity	6.10.3-6
6.10.3.4	Single Package Evaluation.....	6.10.3-8
6.10.3.4.1	Configuration	6.10.3-8
6.10.3.4.2	Results.....	6.10.3-9
6.10.3.5	Evaluation of Package Arrays under Normal Conditions of Transport.....	6.10.3-10
6.10.3.5.1	Configuration	6.10.3-10
6.10.3.5.2	Results.....	6.10.3-10
6.10.3.6	Package Arrays under Hypothetical Accident Conditions	6.10.3-11
6.10.3.7	Fissile Material Packages for Air Transport	6.10.3-12
6.10.3.8	Benchmark Evaluations	6.10.3-13
6.10.3.8.1	Applicability of Benchmark Experiments	6.10.3-13
6.10.3.8.2	Bias Determination	6.10.3-14
6.10.3.9	Appendix.....	6.10.3-16
6.10.3.9.1	References.....	6.10.3-16
	Proprietary Information Withheld Pursuant to 10 CFR 2.390.	
6.10.3.9.3	Parametric Evaluations	6.10.3-31

LIST OF TABLES

Table 6.10.3-1	Summary of TN-LC-TRIGA Criticality Evaluations	6.10.3-33
Table 6.10.3-2	Characteristics of TRIGA Fuel Elements	6.10.3-33
Table 6.10.3-3	Number Densities of TRIGA Fuel.....	6.10.3-34
Table 6.10.3-4	Dimensions Used in the Cask Model.....	6.10.3-34
Table 6.10.3-5	Composition of Stainless Steel	6.10.3-35
Table 6.10.3-6	Composition of Poison Plates	6.10.3-35
Table 6.10.3-7	Cross-Section Libraries Utilized.....	6.10.3-36
Table 6.10.3-8	TN-LC-TRIGA Single Package Results	6.10.3-36
Table 6.10.3-9	TN-LC-TRIGA NCT Array Results	6.10.3-37
Table 6.10.3-10	Benchmark Experiments Utilized	6.10.3-37
Table 6.10.3-11	USL Results	6.10.3-37
Table 6.10.3-12	Benchmark Experiment Data.....	6.10.3-38
Table 6.10.3-13	Evaluation of the Most Reactive Fuel Element	6.10.3-39
Table 6.10.3-14	Effect of Water Density on Reactivity	6.10.3-39
Table 6.10.3-15	Evaluation of the Most Reactive Geometry	6.10.3-40

LIST OF FIGURES

Figure 6.10.3-1	A Typical Stainless-Steel Clad TRIGA Fuel Element.....	6.10.3-41
Figure 6.10.3-2	MCNP Model of the Cask.....	6.10.3-42
Figure 6.10.3-3	TRIGA Radial Fuel Configuration	6.10.3-43
Figure 6.10.3-4	TRIGA Axial Fuel Configurations	6.10.3-44
Figure 6.10.3-5	MCNP TN-LC-TRIGA NCT Array Model	6.10.3-45
Figure 6.10.3-6	MCNP Model of a Single Compartment with Four TRIGA Fuel Elements.....	6.10.3-46
Figure 6.10.3-7	Radial Geometry Configurations	6.10.3-47

Appendix 6.10.3 TN-LC-TRIGA Basket Criticality Evaluation

NOTE: References in this Appendix are shown as [1], [2], etc. and refer to the reference list in Appendix 6.10.3.9.1.

The Appendix presents the criticality evaluation of the TN-LC-TRIGA basket with a payload of up to 180 TRIGA fuel assemblies or assemblies. The following analyses demonstrate that the TN-LC package complies with the requirements of 10CFR71.55 and 71.59. The Criticality Safety Index (CSI), per 10CFR71.59, is 100.

6.10.3.1 Description of the Criticality Design

6.10.3.1.1 Design Features

The cask holds five TN-LC-TRIGA baskets that are used to contain and properly position the fuel during transport

Proprietary Information Withheld Pursuant to 10 CFR 2.390.

The design includes poison plates between adjacent compartments containing the TRIGA fuel. The B-10 areal density is modeled at 5 mg/cm². Therefore, the minimum B-10 areal density in the fabricated product is 5.56 g/cm² if 90 percent B-10 credit is utilized and 6.67 g/cm² if 75 percent B-10 credit is utilized. Criticality safety is maintained by the combination of the neutron poison and the separation provided by the packaging.

6.10.3.1.2 Summary Table of Criticality Evaluation

The upper subcritical limit (USL) for ensuring that the package is acceptably subcritical, as determined in Section 6.10.3.8 is:

$$USL = 0.9297$$

The package is considered to be acceptably subcritical if the computed k_{safe} (k_s), which is defined as $k_{effective}$ (k_{eff}) plus twice the statistical uncertainty (σ), is less than or equal to the USL, or:

$$k_s = k_{eff} + 2\sigma \leq USL$$

The USL is determined on the basis of a benchmark analysis and incorporates the combined effects of code computational bias, the uncertainty in the bias based on both benchmark-model and computational uncertainties, and an administrative margin. The results of the benchmark analysis indicate that the USL is adequate to ensure subcriticality of the package.

The results of this analysis demonstrate that the packaging design meets the requirements of 10CFR71.55(b). No credit is taken for burnup in any of the analyses, and no credit is taken for the leak-tight performance of the cask.

Since the Criticality Safety Index (CSI) of this cask is assumed to be 100, the HAC analysis of an array of casks is not necessary. Calculations with an array of three casks, the minimum required for a CSI of 100, were performed as part of the NCT analysis.

The results of the criticality calculations are summarized in Table 6.10.3-1 which includes the maximum values of each type of analysis. The maximum value of k_c calculated in this analysis is 0.896 which is calculated for an array of packages under NCT and is below the USL of 0.9297.

6.10.3.1.3 Criticality Safety Index

No HAC array models are developed ($2N=1$). Therefore, per 10CFR71.59, $N=0.5$, and the criticality safety index (CSI) is $50/N = 100$. In the NCT array cases, $5N=2.5$, so that 3 packages are modeled.

6.10.3.2 Fissile Material Contents

Proprietary Information Withheld Pursuant to 10 CFR 2.390.

The fuel assembly consists of a cylindrical active fuel region located between two axial graphite reflectors. The fuel consists of a matrix that is a mixture of uranium and zirconium hydride. Therefore, all TRIGA fuel assemblies contain a hydrogen moderator material. TRIGA fuel assemblies manufactured before 1964 incorporate thin samarium trioxide discs, which serve as a burnable poison, between the active fuel and graphite reflectors. These discs and the erbium poison that is present in some TRIGA fuel assemblies have not been included in the models used for this analysis which is a conservative assumption. Later fuel used a thin molybdenum disc between the active fuel and the lower reflector. This disc, which has a thickness of 0.031 in, has a negligible effect on reactivity and is also omitted from the models.

All but one type of TRIGA fuel assembly (type 1) have a 0.225 in. diameter zirconium rod located in the center of the fuel pellet. The inner diameter of the pellet is assumed to be slightly larger, with a diameter of 0.25 in, to provide a small clearance between the rod and the fuel.

The design basis payload also includes three types of Fuel Follower Control Rod (FFCR) assemblies. These assemblies, which consist of a 15 in. boron carbide section, a 15 in. active fuel section, and upper and lower void sections are longer (with a total length of 45 in.) than standard

TRIGA fuel assemblies and, therefore, must be held in the longer of the two TRIGA basket designs, with dimensions labeled “option 2” in the Chapter 1 drawings. The basket loading scheme used by the TN-LC package allows only one of these longer baskets in each cask, if it is present at all. The remaining four baskets in the cask must be short (with the dimensions labeled “option 1”) and contain standard TRIGA fuel assemblies. The three types of FFCR assemblies have active fuel regions that are similar to the fuel in types 3, 4, and 6 in Table 6.10.3-2. However, since the FFCR assemblies lack graphite reflectors, contain boron carbide, and in some cases have lower uranium loadings, they are less reactive than their standard TRIGA assembly counterparts. Thus, the FFCR assemblies are not modeled since the standard TRIGA fuel types are bounding for criticality safety analysis.

In the calculations performed for this analysis, only the fuel, cladding, the zirconium rod (if present), and the two graphite reflectors of the fuel assembly are modeled explicitly. The upper and lower end fittings have not been included, a conservative assumption that simplifies the model. Similarly, the two graphite reflectors are modeled as though they have the same diameter as the fuel pellets, although they are slightly smaller in size.

The number densities for the seven types of TRIGA fuel are calculated using the information in Table 6.10.3-2. Only two isotopes of uranium, U-235 and U-238, are included in the model for simplicity. The number densities of the components of the fuel were calculated from the mass of uranium, the mass fraction of U-235, the mass of zirconium, the H-to-Zr ratio, and the physical dimensions of the assembly. The mass fraction of uranium in the fuel given in Table 6.10.3-2 is a maximum value for each type of fuel assembly and is not used in this calculation. The number densities are given in Table 6.10.3-3 for all seven types of fuel.

6.10.3.3 General Considerations

6.10.3.3.1 Model Configuration

The fuel, basket, and packaging are modeled explicitly in the MCNP5 V1.4 computer program [1]. The TN-LC package model is a simplified representation of the cask and baskets. The body of the casks is represented by coaxial cylinders of steel and lead, with no effort to model minor details of the design since they have a negligible effect on the reactivity calculation. The impact limiters at the ends of the cask and the neutron shield have also been omitted. The entire cask is surrounded in the model by a reflective region of water that is 12 in. thick.

The model of the cask is shown in Figure 6.10.3-2. The dimensions of the cask that were used to construct the model are given in Table 6.10.3-4. The cask contains five baskets that hold the TRIGA fuel. The remaining space in the cask is occupied by a steel spacer which is not included in the model for simplicity. The length of the spacer in the Chapter 1 drawings is 23.50 in. The model is based on a spacer that is 1.25 in. shorter, but this should have a negligible effect on the results of these calculations. Only the short TN-LC-TRIGA basket design, with the dimensions labeled “option 1,” is modeled since the long TN-LC-TRIGA basket is used for FFCR assemblies which are less reactive than standard fuel assemblies, as discussed in Section 6.10.3.2.

The model of the basket is also simplified, and only the key features of the basket that are relevant to criticality analysis are included. Thus, the lifting lugs, the steel inserts, and the fasteners are not modeled. The model of the poison plates includes 1 in. × 1 in. drainage holes at the bottom of the plates which were present in an earlier version of the design but do not appear in the final drawings. Thus, the model conservatively underestimates the amount of poison that is in the basket.

Since the fuel assemblies are held in fairly small compartments, without much room to move during an accident, the baskets and fuel are assumed to be undamaged in all calculations performed for this analysis under both normal conditions of transport (NCT) and hypothetical accident conditions (HAC). Although the cask is designed to be sealed to prevent the entrance of water into the cavity and to remain leak tight under accident conditions, all of the calculations assume that water is present inside the cask, and the density of this water is allowed to vary to ensure that the calculation that maximizes reactivity is performed and used for this analysis. The drainage holes in the basket (although they are not completely represented in the MCNP model) allow water to flow throughout the inner cavity of the cask. Thus, *preferential flooding is not credible*, and the calculations here assume that the density of water is the same everywhere inside the cask. While it is possible that the cask could be partially filled with water, with some fuel assemblies submerged and others uncovered, this scenario was not modeled because it is less reactive (due to less moderation) than the case in which all fuel assemblies are submerged. *It is demonstrated that the reactivity of TRIGA fuels reduces in the absence of moderation. It is demonstrated explicitly in Section 6.10.2.4 for HEU NRU fuel that a partially flooded cavity results in lower reactivities, and TRIGA fuel will behave in a similar manner. For these reasons, cases are not developed for partial and/or preferential flooding.*

6.10.3.3.2 Material Properties

The composition of the TRIGA fuel is presented in Table 6.10.3-3. The stainless steel components, including the cladding of some types of TRIGA fuel assemblies, the basket, and parts of the cask, are modeled as SS304 using the standard composition provided in the SCALE

material library [2] (presented in Table 6.10.3-5), which is the standard for criticality analysis. Although the TN-LC design uses XM-19 stainless steel for the outer steel parts of the cask,

SS304 is used for all stainless steel components in the model for simplicity. This substitution has no significant effect on the results.

The other components of the TRIGA fuel are assumed to be pure. That is, the graphite reflectors are modeled as pure carbon with a density of 2.3 g/cm^3 [2], and the zirconium rod that is present in many of the TRIGA fuel assemblies is modeled as pure zirconium with a density of 6.5 g/cm^3 [2].

Cask lead is modeled as pure with a density of 11.35 g/cm^3 .

The poison plates are assumed to be a mixture of B_4C and aluminum. The composition of these plates, corresponding to a loading of 5 mg/cm^2 of ^{10}B , is given in Table 6.10.3-6. Water, H_2O , appears in the model with various densities, up to a maximum of 1.0 g/cm^3 , inside or outside of the cask depending on the calculation. The water in the 12 in reflective zone around the model always has a density of 1.0 g/cm^3 .

6.10.3.3.3 Computer Codes and Cross-Section Libraries

MCNP5 v1.40 is used for the criticality analysis [1]. All cross-sections utilized are at room temperature (293 K). The uranium isotopes utilize preliminary ENDF/B-VII cross-section data that are considered by Los Alamos National Laboratory to be more accurate than ENDF/B-VI cross-sections. ENDF/B-V cross-sections are utilized for chromium, nickel, iron, and lead because natural composition ENDF/B-VI cross-sections are not available for these assemblies. The remaining isotopes utilize ENDF/B-VI cross-sections. Titles of the cross-sections utilized in the models have been extracted from the MCNP output (when available) and provided in Table 6.10.3-7. The $S(\alpha, \beta)$ cards LWTR.60T, H/ZR.60T, and ZR/H.60T are used to properly account for the hydrogen bound to water and the hydrogen and zirconium in the zirconium hydride in the TRIGA fuel.

All calculations reported here use 250 cycles with 5000 neutrons per cycle. Only the last 200 cycles are used to determine the results (the first 50 are skipped). This configuration yields a 68 percent statistical uncertainty (1σ) that is typically 0.001 or less.

6.10.3.3.4 Demonstration of Maximum Reactivity

No credit is taken for fuel assembly burnup. An array of packages under NCT is the most reactive, since the presence of multiple casks increases the reactivity. The reactivity for this configuration is maximized when no water is present in the space between the casks.

Since water is allowed to enter the cask, the reactivity is maximized when the assemblies in each compartment are far from each other, allowing water to occupy the center of the compartment. The most reactive axial configuration is that in which the assemblies in adjacent baskets are located next to each other with the assemblies arranged so that the ends of the assemblies with the smaller graphite reflector are facing each other.

Although the calculations show that maximum reactivity is achieved by assuming that the thicknesses of the poison plates is at its minimum tolerance, the effect of reducing the thickness of these plates is quite small and is within the statistical uncertainty of the calculations.

Structural analysis of the cask and basket in Chapter 2 has demonstrated that they maintain their structural integrity after an accident. Therefore, these calculations assume that both the basket and the fuel are completely undamaged and intact. Nevertheless, because the end fittings are not modeled, the most reactive geometry in the calculations here bounds the case in which the fuel assemblies are damaged by losing their end fittings and cladding beyond the active fuel region and are free to move within the compartment.

The most reactive case for TRIGA fuel is the NCT scenario with an array of packages for which $k_s = 0.896$ which is below the USL of 0.9297.

6.10.3.4 Single Package Evaluation

6.10.3.4.1 Configuration

The bounding fuel assembly is discussed in Section 6.10.3.9.3 where it is demonstrated that the fifth type of fuel assembly, the FLIP assembly with up to 8.5 wt.% HEU, is the most reactive of the fuel types considered in this study. Therefore, all calculations discussed here use this type of fuel.

Since no credit is taken for the leak-tight performance of the cask, it is assumed that water is present in the basket, and the parametric calculations presented in Section 6.10.3.9.3 demonstrate that the TRIGA fuel is most reactive when the fuel assemblies are located at the four corners of each fuel compartment, allowing the water to fill the intermediate space. Thus, all single package cases use this radial configuration, which is shown in Figure 6.10.3-3.

Because water is assumed to be present during NCT, separate NCT and HAC single package calculations are not performed. Although the fuel is assumed to be undamaged, the most reactive geometry has the graphite reflectors of the TRIGA assemblies touching the end of the basket which normally would be prevented by the end fittings and cladding beyond the active fuel zone. Therefore, this configuration can be considered to be a bounding geometry for a scenario under HAC in which the fuel is damaged.

The calculations are labeled TA01 to TA12, and their results are presented in Table 6.10.3-8. The first three cases differ in the axial arrangement of the assemblies. In Case TA01, the fuel assemblies are axially positioned in the basket such that the active fuel region is centered in the compartment. Since the bounding fuel assemblies are not symmetric in the axial direction, because the graphite reflectors on either side of the active fuel region are different in length, the fuel assemblies in two of the baskets are oriented in the opposite direction of the assemblies in the other three. In Case TA02, the fuel has been moved so that the fuel assemblies in adjacent baskets are next to each other in four of the five baskets, with the graphite reflectors touching the end of the basket. (In actual practice, it would not be possible to shift the fuel all the way to the end of the basket due to the presence of the end fittings.) The fuel in the remaining basket has been moved so that it is as close as possible to the other fuel assemblies. The assemblies are oriented so that the sides of adjacent assemblies with the longer graphite reflector (the “long ends” of the assemblies) are next to each other. Case TA03 is similar to Case TA02, but the orientations of the assemblies have been reversed, so that the sides of adjacent assemblies with the shorter graphite reflector (the “short ends”) are next to each other. The three axial configurations are shown in Figure 6.10.3-4.

Of the first three cases, the last, Case TA03, is the most reactive. Therefore, this axial configuration is used for the remaining cases.

In Case TA04, the inner dimensions of each fuel compartment are increased to their maximum tolerance in each direction from 3.48 in to 3.53 in. The outer dimensions, which are determined by the size of the basket’s wrap and the thickness of the poison plates, remain the same. Thus, this change has the effect of reducing the thickness of each side wall of the compartment by 0.025 in, or 18.5 percent of its original thickness.

In Case TA05, the thickness of the poison plates is reduced to its minimum tolerance, from 0.31 in to 0.30 in. The thickness of the walls of the fuel compartments remains unchanged, so that the

inner dimensions of each fuel compartment increase from 3.48 in to 3.487 in. The density and composition of the poison plates also remain unchanged (their values are given in Table 6.10.3-6). Thus, this dimensional change results in a reduction of the amount of poison in the basket.

In Case TA06, the dimensional changes of the previous two cases are combined. Thus, both the walls of the fuel compartments and the poison plates are reduced in thickness. The space inside each fuel compartment expands in both directions to 3.537 in.

Reducing the thickness of the walls decreases the reactivity in the cask, since the fuel assemblies, which are pressed against the compartment walls to maximize the reactivity, are moved closer to the poison plates between the compartments. Reducing the thickness of the poison plates increases the reactivity, as the amount of poison in the basket is decreased; however, the observed increase in reactivity is small and is within the statistical uncertainty of the calculations.

The remaining cases, labeled TA07 to TA12, examine the effect of the density of the water in the cask. They repeat the conditions in Case TA06 with the density of the water inside the basket reduced in increments, from 0.9 g/cm^3 to 0.4 g/cm^3 . Since the system is under-moderated, the reactivity decreases with decreasing water density. Therefore, the most reactive case is TA05, with $k_s = 0.887$.

6.10.3.4.2 Results

The tabulated results for the single package cases are presented in Table 6.10.3-8. The most reactive configuration is indicated by bold type.

6.10.3.5 Evaluation of Package Arrays under Normal Conditions of Transport

6.10.3.5.1 Configuration

Since the CSI of this package is assumed to be 100, an array of only three packages needs to be evaluated under NCT. Case TA05, with thin poison plates, is used as the basis for this analysis to conservatively reduce the amount of poison in the basket.

The three casks are arranged in the triangular configuration shown in Figure 6.10.3-5. This configuration represents a close-packed array of packages. Since the impact limiters and the neutron shield are not modeled, this array is a conservative geometry that minimizes the separation between the casks and therefore increases the reactivity of the array. A 12 in. thick cylindrical layer of reflective water surrounds the array on the sides, top, and bottom.

Five calculations were performed, which are labeled TB01 to TB05. The five cases differ in the density of water in the space between the casks, from Case TB01 with a density of 1.0 g/cm³ to Case TB05 with no water at all.

The results are summarized in Table 6.10.3-9. Case TB05, with no water between the casks, is the most reactive, with $k_s = 0.896$.

6.10.3.5.2 Results

The tabulated results for the NCT array analysis cases are presented in Table 6.10.3-9. The most reactive configuration is indicated by bold type.

6.10.3.6 Package Arrays under Hypothetical Accident Conditions

Because the CSI = 100, no HAC array cases are performed.

6.10.3.7 Fissile Material Packages for Air Transport

This section does not apply.

6.10.3.8 Benchmark Evaluations

The Monte Carlo computer program MCNP5 v1.40 is utilized for this benchmark analysis [1]. MCNP has been used extensively in criticality evaluations for several decades and is considered a standard in the industry.

A listing of the cross-section libraries used in the analysis is provided in Table 6.10.3-7. These cross-sections are consistent with the cross-sections utilized in the benchmarks.

The ORNL USLSTATS computer program [3] is used to establish a USL for the analysis. USLSTATS provides a simple means of evaluating and combining the statistical error of the calculation, code biases, and benchmark uncertainties. The USLSTATS calculation uses the combined uncertainties and data to provide a linear trend and an overall uncertainty. Computed multiplication factors, k_{eff} , for the package are deemed to be adequately subcritical if the computed value of k_s is less than or equal to the USL as follows:

$$k_s = k_{\text{eff}} + 2\sigma \leq \text{USL}$$

The USL is determined on the basis of a benchmark analysis and incorporates the combined effects of code computational bias, the uncertainty in the bias based on both benchmark-model and computational uncertainties, and an administrative margin. This methodology has accepted precedence in establishing criticality safety limits for transportation packages complying with 10CFR71.

6.10.3.8.1 Applicability of Benchmark Experiments

The critical experiment benchmarks were selected from the International Handbook of Evaluated Criticality Safety Benchmark Experiments [4]. Three sets of benchmarks are used which are listed in Table 6.10.3-10.

The first set consists of two intermediate-enriched (20 percent) TRIGA benchmarks for an entire Mark II core. These benchmarks include graphite reflectors and absorber materials, both of which also appear in the TN-LC criticality analysis. These experiments are the most similar benchmarks that are available.

Since a set of only two benchmarks is insufficient to provide a statistical distribution, two additional sets of benchmarks were selected: a set of 10 highly enriched (93 percent) uranium solution benchmarks and set of 9 low-enriched (10 percent) uranium solution benchmarks. These benchmarks were chosen to simulate fuel intimately mixed with a moderator since the zirconium hydride fuel in the TRIGA assemblies contains moderator in the fuel matrix.

The 21 benchmark experiments were divided into three groups for computing trends:

- A group consisting of all 21 benchmarks
- A group consisting of the 10 HEU benchmarks and the 2 TRIGA benchmarks
- A group consisting of the 9 LEU benchmarks and the 2 TRIGA benchmarks

The USL used for the criticality analysis is the minimum of the values calculated for these three benchmark groups.

6.10.3.8.2 Bias Determination

The USL is calculated by application of the USLSTATS computer program [3]. USLSTATS receives as input the k_{eff} as calculated by MCNP, the total 1- σ uncertainty (combined benchmark and MCNP uncertainties), and a trending parameter. Three trending parameters have been selected: (1) Energy of the Average neutron Lethargy causing Fission (EALF), (2) the number density of U-235, and (3) the ratio of the number of hydrogen atoms to the number of U-235 atoms in the fuel matrix (H/U-235).

The uncertainty value, σ_{total} , assigned to each case is a combination of the benchmark uncertainty for each experiment, σ_{bench} , and the Monte Carlo uncertainty associated with the particular computational evaluation of the case, σ_{MCNP} , or:

$$\sigma_{\text{total}} = (\sigma_{\text{bench}}^2 + \sigma_{\text{MCNP}}^2)^{1/2}$$

These values are input into the USLSTATS program in addition to the following parameters which are the values recommended by the USLSTATS user's manual [3]:

- P, proportion of population falling above lower tolerance level = 0.995 (note that this parameter is required input but is not utilized in the calculation of USL Method 1)
- 1- γ , confidence on fit = 0.95
- α , confidence on proportion P = 0.95 (note that this parameter is required input but is not utilized in the calculation of USL Method 1)
- Δk_m , administrative margin used to ensure subcriticality = 0.05.

These data are followed by triplets of trending parameter value, computed k_{eff} , and uncertainty for each case. A confidence band analysis is performed on the data for each trending parameter using USL Method 1. The USL calculated for each of the trending parameters and group of experiments is provided in Table 6.10.3-11. All benchmark data used as input to USLSTATS are reported in Table 6.10.3-12. The results are discussed below.

Energy of the Average Neutron Lethargy Causing Fission (EALF):

Using EALF as a trending parameter provides information on neutron spectral dependencies. The minimum USL in the range of applicability is 0.9297 which is calculated for the group of 12 experiments consisting of the HEU and TRIGA benchmarks.

Most of the cases, including the most reactive case, TB05, fall within the range of applicability of this parameter. The two exceptions are Cases TA11 and TA12 (with EALFs of 3.0178×10^{-7} MeV and 3.4775×10^{-7} MeV, respectively) with low-density water inside the cask; however, these cases resulted in relatively low reactivity. Thus, this parameter is acceptable.

Number Density of U-235:

The minimum USL in the range of applicability of the second trending parameter is 0.9300 which is calculated for the group of 12 experiments consisting of the HEU and TRIGA benchmarks.

The ^{235}U number density of the bounding fuel assembly used in the NCT and HAC calculations (type 5 in Table 6.10.3-3) is 9.119×10^{-4} atom/b-cm which is slightly outside of the range of applicability. Nevertheless, since this number density is close to the maximum value of the range, 8.5392×10^{-4} atom/b-cm, this parameter is acceptable.

H/U-235 Number Ratio:

The minimum USL in the range of applicability of the third trending parameter is 0.9307 which is calculated for the group of 12 experiments consisting of the HEU and TRIGA benchmarks.

The atom ratio in the bounding fuel assembly (type 5 in Table 3.1-2) is 61.9 which is slightly outside of the range of applicability. Nevertheless, since this ratio is close to the minimum value of the range, 68.2, this parameter is acceptable.

Recommended USL:

The minimum USL of 0.9297 is calculated using EALF as a trending parameter over the subset of HEU solution and TRIGA benchmarks. This USL is recommended for the criticality analysis of the TN-LC package containing TRIGA fuel.

6.10.3.9 Appendix

6.10.3.9.1 References

1. MCNP5, "MCNP – A General Monte Carlo N-Particle Transport Code, Version 5; Volume II: User's Guide," LA-CP-03-0245, Los Alamos National Laboratory, April 2003.
2. SCALE: A Modular Code System for Performing Standardized Computer Analyses for Licensing Evaluations, ORNL/TM-2005/39, Version 6, Vols. I-III, January 2009.
3. USLSTATS, "USLSTATS: A Utility To Calculate Upper Subcritical Limits For Criticality Safety Applications," Version 1.4.2, Oak Ridge National Laboratory, April 23, 2003. Note: USLSTATS is described in Appendix C, User's Manual for USLSTATS V1.0, in NUREG/CR-6361 Criticality Benchmark Guide for Light-Water-Reactor Fuel in Transportation and Storage Packages, March 1997.
4. International Handbook of Evaluated Criticality Safety Benchmark Experiments, Nuclear Energy Agency, NEA/NSC/DOC(95)03, September 2009.

**Proprietary Information on Pages 6.10.3-17 through 6.10.3-30
Withheld Pursuant to 10 CFR 2.390.**

6.10.3.9.3 Parametric Evaluations

Determination of the Most Reactive Fuel Type

The seven types of TRIGA fuel assemblies are compared so that a bounding fuel type could be selected for use in the criticality analysis. For this evaluation, a unit cell consisting of a single fuel compartment from the basket with four fuel assemblies is modeled in MCNP. This model is shown in Figure 6.10.3-6. Each of the seven types of fuel in Table 6.10.3-2 is modeled, and all four assemblies in each model are of the same type. Only the fuel, cladding, the zirconium rod (if present), and the two graphite reflectors are modeled explicitly. The upper and lower end fittings are omitted for simplicity.

Reflecting boundary conditions are imposed on the sides, top, and bottom of the model to simulate an infinite array of fuel compartments with no leakage. Calculations were performed for both dry conditions (no water present in the model) and wet conditions (water with a density of 1.0 g/cm^3 occupying the spaces between fuel assemblies). No poison is included in the model.

The results are summarized in Table 6.10.3-13. The most reactive dry and wet cases are highlighted with bold type. The HEU fuel assembly, Type 5, is the most reactive fuel assembly in both dry and wet conditions. This type of fuel is used as the bounding fuel assembly in the other calculations reported here.

An additional set of calculations is performed to find the density of water that maximizes the reactivity with this type of fuel. The results of these calculations are summarized in Table 6.10.3-14. These calculations demonstrate that the maximum reactivity occurs when the water between the assemblies is absent, indicating that the infinite array of fuel compartments is over-moderated due to the graphite reflectors and the presence of hydrogen in the fuel. However, the analysis of the TN-LC-TRIGA basket involves at most three packages, and, in a small array, full-water moderation is more reactive than dry or reduced water moderation.

Determination of the Most Reactive Fuel Geometry

These parametric calculations are performed to determine the most reactive configuration of fuel in the TN-LC-TRIGA basket. The bounding fuel type from the previous section is used in this analysis. To study geometrical configurations, an MCNP model of a TN-LC-TRIGA fuel basket is constructed. This model includes the fuel compartments (with four fuel assemblies each), the poison plates, the aluminum rail, the cylindrical sides of the cask, and a 12 in. thick reflective region of water outside the cask. Only one TN-LC-TRIGA basket is explicitly represented, and reflective boundary conditions on the top and bottom of the model simulate an infinite array of casks in the axial direction.

Four cases, labeled TP01 to TP04, are studied. All four cases assume that the basket is filled with water (with a density of 1.0 g/cm^3) and have poison plates consisting of a loading of 5 mg/cm^2 of ^{10}B . The composition of these plates is given in Table 6.10.3-6.

The results of four radial configurations of fuel assemblies, shown in Figure 6.10.3-7, are presented here. They are identified by the following labels:

- Spaced The fuel assemblies are evenly spaced so that the distance between adjacent assemblies and the distance between an assembly and a wall of the compartment are equal.
- Center All fuel assemblies are pushed to the center of each compartment and are touching.
- Corners All fuel assemblies are pushed to the four corners of each compartment.
- Inside All fuel assemblies are touching and are pushed as close to the center of the basket as possible.

The results of the calculations are presented in Table 6.10.3-15. The most reactive case is indicated by bold type.

The most reactive configuration is Case TP03 with the fuel assemblies located at the four corners of each compartment (labeled "corners"). This geometrical configuration is the recommended horizontal arrangement of TRIGA assemblies for criticality safety analysis.

Table 6.10.3-1
 Summary of TN-LC-TRIGA Criticality Evaluations

Normal Conditions of Transport (NCT)	
Case	k_s
Single Unit Maximum	0.887
Array Maximum (3 packages)	0.896
Hypothetical Accident Conditions (HAC)	
Case	k_s
Single Unit Maximum	0.887
Array Maximum (1 package)	0.887
USL = 0.9297	

Table 6.10.3-2
 Characteristics of TRIGA Fuel Elements

Proprietary Information Withheld Pursuant to 10 CFR 2.390.

Table 6.10.3-3
Number Densities of TRIGA Fuel

Fuel Type	Number Density (atom/b-cm)				
	H	Zr	²³⁵ U	²³⁸ U	Total
1	4.239×10^{-2}	4.239×10^{-2}	2.932×10^{-4}	1.16×10^{-3}	8.622×10^{-2}
2	4.084×10^{-2}	4.084×10^{-2}	2.826×10^{-4}	1.12×10^{-3}	8.309×10^{-2}
3	6.011×10^{-2}	3.536×10^{-2}	3.917×10^{-4}	1.55×10^{-3}	9.740×10^{-2}
4	6.696×10^{-2}	3.939×10^{-2}	2.725×10^{-4}	1.08×10^{-3}	1.077×10^{-2}
5	5.645×10^{-2}	3.528×10^{-2}	9.119×10^{-4}	3.86×10^{-4}	9.302×10^{-2}
6	5.447×10^{-2}	3.405×10^{-2}	6.700×10^{-4}	2.65×10^{-3}	9.183×10^{-2}
7	5.168×10^{-2}	3.230×10^{-2}	1.123×10^{-3}	4.44×10^{-3}	8.954×10^{-2}

Table 6.10.3-4
Dimensions Used in the Cask Model

Proprietary Information Withheld Pursuant to 10 CFR 2.390.

Table 6.10.3-5
Composition of Stainless Steel

Component	Wt.%
C	0.08
Si	1.0
P	0.045
Cr	19.0
Mn	2.0
Fe	68.375
Ni	9.5
Density = 7.94 g/cm ³	

Table 6.10.3-6
Composition of Poison Plates

Component	Wt.%
Al	98.37
C	0.354
¹⁰ B	0.235
¹¹ B	1.04
Density = 2.67 g/cm ³	

Table 6.10.3-7
Cross-Section Libraries Utilized

Isotope or Element	Cross-Section Description (From MCNP Output)
1001.62c	1-h-1 at 293.6K from endf-vi.8 njoy99.50
5010.66c	5-b-10 at 293.6K from endf-vi.1 njoy99.50
5011.66c	5-b-11 at 293.6K from endf-vi.0 (MOD) njoy99.50
6000.66c	6-c-0 at 293.6K from endf-vi.6 njoy99.50
8016.62c	8-o-16 at 293.6K from endf-vi.8 njoy99.50
13027.62c	13-al-27 at 293.6K from endf-vi.8 njoy99.50
14000.60c	14-si-nat from endf/b-vi
15031.66c	15-p-31 at 293.6K from endf-vi.6 njoy99.50
24000.50c	njoy
25055.62c	25-mn-55 at 293.6K from endf/b-vi.8 njoy99.50
26000.55c	njoy
28000.50c	njoy
40000.66c	40-zr-0 at 293.6K from endf-vi.1 njoy99.50
82000.50c	njoy
92235.69c	92-u-235 at 293.6K from t16 u2351a9d njoy99.50
92238.69c	92-u-238 at 293.6K from t16 u2381a8h njoy99.50

Table 6.10.3-8
TN-LC-TRIGA Single Package Results

Case Id.	Geometry	Water Density (g/cm ³)	k _{eff}	σ	k _s (k _{eff} + 2σ)
Proprietary Information Withheld Pursuant to 10 CFR 2.390.	Middle	1.0	0.87207	0.00083	0.87373
	Long touching	1.0	0.87655	0.00084	0.87823
	Short touching	1.0	0.88556	0.00081	0.88718
	Short touching, thin walls	1.0	0.88290	0.00079	0.88448
	Short touching, thin plates	1.0	0.88567	0.00081	0.88729
	Short touching, thin walls/plates	1.0	0.88429	0.00081	0.88591
	Short touching, thin walls/plates	0.9	0.87270	0.00085	0.87440
	Short touching, thin walls/plates	0.8	0.86432	0.00082	0.86596
	Short touching, thin walls/plates	0.7	0.85229	0.00081	0.85391
	Short touching, thin walls/plates	0.6	0.83700	0.00089	0.83878
	Short touching, thin walls/plates	0.5	0.81810	0.00082	0.81974
Short touching, thin walls/plates	0.4	0.79878	0.00090	0.80058	

Table 6.10.3-9
TN-LC-TRIGA NCT Array Results

Case Id.	Ext. Water Density (g/cm ³)	k _{eff}	σ	k _s (k _{eff} + 2σ)
Proprietary Information Withheld Pursuant to 10 CFR 2.390.	1.00	0.88864	0.00090	0.89044
	0.75	0.88847	0.00084	0.89015
	0.50	0.89106	0.00084	0.89274
	0.25	0.88931	0.00083	0.89097
	0.00	0.89411	0.00087	0.89585

Proprietary Information Withheld Pursuant to 10 CFR 2.390.

Table 6.10.3-10
Benchmark Experiments Utilized

Series	Title
IEU-COMP-THERM-003	TRIGA Mark II Reactor: U(20) – Zirconium Hydride Fuel Rods in Water with Graphite Reflector
HEU-SOL-THERM-001	Minimally Reflected Cylinders of Highly Enriched Solutions of Uranyl Nitrate
LEU-SOL-THERM-003	Full and Truncated Bare Spheres of 10% Enriched Uranyl Nitrate Water Solutions

Table 6.10.3-11
USL Results

Experiment Set	Trending Parameter (X)	Minimum USL	Range of Applicability
21 Experiments HEU + LEU + TRIGA	Proprietary Information Withheld Pursuant to 10 CFR 2.390.	0.9318	$3.42760 \times 10^{-8} \leq X \leq 2.95740 \times 10^{-7}$
		0.9325	$4.33640 \times 10^{-5} \leq X \leq 8.53920 \times 10^{-4}$
		0.9344	$68.2 \leq X \leq 1437.5$
12 Experiments HEU + TRIGA		0.9297	$4.29310 \times 10^{-8} \leq X \leq 2.95740 \times 10^{-7}$
		0.9300	$1.31030 \times 10^{-4} \leq X \leq 8.53920 \times 10^{-4}$
		0.9307	$68.2 \leq X \leq 499.40$
11 Experiments LEU + TRIGA		0.9328	$3.42760 \times 10^{-8} \leq X \leq 4.09840 \times 10^{-8}$
		0.9330	$4.33640 \times 10^{-5} \leq X \leq 7.64030 \times 10^{-5}$
		0.9335	$770.3 \leq X \leq 1437.5$

Table 6.10.3-12
Benchmark Experiment Data

Case Id.	EALF (MeV)	²³⁵ U (atom/b-cm)	H/ ²³⁵ U	k _{eff}	σ _{MCNP}	σ _{bench}	σ _{total}
Proprietary Information Withheld Pursuant to 10 CFR 2.390.	8.1466×10^{-8}	3.4777×10^{-4}	181.8	0.99686	0.00068	0.0060	0.0060
	2.7629×10^{-7}	8.2771×10^{-4}	70.6	0.99418	0.00072	0.0072	0.0072
	8.0140×10^{-8}	3.4118×10^{-4}	185.7	1.00015	0.00067	0.0035	0.0036
	2.9574×10^{-7}	8.5392×10^{-4}	68.2	0.99470	0.00069	0.0053	0.0053
	4.2931×10^{-8}	1.3103×10^{-4}	499.4	0.99727	0.00059	0.0049	0.0049
	4.4497×10^{-8}	1.4240×10^{-4}	458.8	1.00351	0.00057	0.0046	0.0046
	7.7095×10^{-8}	3.2800×10^{-4}	193.3	0.99609	0.00071	0.0040	0.0041
	8.1742×10^{-8}	3.4777×10^{-4}	181.8	0.99648	0.00067	0.0038	0.0039
	2.9544×10^{-7}	8.5392×10^{-4}	68.2	0.99068	0.00068	0.0054	0.0054
	4.6087×10^{-8}	1.5266×10^{-4}	427.4	0.99130	0.00055	0.0054	0.0054
	8.7120×10^{-8}	3.6801×10^{-4}	150.1	0.99699	0.00052	0.0056	0.0056
	8.6658×10^{-8}	3.6801×10^{-4}	150.1	1.00139	0.00052	0.0056	0.0056
	4.0984×10^{-8}	7.6403×10^{-5}	770.3	0.99485	0.00044	0.0039	0.0039
	3.9213×10^{-8}	6.8143×10^{-5}	877.6	0.99401	0.00042	0.0042	0.0042
	3.8855×10^{-8}	6.7111×10^{-5}	897.0	0.99902	0.00041	0.0042	0.0042
	3.8754×10^{-8}	6.5820×10^{-5}	913.2	0.99249	0.00039	0.0042	0.0042
	3.5930×10^{-8}	5.2398×10^{-5}	1173.4	0.99573	0.00035	0.0048	0.0048
	3.5644×10^{-8}	5.0849×10^{-5}	1213.1	0.99694	0.00031	0.0049	0.0049
	3.5539×10^{-8}	4.9817×10^{-5}	1239.8	0.99602	0.00031	0.0049	0.0049
	3.4471×10^{-8}	4.4138×10^{-5}	1411.6	0.99930	0.00028	0.0052	0.0052
3.4276×10^{-8}	4.3364×10^{-5}	1437.5	0.99606	0.00027	0.0052	0.0052	

Table 6.10.3-13
Evaluation of the Most Reactive Fuel Element

Fuel Description	Case Id.	Water Density (g/cm ³)	k _{eff}	σ	k _s (k _{eff} + 2σ)
Type 1: 8.5 wt.% LEU 14 in, aluminum clad	Proprietary Information Withheld Pursuant to 10 CFR 2.390.	0.0	1.09966	0.00081	1.10128
		1.0	1.02449	0.00097	1.02643
Type 2: 8.5 wt.% LEU 15 in, aluminum clad		0.0	1.07874	0.00080	1.08034
		1.0	1.01324	0.00095	1.01514
Type 3: 12.5 wt.% LEU Stainless steel clad		0.0	1.13581	0.00078	1.13737
		1.0	1.02260	0.00092	1.02444
Type 4: 12.0 wt.% LEU Stainless steel clad		0.0	1.08059	0.00075	1.08209
		1.0	0.97761	0.00082	0.97925
Type 5: 8.5 wt.% HEU stainless steel clad		0.0	1.48748	0.00083	1.48914
		1.0	1.34293	0.00100	1.34493
Type 6: 20 wt.% LEU Stainless steel clad		0.0	1.30518	0.00086	1.30690
		1.0	1.21059	0.00101	1.21261
Type 7: 31 wt.% LEU Stainless steel clad	0.0	1.35907	0.00094	1.36095	
	1.0	1.28885	0.00105	1.29095	

Table 6.10.3-14
Effect of Water Density on Reactivity

Case Id.	Water Density (g/cm ³)	k _{eff}	σ	k _s (k _{eff} + 2σ)
Proprietary Information Withheld Pursuant to 10 CFR 2.390.	0.0	1.48748	0.00083	1.48914
	0.1	1.45905	0.00082	1.46069
	0.2	1.43523	0.00089	1.43701
	0.3	1.41503	0.00089	1.41681
	0.4	1.40042	0.00087	1.40216
	0.5	1.38666	0.00091	1.38848
	0.6	1.37796	0.00107	1.38010
	0.7	1.37008	0.00103	1.37214
	0.8	1.35806	0.00099	1.36004
	0.9	1.35073	0.00106	1.35285
	1.0	1.34293	0.00100	1.34493

Table 6.10.3-15
Evaluation of the Most Reactive Geometry

Case Id.	Geometry	k_{eff}	σ	k_s ($k_{eff} + 2\sigma$)
Proprietary Information Withheld Pursuant to 10 CFR 2.390.	Spaced	0.86128	0.00088	0.86304
	Center	0.83356	0.00085	0.83526
	Corners	0.87107	0.00088	0.87283
	Inside	0.85305	0.00097	0.85499

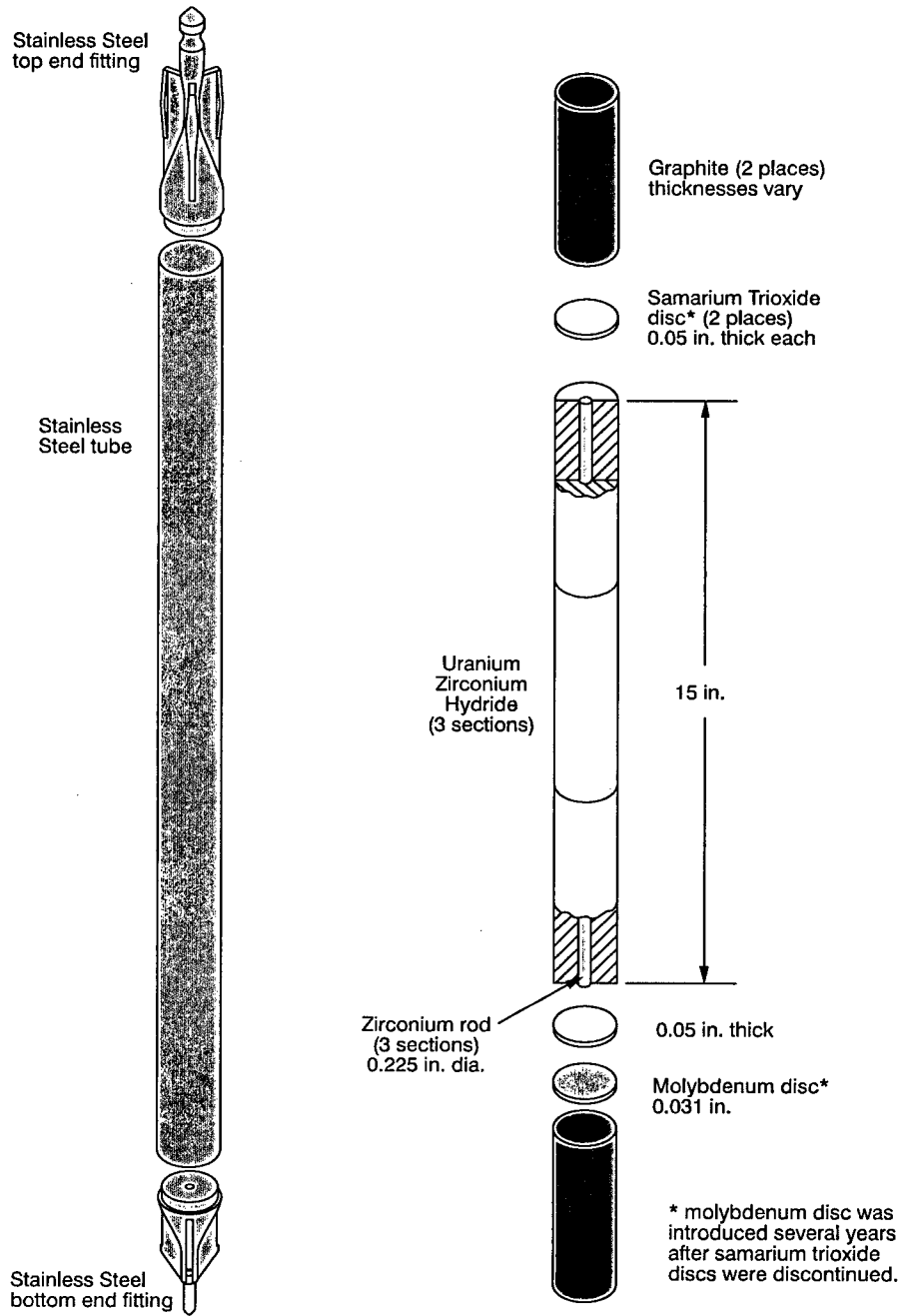


Figure 6.10.3-1
A Typical Stainless-Steel Clad TRIGA Fuel Element

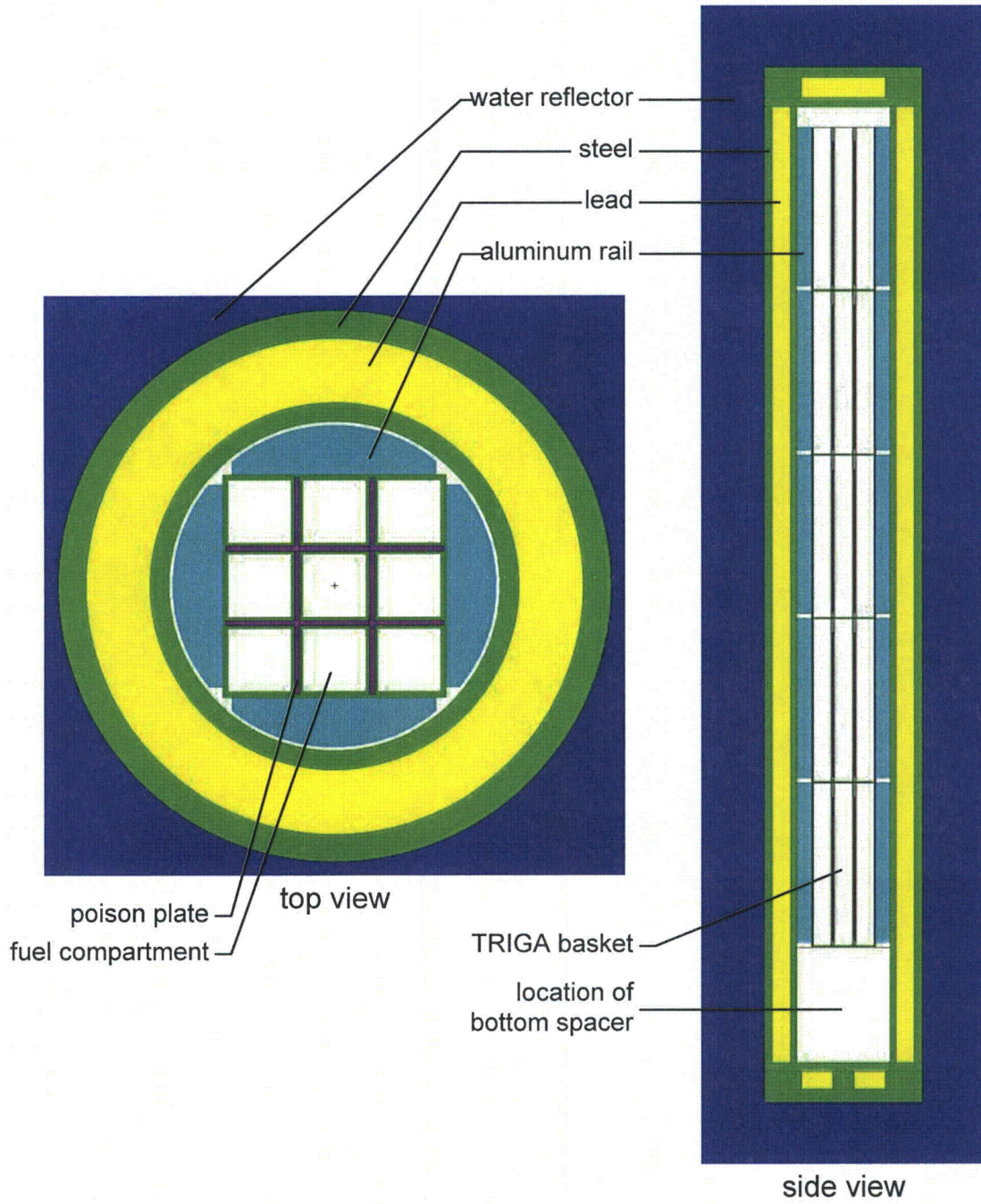


Figure 6.10.3-2
MCNP Model of the Cask

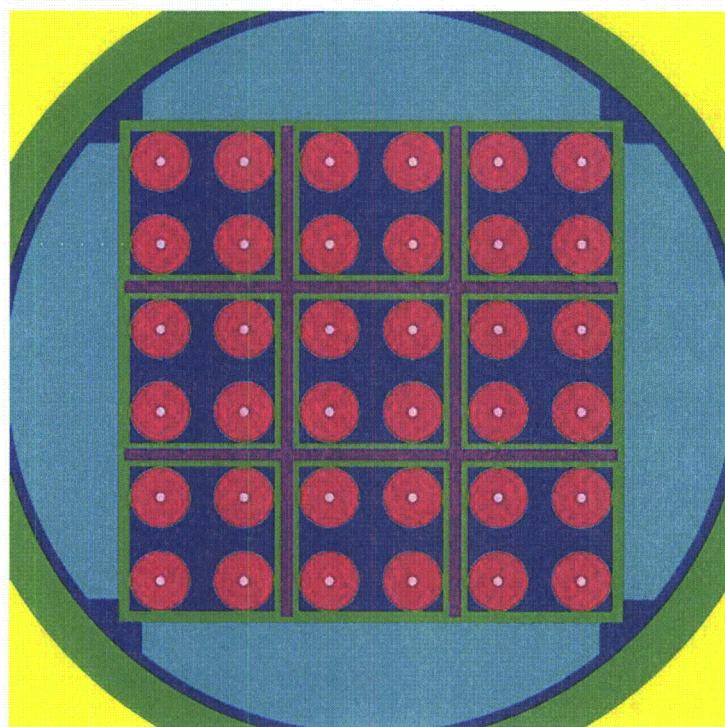


Figure 6.10.3-3
TRIGA Radial Fuel Configuration

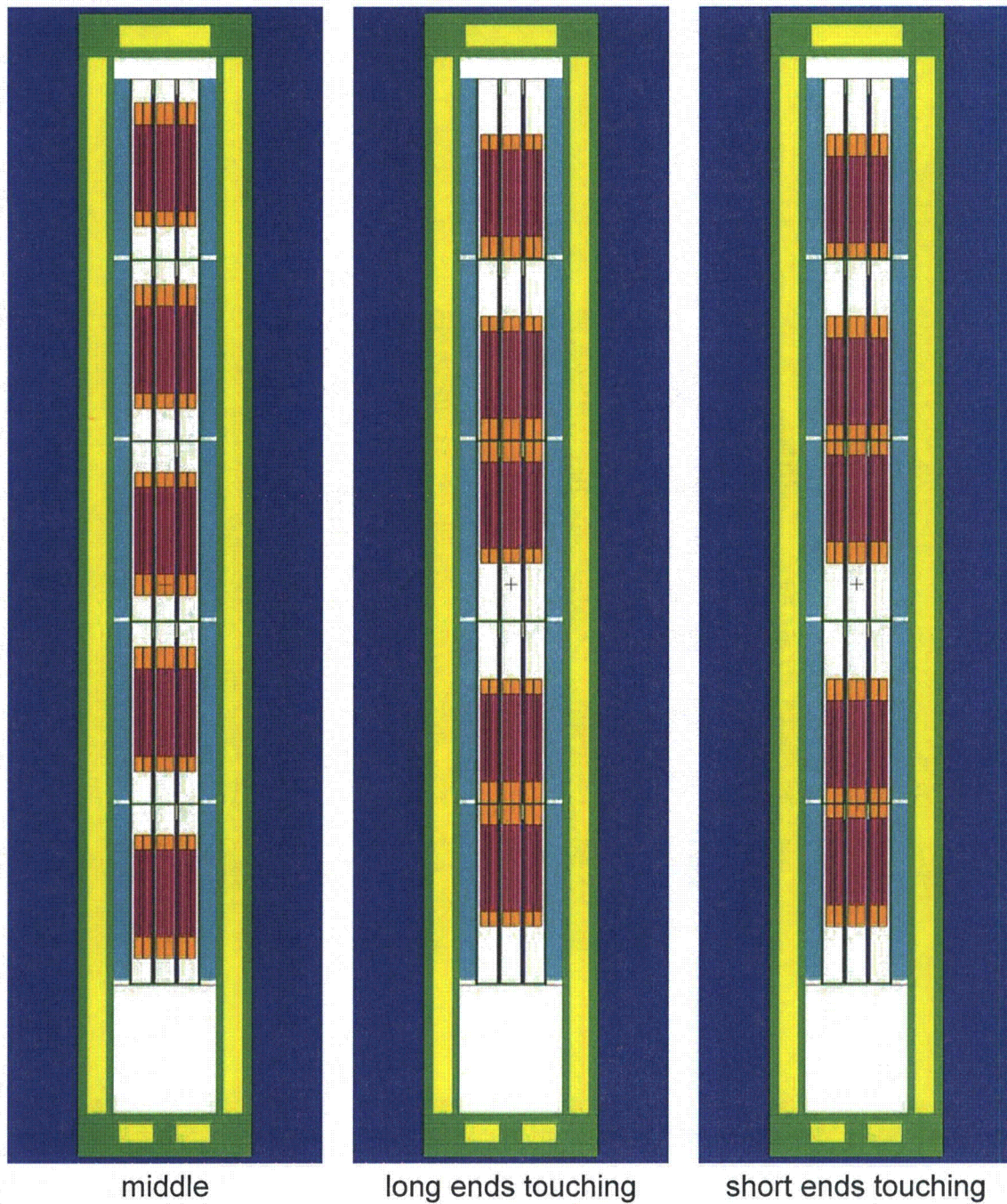


Figure 6.10.3-4
TRIGA Axial Fuel Configurations

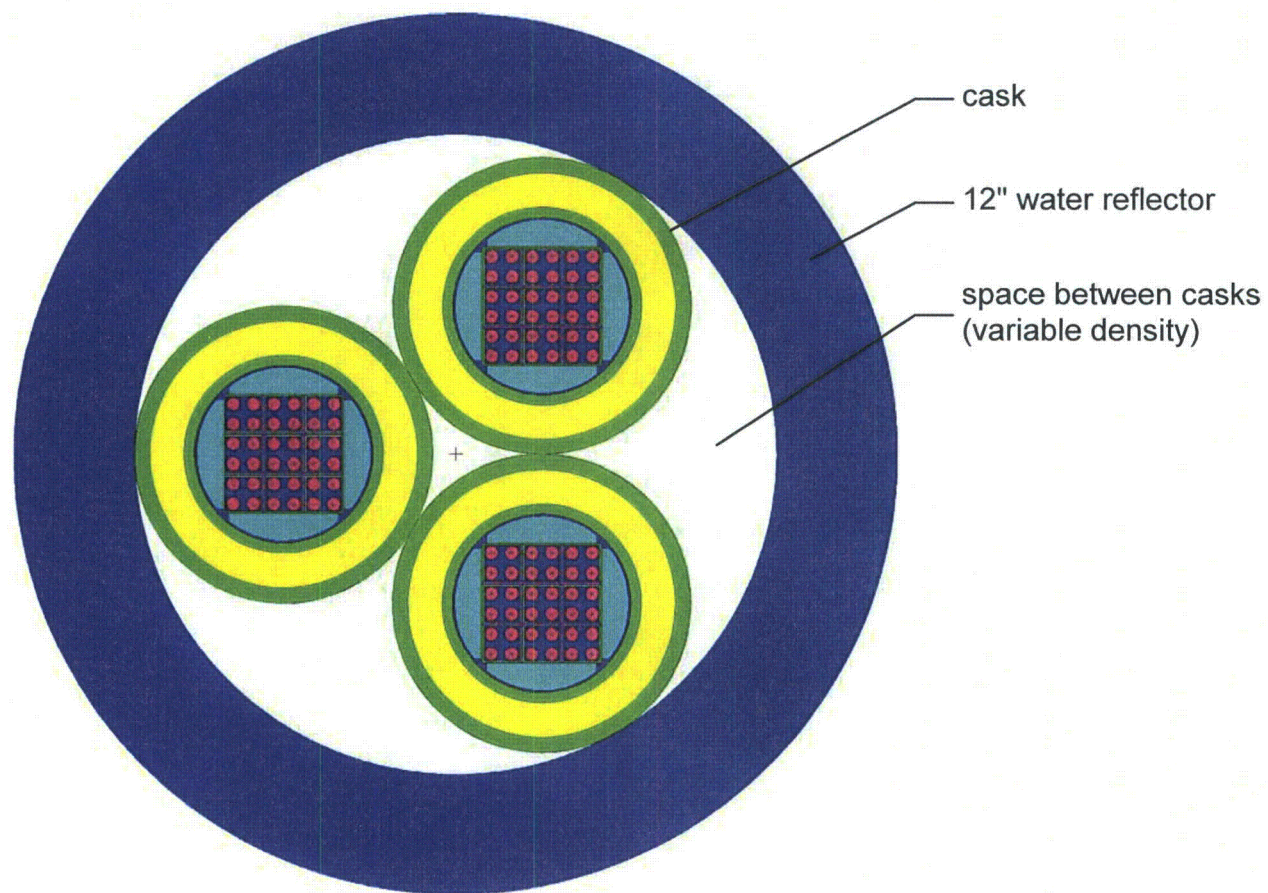


Figure 6.10.3-5
MCNP TN-LC-TRIGA NCT Array Model

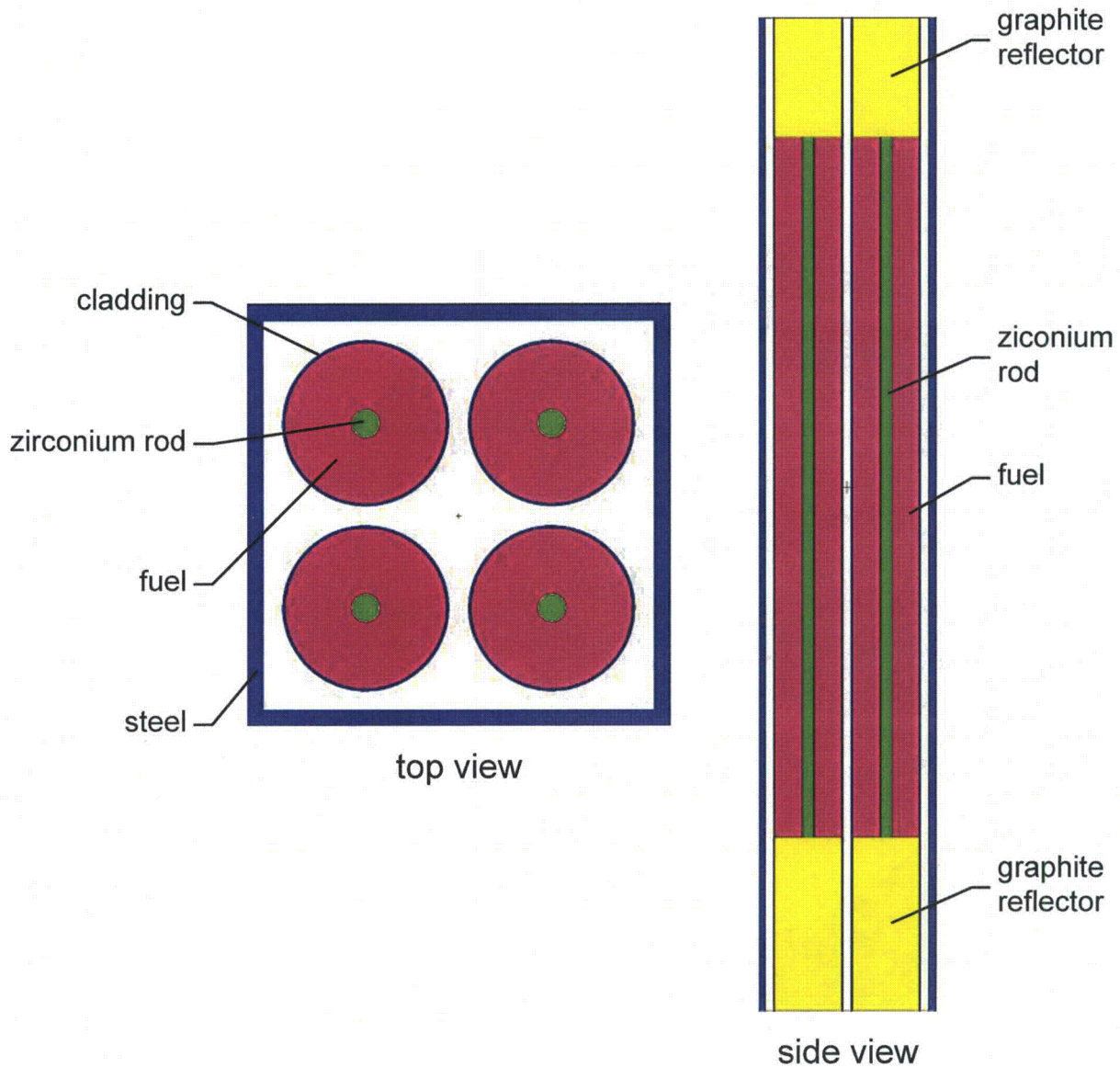


Figure 6.10.3-6
 MCNP Model of a Single Compartment with Four TRIGA Fuel Elements

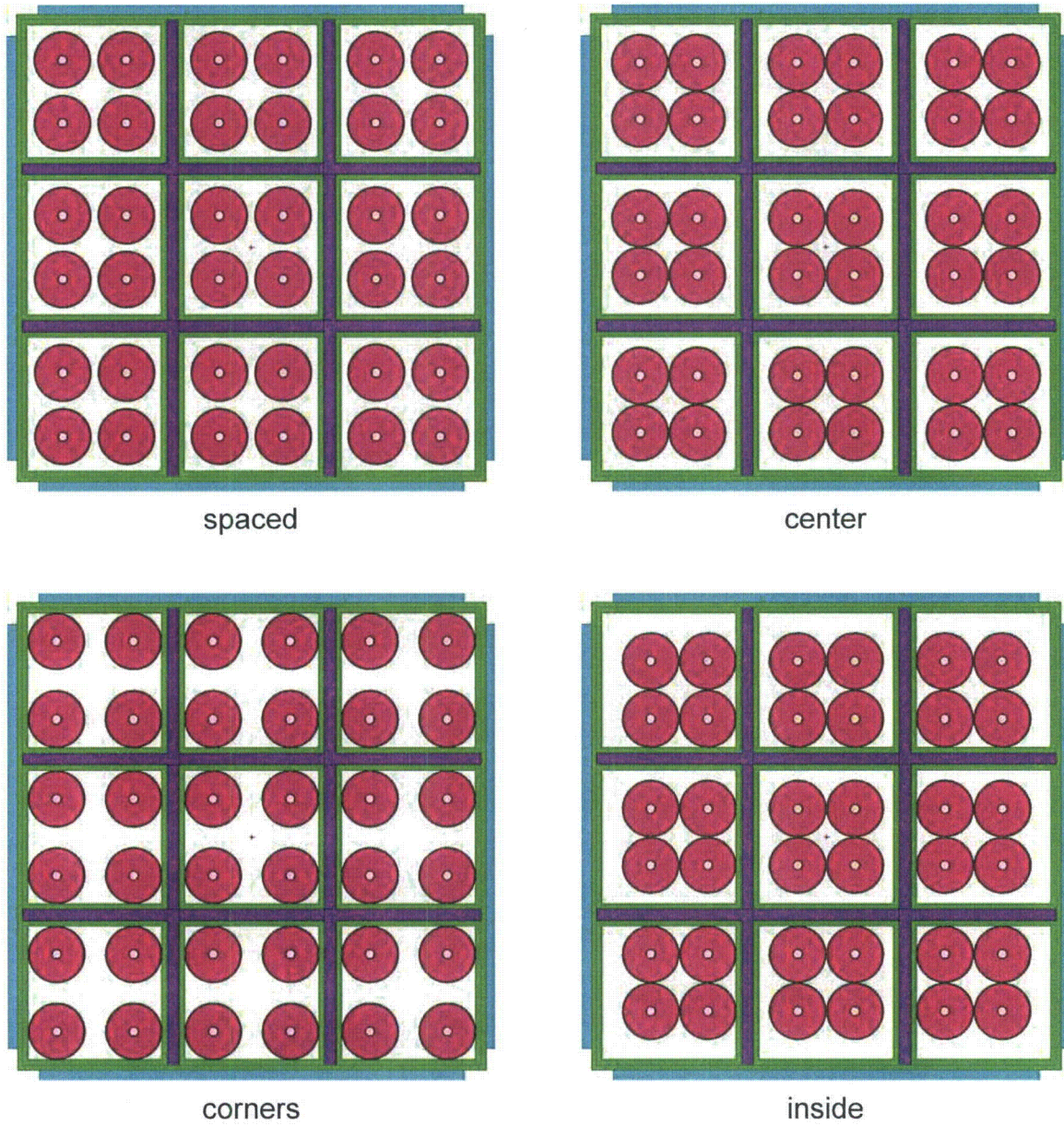


Figure 6.10.3-7
Radial Geometry Configurations

Appendix 6.10.4 1FA Basket Criticality Evaluation

TABLE OF CONTENTS

6.10.4.1	Description of the Criticality Design.....	6.10.4-1
6.10.4.1.1	Design Features.....	6.10.4-1
6.10.4.1.2	Summary Table of Criticality Evaluation.....	6.10.4-2
6.10.4.1.3	Criticality Safety Index.....	6.10.4-3
6.10.4.2	Fissile Material Contents.....	6.10.4-4
6.10.4.3	General Considerations	6.10.4-5
6.10.4.3.1	Model Configuration.....	6.10.4-5
6.10.4.3.2	Material properties.....	6.10.4-6
6.10.4.3.3	Computer Codes and Cross-Section Libraries.....	6.10.4-7
6.10.4.3.4	Demonstration of Maximum Reactivity	6.10.4-7
6.10.4.4	Single Package Evaluation	6.10.4-11
6.10.4.4.1	Configuration.....	6.10.4-11
6.10.4.4.2	Results.....	6.10.4-13
6.10.4.5	Evaluation of Package Arrays under Normal Conditions of Transport	6.10.4-14
6.10.4.5.1	Configuration.....	6.10.4-14
6.10.4.5.2	Results.....	6.10.4-14
6.10.4.6	Package Arrays under Hypothetical Accident Conditions.....	6.10.4-15
6.10.4.7	Fissile Material Packages for Air Transport.....	6.10.4-16
6.10.4.8	Benchmark Evaluations.....	6.10.4-17
6.10.4.8.1	Applicability of Benchmark Experiments	6.10.4-17
6.10.4.8.2	Bias Determination	6.10.4-17
6.10.4.9	Appendix	6.10.4-19
6.10.4.9.1	References.....	6.10.4-19

Proprietary Information Withheld Pursuant to 10 CFR 2.390.

LIST OF TABLES

Table 6.10.4-1	Summary of Criticality Evaluation.....	6.10.4-23
Table 6.10.4-2	PWR Fuel Assembly Parameters	6.10.4-24
Table 6.10.4-3	BWR Fuel Assembly Parameters.....	6.10.4-27
Table 6.10.4-4	Parameters Used for MOX Fuel Rods.....	6.10.4-29
Table 6.10.4-5	Parameters Used for EPR and Generic Fuel Rods	6.10.4-29
Table 6.10.4-6	Cask Dimensions for Modeling.....	6.10.4-30
Table 6.10.4-7	Materials Modeled.....	6.10.4-30
Table 6.10.4-8	Most Reactive PWR Fuel	6.10.4-31
Table 6.10.4-9	Internal Moderator Density Variation Results – PWR Fuels	6.10.4-33
Table 6.10.4-10	Assembly Positioning – PWR Fuels	6.10.4-34
Table 6.10.4-11	Dimension Variation Study – PWR Fuels.....	6.10.4-34
Table 6.10.4-12	Rod Pitch Variation – PWR Fuels.....	6.10.4-34
Table 6.10.4-13	Single-Ended Shear Analysis – PWR Fuels.....	6.10.4-35
Table 6.10.4-14	Double-Ended Shear Analysis – PWR Fuels	6.10.4-35
Table 6.10.4-15	Most Reactive BWR Fuel in Each Fuel Category.....	6.10.4-36
Table 6.10.4-16	Dimension Variation Study – BWR Fuels	6.10.4-37
Table 6.10.4-17	Rod Pitch Variation – BWR Fuels	6.10.4-38
Table 6.10.4-18	25 Pin Can Analyses.....	6.10.4-40
Table 6.10.4-19	Possible PRA Configuration for WE 14x14 Class Assemblies	6.10.4-40
Table 6.10.4-20	Evaluation of Effects due to PRA Clad Variation, Single Package	6.10.4-41
Table 6.10.4-21	Design Basis PRA Configuration for Various PWR Assemblies, HAC Single Package	6.10.4-41
Table 6.10.4-22	NCT and HAC Results for Single Package Transport	6.10.4-42
Table 6.10.4-23	NCT Package Array Results at Varying External Moderator Density – PWR Fuels (no PRAs).....	6.10.4-42
Table 6.10.4-24	NCT Package Array Results with PRAs for the Most Reactive PWR Configuration.....	6.10.4-43
Table 6.10.4-25	NCT Package Array Results at Varying External Moderator Density – BWR Fuels	6.10.4-43
Table 6.10.4-26	Summary of PRA Requirements Under all Conditions of Transport for PWR Fuel Assembly Classes.....	6.10.4-1
Table 6.10.4-27	Criticality Experiment Benchmark Results.....	6.10.4-2
Table 6.10.4-28	USL Functions.....	6.10.4-6
Table 6.10.4-29	USL Determination for Criticality Analysis	6.10.4-6

LIST OF FIGURES

<i>Figure 6.10.4-1</i>	<i>1FA Basket with All Functional Components</i>	<i>6.10.4-50</i>
<i>Figure 6.10.4-2</i>	<i>PWR Compartment Components</i>	<i>6.10.4-51</i>
<i>Figure 6.10.4-3</i>	<i>BWR Compartment Sleeve and Hold-Down Ring</i>	<i>6.10.4-52</i>
<i>Figure 6.10.4-4</i>	<i>25 Pin Can and Fuel Rod Tubes</i>	<i>6.10.4-53</i>
<i>Figure 6.10.4-5</i>	<i>Radial and Axial Cross Sections of the 1FA Basket KENO Model</i>	<i>6.10.4-54</i>
<i>Figure 6.10.4-6</i>	<i>TN-LC 1FA Basket KENO Model</i>	<i>6.10.4-55</i>
<i>Figure 6.10.4-7</i>	<i>BWR and PWR Fuel Models</i>	<i>6.10.4-56</i>
<i>Figure 6.10.4-8</i>	<i>Array of Casks for NCT Analysis</i>	<i>6.10.4-57</i>
<i>Figure 6.10.4-9</i>	<i>Damaged Fuel Models</i>	<i>6.10.4-58</i>
<i>Figure 6.10.4-10</i>	<i>25 Pin Can Model with PWR Fuel</i>	<i>6.10.4-59</i>
<i>Figure 6.10.4-11</i>	<i>Assembly Positioning</i>	<i>6.10.4-60</i>
<i>Figure 6.10.4-12</i>	<i>PRA Locations for PWR Fuel Requiring 5 PRAs</i>	<i>6.10.4-61</i>
<i>Figure 6.10.4-13</i>	<i>Possible PRA Configuration for WE 14x14 and WE 15x15 Class Assemblies – NCT and HAC</i>	<i>6.10.4-62</i>
<i>Figure 6.10.4-14</i>	<i>BWR Modeling Cases to Assess Hold Down Ring Effects</i>	<i>6.10.4-63</i>
<i>Figure 6.10.4-15</i>	<i>PRA Configuration for BW 15x15, BW 17x17 and WE 17x17 Class Fuel Assemblies – NCT and HAC</i>	<i>6.10.4-64</i>
<i>Figure 6.10.4-16</i>	<i>KENO Model of the Most Reactive Case with Poison Plate Bolt Holes</i>	<i>6.10.4-65</i>

Appendix 6.10.4 1FA Basket Criticality Evaluation

NOTE: References in this Appendix are shown as [1], [2], etc. and refer to the reference list in Appendix 6.10.4.9.1.

This Appendix presents the criticality evaluation of the 1FA basket. The 1FA basket allows the transportation of one intact PWR or BWR fuel assembly, or up to 25 intact individual PWR, BWR, EPR or MOX fuel pins. The following analyses demonstrate that the TN-LC complies with the requirements of 10CFR71.55 and 71.59. The Criticality Safety Index (CSI), per 10CFR71.59, is 100.

6.10.4.1 Description of the Criticality Design

6.10.4.1.1 Design Features

Light Water Reactor (LWR) assemblies and individual pins are transported by the 1FA Basket, as shown in Figure 6.10.4-1. Components labeled B through E in this figure are shown in further detail in subsequent figures.

The PWR compartment is attached to the aluminum rail as shown in Figure 6.10.4-2. **(Proprietary Information Withheld Pursuant to 10 CFR 2.390.)** The tolerances are important in the analysis to determine the most reactive configuration.

The BWR compartment **(Proprietary Information Withheld Pursuant to 10 CFR 2.390.)** to ensure that the resultant reactivity is conservative.

The 25 pin can accommodates PWR, BWR, MOX or EPR fuel rods. Two types of pin can are available, with different cavity lengths and end lead shielding. Because axial details are ignored in the criticality models, these two types are equivalent for criticality analysis. There are two fabrication options that exist for the 25 pin can. The option used in the calculation models is Option 2, which is displayed in Figure 6.10.4-4. A notable difference between Options 1 and 2 is that in Option 1, the corners are rounded and the tubes in the corner positions fit without the gaps as shown for Option 2. The choice of one option over the other does not make a difference in the criticality results. Option 2 is used to simplify the modeling.

Proprietary Information Withheld Pursuant to 10 CFR 2.390.

(Proprietary Information Withheld Pursuant to 10 CFR 2.390.) The Boron-10 content represents the minimum loading specification after either 75 percent or 90 percent credit is applied, depending on the poison plate material used. Therefore, if a 75 percent credit is applied, the loading will actually be 20 mg/cm², and if the credit applied is 90 percent, the loading will be 16.7 mg/cm². The boron loading in the

poison plates remains the same regardless of whether a PWR assembly, BWR assembly, or individual pins are transported.

Also shown in Figure 6.10.4.2 are stainless steel bolts that bore through the poison plates. These bolts attach the aluminum rails to the basket frames and pass through the poison plates. In Section 6.10.4.4.1 the effect of these stainless steel holes is evaluated by modifying the system with the most reactive fuel and configuration.

Additionally, Poison Rod Assemblies (PRAs) are required while transporting PWR fuel assemblies in order to ensure that the maximum reactivity is subcritical and below the Upper Subcritical Limit (USL). The minimum required B₄C content of the absorber rods in the PRAs is 40 percent theoretical density (TD) (75 percent credit is taken in the criticality analysis, or 30 percent TD). The minimum required B₄C content of the absorber rods is only 30 percent (in the KENO input) because assuming a higher B₄C content is not expected to reduce the reactivity of the system since the absorber rods are already “black” to the neutrons in the system. Note that the absorber rods are also referred to as PRAs in this Appendix.

The BWR fuel assembly compartment is surrounded by the PWR compartment and the 25 pin can is placed in the BWR compartment. Additional reactivity control is not necessary for the BWR and 25 pin can transportation.

6.10.4.1.2 Summary Table of Criticality Evaluation

The upper subcritical limit (USL) for ensuring that the package is acceptably subcritical as determined in Section 6.10.4.8 is:

$$\text{USL} = 0.9420$$

The package is considered to be acceptably subcritical if the computed k_{safe} (k_s), which is defined as $k_{\text{effective}}$ (k_{eff}) plus twice the statistical uncertainty (σ), is less than or equal to the USL, or:

$$k_s = k_{\text{eff}} + 2\sigma \leq \text{USL}$$

The USL is determined on the basis of a benchmark analysis and incorporates the combined effects of code computational bias, the uncertainty in the bias based on computational uncertainties, and an administrative margin. The results of the benchmark analysis indicate that the USL is adequate to ensure subcriticality of the package.

The package design is shown to meet the requirements of 10 CFR 71.55(b). No credit is taken for fuel burnup; in other words, the fuel rods are modeled as fresh fuel, which ensures that a highly conservative k_s is obtained. The package is evaluated under Normal Conditions of Transport (NCT) and Hypothetical Accident Conditions (HAC) in accordance with the requirements of 10 CFR 71.55 and 10 CFR 71.59. In all single package evaluations, water is modeled in all cavities with the most reactive density for both NCT and HAC conditions. Close full reflection of the package is achieved using 12 feet of water.

In the NCT array models, a close-packed array of three packages is utilized. The entire array is reflected with 12 feet of water. No HAC array models are developed. Therefore, the HAC array result is the same as the single package result.

The maximum results of the criticality calculations are summarized in Table 6.10.4-1. The maximum calculated k_s is 0.9366, which occurs for HAC with a PWR fuel assembly. The maximum reactivity is below the USL of 0.9420.

6.10.4.1.3 Criticality Safety Index

No HAC array models are developed ($2N=1$). Therefore, per 10CFR71.59, $N=0.5$, and the criticality safety index (CSI) is $50/N = 100$. In the NCT array cases, $5N=2.5$, so that 3 packages are modeled.

6.10.4.2 Fissile Material Contents

The fissile materials are a single PWR or BWR fuel assembly. Additionally, PWR, BWR, EPR and MOX fuel pins are allowed in the 25 pin can.

The PWR fuel assemblies and their parameters are provided in Table 6.10.4-2. The KENO model fuel assemblies are constructed using these parameters.

Similarly, the BWR fuel assembly parameters are provided in Table 6.10.4-3. As stated, no credit is taken for burn up of fuel in the calculations. A maximum enrichment of 5.0 wt. percent U-235 is used for all fuel assemblies listed in Table 6.10.4-2 and Table 6.10.4-3, with the following exception. For the CE 15x15 class assemblies, the maximum enrichment is 3.7 wt. percent U-235.

Each fuel assembly listed for the PWR assemblies is modeled using nominal dimensions within the cask to obtain a limiting assembly with the highest k_s for subsequent analyses. For BWR fuel, the most reactive fuel assembly for each lattice group is obtained. In addition, since the BWR LaCrosse fuel assemblies have a much smaller active fuel length than the other 10x10 assemblies, both are evaluated individually. The two LaCrosse fuel assemblies are Allis Chalmers and Exxon/ANF.

In order to qualify individual fuel rods for transport, the fuel rods from the most reactive PWR and BWR assembly calculations are inserted in the fuel rod tubes located in the 25 pin can. The MOX and EPR fuel rods are modeled according to the parameters provided in Table 6.10.4-4 and Table 6.10.4-5, respectively. Additionally, a generic UO₂ fuel model is considered in the 25 pin can with parameters shown in Table 6.10.4-5. The plutonium isotopic vector provides a bounding k_s and the analysis is performed with three different plutonium concentrations: 6.0, 8.0 and 10.2 wt. percent plutonium.

6.10.4.3 General Considerations

6.10.4.3.1 Model Configuration

The cask model comprises the fuel, basket, and packaging, which are modeled explicitly in SCALE [1]. The packaging is conservatively modeled without the neutron shield and impact limiters in both the NCT and HAC conditions. The length of the cask modeled covers the active length of the fuel and 12 feet of water is modeled in the axial directions as well as the sides of the cask. A KENO model of the cask without fuel is shown in Figure 6.10.4-5. The figure on the left shows the radial cross section of the cask with the 25 pin can. In the same figure, the axial cross section is also presented on the right.

A more detailed view of the KENO model is shown in Figure 6.10.4-6. In the figure, all the compartments are shown to provide an overall view of the compartments relative to one another. The cask model is based on materials and dimensions shown in the drawings in Chapter 1. The dimensions of the components labeled in Figure 6.10.4-6 are listed in the accompanying Table 6.10.4-6.

In the simulation models, only the lengths of the compartments/components that cover the active length of the fuels to be transported are modeled.

In both the NCT and HAC models, water is modeled inside the package at the density that maximizes reactivity. Because the cask is designed for wet loading, water drains freely inside the basket, and preferential flooding scenarios are not credible. However, the cavity could be partially flooded. Because the baskets drain freely, if the TN-LC cavity is partially flooded, the only credible scenario is that some fuel would be submerged in water, and the remaining fuel would remain unsubmerged. Therefore, any partial flooding scenarios would result in unmoderated fuel. LWR fuels have very low reactivity in the absence of moderation. Therefore, any partial flooding would uncover fuel and decrease the reactivity. For these reasons, cases are not developed for partial and/or preferential flooding.

Normal Conditions of Transport Fuel Models:

The intact fuel models constructed are used for the NCT analysis. The NCT analysis calls for simulation of single package transport and an array of packages. For BWR and PWR fuels, the assemblies are modeled, centered in their respective compartments with the fuel rods also centered in each lattice cell. Water is modeled in the compartment cavity and fuel gap with Zircalloy as the cladding material. The fuel parameters used are presented in Table 6.10.4-2 and Table 6.10.4-3. The PWR and BWR fuel models for NCT single package analysis are shown in Figure 6.10.4-7. The model on the left represents the most reactive BWR fuel assembly for the 10x10 assemblies, while the model on the right represents the most reactive PWR fuel assembly in NCT.

In Figure 6.10.4-8, a model of the three array package used for NCT analysis is shown. The figure shows that some space exists between the casks by the virtue of the arrangement of the casks. The three casks are surrounded by 12 feet of water in all directions, while the space between the casks is modeled with various moderator densities to determine the most reactive external moderator density for the configuration shown.

Hypothetical Accident Condition Fuel Models:

The analytical results reported in Chapter A.2, Appendix A.2.13.1 demonstrate that the cask containment boundary and basket structure do not experience any significant distortion under hypothetical accident conditions. Therefore, the basket and cask geometry remain intact in HAC.

This analysis addresses potential fuel damage scenarios under HAC of transportation. The type and extent of fuel rod damage under HAC can be broken down into several categories. The worst case gross damage from a cask-drop accident is assumed to be either a single-ended or double-ended rod shear with fresh water intrusion. The bent or bowed fuel rod cases assume that the fuel is intact but not in its nominal fuel rod pitch. It is possible that the fuel rods may be crushed

inward or bow outward to a certain degree. Therefore, this will be evaluated by varying the fuel rod pitch from a minimum pitch that is limited by the clad outer diameter, and a maximum pitch that is limited by the compartment inner width. All pitch variations assume a uniform rod pitch throughout the entire fuel matrix.

The single-ended fuel rod shear cases assume that a row of fuel rods shears radially away from the parent assembly and is displaced to a new location. The fuel pellets are assumed to remain in the fuel rod. This case will be evaluated by displacing one row of rods from the base fuel assembly matrix at small increments toward the compartment wall. The base fuel assembly will be at nominal pitch and positioned at the left corner of the compartment to maximize the spacing of the sheared row of rods. A smaller rod pitch for the base fuel assembly matrix was not chosen because it has been shown from the pitch cases that decreasing the rod pitch decreases reactivity. Increasing the rod pitch will increase reactivity; however, the resulting model is similar to and is bounded by the rod pitch varying cases described above and therefore will not be duplicated here.

The double-ended fuel rod shear cases assume that a row of fuel rods shears radially from the parent fuel assembly and then breaks axially into two pieces. The broken fuel rods are then conservatively modeled with the same length as the intact fuel rods. These two rows of rods are free to move away or toward the parent fuel assembly. In order to bound all scenarios of this case, the base assembly is reduced by one row, and two sheared rows are added. The length of the sheared rods is the same as the remaining rods in the assembly. The two rows of rods are then shifted toward and away from the base assembly at incremental distances. Pitch and location of the base assembly remain as described in the single-shear case. Figure 6.10.4-9 illustrates the typical models used for the (a) single-ended shear analysis, (b) rod pitch analysis, and (c) double-ended shear analysis. The actual model is the WE 14x14 Std. assembly. These figures are for illustration purposes only.

The models shown in Figure 6.10.4-9 are those used in the PWR fuel analysis. Only the rod pitch analysis is performed for BWR fuels since it is demonstrated that the most reactive fuel is the PWR, and any BWR damaged fuel will be bounded by that of the PWR fuel.

25 Pin Can Fuel Models:

Proprietary Information Withheld Pursuant to 10 CFR 2.390. Only the active fuel length of the tubes is modeled. A model of the can with 25 PWR fuels is displayed in Figure 6.10.4-10.

6.10.4.3.2 Material properties

In Table 6.10.4-7, the different materials, the mixture number as shown in KENO inputs, and other relevant parameters are shown. Water has more than one entry in the material data cards because it is important to distinguish between water in the fuel lattice and water that exists between the casks, as shown in Figure 6.10.4-8. The materials used are part of the Standard Composition library with built-in densities. Only the poison plate definition required an explicit density definition of 2.693 g/cm³. See also the sample input file in Section 6.10.4.9.2.

6.10.4.3.3 Computer Codes and Cross-Section Libraries

The CSAS5 control module of the SCALE6 program [1] is used to calculate the effective multiplication factor of the fuel in the cask. The maximum k_s for the calculation was determined with the following formula:

$$k_s = k_{\text{eff}} + 2\sigma$$

The CSAS5 control module allows simplified data input to the functional modules BONAMI, NITAWL, and KENO V.a. These modules process the required cross sections and calculate the k_{eff} of the system. BONAMI performs resonance self-shielding calculations for nuclides that have Bondarenko data associated with their cross sections. NITAWL applies a Nordheim resonance self-shielding correction to nuclides having resonance parameters. Finally, KENO V.a calculates the k_{eff} of a three-dimensional system. A sufficiently large number of neutron histories are run so that the standard deviation is below 0.0010 for all calculations. The criticality analysis used the 44-group cross-section library built into the SCALE6 program. ORNL uses ENDF/B-V data to develop this broad-group library specifically for criticality analysis of a wide variety of thermal systems.

6.10.4.3.4 Demonstration of Maximum Reactivity

The criticality analysis methodology used to select the bounding fuel assemblies is as follows:

1. Evaluate the PWR and BWR fuel assemblies shown in Table 6.10.4-2 and Table 6.10.4-3, respectively, to determine the most reactive fuel. At this stage, the cask component dimensions will be at their nominal values. The PWR fuels will be evaluated at nominal pitch and maximum pitch. The maximum pitch is obtained by dividing the inner width value of the compartment by the number of rods in one row of the assembly. This is done to determine whether the most reactive fuel in NCT is different from the most reactive fuel in HAC. For BWR, the most reactive fuel for each fuel category is obtained at nominal pitch.
2. Once the most reactive fuel assemblies are determined, changes in reactivity are assessed for internal moderator densities between 0.01% and 100%.
3. In Steps 1 and 2, the fuel assembly is centered in the compartment. A set of calculations is performed to maximize reactivity by changing the placement of the fuel assembly to the bottom-center and left corner of the compartment.
4. The manufacturing tolerances on the cask body have a negligible effect on the reactivity. However, the tolerances on basket dimensions may affect the reactivity and are explicitly addressed. The stainless steel PWR fuel compartment thickness has a tolerance of ± 0.05 in., while the poison plate has a thickness tolerance of ± 0.05 in. The tolerance for the BWR fuel compartment is the same as that of the PWR fuel. Also, a gap of 0.1875 in. that exists between the two compartments is subject to variation. The effect on reactivity of varying these dimensions is evaluated once the most reactive assembly location is determined in Step 3.
5. The most reactive fuel under HAC obtained in Step 1 for PWR fuel is used to evaluate the behavior of this fuel assembly in the various damaged fuel scenarios described in Section

6.10.4.3.1. These evaluations entail three independent damaged fuel evaluations: Rod Pitch Variation, Single-Shear Analysis, and Double-Shear Analysis. Only the Rod Pitch Variation for each fuel category is considered for BWR fuel. The most reactive damaged fuel scenario obtained is the design basis model to perform criticality calculations for HAC.

6. The PWR fuel assembly results from Steps 1 through 5 exceed the USL, both for NCT and HAC. Therefore, the PWR fuel assemblies must be poisoned with PRAs that are inserted into the fuel assembly. The BWR fuel assemblies do not require PRAs.
7. For the 25 fuel pin can, the design basis fuel for the most reactive PWR and BWR fuel are considered. Additionally, MOX and EPR fuel pins are considered

The steps delineated above are followed in order to determine the maximum reactivity under several postulated scenarios.

PWR Fuel Assembly:

In Step 1, the most reactive PWR fuel assembly is determined. The basket and other components are modeled using nominal dimensions for the PWR case. The results are presented in Table 6.10.4-8. Note that the results exceed the USL in this and subsequent tables because PRAs are not modeled.

As shown in Table 6.10.4-8, the most reactive PWR fuel under NCT is the BW 15x15 B11 (Case ID: P_A010), and for HAC, it is the WE 14x14 Std/LOPAR/ZCA/ZCB (Case ID: P_A045).

In Step 2, internal moderator density for the most reactive fuel assemblies was varied to determine the density that would result in the highest reactivity. As shown in Table 6.10.4-9, the PWR fuel is most reactive at 100% internal moderator density, under both NCT and HAC scenarios. The PWR internal moderator density variation results are performed with nominal cask and compartment dimensions.

The drawing of the compartment shown in Figure 6.10.4-2 depicts a radial cavity created by virtue of the presence of the poison plates between the aluminum rail and compartment. As illustrated in Figure 6.10.4-6, this cavity is not included in the model. Therefore, a scoping calculation has been performed to quantify the difference in reactivity due to the presence of the cavity. The WE 17x17 RFA fuel assembly is selected for both NCT and HAC scenarios. In Table 6.10.4-8, the k_s for this fuel assembly under NCT condition is 0.9893 without the presence of the cavity, while it is 0.9830 for the case with the cavity. For HAC, Table 6.10.4-8 indicates that the k_s is 1.0171 for the case without the cavity, and the case with the cavity results in k_s of 1.0133. Therefore, in terms of modeling, it is concluded that the absence of the cavity results in a bounding analysis.

In Step 3, the effect of varying the fuel assembly position within the compartment is determined. The three positions compared are the center, bottom-center, and bottom left-corner positions. Nominally, the central position result should be the same as the result that was obtained for the moderator variation cases performed in Step 2 for the 100 percent internal moderator density case (compare Case P_B011 and P_C002). There exists an inconsistency due to the following negligible effect: the fuel rod models used in Step 2 are centered in their lattices regardless of their position in the assembly (i.e., the outer fuel rods do not touch the compartment). In Step 3,

the outer rods touch the sides of the compartment, which results in a slightly larger pitch. This will result in slight increase in reactivity. Nevertheless, out of the three positions, the central case is most reactive and that will be picked as the standard most reactive position for NCT and HAC. The results are presented in Table 6.10.4-10 with Figure 6.10.4-11 to illustrate the positioning.

In Step 4, the compartment and poison plate dimensions are changed to reflect tolerance effects. **(Proprietary Information Withheld Pursuant to 10 CFR 2.390.)** The results, presented in Table 6.10.4-11 show that the nominal compartment thickness and a poison plate thickness of 0.20 in. results in the most reactive configuration (Case ID: P_D001). The B-10 loading is held constant during this analysis, i.e. the 15 mg B-10/cm² is modeled in each case. The result in Case ID P_D001 also represents the most reactive PWR fuel under NCT.

In Step 5, the compartment and poison plate configuration from Case P_D001 is used to obtaining the most reactive fuel for HAC. That is, the most reactive fuel obtained in Table 6.10.4-8 (P_A045) is modeled for further analysis in the three damaged fuel scenarios described in Section 6.10.4.3.1.

In the HAC analysis, the PWR fuels undergo the aforementioned three different damaged fuel analyses. In Table 6.10.4-12, it is shown that when the PWR fuel (WE 14x14 Std/LOPAR/ZCA/ZCB) is at its maximum pitch, reactivity is maximized for the rod pitch study. In Table 6.10.4-13 and Table 6.10.4-14, the single- and double- ended shear scenario results are presented. The configuration of the cask is at the most reactive state determined thus far.

For single shear and double shear analyses, it is shown that the BW 15x15 B11 fuel assembly results in the most reactive configuration. However, the WE 14x14 Std/LOPAR/ZCA/ZCB fuel assembly remains the most reactive for damaged fuel cases, as shown in Table 6.10.4-12.

The results presented thus far exceed the USL. In Step 6, PRAs are added to the fuel assembly to reduce the reactivity below the USL. The PRA analysis is presented in Section 6.10.4.4.

BWR Fuel Assembly:

The methodology is repeated for BWR fuel. Where the specific step is modified, it is explicitly stated below. For the BWR case, the most reactive component dimensions are used. In step 1, the most reactive BWR fuel for each array type is presented in Table 6.10.4-15. For the 10x10 type, the LaCrosse fuels have a smaller active fuel length and are also more reactive than all the other array types. Therefore, they are analyzed individually.

In the models, the BWR fuel assembly is modeled in the axial center of the cavity. Since the fuel assembly is modeled in an axially centered position along the compartment, some of the fuel assemblies were modeled as if they extend to the hold-down ring. As a result, in some cases the hold down ring is included. The effect of modeling the BWR fuel so that the fuel is not axially centered and the hold down ring is not included is evaluated. Case B_A005, for Group 1 assemblies is rerun without the hold down ring and resulted in a k_s of 0.7258 (Case B_A005-1). Therefore, modeling the assembly in a central position axially has no effect in reactivity. The difference between the two models is illustrated in Figure 6.10.4-14. These two cases indicate

that the location of the fuel axially does not affect reactivity and covers the use of spacers placed either at the top or the bottom of the fuel assembly in the cask.

Not all fuel assemblies in the BWR fuel list given in Table 6.10.4-3 are evaluated. This is due to the fact that those grouped into one category, such as GE, Group 1, have similar parameters that allow this grouping process. The groups are as follows: the GE Group 1 includes GE5, GE-Pres, GE-Barrier, and GE8 Type I, the GE Group 2 includes GE8 Type II, GE9, and GE10, and the Framatome ANP Group represents the 9x9 – 79/2, 72, 80, and 81 fuel assemblies. The most reactive BWR fuel assembly in each class are highlighted bold in Table 6.10.4-15.

Based on the analyses performed for PWR fuel, it is clear that an internal moderator density of 100 percent and a central fuel assembly position will result in the most reactive states. As a result, Steps 2 and 3 are skipped, and the dependence of reactivity on tolerance is assessed in Step 4.

Proprietary Information Withheld Pursuant to 10 CFR 2.390.

As the results in Table 6.10.4-16 indicate, decreasing the size of the gap between the BWR and PWR compartments (increasing the BWR compartment thickness) increases the k_s of the system. For the 8x8 fuel assembly class, the GE group 1 assembly is selected as the most reactive fuel. Under NCT, these six assemblies (for further analysis, the GE group 2 assembly is not considered) are the most reactive fuel assemblies. These assemblies are also considered in HAC.

In the HAC scenario, unlike the three different damaged fuel models analyzed for PWR fuels as described by Step 5, only the fuel pitch variation analysis is performed. This is sufficient to show that HAC of PWR fuel transport bounds that of BWR fuels. The results are shown in Table 6.10.4-17.

For BWR fuels, the most reactive fuel for HAC is taken to be the Allis Chalmers – LaCrosse fuel, as shown in Table 6.10.4-17, which has the highest reactivity. For the BWR fuel assemblies, PRAs are not required.

25 Pin Can:

Step 7 specifies fuel pins from the most reactive PWR and BWR fuels, as well as fuel parameters for MOX, EPR and generic UO₂ fuel. The PWR fuel pins modeled are the BW 15x15 Mark B11 and WE 14x14 Std/LOPAR/ ZCA/ZCB. For BWR fuel pins, the Allis Chalmers Lacrosse was modeled because it resulted in the highest k_s . Since the active fuel height of this fuel assembly is much smaller than the other BWR fuel assemblies considered, the next reactive fuel assembly, the Siemens QFA 9x9 fuel pin, is also modeled. The MOX, EPR and generic UO₂ parameters are obtained from Table 6.10.4-4 and Table 6.10.4-5. The results shown in Table 6.10.4-18 point out two facts: the highest reactivity is obtained while transporting 25 MOX fuel pins, and this reactivity is bounded by the reactivity obtained with PWR and BWR fuel assemblies.

6.10.4.4 Single Package Evaluation

6.10.4.4.1 Configuration

The single package models for both NCT and HAC are described in Section 6.10.4.3.1. The NCT scenario is modeled with an intact fuel assembly in its compartment flooded with fresh water at 100% density. The BWR fuels will remain subcritical and under the USL without any PRAs. The PRA requirement for PWR fuels is provided below.

In the material specification, the PRA model has a density that is 30 percent of the theoretical density of B₄C, as provided in SCALE6. As stated earlier, the PRA is composed of B₄C with a theoretical density of 2.52 g/cm³. The minimum required B₄C content is 40% of Theoretical Density (TD). In this analysis 75% credit is taken or 30% of the theoretical density or 0.756 g/cm³. The product of the cross-sectional area of the PRA with the volume density provides the linear density.

In the KENO models, the PRA is inserted in the guide tube locations. That is, the model consists of PRA material, PRA cladding, and Guide Tube Material. In all models, the Guide Tube material is Zircalloy. The PRA diameter modeled is the minimum required to ensure that the system is under the USL. In order to assess dependence of cladding material and geometry of the PRAs, three cases are considered: Case 1 is a PRA model with solid zircalloy clad determined by the size of the guide tube it is inserted in, Case 2 is a zircalloy clad with gap between the clad and the guide tube wall, and Case 3 is similar to Case 2 except the PRA clad is SS304. In the four assemblies considered for this sensitivity analysis, the number of PRAs modeled is indicated in the Table 6.10.4-20. As these cases only evaluate cladding effects, the models do not represent the final design basis cases. One of the main differences between these cases and the final results is that the cases evaluated in this table are not at their maximum, most reactive pitch. The only purpose they serve is to show PRA cladding effects. The results in Table 6.10.4-20 show that the dependence in modeling of clad is negligible. However for consistency, Case 3 is used to perform the bounding analysis that provides the maximum reactivity for each bounding assembly considered.

The PRA configuration for the assembly classes that require 5 PRAs is shown in Figure 6.10.4-12. For the WE 14x14 and WE 15x15 assembly classes, Configuration 1 or Configuration 2, shown in Figure 6.10.4-13, is employed. For the B&W 15x15, B&W 17x17, and WE 17x17 assembly classes, Configuration 3 or Configuration 4, shown in Figure 6.10.4-15, is employed. In general, for the fuel assemblies that require 8 PRAs, the four guide tubes located in the immediate corners from the instrument tube accept one PRA each. Then the immediate east, west, north and south guide tube locations relative to the "square" shape created by the four corners accept one PRA each. Note that in each direction only one PRA is inserted, as shown in the figures.

The PRA requirement for each assembly class is addressed as follows:

WE 14x14 Class Assemblies:

The WE 14x14 Std fuel assembly utilized for HAC does not have a central instrument tube. This applies for all WE 14x14 class assemblies. The number of PRAs is selected such that possible

configurations for PRA locations are minimized. This will eliminate any error that will result due to selection of PRA locations. To this end, the configurations illustrated in Figure 6.10.4-13 are selected. The reactivity of these configurations as shown in Table 6.10.4-19 is below the USL. The minimum PRA diameter required is 0.88 cm and a resulting linear density of 0.460 g/cm B₄C per PRA, at a maximum U-235 enrichment of 5.00 weight percent. The WE 14x14 has a substantially less k_s than other assembly classes evaluated in HAC. This is due to the 8-PRA requirement and does not change the analysis that it is the most reactive fuel assembly in HAC. All rotationally symmetric configurations of the absorber rods are also acceptable.

WE 15x15 Class Assemblies:

For the WE 15x15 class assemblies, the most reactive WE 15x15 assembly evaluated is the WE 15x15 Std, as shown in Table 6.10.4-8 for HAC results. This class of assembly remains subcritical and below the USL with the PRA configuration as shown in Figure 6.10.4-13. The number of PRAs required is 8, each at a minimum diameter of 0.88 cm. The maximum allowable U-235 enrichment is 5.00 weight percent. All rotationally symmetric configurations of the absorber rods are also acceptable.

WE 17x17 Class Assemblies:

The most reactive WE 17x17 assembly evaluated is the WE 17x17 OFA fuel assembly, as shown in Table 6.10.4-8. These class of assemblies will remain subcritical and below the USL with the PRA configuration as shown in Figure 6.10.4-15. The number of PRAs required is 8, each at a minimum diameter of 0.88 cm. The maximum allowable U-235 enrichment is 5.00 weight percent. All rotationally symmetric configurations of the absorber rods are also acceptable.

BW 15x15 Class Assemblies:

The most reactive BW 15x15 assembly is the BW 15x15, Mark B11 fuel assembly as shown in Table 6.10.4-8. The number of PRAs required is 8, each at a minimum diameter of 0.88 cm. The maximum allowable U-235 enrichment is 5.00 weight percent. The configuration of PRA location is as shown in Figure 6.10.4-15. All rotationally symmetric configurations of the absorber rods are also acceptable.

CE 14x14 Class Assemblies:

The most reactive CE 14x14 assembly is the Framatome CE 14x14 fuel assembly as shown in Table 6.10.4-8. The number of PRAs required is 5, each at a minimum diameter of 1.02 cm. This translates to a linear density of 0.618 g/cm. The maximum allowable U-235 enrichment is 5.00 weight percent. The configuration of PRA location is as shown in Figure 6.10.4-12.

CE 15x15 Class Assemblies:

For CE 15x15 Class assemblies that have just one location for PRA insertion, the maximum enrichment is reduced to 3.70 weight percent U-235. The analysis is performed with a PRA diameter of 0.76 cm or linear density of 0.343 g/cm B₄C per PRA.

CE 16x16 Class Assemblies:

The most reactive CE 16x16 assembly is the CE 16x16 System 80 fuel assembly as shown in Table 6.10.4-8. The number of PRAs required is 5, each at a minimum diameter of 1.02 cm. The maximum allowable U-235 enrichment is 5.00 weight percent. The configuration of PRA location is as shown in Figure 6.10.4-12.

BW 17x17 Class Assemblies:

In the case of B&W 17x17 Mark C, a PRA diameter of 0.76 cm or a linear density of 0.343 g/cm is required. The maximum allowable enrichment is 5.00 weight percent U-235. The PRA Configuration is as illustrated in Figure 6.10.4-15.

For each class, the result is shown in Table 6.10.4-21 with HAC scenario. As a resultant, the PRA requirement under all conditions of transport is as summarized in Table 6.10.4-26. This table contains the number of PRAs necessary for each assembly class, maximum enrichment allowed, the linear density of each PRA before the 75% credit is applied for analysis, or the actual minimum 40% TD required, and the minimum diameter of each PRA. Note that in Table 6.10.4-21; only PRA Configuration 1 is evaluated, since it has been shown that both Configurations 1 and 2 are acceptable in Table 6.10.4-19.

Under HAC, the PRA configuration is not expected to change. All rotationally symmetric configurations of the absorber rods are also acceptable.

Proprietary Information Withheld Pursuant to 10 CFR 2.390.

As the results in Table 6.10.4-17 demonstrate, BWR fuels will remain subcritical and under the USL for HAC. For the transportation of 25 individual fuel rods, HAC is not evaluated. This is due to the fact that the reactivity of the system is bounded by PWR fuel assembly transportation by more than 0.30 in Δk for NCT, and any postulated HAC is also bounded by PWR fuel rod pitch expansion analysis performed. These scenarios have been explored for PWR and BWR fuels to show that the 25 fuel rods are bounded.

6.10.4.4.2 Results

The results for single package transport are presented in Table 6.10.4-22. In this table, taking the most reactive fuel under NCT, the B&W 15x15 Mark B11 fuel assembly from Table 6.10.4-9 (Case ID P_B011), eight PRAs are added to the system. Additionally, the most reactive CE 16x16 and CE 15x15 fuel assemblies are selected and evaluated with five PRAs and one PRA, respectively, to demonstrate that they remain subcritical and under the USL. The remaining cases presented in this table are reproduced with their original Case IDs.

The most reactive configuration results from the PWR fuel assembly under HAC. In HAC, it has been shown that the WE 14x14 class assemblies are the most reactive. However, the CE 15x15 Assembly Class accepts only 1 PRA and would result in a higher k_{eff} . The CE 16x16 Assembly Class with five PRAs is added for completeness in this result, although, without control components, the WE 14x14 Assembly Class remains the most reactive. For BWR fuel, the Allis Chalmers - LaCrosse assemblies are the most reactive.

6.10.4.5 Evaluation of Package Arrays under Normal Conditions of Transport

6.10.4.5.1 Configuration

Consistent with the PWR NCT results in Table 6.10.4-8, B&W 15x15 Mark B11 fuel is used in the PWR NCT array calculations. For the package arrays under NCT, only PWR and BWR fuel assembly transport was considered because transport of 25 fuel rods will be bounded by the assembly transport conditions. Since CSI is 100, an array of three casks is modeled, as shown in Figure 6.10.4-8, and the gap between them is filled with water or air. The water density was varied between 0.01 and 100 percent. The PWR results are presented in Table 6.10.4-23 without PRAs. Because PRAs are not included in this step, the results exceed the USL. The BWR fuel, NCT array configuration is similar to that of PWR fuels. Consistent with the BWR NCT results in Table 6.10.4-15, the most reactive BWR assembly of all types, Allis Chalmers – LaCrosse, is selected as the design basis BWR fuel.

6.10.4.5.2 Results

The results show that for an external moderator density (EMD) or density of water located between the casks of 0.01 percent, the most reactive configuration under NCT exists. This configuration will be subcritical and under the USL with five PRAs located in the prescribed locations of the CE 16x16 assembly class, one (1) PRA for the CE 15x15 class, and eight (8) PRAs for the remaining fuel classes. The resulting PWR reactivity for the NCT array with PRAs is presented in Table 6.10.4-24. For BWR fuel, the most reactive fuel assembly, the Allis Chalmers LaCrosse fuel assembly, is used to perform the 3-array NCT analysis. As shown in Table 6.10.4-25, the system remains subcritical.

6.10.4.6 Package Arrays under Hypothetical Accident Conditions

Because the CSI = 100, no HAC array cases are performed.

6.10.4.7 Fissile Material Packages for Air Transport

This section does not apply.

6.10.4.8 Benchmark Evaluations

In this calculation, the Upper Subcritical Limit (USL) for use in the criticality analysis of the TN-LC-1FA system is determined. The USL is expressed as a function of the geometrical and material composition characteristics of the TN-LC-1FA.

The SCALE 6 program [1] is used to perform KENO V.a. k_{eff} calculations for the critical experiments. In the KENO V.a. calculation, the 44 group ENDF/B-V cross section library and the NITAWL option are used.

The USLSTATS 6 program [2] is used to evaluate the USL functions with the USL method 1 [3].

6.10.4.8.1 Applicability of Benchmark Experiments

The parameters of USL functions are U-235 enrichment, energy of average lethargy of fission (EALF), H₂O/UO₂ volume ratio, and fuel rod pitch.

The criticality benchmark analysis uses 118 LWR critical experiments provided by Oak Ridge National Laboratory (ORNL) [3], and 32 MOX experiments obtained from [4, 5]. All 150 experiments are selected for developing H₂O/UO₂ USL function. The volume ratio in the 150 experiments ranges from 0.3830 to 10.750. All 150 experiments are selected for developing lethargy USL function. The lethargy in the 150 experiments ranges from 0.0826 and 1.4006 eV. All 150 experiments are selected for developing pitch USL function. The pitch in the experiments ranges from 1.105 to 3.5204 cm. For U-235 enrichment, all 150 experiments are used for developing enrichment USL function. The range of enrichment in the 150 experiments is between 2.35 and 5.74 wt. percent. All 32 experiments are selected for developing the MOX USL functions. The PUO₂ enrichment ranges from 2.0 to 6.60 wt. percent.

6.10.4.8.2 Bias Determination

The USLSTATS inputs are prepared in accordance to User's Manual for USLSTATS V1.0 [2]. The input consists of a title and seven (7) parameters followed by a set of triplets; USL parameter value, k_{eff} and its standard deviation.

The parameter input values are described below:

- $P = 0.995$

This input is the proportion of population falling above lower tolerance level. The typical value is 0.995. It is a statistical parameter that is used only in the USL Method 2.

- $1 - \gamma = 0.95$

This input is the confidence level.

- $\sigma = 0.95$

This input represents the confidence on the proportion P. The typical value is 0.95.

- $X_{\text{MINIMUM}} = 0.0$

The lower limit of the parameter input value. The value of 0.0 indicates that no lower limit is imposed on the input values.

- $X_{\text{MAXIMUM}} = 0.0$

The upper limit of the parameter input value. The value of 0.0 indicates that no upper limit is imposed on the input values.

- σ_{SAMPLE} less or greater than 0.0

It is the standard deviation for all k_{eff} values. The value of less than 0.0 indicates that each k_{eff} has its own standard deviation.

- $\Delta k_M = 0.05$

It is the administrative margin.

The SCALE6 runs for the 150 critical experiments are performed such that their k_{eff} satisfy the χ^2 test for the normality at either 95% or 99% level. The SCALE6 calculation results (k_{eff} , σ , and EALF) along with the critical experiment parameters are listed in Table 6.10.4-27. The k_{eff} and standard deviation are needed for the USLSTATS6 calculations.

The USL functions are developed for five USL parameters: U-235 enrichment in wt. percent, PUO_2 content, the fuel rod pitch in cm, the $\text{H}_2\text{O}/\text{UO}_2$ volume ratio, and the energy of average lethargy of fission. The selection of the experiments is made in accordance with each parameter. All four USLSTATS6 runs meet the normality test. The USL 1 functional forms with their applicable range are given in Table 6.10.4-28. From these equations, limiting USL values are determined in Table 6.10.4-29 for each of the parameters examined. The limiting USL of 0.9420 is used in the criticality analysis.

6.10.4.9 Appendix

6.10.4.9.1 References

1. SCALE: A Modular Code System for Performing Standardized Computer Analyses for Licensing Evaluations, ORNL/TM-2005/39, Version 6, Vols. I-III, January 2009.
2. USLSTATS: A Utility to Calculate Upper Subcritical Limits for Criticality Safety Applications, Version 6, Oak Ridge National Laboratory, January 2009.
3. NUREG/CR-6361, LWR Fuel Validation Cases, Oak Ridge National Laboratory, December 2006.
4. DeHart, M.D. and S. M. Bowman "Analysis of Fresh Fuel Critical Experiments Appropriate for Burnup Credit Validation," Oak Ridge National Laboratory, October 1999, ORNL/TM-12959.
5. NEA/NSC/DOC(95)03, "International Handbook of Evaluated Criticality Safety Benchmark Experiments," September 2009.

**Proprietary Information on Pages 6.10.4-20 through 6.10.4-22
Withheld Pursuant to 10 CFR 2.390.**

Table 6.10.4-1
Summary of Criticality Evaluation

Proprietary Information Withheld Pursuant to 10 CFR 2.390.

Description	k_{eff}	USL
Normal Conditions of Transport: PWR fuel		
Single Package Maximum	0.8895	0.9420
3 Package Array Maximum	0.9047	0.9420
Normal Conditions of Transport: BWR fuel		
Single Package Maximum	0.7806	0.9420
3 Package Maximum	0.8202	0.9420
Hypothetical Accident Conditions: PWR fuel		
Single Package Maximum	0.9366	0.9420
Infinite Array Maximum	0.9366	0.9420
Hypothetical Accident Conditions: BWR fuel		
Single Package Maximum	0.8118	0.9420
Infinite Array Maximum	0.8118	0.9420
Normal Conditions of Transport: 25 Pin Can		
Single Package PWR	0.3782	0.9420
Single Package BWR	0.3865	0.9420
Single Package MOX	0.5210	0.9420
Single Package EPR	0.3616	0.9420

Table 6.10.4-2
PWR Fuel Assembly Parameters
(Part 1 of 3)

Proprietary Information Withheld Pursuant to 10 CFR 2.390.

Table 6.10.4-2

(Part 2 of 3)

Proprietary Information Withheld Pursuant to 10 CFR 2.390.

Table 6.10.4-2
(Part 3 of 3)

Proprietary Information Withheld Pursuant to 10 CFR 2.390.

Table 6.10.4-3
BWR Fuel Assembly Parameters
(Part 1 of 2)

Proprietary Information Withheld Pursuant to 10 CFR 2.390.

Table 6.10.4-3
BWR Fuel Assembly Parameters
(Part 2 of 2)

Proprietary Information Withheld Pursuant to 10 CFR 2.390.

Table 6.10.4-4
Parameters Used for MOX Fuel Rods

Parameter	Value	
	Inches	cm
Active Length	145.7	370.0
Pellets Diameter	0.33	0.8382
Clad OD	0.38	0.9652
Clad Thickness	0.02	0.0508
Max Density of Oxide	10.96 gm/cm ³	
Max U-235	0.7 wt.%	
Isotopic Vector for Pu	Vector	
Max. Plutonium wt. % Pu/(U+Pu) _{tot}	6.0, 8.0, 10.2	
Pu-240 wt. % - Pu-240/Pu _{total}	5.0	
Pu-239 wt. % - Pu-239/Pu _{total}	94.0	
Pu-241 wt. % - Pu-241/Pu _{total}	1.0	

Table 6.10.4-5
Parameters Used for EPR and Generic Fuel Rods

Parameter	Proprietary Information Withheld Pursuant to 10 CFR 2.390.	Generic (UO ₂) Value	
		Inches	Cm
Active Length		168	426.7
Pellet Diameter		0.33	0.8382
Clad OD		0.38	0.9652
Clad Thickness		0.02	0.0508
Max Density of Oxide	10.96 gm/cm ³		
Max U-235	5.0 wt.%		

Table 6.10.4-6
Cask Dimensions for Modeling

Proprietary Information Withheld Pursuant to 10 CFR 2.390.

Table 6.10.4-7
Materials Modeled

MIX ID	Material Type
1	UO ₂ Fuel
2	Zircalloy 4 Cladding
3, 5, 10, 13	Water
4	Stainless Steel
6	PRA Material
8	Aluminum
9	Poison Material
11	Lead Shield

Table 6.10.4-8
 Most Reactive PWR Fuel
 (Part 1 of 2)

Normal Conditions of Transport						
Case ID	Manufacturer	Array	Version	k_{eff}	1σ	k_s
	WE	17x17	LOPAR	0.9875	0.0009	0.9893
	WE	17x17	OFA/Van 5	0.9982	0.0009	1.0000
	Framatome	17x17	MK BW	0.9915	0.0009	0.9934
	WE	17x17	RFA	0.9875	0.0010	0.9893
	WE	17x17	RFA	0.9810	0.0010	0.9830
	CE	16x16	System 80	0.9719	0.0009	0.9737
	CE	16x16	Standard	0.9674	0.0009	0.9691
	B&W	15x15	Mark B2 – B8	0.9916	0.0010	0.9936
	B&W	15x15	Mark B9	0.9889	0.0009	0.9906
	B&W	15x15	Mark B10	0.9908	0.0009	0.9925
	B&W	15x15	Mark B11	0.9995	0.0009	1.0014
	B&W	17x17	Mark C	0.9893	0.0009	0.9911
	CE	15x15	Palisades	0.9573	0.0009	0.9591
	Exxon/ANF (ANP)	15x15	CE	0.9504	0.0009	0.9522
	Exxon/ANF (ANP)	15x15	WE	0.9853	0.0009	0.9870
	WE	15x15	Std/ZC	0.9938	0.0010	0.9958
	WE	15x15	LOPAR/OFA/DRFA/Van 5	0.9702	0.0008	0.9719
	CE	14x14	Std/Gen	0.9644	0.0009	0.9662
	CE	14x14	Ft. Calhoun	0.9635	0.0010	0.9655
	Framatome	14x14	CE	0.9684	0.0009	0.9702
	Exxon/ANF (ANP)	14x14	WE	0.9526	0.0009	0.9544
	Exxon/ANF (ANP)	14x14	Top rod	0.9525	0.0009	0.9543
	WE	14x14	Std/LOPAR/ZCA/ZCB	0.9581	0.0009	0.9599
	WE	14x14	OFA	0.9641	0.0009	0.9660

Proprietary Information Withheld Pursuant to 10 CFR 2.390.

Table 6.10.4-8
Most Reactive PWR Fuel
(Part 2 of 2)

Hypothetical Accident Conditions						
Case ID	Manufacturer	Array	Version	k_{eff}	1σ	k_s
	WE	17x17	LOPAR	1.0153	0.0009	1.0171
	WE	17x17	OFA/Van 5	1.0211	0.0009	1.0229
	Framatome	17x17	MK BW	1.0198	0.0009	1.0215
	WE	17x17	RFA	1.0153	0.0009	1.0171
	WE	17x17	RFA	1.0115	0.0009	1.0133
	CE	16x16	System 80	1.0170	0.0010	1.0190
	CE	16x16	Standard	1.0154	0.0009	1.0172
	B&W	15x15	Mark B2 – B8	1.0131	0.0008	1.0147
	B&W	15x15	Mark B9	1.0110	0.0008	1.0126
	B&W	15x15	Mark B10	1.0130	0.0009	1.0148
	B&W	15x15	Mark B11	1.0200	0.0009	1.0218
	B&W	17x17	Mark C	1.0109	0.0009	1.0127
	CE	15x15	Palisades	1.0028	0.0008	1.0045
	Exxon/ANF (ANP)	15x15	CE	0.9984	0.0009	1.0002
	Exxon/ANF (ANP)	15x15	WE	1.0147	0.0009	1.0165
	WE	15x15	Std/ZC	1.0213	0.0008	1.0229
	WE	15x15	LOPAR/OFA /DRFA/Van 5	0.9983	0.0010	1.0002
	CE	14x14	Std/Gen	1.0065	0.0009	1.0083
	CE	14x14	Ft. Calhoun	1.0064	0.0010	1.0084
	Framatome	14x14	CE	1.0099	0.0008	1.0115
	Exxon/ANF (ANP)	14x14	WE	1.0168	0.0008	1.0185
	Exxon/ANF (ANP)	14x14	Top rod	1.0179	0.0009	1.0197
	WE	14x14	Std/LOPAR/ ZCA/ZCB	1.0276	0.0009	1.0294
	WE	14x14	OFA	1.0234	0.0009	1.0252

Proprietary Information Withheld Pursuant to 10 CFR 2.390.

Table 6.10.4-9
Internal Moderator Density Variation Results – PWR Fuels

Case ID	Description	k_{eff}	1σ	k_s
Proprietary Information Withheld Pursuant to 10 CFR 2.390.	B&W 15x15 MARK B11			
	0.01 IMD	0.2078	0.0004	0.2086
	10 IMD	0.2943	0.0004	0.2952
	20 IMD	0.4183	0.0006	0.4195
	30 IMD	0.5352	0.0007	0.5365
	40 IMD	0.6372	0.0008	0.6388
	50 IMD	0.7257	0.0009	0.7276
	60 IMD	0.7990	0.0009	0.8008
	70 IMD	0.8600	0.0009	0.8618
	80 IMD	0.9150	0.0009	0.9167
	90 IMD	0.9622	0.0009	0.9639
	100 IMD	0.9995	0.0009	1.0014
	WE 14x14 Std/LOPAR/ZCA/ZCB			
	0.01 IMD	0.1923	0.0004	0.1931
	10 IMD	0.2870	0.0004	0.2879
	20 IMD	0.4281	0.0006	0.4293
	30 IMD	0.5559	0.0007	0.5574
	40 IMD	0.6659	0.0009	0.6676
	50 IMD	0.7581	0.0008	0.7597
	60 IMD	0.8314	0.0008	0.8330
	70 IMD	0.8944	0.0008	0.8960
	80 IMD	0.9477	0.0008	0.9494
	90 IMD	0.9928	0.0009	0.9946
100 IMD	1.0276	0.0009	1.0294	

Table 6.10.4-10
Assembly Positioning – PWR Fuels

Case ID	Description	k_{eff}	1σ	k_s
Proprietary Information Withheld Pursuant to 10 CFR 2.390.	Bottom Center	0.9988	0.0010	1.0008
	Central	0.9999	0.0009	1.0016
	Left Corner	0.9955	0.0009	0.9972

Table 6.10.4-11
Dimension Variation Study – PWR Fuels

Case ID	Description	k_{eff}	1σ	k_s
Proprietary Information Withheld Pursuant to 10 CFR 2.390.	Vary Poison Plate Thickness			
	pp-0.20 in, comp-1.00 in	1.0022	0.0009	1.0040
	pp-0.30 in, comp-1.00 in	0.9998	0.0010	1.0018
	Vary Compartment Thickness – poison plate 0.20"			
	pp-0.20in, comp-0.95 in	1.0007	0.0009	1.0025
	pp-0.20in, comp-1.05 in	1.0015	0.0009	1.0033

Table 6.10.4-12
Rod Pitch Variation – PWR Fuels

Case ID	Pitch	k_{eff}	1σ	k_s
Proprietary Information Withheld Pursuant to 10 CFR 2.390.	0.559	0.9627	0.0009	0.9646
	0.582	0.9896	0.0010	0.9915
	0.605	1.0092	0.0009	1.0110
	0.627	1.0250	0.0009	1.0269
	0.634	1.0290	0.0010	1.0310
	0.650	1.0331	0.0009	1.0349

Table 6.10.4-13
Single-Ended Shear Analysis – PWR Fuels

Case ID	Separation Distance (in)	k_{eff}	1σ	k_s
Proprietary Information Withheld Pursuant to 10 CFR 2.390.	0.000	0.9924	0.0009	0.9942
	0.165	0.9979	0.0009	0.9996
	0.330	1.0030	0.0010	1.0049
	0.494	1.0057	0.0008	1.0074
	0.659	1.0053	0.0009	1.0072
	0.494 - Shifted Up	1.0050	0.0010	1.0070
	0.659 - Shifted Up	1.0042	0.0008	1.0059
	0.000	0.9422	0.0009	0.9440
	0.340	0.9580	0.0009	0.9598
	0.680	0.9678	0.0009	0.9696
	1.019	0.9678	0.0009	0.9696
	1.360	0.9588	0.0009	0.9605

Table 6.10.4-14
Double-Ended Shear Analysis – PWR Fuels

Case ID	Separation Distance (in)	k_{eff}	1σ	k_s
Proprietary Information Withheld Pursuant to 10 CFR 2.390.	0.000	1.0016	0.0009	1.0033
	0.122	1.0049	0.0009	1.0067
	0.243	1.0070	0.0008	1.0087
	0.243 - Shifted Up	1.0079	0.0009	1.0097
	0.000	0.9568	0.0010	0.9587
	0.470	0.9774	0.0009	0.9791
	0.940	0.9776	0.0010	0.9796

Table 6.10.4-15
Most Reactive BWR Fuel in Each Fuel Category

Case ID	Manufacturer	Version	k_{eff}	1σ	k_s
7 x 7 array					
	GE	GE1, 2, 3	0.7168	0.0009	0.7185
	Exxon/ANF	ENC III-A	0.7118	0.0009	0.7136
	Exxon/ANF	ENC III	0.7092	0.0009	0.7110
8 x 8 array					
	GE	GE4	0.7126	0.0008	0.7143
	GE	Group 1	0.7240	0.0009	0.7258
	GE	Group 1	0.7240	0.0009	0.7258
	GE	Group 2	0.7268	0.0010	0.7288
	Exxon/ANF	ENC Va and Vb	0.6951	0.0009	0.6969
	Framatome ANP	8x8-62/2	0.7173	0.0008	0.7189
9 x 9 array					
	GE	GE11/13	0.7222	0.0009	0.7240
	Framatome ANP	Group	0.7215	0.0009	0.7232
	ABB	ABB-8-1,2, SVEA -64	0.7070	0.0009	0.7088
	Siemens	QFA	0.7258	0.0008	0.7275
10 x 10 array					
	GE	GE12/14	0.7248	0.0008	0.7264
	Framatome-ANP	ATRIUM 10, ATRIUM 10XM	0.7222	0.0010	0.7242
	ABB	ABB-10-1,2, SVEA-92	0.7219	0.0009	0.7237
	ABB	ABB-10-3,4, SVEA-96	0.7018	0.0009	0.7036
	ABB	ABB-10-5,6, SVEA-100	0.6911	0.0009	0.6929
	ABB	OPTIMA, OPTIMA 2	0.7154	0.0009	0.7172
10 x 10 array – Lacrosse					
	Allis Chalmers	LaCrosse	0.7691	0.0009	0.7709
	Exxon/ANF	LaCrosse	0.7570	0.0009	0.7588

Proprietary Information Withheld Pursuant to 10 CFR 2.390.

Note: Poison plate thickness is 0.20 in. with B-10 areal density of 15 mg/cm².

Table 6.10.4-16
Dimension Variation Study – BWR Fuels

Case ID	Description	k_{eff}	1σ	k_s
Proprietary Information Withheld Pursuant to 10 CFR 2.390.	Poison Thickness: 0.20in, PWR Comp. Thickness: 1.00in, Gap: 0.125in			
	7x7	0.7258	0.0008	0.7275
	8x8 Group 1	0.7331	0.0009	0.7348
	8x8 Group 2	0.7323	0.0009	0.7342
	9x9	0.7346	0.0009	0.7363
	10x10	0.7314	0.0008	0.7330
	Allis Chalmers	0.7788	0.0009	0.7806
	Exxon/ANF-LaCrosse	0.7664	0.0009	0.7682

Table 6.10.4-17
 Rod Pitch Variation – BWR Fuels
 (Part 1 of 2)

Case ID	Pitch	k_{eff}	1σ	k_s
7x7 Array Assembly Group				
	0.563	0.5488	0.0008	0.5503
	0.597	0.5880	0.0008	0.5895
	0.632	0.6232	0.0009	0.6250
	0.666	0.6624	0.0010	0.6643
	0.700	0.6939	0.0009	0.6957
	0.738	0.7271	0.0009	0.7288
	0.769	0.7488	0.0009	0.7505
	0.803	0.7696	0.0009	0.7713
	0.838	0.7863	0.0009	0.7880
	0.872	0.7964	0.0008	0.7980
	0.906	0.8025	0.0009	0.8043
8x8 Array Assembly Group				
	0.483	0.5541	0.0008	0.5556
	0.514	0.5919	0.0009	0.5937
	0.544	0.6331	0.0009	0.6349
	0.575	0.6673	0.0008	0.6690
	0.605	0.7012	0.0009	0.7031
	0.640	0.7349	0.0009	0.7368
	0.666	0.7544	0.0009	0.7561
	0.697	0.7741	0.0009	0.7758
	0.727	0.7906	0.0009	0.7924
	0.758	0.7980	0.0009	0.7998
	0.788	0.8028	0.0010	0.8047
9x9 Array Assembly Group				
	0.433	0.5828	0.0008	0.5844
	0.459	0.6168	0.0008	0.6184
	0.486	0.6524	0.0008	0.6541
	0.512	0.6812	0.0008	0.6829
	0.538	0.7084	0.0009	0.7102
	0.569	0.7346	0.0009	0.7363
	0.591	0.7489	0.0009	0.7507
	0.617	0.7631	0.0010	0.7650
	0.643	0.7700	0.0008	0.7717
	0.670	0.7729	0.0009	0.7747
	0.696	0.7685	0.0008	0.7702

Proprietary Information Withheld Pursuant to 10 CFR 2.390.

Table 6.10.4-17
 Rod Pitch Variation – BWR Fuels
 (Part 2 of 2)

Case ID	Pitch	k_{eff}	1σ	k_s
10x10 Array Assembly Group				
	0.404	0.5840	0.0008	0.5856
	0.426	0.6183	0.0008	0.6199
	0.448	0.6502	0.0008	0.6518
	0.469	0.6803	0.0010	0.6823
	0.491	0.7084	0.0010	0.7104
	0.513	0.7346	0.0009	0.7364
	0.535	0.7542	0.0009	0.7560
	0.556	0.7724	0.0009	0.7742
	0.578	0.7854	0.0009	0.7872
	0.600	0.7947	0.0008	0.7963
	0.622	0.7969	0.0009	0.7987
LaCrosse - Allis Chalmers Assembly Type				
	0.396	0.5485	0.0007	0.5500
	0.419	0.5844	0.0009	0.5861
	0.464	0.6558	0.0008	0.6574
	0.487	0.6865	0.0008	0.6882
	0.509	0.7181	0.0009	0.7198
	0.532	0.7454	0.0009	0.7471
	0.555	0.7679	0.0009	0.7697
	0.565	0.7752	0.0008	0.7768
	0.577	0.7867	0.0010	0.7886
	0.600	0.8014	0.0009	0.8032
	0.623	0.8099	0.0009	0.8118
LaCrosse - Exxon/ANF				
	0.394	0.5477	0.0008	0.5492
	0.417	0.5835	0.0008	0.5851
	0.440	0.6196	0.0008	0.6212
	0.463	0.6540	0.0009	0.6558
	0.486	0.6873	0.0010	0.6892
	0.508	0.7177	0.0009	0.7195
	0.531	0.7445	0.0010	0.7465
	0.557	0.7703	0.0008	0.7720
	0.577	0.7852	0.0009	0.7870
	0.600	0.8011	0.0009	0.8029
	0.623	0.8093	0.0010	0.8113

Proprietary Information Withheld Pursuant to 10 CFR 2.390.

Table 6.10.4-18
25 Pin Can Analyses

Case ID	Description	k_{eff}	1σ	k_s
Proprietary Information Withheld Pursuant to 10 CFR 2.390.	BW15: Mark B11	0.3770	0.0006	0.3782
	EPR	0.3604	0.0006	0.3616
	Allis Chalmers: LaCrosse	0.3653	0.0007	0.3667
	MOX – 10.2 % Pu	0.5194	0.0008	0.5210
	MOX – 6.0 % Pu	0.4648	0.0007	0.4662
	MOX – 8.0 % Pu	0.4957	0.0007	0.4971
	Siemens: QFA	0.3851	0.0007	0.3865
	UO ₂	0.3495	0.0006	0.3507
	WE14: Std/LOPAR/ ZCA/ZCB	0.3827	0.0006	0.3839

Table 6.10.4-19
Possible PRA Configuration for WE 14x14 Class Assemblies

Case ID	Description	k_{eff}	1σ	k_s
Proprietary Information Withheld Pursuant to 10 CFR 2.390.	Configuration 1	0.9090	0.0009	0.9108
	Configuration 2	0.9086	0.0009	0.9104

Table 6.10.4-20
Evaluation of Effects due to PRA Clad Variation, Single Package

Case ID	Description	k_{eff}	1σ	k_s
Proprietary Information Withheld Pursuant to 10 CFR 2.390.	BW 15x15 Fuel Assembly – Single Package NCT, 5 PRAs			
	Case 1 - PRA Clad: solid zirc	0.9110	0.0008	0.9126
	Case 2 - PRA Clad: zirc-with gap	0.9111	0.0010	0.9131
	Case 3 - PRA Clad: ss304-with gap	0.9128	0.0009	0.9146
	CE 15x15 Palisade Fuel Assembly HAC, 1 PRA			
	Case 1 - PRA Clad: solid zirc	0.9295	0.0008	0.9311
	Case 2 - PRA Clad: zirc-with gap	0.9294	0.0008	0.9310
	Case 3 - PRA Clad: ss304-with gap	0.9270	0.0009	0.9288
	Exxon/ANP 15x15 CE Fuel Assembly HAC, 1 PRA			
	Case 1 - PRA Clad: solid zirc	0.9235	0.0008	0.9251
	Case 2 - PRA Clad: zirc-with gap	0.9231	0.0009	0.9249
	Case 3 - PRA Clad: ss304-with gap	0.9254	0.0010	0.9274
	WE 14x14 Fuel Assembly HAC, 6 PRAs			
	Case 1 - PRA Clad: solid zirc	0.9316	0.0009	0.9334
	Case 2 - PRA Clad: zirc-with gap	0.9353	0.0010	0.9373
Case 3 - PRA Clad: ss304-with gap	0.9350	0.0008	0.9366	

Table 6.10.4-21
Design Basis PRA Configuration for Various PWR Assemblies, HAC Single Package

Case ID	Description	k_{keno}	1σ	k_{eff}
Proprietary Information Withheld Pursuant to 10 CFR 2.390.	BW 15x15, 8 PRAs	0.8914	0.0010	0.8934
	CE 15x15, 1 PRA	0.9331	0.0010	0.9351
	CE 16x16, 5 PRAs	0.9231	0.0009	0.9249
	Framatome, CE, 14x14, 5 PRAs	0.9243	0.0009	0.9261
	BW 17x17, 8 PRAs	0.9225	0.0008	0.9241
	Framatome, MK BW 17x17, 8 PRAs	0.9127	0.0009	0.9145
	WE 15x15, 8 PRAs	0.9119	0.0009	0.9137
	WE 17x17, 8 PRAs	0.9168	0.0009	0.9186
	CE 15x15, 1 PRA- Poison Plate Bolt Holes	0.9348	0.009	0.9366

Table 6.10.4-22
NCT and HAC Results for Single Package Transport

Case ID	Description	k_{eff}	1σ	k_s
Proprietary Information Withheld Pursuant to 10 CFR 2.390.	Normal Conditions of Transport: PWR fuel			
	Single Package Maximum, 8 PRAs	0.8596	0.0008	0.8612
	Single Package Maximum, 1 PRA	0.8875	0.0010	0.8895
	Single Package Maximum, 5 PRAs	0.8724	0.0009	0.8742
	Normal Conditions of Transport: BWR fuel			
	Single Package Maximum	0.7788	0.0009	0.7806
	Hypothetical Accident Conditions: PWR fuel			
	Single Package Maximum	0.9348	0.0009	0.9366
	Hypothetical Accident Conditions: BWR fuel			
	Single Package Maximum	0.8099	0.0009	0.8118
	Normal Conditions of Transport: 25 Pin Can			
	Single Package Maximum	0.5194	0.0008	0.5210

Table 6.10.4-23
NCT Package Array Results at Varying External Moderator Density – PWR Fuels (no PRAs)

Case ID	Description	k_{keno}	1σ	k_{eff}
Proprietary Information Withheld Pursuant to 10 CFR 2.390.	AIR	1.0172	0.0009	1.0190
	0.01% EMD	1.0177	0.0009	1.0195
	10% EMD	1.0116	0.0009	1.0133
	20% EMD	1.0092	0.0010	1.0112
	30% EMD	1.0092	0.0009	1.0110
	40% EMD	1.0079	0.0010	1.0098
	50% EMD	1.0073	0.0010	1.0093
	60% EMD	1.0077	0.0009	1.0095
	70% EMD	1.0063	0.0009	1.0080
	80% EMD	1.0061	0.0009	1.0079
	90% EMD	1.0044	0.0009	1.0063
	100% EMD	1.0049	0.0009	1.0067

Table 6.10.4-24
 NCT Package Array Results with PRAs for the Most Reactive PWR Configuration

Case ID	Description	k_{keno}	1σ	k_{eff}
Proprietary Information Withheld Pursuant to 10 CFR 2.390.	3 Array, CE 15x15, 1 PRA	0.9029	0.0009	0.9047
	3 Array, CE 16x16, 5 PRAs	0.8867	0.0010	0.8887
	3 Array, BW 15x15, 8 PRAs	0.8925	0.0009	0.8943

Table 6.10.4-25
 NCT Package Array Results at Varying External Moderator Density – BWR Fuels

Case ID	Description	k_{eff}	1σ	k_s
Proprietary Information Withheld Pursuant to 10 CFR 2.390.	0.01% EMD	0.8184	0.0009	0.8202
	10% EMD	0.8175	0.0009	0.8193
	20% EMD	0.8157	0.0009	0.8174
	30% EMD	0.8146	0.0009	0.8163
	40% EMD	0.8155	0.0009	0.8173
	50% EMD	0.8146	0.0009	0.8164
	60% EMD	0.8131	0.0009	0.8148
	70% EMD	0.8144	0.0008	0.8161
	80% EMD	0.8132	0.0009	0.8151
	90% EMD	0.8129	0.0009	0.8146
	100% EMD	0.8130	0.0010	0.8150

Table 6.10.4-26
Summary of PRA Requirements Under all Conditions of Transport for PWR Fuel Assembly
Classes

Assembly Class	Number of PRAs	Diameter of PRAs (cm)	Minimum B₄C Content (g/cm)	Max U-235 Enrichment (wt %)
WE 17x17	8	0.88	0.613	5.00
CE 16x16	5	1.02	0.824	5.00
BW 15x15	8	0.88	0.613	5.00
CE 15x15	1	0.76	0.475	3.70
WE 15x15	8	0.88	0.613	5.00
CE 14x14	5	0.88	0.613	5.00
WE 14x14	8	0.88	0.613	5.00
BW 17x17	8	0.76	0.475	5.00

Table 6.10.4-27
 Criticality Experiment Benchmark Results
 (Part 1 of 4)

Experiment ID	U-235 Enrichment in wt%	Fuel Rod Pitch in cm	H ₂ O/UO ₂ Volume Ratio	Boron Loading in PPM	Separation Distance in cm	PUO ₂	EALF in eV	K _{EFFECTIVE}	σ
b1645s01	2.46	1.41	1.015	1068	1.78	-	0.4088	0.9958	0.0009
b1645s02	2.46	1.41	1.015	1156	1.78	-	0.4159	0.9999	0.0009
bw1231b1	4.02	1.511	1.139	1152	-	-	0.73	0.9953	0.0008
bw1231b2	4.02	1.511	1.139	3389	-	-	1.1985	0.9961	0.0007
bw1273m	2.46	1.511	1.376	1675	-	-	0.5209	0.9952	0.0007
bw1484a1	2.46	1.636	1.841	15	1.64	-	0.1952	0.9975	0.0008
bw1484a2	2.46	1.636	1.841	72	4.92	-	0.153	0.9922	0.0008
bw1484b1	2.46	1.636	1.841	1037	-	-	0.2498	0.9982	0.0008
bw1484b2	2.46	1.636	1.841	769	1.64	-	0.1924	0.9964	0.0008
bw1484b3	2.46	1.636	1.841	143	4.92	-	0.1481	0.997	0.0007
bw1484c1	2.46	1.636	1.841	-	1.64	-	0.1901	0.9924	0.0009
bw1484c2	2.46	1.636	1.841	-	1.64	-	0.1486	0.9951	0.0009
bw1484s1	2.46	1.636	1.841	432	1.64	-	0.1968	0.9987	0.0007
bw1484s2	2.46	1.636	1.841	514	1.64	-	0.1933	0.9991	0.0008
bw1484sl	2.46	1.636	1.841	-	6.54	-	0.1387	0.9954	0.0009
bw1645s1	2.46	1.209	0.383	746	1.78	-	1.3362	0.9981	0.0008
bw1645s2	2.46	1.209	0.383	886	1.78	-	1.4006	1.0018	0.0007
bw1810a	2.46	1.636	1.841	1239	-	-	0.2478	0.999	0.0006
bw1810b	2.46	1.636	1.841	1170	-	-	0.2463	0.9991	0.0006
bw1810c	2.46	1.636	1.841	1499	-	-	0.3321	0.9984	0.0008
bw1810d	2.46	1.636	1.841	1654	0.18973	-	0.3386	0.9963	0.0008
bw1810e	2.46	1.636	1.841	1579	-	-	0.3319	0.9982	0.0008
bw1810f	2.46	1.636	1.841	1337	-	-	0.2463	1.0034	0.0008
bw1810g	2.46	1.636	1.841	1776	-	-	0.3581	0.9977	0.0007
bw1810h	2.46	1.636	1.841	1899	-	-	0.3585	0.9993	0.0008
bw1810i	2.46	1.636	1.841	1250	-	-	0.2471	1.0017	0.0007
bw1810j	2.46	1.636	1.532	1635	-	-	0.3343	0.9991	0.0008
epru65b	2.35	1.562	1.196	463	-	-	0.319	0.9986	0.001
epru65	2.35	1.562	1.196	-	-	-	0.2571	0.9966	0.001
epru75b	2.35	1.905	2.408	568	-	-	0.1421	0.9992	0.001
epru75	2.35	1.905	2.408	-	-	-	0.1131	0.9966	0.0008
epru87b	2.35	2.21	3.687	286	-	-	0.093	0.9999	0.0007
epru87	2.35	2.21	3.687	-	-	-	0.0826	0.9983	0.0008
nse71sq	4.74	1.26	1.823	-	-	-	0.2465	0.9999	0.001
nse71w1	4.74	1.26	1.823	-	-	-	0.2243	0.9989	0.001
nse71w2	4.74	1.26	1.823	-	-	-	0.1916	0.9979	0.001

Table 6.10.4-27
 Criticality Experiment Benchmark Results
 (Part 2 of 4)

Experiment ID	U-235 Enrichment in wt%	Fuel Rod Pitch in cm	H ₂ O/UO ₂ Volume Ratio	Boron Loading in PPM	Separation Distance in cm	PUO ₂	EALF in eV	K _{EFFECTIVE}	σ
p2438ba	2.35	2.032	2.918	-	5.05	-	0.098	0.9972	0.0009
p2438slg	2.35	2.032	2.918	-	8.39	-	0.0957	0.996	0.0008
p2438ss	2.35	2.032	2.918	-	6.88	-	0.0963	0.9969	0.0008
p2438zr	2.35	2.032	2.918	-	8.79	-	0.0955	0.9958	0.0007
p2615ba	4.31	2.54	3.883	-	6.72	-	0.1155	0.9973	0.001
p2615ss	4.31	2.54	3.883	-	8.58	-	0.1143	0.9991	0.0009
p2615zr	4.31	2.54	3.883	-	10.92	-	0.1139	0.9996	0.001
p282711	2.35	2.032	2.918	-	13.72	-	0.0972	1.0014	0.0007
p282712	2.35	2.032	2.918	-	11.25	-	0.0948	0.9991	0.0008
p282713	4.31	2.54	3.883	-	20.78	-	0.1169	1.01	0.0009
p282714	4.31	2.54	3.883	-	19.04	-	0.1151	1.0075	0.0008
p2827slg	2.35	2.032	2.918	-	8.31	-	0.0949	0.9957	0.001
p3314ba	4.31	1.892	1.6	-	4.8	-	0.3252	1.0007	0.0009
p3314bc	4.31	1.892	1.6	-	3.53	-	0.3188	1.0004	0.001
p3314bf1	4.31	1.892	1.6	-	3.6	-	0.3158	1.0027	0.0009
p3314bf2	4.31	1.892	1.6	-	4.94	-	0.3197	1.0024	0.001
p3314bs1	2.35	1.684	1.6	-	3.86	-	0.1746	0.9952	0.0009
p3314bs2	2.35	1.684	1.6	-	3.46	-	0.176	0.9936	0.0008
p3314bs3	4.31	1.892	1.6	-	7.23	-	0.2941	0.9979	0.0011
p3314bs4	4.31	1.892	1.6	-	6.63	-	0.298	0.9996	0.0009
p3314slg	4.31	1.892	1.6	-	10.86	-	0.2337	0.9974	0.0009
p3314ss1	4.31	1.892	1.6	-	3.38	-	0.2372	0.9988	0.0009
p3314ss2	4.31	1.892	1.6	-	11.55	-	0.2568	1.0018	0.0009
p3314ss3	4.31	1.892	1.6	-	4.47	-	0.2436	0.9985	0.001
p3314ss4	4.31	1.892	1.6	-	8.36	-	0.2572	0.9969	0.0009
p3314ss5	2.35	1.684	1.6	-	7.8	-	0.168	0.9957	0.0011
p3314ss6	4.31	1.892	1.6	-	10.52	-	0.2819	1.0009	0.0009
p3314w1	4.31	1.892	1.6	-	-	-	0.1996	1.001	0.0009
p3314w2	2.35	1.684	1.6	-	-	-	0.1501	0.9974	0.0008
p3314zr	4.31	1.892	1.6	-	2.83	-	0.2397	1.0004	0.0009
p3602bb	4.31	1.892	1.6	-	8.3	-	0.3056	1.003	0.0009
p3602bs1	2.35	1.684	1.6	-	4.8	-	0.1785	1.0003	0.0008
p3602bs2	4.31	1.892	1.6	-	9.83	-	0.3026	1.0035	0.0011
p3602n11	2.35	1.684	1.6	-	8.98	-	0.1795	1.0029	0.001
p3602n12	2.35	1.684	1.6	-	9.58	-	0.1739	1.0039	0.0009
p3602n13	2.35	1.684	1.6	-	9.66	-	0.1672	1.0006	0.0009
p3602n14	2.35	1.684	1.6	-	8.54	-	0.1617	0.9987	0.0009
p3602n21	2.35	2.032	2.918	-	10.36	-	0.0957	0.9997	0.0009

Table 6.10.4-27
 Criticality Experiment Benchmark Results
 (Part 3 of 4)

Experiment ID	U-235 Enrichment in wt%	Fuel Rod Pitch in cm	H ₂ O/UO ₂ Volume Ratio	Boron Loading in PPM	Separation Distance in cm	PUO ₂	EALF in eV	K _{EFFECTIVE}	σ
p3602n22	2.35	1.892	2.918	-	11.2	-	0.0983	1.0016	0.0009
p3602n31	4.31	1.892	1.6	-	14.87	-	0.3169	1.0083	0.001
p3602n32	4.31	1.892	1.6	-	15.74	-	0.3042	1.0069	0.0009
p3602n33	4.31	1.892	1.6	-	15.87	-	0.2945	1.0064	0.001
p3602n34	4.31	1.892	1.6	-	15.84	-	0.2871	1.0045	0.001
p3602n35	4.31	1.892	1.6	-	15.45	-	0.2819	1.0049	0.0009
p3602n36	4.31	2.54	1.6	-	13.82	-	0.2761	1.0021	0.0009
p3602n41	4.31	2.54	3.883	-	12.89	-	0.1237	1.0126	0.0009
p3602n42	4.31	2.54	3.883	-	14.12	-	0.1168	1.0098	0.0008
p3602n43	4.31	1.684	3.883	-	12.44	-	0.114	1.0038	0.0008
p3602ss1	2.35	1.684	1.6	-	8.28	-	0.1718	1.0011	0.0008
p3602ss2	4.31	1.892	1.6	-	13.75	-	0.2937	1.0039	0.001
p3926l1	2.35	1.684	1.6	-	10.06	-	0.1741	1.0003	0.0008
p3926l2	2.35	1.684	1.6	-	10.11	-	0.1676	1	0.0007
p3926l3	2.35	1.684	1.6	-	8.5	-	0.1601	0.9977	0.0008
p3926l4	4.31	1.892	1.6	-	17.74	-	0.3045	1.0069	0.0009
p3926l5	4.31	1.892	1.6	-	18.18	-	0.2951	1.0058	0.0009
p3926l6	4.31	1.892	1.6	-	17.43	-	0.2837	1.0024	0.0009
p3926sl1	2.35	1.684	1.6	-	6.59	-	0.1597	0.9945	0.0008
p3926sl2	4.31	1.892	1.6	-	12.97	-	0.278	1	0.0009
p4267b1	4.31	1.89	1.59	2150	-	-	0.5539	0.9969	0.0008
p4267b2	4.31	1.89	1.59	2550	-	-	0.6135	1.0022	0.001
p4267b3	4.31	1.715	1.09	1030	-	-	0.7892	1.0042	0.0009
p4267b4	4.31	1.715	1.09	1820	-	-	0.9554	0.9987	0.0009
p4267b5	4.31	1.715	1.09	2550	-	-	1.1237	1.0005	0.0008
p4267sl1	4.31	1.89	1.59	-	-	-	0.2894	1.001	0.001
p4267sl2	4.31	1.715	1.09	-	-	-	0.5452	0.9989	0.0009
p62ft231	4.31	1.891	1.6	-	5.67	-	0.3636	1.0026	0.0009
p71f14f3	4.31	1.891	1.6	-	5.19	-	0.3796	1.0002	0.0009
p71f14v3	4.31	1.891	1.6	-	5.19	-	0.3677	0.9988	0.0009
p71f14v5	4.31	1.891	1.6	-	5.19	-	0.3707	0.9989	0.0009
p71f214r	4.31	1.891	1.6	-	5.19	-	0.3673	0.9975	0.0009
pat80l1	4.74	1.6	3.807	-	2	-	0.1486	1.0008	0.0009
pat80l2	4.74	1.6	3.807	-	2	-	0.1438	0.9964	0.0009
pat80ss1	4.74	1.6	3.807	-	2	-	0.1506	0.9992	0.0009
pat80ss2	4.74	1.6	3.807	-	2	-	0.1442	0.9941	0.0009
w3269a	5.7	1.422	1.93	-	-	-	0.3093	0.9967	0.001
w3269c	3.7	1.105	1.432	-	-	-	0.268	0.9978	0.0009
w3269sl1*	2.72	1.524	1.494	-	-	-	0.3281	0.9954	0.0010

Table 6.10.4-27
 Criticality Experiment Benchmark Results
 (Part 4 of 4)

Experiment ID	U-235 Enrichment in wt%	Fuel Rod Pitch in cm	H ₂ O/UO ₂ Volume Ratio	Boron Loading in PPM	Separation Distance in cm	PUO ₂	EALF in eV	K _{EFFECTIVE}	σ
w3269sl2	5.7	1.422	1.932	-	-	-	0.3179	1.0038	0.0009
w3269w1	2.72	1.524	1.494	-	-	-	0.3112	0.9975	0.0009
w3269w2	5.7	1.422	1.932	-	-	-	0.3063	1.001	0.001
w3385sl1	5.74	1.422	1.933	-	-	-	0.2983	0.9965	0.001
w3385sl2	5.74	2.011	5.067	-	-	-	0.1031	1.0019	0.0009
epri70un	0.71	1.778	1.2000	-	-	2	0.56944	0.99937	0.00078
epri70b	0.71	1.778	1.2000	-	-	2	0.76425	0.99967	0.00094
epri87b	0.71	2.2098	1.5300	-	-	2	0.27909	1.00765	0.00073
epri99un	0.71	2.5146	3.6400	-	-	2	0.13497	1.00879	0.00086
epri99b	0.71	2.5146	3.6400	-	-	2	0.18214	1.00823	0.00070
saxton52	0.71	1.3208	1.6800	-	-	6.6	0.88355	0.99856	0.00094
saxton56	0.71	1.4224	2.1600	-	-	6.6	0.53825	0.99948	0.00098
saxton56b	0.71	1.4224	2.1600	-	-	6.6	0.64213	1.00008	0.00092
saxtn735	0.71	1.8669	4.7000	-	-	6.6	0.18694	1.00090	0.00100
saxtn792	0.71	2.01168	5.6700	-	-	6.6	0.15417	1.00270	0.00100
saxtn104	0.71	2.6416	10.7500	-	-	6.6	0.09961	1.00523	0.00089
mct-007-c01	0.72	2.3622	2.4878	-	-	2	0.19439	1.00202	0.00036
mct-007-c02	0.72	2.667	3.5152	-	-	2	0.13932	0.99888	0.00038
mct-007-c03	0.72	2.90322	4.3970	-	-	2	0.11753	1.00152	0.00031
mct-007-c04	0.72	3.3528	6.2819	-	-	2	0.09532	1.00192	0.00035
mct-007-c05	0.72	3.52044	7.0541	-	-	2	0.09052	1.00099	0.00032
mct-007-c06-A1	0.72	2.667	3.5152	-	-	2	0.13823	0.99687	0.00038
mct-007-c07-B1	0.72	2.667	3.5152	-	-	2	0.13988	0.99383	0.00034
mct-007-c08-B2	0.72	2.667	3.5152	-	-	2	0.13935	0.99521	0.00034
mct-007-c09-B3	0.72	2.667	3.5152	-	-	2	0.13909	0.99611	0.00036
mct-007-c10-B4	0.72	2.667	3.5152	-	-	2	0.13864	0.99619	0.00033
mct-008-c01	0.72	2.032	1.5154	-	-	2	0.39526	0.99309	0.00026
mct-008-c02	0.72	2.3622	2.4878	-	-	2	0.19679	0.99665	0.00025
mct-008-c03	0.72	2.667	3.5152	-	-	2	0.13996	0.99825	0.00026
mct-008-c04	0.72	2.90322	4.3970	-	-	2	0.11796	1.002	0.00026
mct-008-c05	0.72	3.3528	6.2819	-	-	2	0.09557	1.00415	0.00025
mct-008-c06	0.72	3.52044	7.0541	-	-	2	0.09046	1.00379	0.00024
mct-008-c07-A1	0.72	2.667	3.5152	-	-	2	0.13920	0.99896	0.00027
mct-008-c13-B4	0.72	2.667	3.5152	-	-	2	0.13940	0.99619	0.00026
mct-008-c14-B3	0.72	2.667	3.5152	-	-	2	0.13988	0.99607	0.00026
mct-008-c15-B2	0.72	2.667	3.5152	-	-	2	0.14014	0.99555	0.00028
mct-008-c16-B1	0.72	2.667	3.5152	-	-	2	0.14040	0.99464	0.00026

Table 6.10.4-28
USL Functions

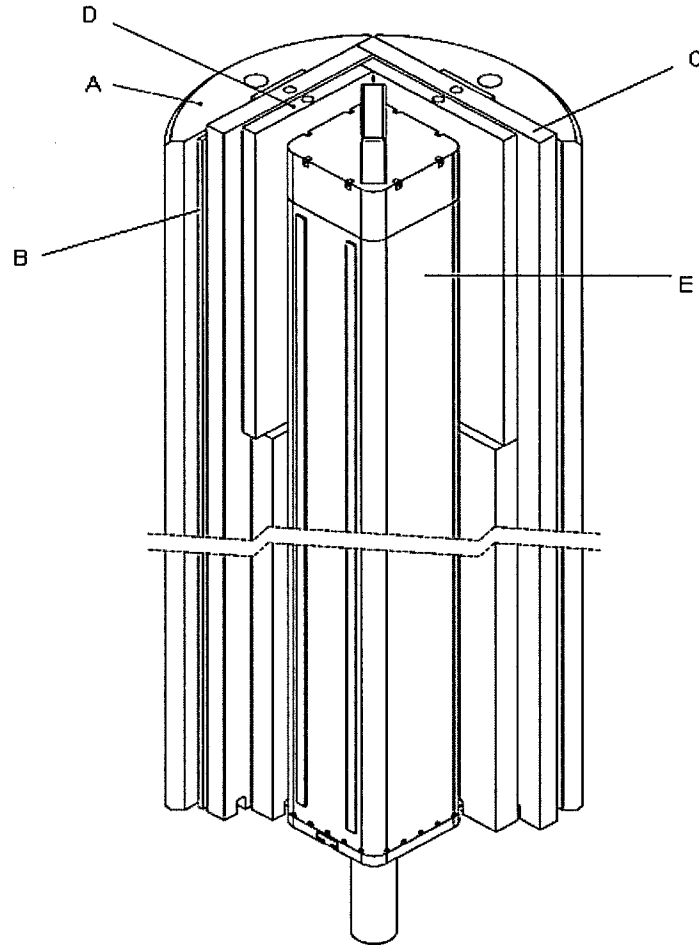
Parameter	Applicable Range	USL Function	
EALF in eV	[0.0826, 1.4006]	0.9430 – 3.6859E-05*X	
Boron Loading in PPM	[15, 3389]	0.9431 + 3.5320E-07*X	
Separation Distance in cm	[0.18973, 20.78]	0.9402 + 5.7045E-04*X	X < 7.7875
		0.9446	X ≥ 7.7875
U-235 Enrichment in wt%	[2.3500, 5.7400]	0.9419 + 4.9961E-04*X	X < 3.4323
		0.9437	X ≥ 3.4323
H ₂ O/UO ₂ Volume Ratio	[0.3830, 10.750]	0.9415 + 5.1558E-04*X	X < 2.9015
		0.9430	X ≥ 2.9015
Pitch in cm	[1.1050 , 3.5204]	0.9397 + 1.8566E-03*X	X < 2.0761
		0.9435	X ≥ 2.0761
PUO ₂	[2.0, 6.6]	0.9411+3.6394E-04*X	X < 3.4172
		0.9423	X ≥ 3.4172

Table 6.10.4-29
USL Determination for Criticality Analysis

Parameter	Value From Limiting Analysis	Bounding USL
EALF in eV	0.4210	0.9430
U-235 Enrichment in wt%	2.00	0.9429
H ₂ O/UO ₂ Volume Ratio	1.52 ⁽¹⁾	0.9423
PUO ₂	6.00	0.9423
Pitch in cm	1.2598 ⁽²⁾	0.9420

Notes:

- (1) Framatome 9x9 from Table 6.10.4-3.
- (2) WE 17x17 from Table 6.10.4-2.



Label	Description	Material
A	Rail	Aluminum 6061
B	Poison Plate (highlighted in blue in Figure 6.10.4-2)	Boron Enriched Aluminum Alloy/ Metal Matrix Composite/ Natural Boron Aluminum
C	PWR fuel Compartment	SA-204 Type 304
D	BWR fuel Compartment	SA-204 Type 304
E	25 Pin Can	SA-204 Type 304

Figure 6.10.4-1
1FA Basket with All Functional Components

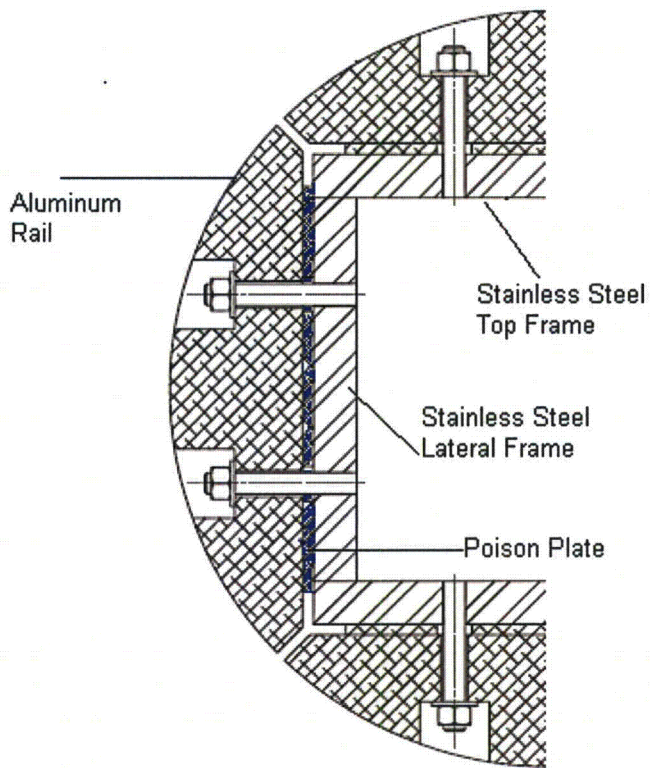


Figure 6.10.4-2
PWR Compartment Components

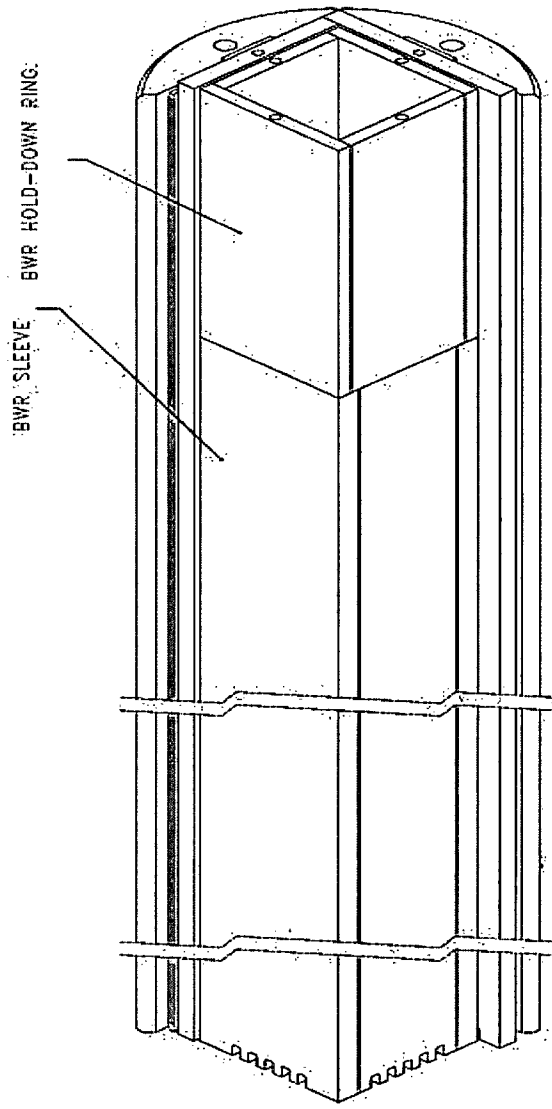


Figure 6.10.4-3
BWR Compartment Sleeve and Hold-Down Ring

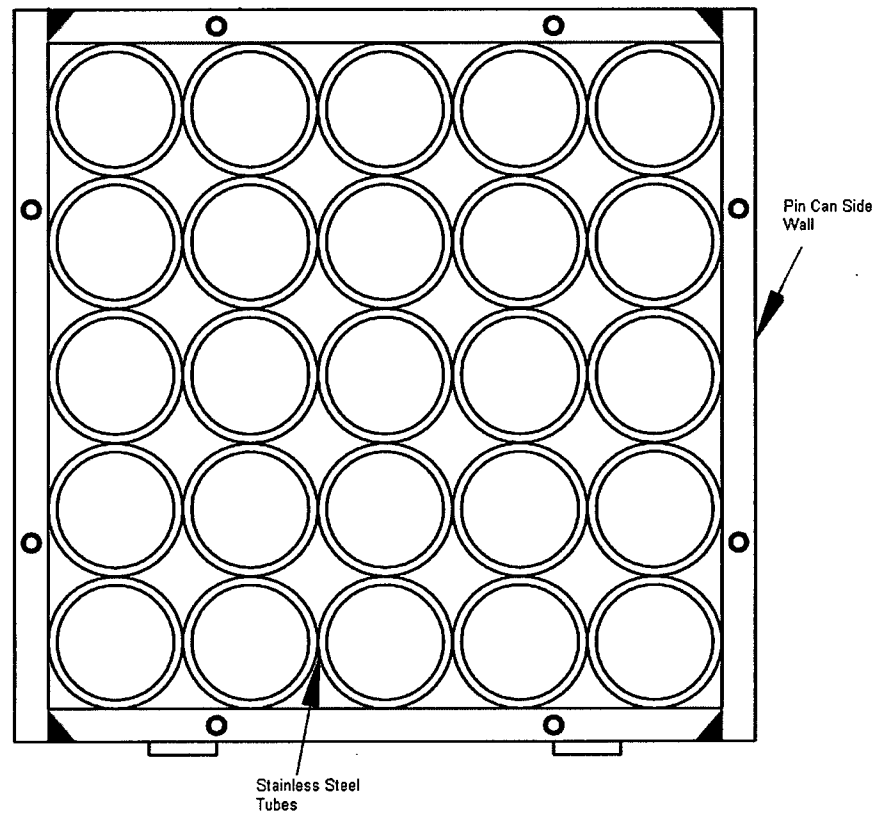


Figure 6.10.4-4
25 Pin Can and Fuel Rod Tubes

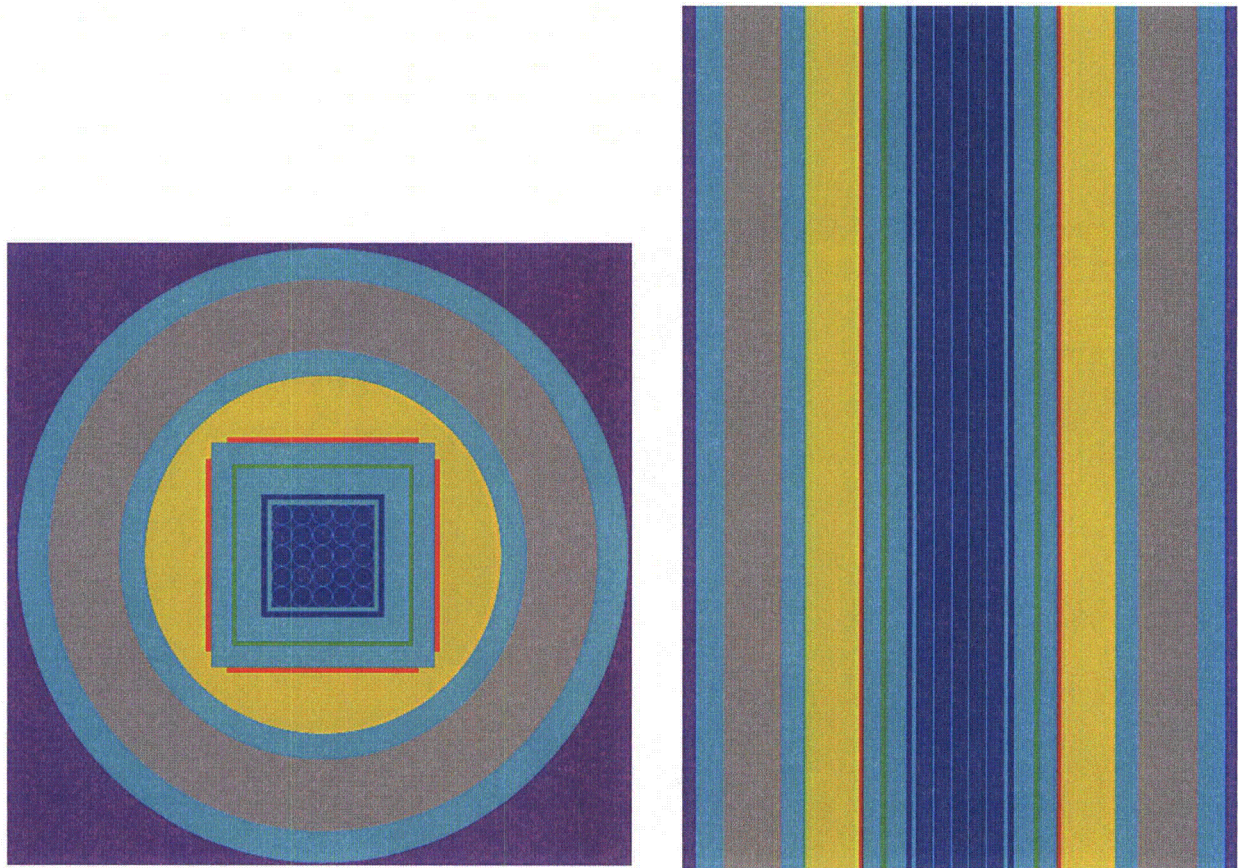


Figure 6.10.4-5
Radial and Axial Cross Sections of the 1FA Basket KENO Model

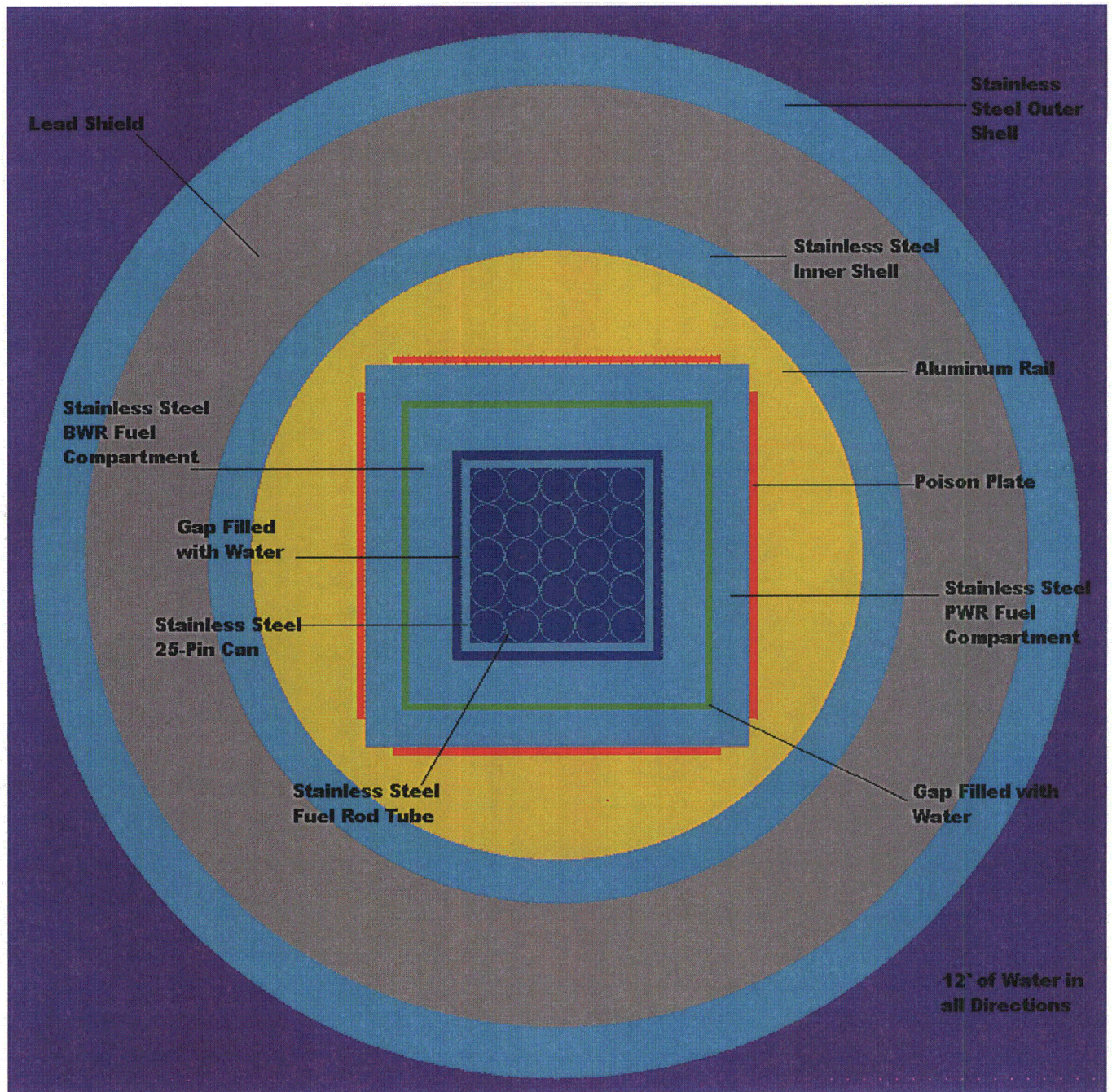
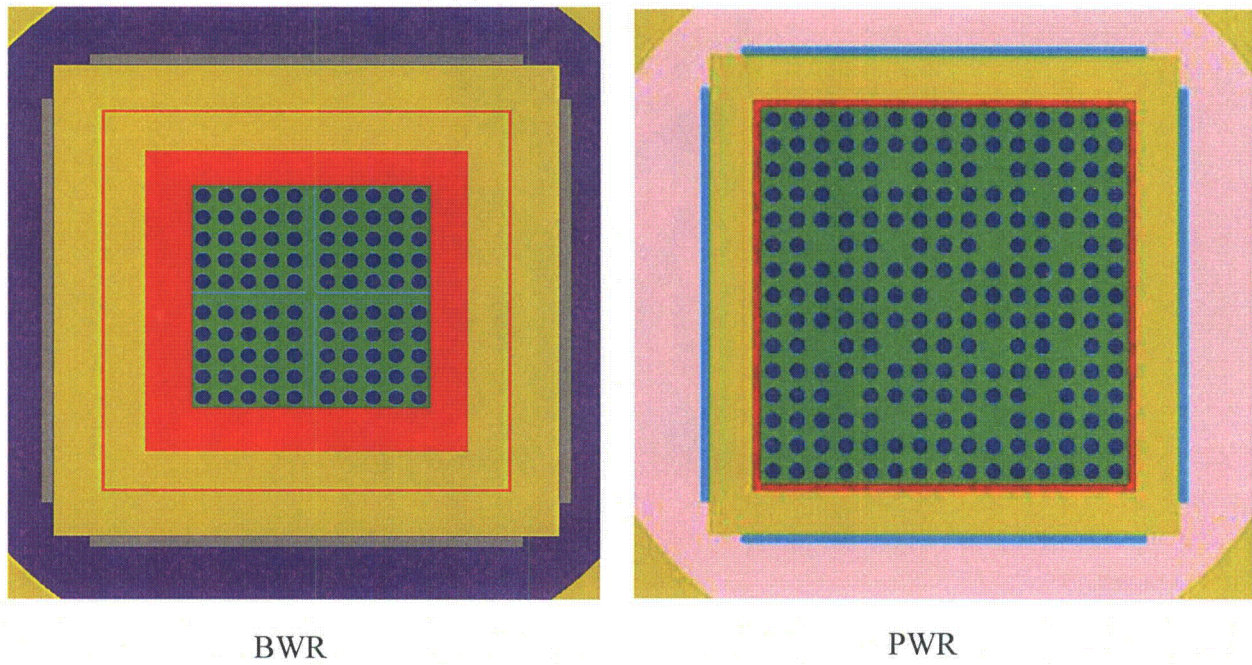


Figure 6.10.4-6
TN-LC 1FA Basket KENO Model



BWR

PWR

Figure 6.10.4-7
BWR and PWR Fuel Models

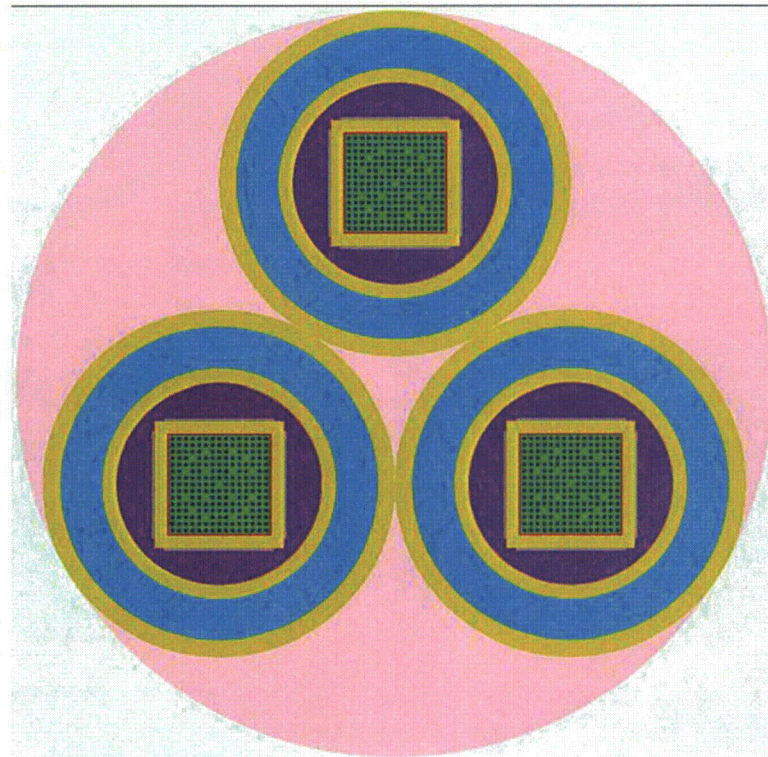
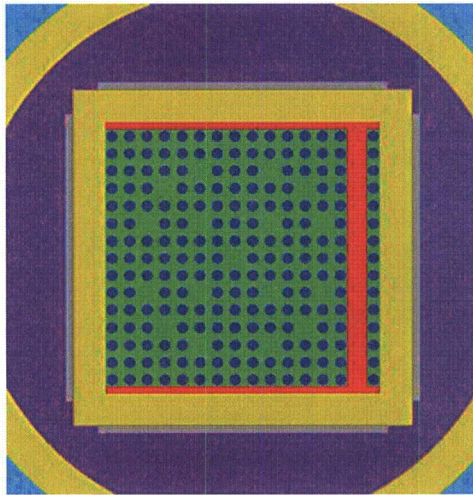
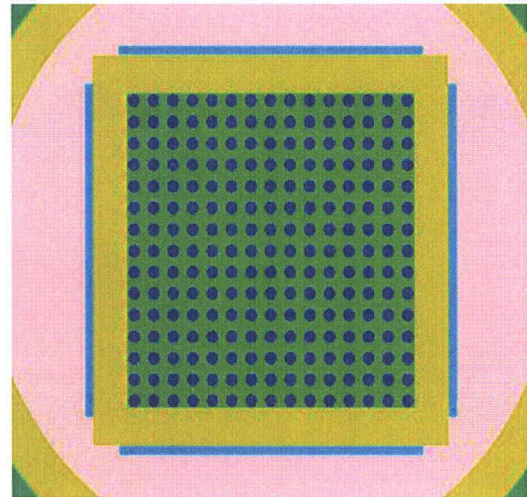


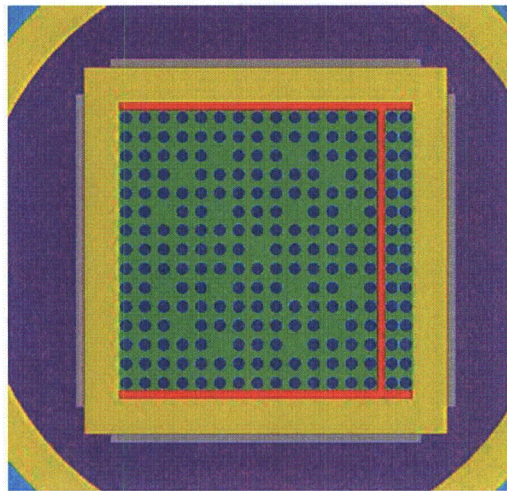
Figure 6.10.4-8
Array of Casks for NCT Analysis



(a) Single Shear Model



(b) Rod Pitch Variation Model



(c) Double Shear Model

Figure 6.10.4-9
Damaged Fuel Models

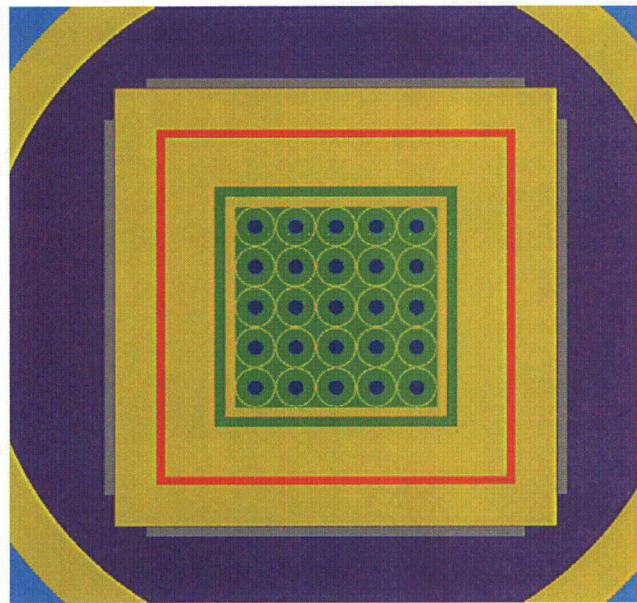


Figure 6.10.4-10
25 Pin Can Model with PWR Fuel

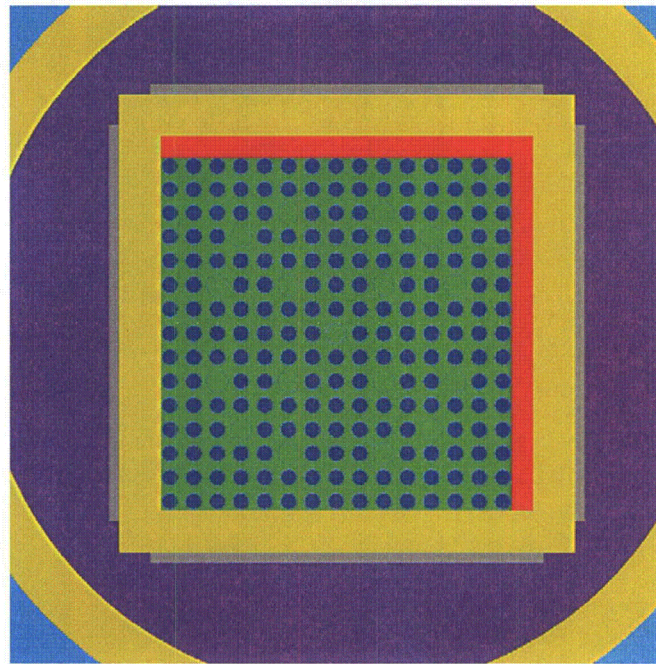


Figure 6.10.4-11
Assembly Positioning

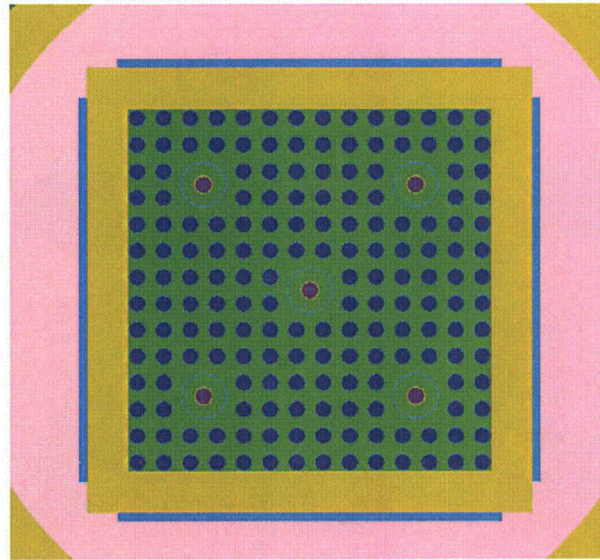
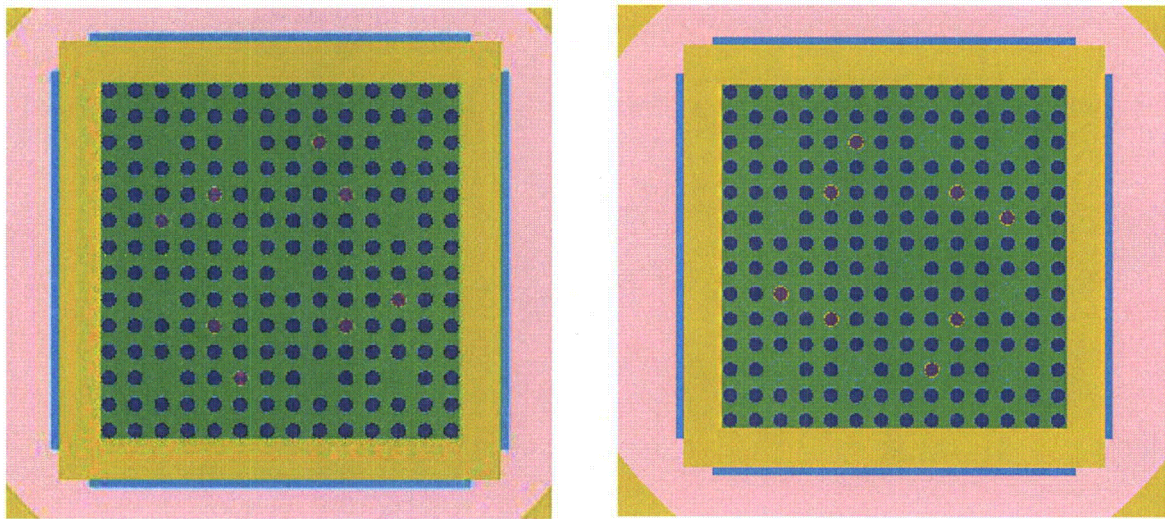


Figure 6.10.4-12
PRA Locations for PWR Fuel Requiring 5 PRAs



Configuration 1

Configuration 2

Figure 6.10.4-13
Possible PRA Configuration for WE 14x14 and WE 15x15 Class Assemblies – NCT and HAC

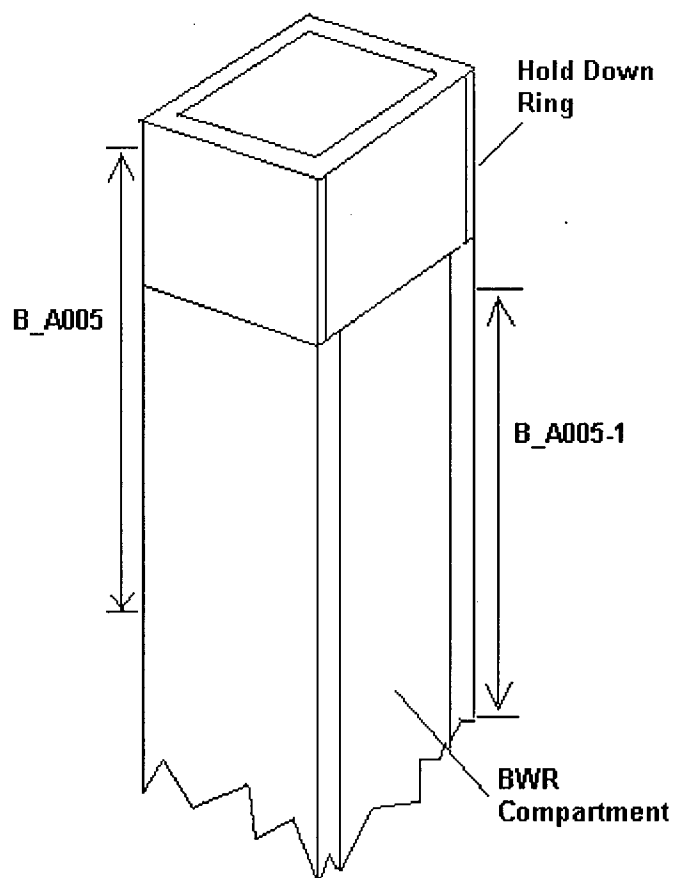
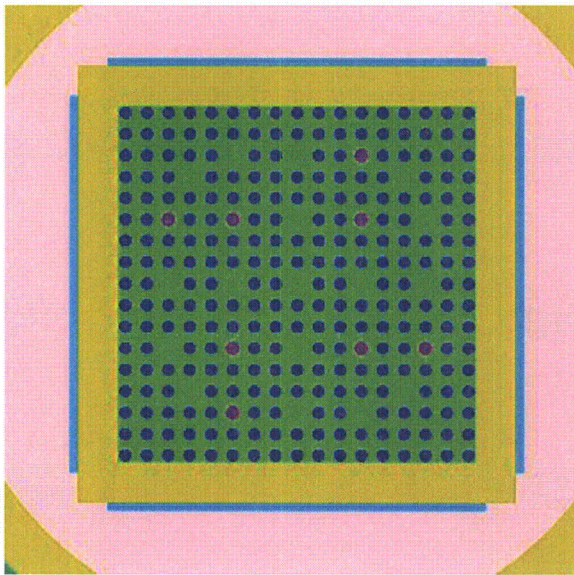
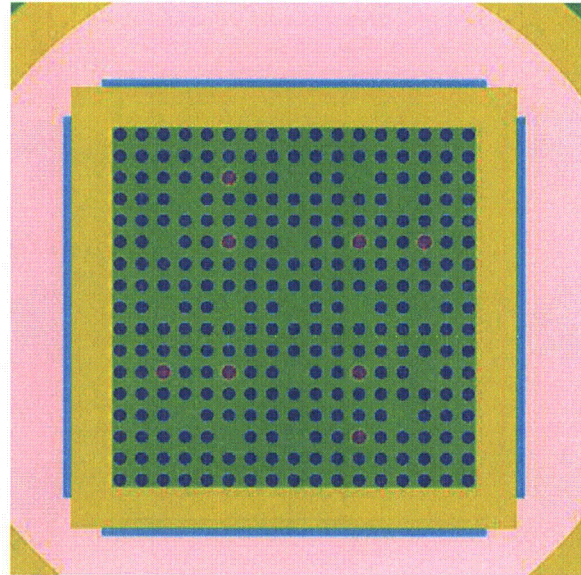


Figure 6.10.4-14
 BWR Modeling Cases to Assess Hold Down Ring Effects



Configuration 3



Configuration 4

Figure 6.10.4-15
PRA Configuration for BW 15x15, BW 17x17 and WE 17x17 Class Fuel Assemblies
– NCT and HAC

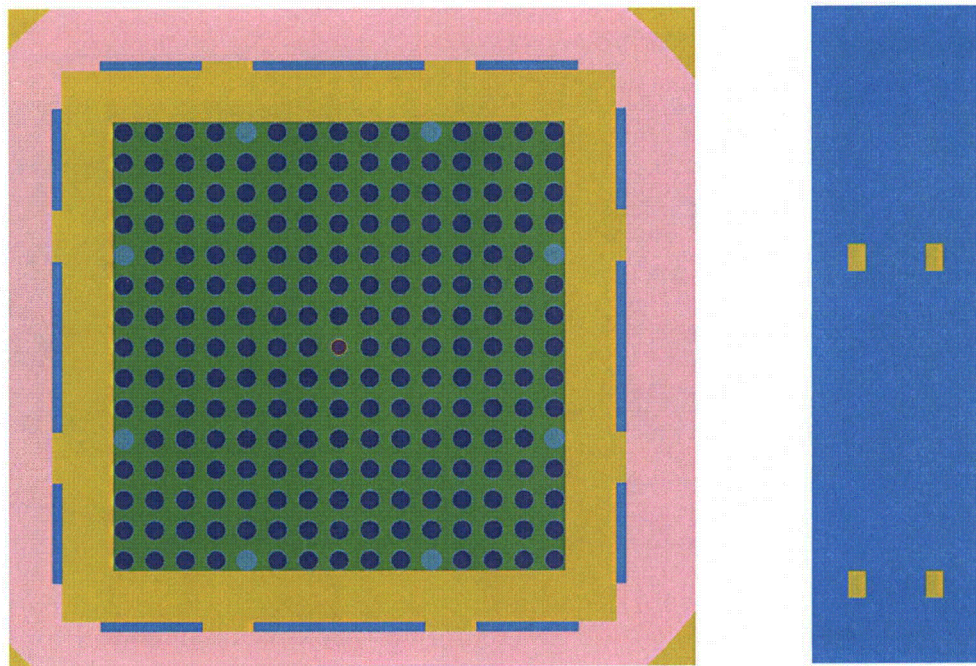


*Figure 6.10.4-16
KENO Model of the Most Reactive Case with Poison Plate Bolt Holes*

Chapter 7 Package Operations

TABLE OF CONTENTS

7.1	TN-LC Package Loading.....	7-1
7.1.1	TN-LC Cask Preparation for Loading.....	7-1
7.1.2	TN-LC Cask Wet Loading.....	7-2
7.1.3	TN-LC Cask Dry Loading.....	7-4
7.1.4	TN-LC Cask Preparation for Transport.....	7-5
7.2	TN-LC Package Unloading.....	7-7
7.2.1	Receipt of Loaded TN-LC Package from Carrier.....	7-7
7.2.2	Removal of Contents from TN-LC Cask.....	7-8
7.3	Preparation of Empty Package for Transport.....	7-11
7.4	Other Operations.....	7-12
7.4.1	Assembly Verification Leakage Testing of the Containment Boundary.....	7-12
7.5	References.....	7-15
7.6	Glossary.....	7-16
7.7	Appendices.....	7-17
7.7.1	TN-LC-NRUX Basket Wet and Dry Loading and Unloading.....	7-17
7.7.2	TN-LC-MTR Basket Wet and Dry Loading and Unloading.....	7-17
7.7.3	TN-LC-TRIGA Basket Wet and Dry Loading and Unloading.....	7-17
7.7.4	TN-LC-1FA Wet and Dry Loading and Unloading.....	7-17

LIST OF TABLES

Table 7-1	Applicable Fuel Specification for Various Fuel Types.....	7-18
Table 7-2	Appendices Containing Loading Procedures for Various TN-LC Baskets.....	7-18
Table 7-3	Appendices Containing Unloading Procedures for Various TN-LC Baskets.....	7-18

LIST OF FIGURES

Figure 7-1	TN-LC Packaging Torquing Patterns.....	7-19
Figure 7-2	Assembly Verification Leakage Test.....	7-20

Chapter 7 Package Operations

NOTE: References in this Chapter are shown as [1], [2], etc., and refer to the reference list in Section 7.5. A glossary of terms used in this Chapter is provided in Section 7.6.

This Chapter contains TN-LC cask loading and unloading procedures that are intended to show the general approach to cask operational activities. The procedures in this chapter are intended to show the types of operations that will be performed and are not intended to be limiting. Site-specific conditions and requirements may require the use of different equipment and ordering of steps to accomplish the same objectives or to meet acceptance criteria to ensure the integrity of the package.

A separate operations manual (OM) will be prepared for the TN-LC cask to describe the operational steps in greater detail. The OM, along with the information in this chapter, will be used to prepare the site-specific procedures that will address the particular operational considerations related to the cask.

7.1 TN-LC Package Loading

The use of the TN-LC cask to transport fuel offsite involves (1) preparation of the empty cask for use; (2) verification that the fuel assemblies or fuel rods to be loaded in the TN-LC cask with the appropriate fuel-specific basket meet the criteria set forth in this document; (3) installation of a basket into the cask; and (4) loading fuel or placing loaded fuel buckets or pin cans in an empty TN-LC cask with the appropriate fuel-specific basket.

Offsite transport involves (1) preparation of the loaded cask for transport; (2) assembly verification leakage-rate testing of the package containment boundary; (3) placement of the cask onto a transportation vehicle; (4) installation of the impact limiters and (5) closure of the transportation container.

During shipment, the package contains any one of the TN-LC basket designs with its authorized contents as described in Chapter 1, Appendices 1.4.2 through 1.4.5. Procedures are provided in this section for (1) transport of the cask directly from a site spent fuel pool and (2) transport of the cask directly from a site hot cell. Appendix 7.7 contains a sub-appendix for each basket design detailing its loading procedures.

7.1.1 TN-LC Cask Preparation for Loading

Procedures for preparing the cask for use after receipt at the loading site are provided in this section and are applicable for shipment of casks loaded with any one of the basket designs and its respective approved contents.

1. Upon arrival of the empty TN-LC Package at the receiving site, perform receipt inspection. Inspect for damage, verify tamper-indicating seal is intact and perform radiation survey.
2. Open the transport container, and remove the empty TN-LC package.

3. Remove the tamper-indicating seals.
4. Remove the impact limiters from the cask.
5. Prior to removing the lid, sample the cask cavity atmosphere.
6. Remove the skid tie-down assembly.
7. Take contamination smears on the outside surfaces of the cask. If necessary, decontaminate the cask.
8. O-ring seals shall be discarded after each use.
9. Remove the trunnion and pocket trunnion plugs.
10. Install the two lifting trunnions in place of the front trunnions plugs. Install the trunnion bolts and torque them to 700-750 ft-lbs following the torquing sequence shown in Figure 7-1.
11. For the specific payload to be transported as part of the TN-LC package, verify that the basket type (TN-LC-NRUX, TN-LC-MTR, TN-LC-TRIGA, or TN-LC-1FA) and spacers, if required, are appropriate for the fuel to be transported.
12. The candidate intact fuel assemblies/elements or fuel rods to be transported in a specific basket must be evaluated to verify that they meet the fuel qualification requirements of the applicable fuel specification as listed in Table 7-1.

7.1.2 TN-LC Cask Wet Loading

NOTE: The wet loading procedure described in this section is applicable only when using the TN-LC cask for loading fuel from a fuel pool into any one of the baskets listed in Chapter 1, Table 1-2.

Site-specific conditions or procedures may require the use of different equipment and ordering of steps than those described below to accomplish the same objectives or to meet acceptance criteria which ensure the integrity of the package.

1. Prior to being placed in service, the cask is to be cleaned or decontaminated, as necessary.
2. Remove the bottom plug assembly, inspect the sealing surfaces, replace the old seals with new seals, lubricate and reinstall the bottom plug assembly (Chapter 1, Appendix 1.4.1, drawing 65200-71-01), torquing the bolts to 40-48 ft-lbs. The option 2 bottom plug assembly MUST only be used when the TN-LC-1FA basket with the 25 pin can is employed.
3. Engage the cask trunnions with the cask lifting yoke.
4. Rotate the cask to a vertical orientation, lift the cask, and place the cask in the designated preparation area.

NOTE: Alternatively, the cask may be lifted in a horizontal orientation and placed on an onsite transfer trailer or upending frame; or the cask/transportation skid may be lifted together and placed in the appropriate location.

5. Install the shear key plug assembly and the pocket trunnion plugs.
6. If the cask lid has not already been removed, remove the bolts from the lid and lift the lid from the cask.
7. Depending on the basket design being loaded, verify that a cask spacer of appropriate height is placed at the bottom of the cask cavity and/or bolted to the underside of the lid.
8. Insert the basket appropriate for the fuel to be transported into the cask, as listed in Table 7-2.

Notes:

- Install a bottom spacer in the basket if required by Chapter 1, Appendix 1.4.1 basket drawings.
 - If loading a BWR fuel assembly in a TN-LC-1FA basket, place a BWR sleeve with a BWR hold down ring in the basket as shown in drawing 65200-71-96.
 - If loading fuel rods in a TN-LC-1FA basket, place a 25 pin can inside the BWR sleeve with a hold down ring in the basket as shown in drawing 65200-71-102.
9. Fill the cask cavity with fuel pool water.
 10. Lift the cask and position it over the cask loading area of the fuel pool.
 11. Lower the cask into the fuel pool.
 12. Place the cask in the fuel pool cask loading area.
 13. Disengage the lifting yoke from the cask trunnions and move the yoke clear of the cask.
 14. The operations for loading fuel into a specific basket type are described in detail in Appendices 7.7.1 through 7.7.4 as listed in Table 7-2.
 15. Lower the lid into place
 16. Visually verify that the lid is properly seated in the cask.
 17. Raise the cask to the pool surface using the cask trunnions and the lifting yoke.
 18. Verify that the lid is properly seated on the cask. If not, lower the cask and reposition the lid. Repeat the above steps as necessary.
 19. Continue to raise the cask from the pool until the top region of the cask is accessible.

20. Perform a radiological survey of the cask as it is raised out of the pool.
21. Install at least two lid bolts hand tight.
22. When the cask drain plug is accessible, open the drain plug and drain the cavity until no appreciable water is noted. Optionally, the cavity may be drained after securing the cask in the site work area. For loading a PWR/BWR fuel assembly, consistent with NUREG-1536 [6] guidance, helium at 1-3 psig is used to backfill the cask cavity with an inert gas (helium) as water is being removed from the cask cavity.
23. Move the cask to the site designated preparation area and secure the cask, as required.

The cask is now ready to be prepared for downending as described in Section 7.1.2.1 below.

7.1.2.1 Preparing the TN-LC Cask for Downending

1. Discard the drain port seal, and install a new drain port seal. Torque the drain port plug to 60-70 ft-lbs and install the drain port plug cover.
2. Verify the lid O-ring seals are new.
3. Install the cask lid. Follow the torquing sequence shown in Figure 7-1, torque the lid bolts to 400-450 ft-lbs.
4. Discard cavity test port seal, and install new cavity test port seal.
5. Using the vacuum pump system, evacuate the cask cavity to 3 torr or less to ensure that the cask cavity has no free standing water and is essentially dry.
6. Backfill with helium to $2.5 \pm$ psig.
7. Perform the assembly verification leakage test following the procedure given in Section 7.4.1.

7.1.2.2 TN-LC Cask Downending

NOTE: Alternate procedures may be developed for plants with unique requirements.

1. Remove the shear key plug assembly and the pocket trunnion plugs from the cask.
2. Lift the cask over the transportation skid.
3. Lower and rotate the cask from vertical to horizontal and secure it to the skid.
4. Prepare the cask for transportation in accordance with the procedure described in Section 7.1.4.

7.1.3 TN-LC Cask Dry Loading

NOTE: The dry loading procedure described in this section is applicable only when using the TN-LC cask for loading fuel from a hot cell into any one of the baskets listed in Chapter 1, Table 1-2.

The procedure for loading the cask from a hot cell is highly dependent on the design of the facility. The procedure described below is intended to show the type of operations that will be performed and is not intended to be limiting. Site-specific conditions or procedures may require the use of different equipment and ordering of steps than those described below to accomplish the same objectives or to meet acceptance criteria which must be met to ensure the integrity of the package.

Steps 1 through 8 for preparation of the TN-LC cask for dry loading are the same as those described above in Section 7.1.2, TN-LC Cask Wet Loading.

1. Place the cask in the location of the hot cell designated as the cask loading area or mate the cask opening with the hot cell portal. Note that this may require downending the cask into a horizontal orientation.
2. If the cask lid has not already been removed, remove the bolts from the lid and, using appropriate slings and/or the cask yoke with appropriate slings, lift the lid from the cask.
3. Disengage the lifting yoke or other lifting device from the trunnions and move the yoke clear of the cask.
4. The operations for loading fuel into a specific basket type are described in detail in Appendices 7.7.1 through 7.7.4 as listed in Table 7-2.
5. Install the lid on the cask. Verify that the lid is properly seated in the cask. If not, reposition the lid.
6. Install and torque the lid bolts to 400-450 ft-lbs following the torquing sequence shown in Figure 7-1.
7. Remove the loaded cask from the hot cell or disengage it from the hot cell portal. Perform a radiological survey of the cask as it is removed.
8. Move the cask to the site designated preparation area and secure the cask, as required.

The cask is now ready to be prepared for downending as described in section 7.1.2.1 above.

7.1.4 TN-LC Cask Preparation for Transport

Once the TN-LC cask has been loaded using either the wet loading procedure described in Section 7.1.2 or the dry loading procedure described in Section 7.1.3 above, the following tasks are performed to prepare the cask for transportation. The cask is assumed to be seated horizontally on the transportation skid. Alternate procedures may be developed for plants with unique requirements.

1. Verify that the cask surface removable contamination levels meet the requirements of 49CFR173.443 [2] and 10CFR71.87 [3].
2. Verify that the assembly verification leakage testing specified in Section 7.4.1 has been performed.

7.1.4.1 Placing the TN-LC Cask onto the Conveyance

The procedure for placement of the cask on the conveyance is given in this section. If the cask is on the transportation skid, but the skid is not on the conveyance, rig the cask/skid, lift and place them onto the conveyance.

1. Install the transportation skid tie-down straps.
2. Install the pocket trunnion plugs.
3. Remove the two trunnions, and install the trunnion plugs.
4. Install the impact limiters on the cask, torquing the attachment bolts to 330-375 ft-lbs.
5. Remove the impact limiter hoist rings and replace them with hex bolts.
6. Install the tamper-indicating seals.
7. Perform a final radiation survey to ensure the cask radiation levels do not exceed 49CFR173.441 [2] and 10CFR71.47 [3] requirements.
8. Place the TN-LC Package in the shipping container.
9. Verify that the temperature on all accessible surfaces is $< 185^{\circ}$ F.
10. Verify that placards, labels, markings and seals are in place and correct.
11. Close the transport container.
12. Prepare the final shipping documentation and release the TN-LC Package for shipment.

7.2 TN-LC Package Unloading

Unloading the TN-LC Package after transport involves removing the cask from the conveyance and removing the fuel from the cask. The cask is designed to allow the fuel to be unloaded from the cask into a hot cell and provisions exist to allow wet unloading in a fuel pool. The necessary procedures for these tasks are essentially the reverse of those described in Section 7.1.

7.2.1 Receipt of Loaded TN-LC Package from Carrier

Procedures for receiving the TN-LC Package after shipment are described in this section. Procedures for preparing an empty package are provided in Section 7.1.1.

1. Upon arrival of the loaded TN-LC Package at the receiving site, perform receipt inspection. Inspect for damage, verify tamper-indicating seal is intact and perform radiation survey.
2. Open the transport container, and remove the TN-LC package.
3. Remove the tamper-indicating seals.
4. Remove the hex bolts from the impact limiters and replace them with the impact limiter hoist rings provided.
5. Remove the impact limiters from the cask.
6. Remove the transportation skid tie-down straps.
7. Prior to removing the lid, sample the cask cavity atmosphere
8. Take contamination smears on the outside surfaces of the cask. If necessary, decontaminate the cask.
9. Remove the pocket trunnion plugs and trunnion plugs.
10. Install the two trunnions in place of the trunnion plugs, torquing the trunnion bolts to 700-750 ft-lbs in the sequence shown in Figure 7-1.
11. Rotate the cask to a vertical orientation, lift the cask, and place the cask in the designated location.
12. Install the shear key plug assembly and the pocket trunnion plugs.
13. Transfer the cask to the fuel pool or a hot cell interface and unload using the procedures described in the following sections.

7.2.2 Removal of Contents from TN-LC Cask

7.2.2.1 Unloading the TN-LC Cask in a Fuel Pool

The procedure for unloading the cask in a fuel pool is summarized in this section. Site-specific conditions and requirements may require the use of different equipment and ordering of steps than those described below to accomplish the same objectives or to meet acceptance criteria to ensure the integrity of the package.

1. Verify that the TN-LC cask receipt process in Section 7.2.1 has been completed.
2. Using the cask port tool, install a pressure gauge, isolation valve and vent line to the site radwaste system on the vent port. Open the cask cavity vent to the site radwaste system and sample the cask cavity atmosphere. Flush the cask cavity if necessary.
3. Remove the drain port plug and install an appropriate fitting in the drain port. Alternatively, cask port tool may be used to perform flooding and draining activities.
4. Install a pressure gauge, isolation valve, check valve, and a supply of clean water to the drain port/fitting.
5. Slowly feed water to enter the cask cavity.
6. Maintain the pressure in the cask cavity below 20 psig.
7. When the cask is filled with water, remove the vent and supply lines.
8. Loosen the lid bolts, leaving the threads engaged. Reverse the torquing sequence shown in Figure 7-1.
9. Slowly lower the cask into the pool until the lid is just above the surface.
10. Remove the lid bolts and lower the cask to its unloading position in the pool.
11. Detach the yoke from the trunnions and lift the lid from the cask.
12. Follow the fuel-specific unloading procedure as listed in Table 7-3 and described in Appendix 7.7.1 through 7.7.4.
13. Following removal of the fuel assemblies or fuel rods and lift the cask from the spent fuel pool.
14. Open the drain and drain the pool water from the cavity. Continue draining the cavity until no appreciable water is noted. Optionally, the cavity may be drained after securing the cask body in the site work area.
15. Decontaminate the cask as necessary and replace the lid.
16. Move the cask to the site designated preparation area and secure the cask, as required.

7.2.2.2 Unloading the TN-LC Cask to a Hot Cell

The procedure for unloading the cask to a hot cell is highly dependent on the design of the dry cell. The procedure described below is intended to show the type of operations that will be performed and is not intended to be limiting. Site-specific conditions and requirements may require the use of different equipment and ordering of steps than those described below to accomplish the same objectives or acceptance criteria which must be met to ensure the integrity of the package.

NOTE: See Section 7.2.2.3 for dry unloading of a 25 pin can.

1. Verify that the TN-LC cask receipt process in Section 7.2.1 has been completed.
2. Using the cask port tool, install a pressure gauge, isolation valve and vent line to the site radwaste system on the vent port. Vent the cask cavity to the site radwaste system and sample the cask cavity atmosphere. Flush the cavity gases if necessary.
3. Place the cask on a designated transfer cart if required.
4. Move the cask to the hot cell cask unloading area or mate the cask opening with the hot cell portal.
5. Remove the lid from the cask. Reverse the torquing sequence shown in Figure 7-1.
6. Follow the specific unloading procedure as listed in Table 7-3 and described in Appendices 7.7.1 through 7.7.4.
7. Retrieve the cask from the hot cell loading area and decontaminate the cask if necessary.
8. Move the cask to the site-designated preparation area and secure the cask, as required.

7.2.2.3 Horizontal Unloading of a 25 Pin Can from the TN-LC Cask

This procedure is for handling a TN-LC cask with a 25 pin can in a 1FA basket at a facility with a hot cell. The procedure described below is intended to show the type of operations that will be performed and is not intended to be limiting. Site-specific conditions and requirements may require the use of different equipment and ordering of steps than those described below to accomplish the same objectives or acceptance criteria which must be met to ensure the integrity of the package.

1. Verify that the TN-LC cask receipt process in Section 7.2.1 has been completed.
2. Using the cask port tool, install a pressure gauge, isolation valve and vent line to the site radwaste system on the vent port. Vent the cask cavity to the site radwaste system and sample the cask cavity atmosphere. Flush the cavity gases if necessary.
3. Lift the cask and downend it to a horizontal position on an unloading cradle.
4. Move the cask to the hot cell and mate the cask to the hot cell.

5. Remove the lid from the cask.

NOTE: Alternatively, the lid may be removed from the cask prior to mating the cask with the hot cell portal, provided that shielding and personnel dose requirements are met.

6. Follow the specific unloading procedure as listed in Table 7-3 and described in Appendices 7.7.1 through 7.7.4.
7. Replace the lid and disconnect the cask from the hot cell.
8. Decontaminate the cask if necessary.
9. Upend the cask and move it to the cask preparation area.

7.3 Preparation of Empty Package for Transport

Previously used and empty TN-LC casks shall be prepared for transport in accordance with the requirements of 49CFR173.427 [2].

7.4 Other Operations

7.4.1 Assembly Verification Leakage Testing of the Containment Boundary

The procedure for leakage testing of the cask containment boundary prior to shipment is given in this section. Assembly verification leakage testing shall conform to the requirements of ANSI N14.5 [1] or ISO -12807 [5]. A flow chart of the assembly verification leakage testing is provided in Figure 7-2. The order in which the leakage test of the various seals are performed may vary. If more than one leakage detector is available, then more than one seal may be tested at a time. Personnel performing the leakage testing shall be specifically trained in leakage testing in accordance with SNT-TC-1A [4].

Vent Port Plug Seal Leakage Test

1. Remove the vent port plug cover. Install the cask port tool in the vent port.
2. Open the vent port plug.
3. Attach a suitable vacuum pump to the cask port tool.
4. Reduce the cask cavity pressure to below 1.0 psia.
5. Fill the cask cavity with helium to atmospheric pressure.
6. Close the vent port plug, torquing it to 60-70 ft-lbs.
7. Remove the helium-saturated cask port tool and install a clean (helium free) cask port tool.
8. Connect a mass spectrometer leak detector to the cask port tool.
9. Evacuate the vent port until the vacuum is sufficient to operate the leakage detection equipment.
10. Perform the leakage test. If the leakage rate is greater than 1×10^{-7} ref cm^3/s , repair or replace the vent port seal as required and retest.

NOTE: Upon removing the vent port plug and seal, it will be necessary to reduce the cask cavity pressure below 1.0 psia and refill with helium through the vent port.
11. Remove the leakage detection equipment.
12. Remove the cask port tool and replace the vent port plug cover.

Lid O-ring Leakage Test

13. Remove the lid test port plug cover.
14. Install the cask port tool in the lid test port.
15. Open the lid test port plug.

16. Connect the vacuum pump to the cask port tool.
17. Connect the leakage detector to the cask port tool.
18. Evacuate the lid test port until the vacuum is sufficient to operate the leakage detection equipment per the manufacturer's recommendations. Perform a pressure rise leakage test to confirm leakage rate past the outer seal is less than 7×10^{-7} ref cm^3/s .
19. Perform the helium leakage test. If the leakage rate is greater than 1×10^{-7} ref cm^3/s , repair or replace the cask lid or the cask lid O-ring seals as required and retest.

NOTE: Upon removing and reinstalling the cask lid, it will be necessary to reduce the cask cavity pressure below 1.0 psia and refill with helium through the vent port. The vent port assembly verification leakage test must also be redone as described above.

20. Remove the leakage detection equipment.
21. Close lid test port plug. Remove the cask port tool from the lid test port and replace the lid test port plug cover.

Drain Port Plug Seal Leakage Test

22. Remove the cask drain port plug cover.
23. Verify that the cask drain port is closed and torqued to 60-70 ft-lbs.
24. Install the cask port tool in the cask drain port.
25. Connect the vacuum pump to the cask port tool.
26. Connect the leakage detector to the cask port tool.
27. Evacuate the drain port until the vacuum is sufficient to operate the leakage detection equipment.
28. Perform the leakage test. If the leakage rate is greater than 1×10^{-7} ref cm^3/s , repair or replace the drain port seal as required and retest.

NOTE: Upon removing the drain port plug and seal, it will be necessary to reduce the cask cavity pressure below 1.0 psia and refill with helium through the vent port. The vent port assembly verification test must also be redone as described above.

29. Remove the leakage detection equipment.
30. Remove the cask port tool from the cask drain port and replace the drain port plug cover.

Bottom Plug O-ring Leakage Test

31. Remove the bottom test port plug cover.

32. Install the cask port tool in the bottom test port.
33. Open the bottom test port plug.
34. Connect the vacuum pump to the cask port tool.
35. Connect the leakage detector to the cask port tool.
36. Evacuate the bottom test port until the vacuum is sufficient to operate the leakage detection equipment per the manufacturer's recommendations. Perform a pressure rise leakage test to confirm leakage rate past the outer seal is less than 7×10^{-7} ref cm^3/s .
37. Perform the helium leakage test. If the leakage rate is greater than 1×10^{-7} ref cm^3/s , repair or replace the bottom plug or the bottom plug O-ring seals as required and retest.

NOTE: Upon removing and reinstalling the bottom plug, it will be necessary to reduce the cask cavity pressure below 1.0 psia and refill with helium through the vent port. The vent port assembly verification leakage test must also be redone as described above.
38. Remove the leakage detection equipment.
39. Close bottom test port plug. Remove the cask port tool from the bottom test port and replace the bottom test port plug cover.

This concludes the assembly verification leakage test procedure.

7.5 References

1. ANSI N14.5-1997, "American National Standard for Radioactive Materials - Leakage Tests on Packages for Shipment," American National Standards Institute, Inc., New York, 1997.
2. Title 49, Code of Federal Regulations, Part 173 (49CFR173), "Shippers - General Requirements for Shipments and Packaging."
3. Title 10, Code of Federal Regulations, Part 71 (10CFR71), "Packaging and Transportation of Radioactive Material."
4. SNT-TC-1A, "American Society for Nondestructive Testing, Personnel Qualification and Certification in Nondestructive Testing."
5. ISO-12807, "Safety Transport of Radioactive Materials – Leakage Testing on Packages," First Edition, 1996.
6. USNRC, NUREG-1536, "Standard Review Plan for Spent Fuel Dry Storage Systems at a General License Facility," Final Report, Revision 1.

7.6 Glossary

The terms used in the above procedures are defined below.

cask lifting yoke: Passive lifting yoke used for vertical lifts and upending of the cask.

conveyance: Any suitable conveyance such as a railcar, heavy haul trailer, barge, ship, etc.

ram: rod with threaded end used to insert/withdraw 25 pin can to/from hot cell.

7.7 Appendices

7.7.1 TN-LC-NRUX Basket Wet and Dry Loading and Unloading

7.7.2 TN-LC-MTR Basket Wet and Dry Loading and Unloading

7.7.3 TN-LC-TRIGA Basket Wet and Dry Loading and Unloading

7.7.4 TN-LC-1FA Wet and Dry Loading and Unloading

Table 7-1
Applicable Fuel Specification for Various Fuel Types

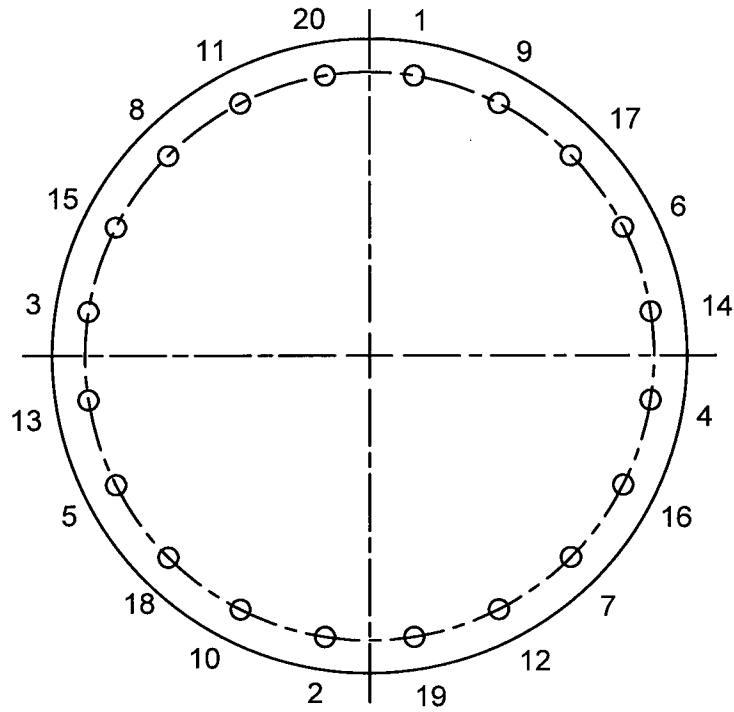
Basket Design	Applicable Fuel Specification from Chapter 1
TN-LC-NRUX	Table 1.4.2-1 and 1.4.2-2
TN-LC-MTR	Table 1.4.3-1 thru Table 1.4.3-3
TN-LC-TRIGA	Table 1.4.4.1 thru 1.4.4-5
TN-LC-1FA	Table 1.4.5-1 thru 1.4.5-14

Table 7-2
Appendices Containing Loading Procedures for Various TN-LC Baskets

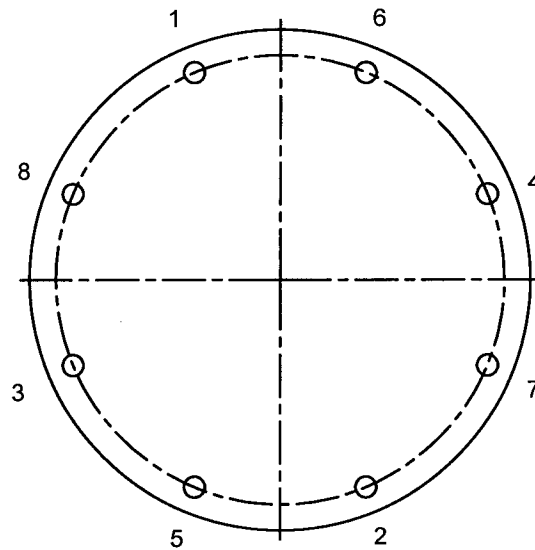
Basket Type	Subbasket Type	Appendix	Bottom Spacer Required?
TN-LC-NRUX	—	7.7.1, Sections 7.7.1.1-2	Yes
	—	7.7.1, Sections 7.7.1.1-2	Yes
TN-LC-MTR	—	7.7.2, Sections 7.7.2.1-2	Yes
TN-LC-TRIGA	—	7.7.3, Sections 7.7.3.1-2	Yes
TN-LC-1FA	1-PWR	7.7.4, Sections 7.7.4.1-2	Yes
	1-BWR	7.7.4, Sections 7.7.4.1-2	Yes
	25 Pin Can	7.7.4, Sections 7.7.4.1-2	No

Table 7-3
Appendices Containing Unloading Procedures for Various TN-LC Baskets

Basket Type	Subbasket Type	Appendix
TN-LC-NRUX	—	7.7.1, Sections 7.7.1.3-4
	—	7.7.1, Sections 7.7.1.3-4
TN-LC-MTR	—	7.7.2, Sections 7.7.2.3-4
TN-LC-TRIGA	—	7.7.3, Sections 7.7.3.3-4
TN-LC-1FA	1-PWR	7.7.4, Sections 7.7.4.3-4
	1-BWR	7.7.4, Sections 7.7.4.3-4
	25 pin can	7.7.4, Sections 7.7.4.3-4



LID



TRUNNION AND BOTTOM PLUG ASSEMBLY

Figure 7-1
TN-LC Packaging Torquing Patterns

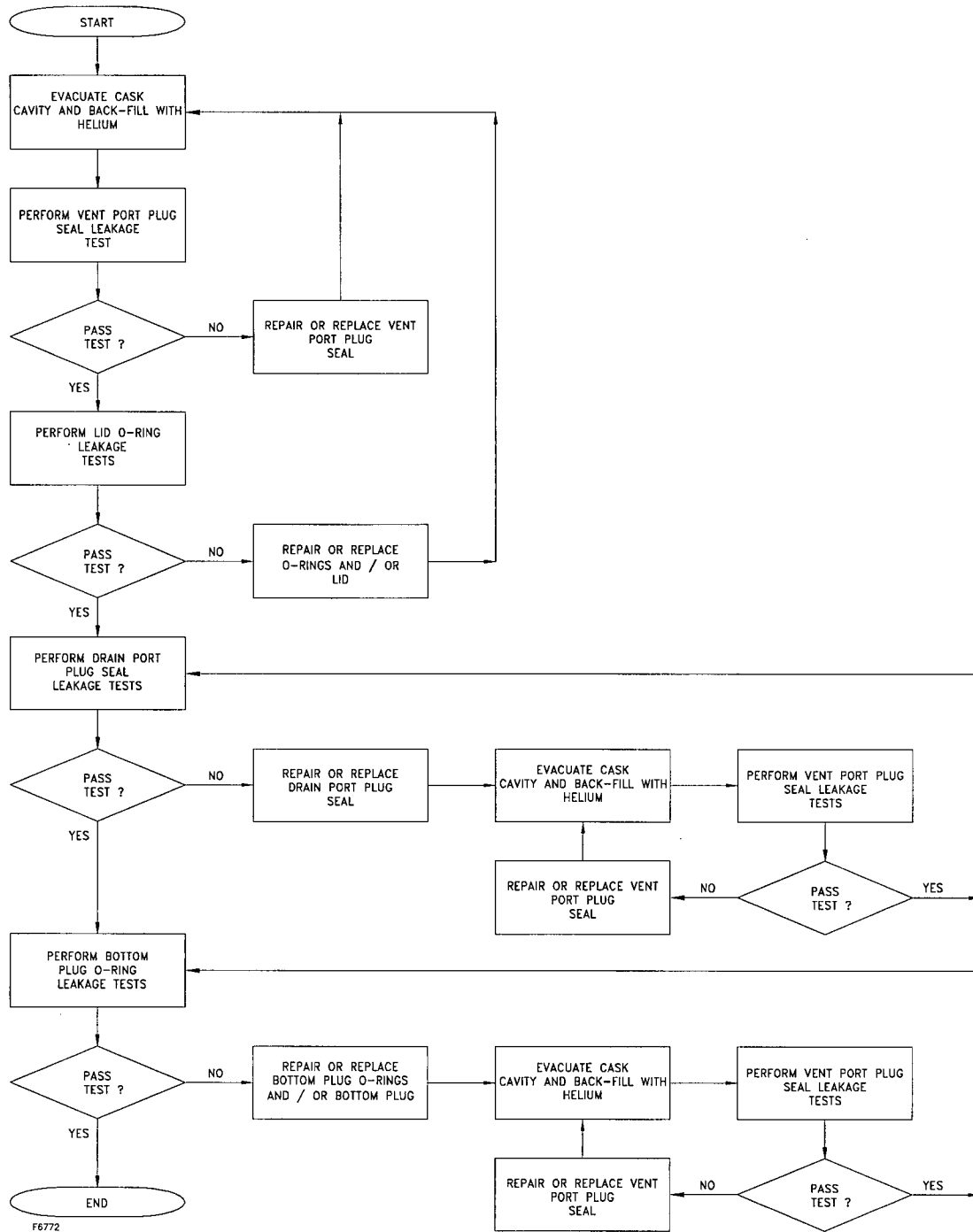


Figure 7-2
 Assembly Verification Leakage Test

Appendix 7.7.1
TN-LC-NRUX Basket Wet and Dry Loading and Unloading

TABLE OF CONTENTS

7.7.1.1	TN-LC-NRUX Basket Wet Loading	7.7.1-1
7.7.1.2	TN-LC-NRUX Basket Dry Loading.....	7.7.1-3
7.7.1.3	TN-LC-NRUX Basket Wet Unloading.....	7.7.1-4
7.7.1.4	TN-LC-NRUX Basket Dry Unloading.....	7.7.1-5

Appendix 7.7.1 TN-LC-NRUX Basket Wet and Dry Loading and Unloading

NOTE: References in this Appendix are shown as [1], [2], etc., and refer to the reference list in Section 7.5. A glossary of terms used in this Appendix is provided in Chapter 7, Section 7.6.

Site-specific conditions and requirements may require the use of different equipment and ordering of steps than those described below to accomplish the same objectives or to meet acceptance criteria to ensure the integrity of the package.

7.7.1.1 TN-LC-NRUX Basket Wet Loading

The starting condition for the following steps assumes completion of the cask preparation steps in Section 7.1.1 and steps 1-14 of Section 7.1.2 of Chapter 7.

The wet loading procedure described in this section is applicable when loading NRU and/or NRX fuel from a fuel pool into the TN-LC cask (containing a TN-LC-NRUX basket) which is submerged in a fuel pool.

The procedure described below assumes that each of the two TN-LC-NRUX basket subassemblies is loaded and staged prior to placement into the TN-LC cask. Alternately, the subassemblies may be pre-placed in the TN-LC cask and loaded in situ.

Prior to the loading, verify that the TN-LC-NRUX basket is in place and that the basket spacer plate has been bolted to the TN-LC lid.

1. Stage the empty TN-LC-NRUX basket subassemblies.
2. The potential for fuel misloading is essentially eliminated through the implementation of procedural and administrative controls. The controls instituted to ensure that acceptable spent fuel assemblies (SFA) are placed into the TN-LC cask will typically consist of the following:
 - A cask loading plan is developed to verify that the candidate intact SFAs meet the fuel qualification requirements of the applicable sections as listed in step 12 of Section 7.1.1.
 - The loading plan is independently verified and approved before fuel load.
 - A fuel movement schedule is then written, verified, and approved based on the loading plan. All fuel movements from any storage cell location are performed under strict compliance with the fuel movement schedule.
3. Prior to loading an SFA into a TN-LC-NRUX basket subassembly, the identity of the SFA is to be verified by two individuals using a video camera or other means. Read and record the identification number from the SFA and check this identification number against the site loading plan which indicates which SFAs are acceptable for transport.

4. Position the SFA for insertion into the selected TN-LC-NRUX subassembly compartment and load the SFA. Repeat steps 2 and 3 for each SFA to be transported in the specific TN-LC cask shipment. Record the compartment position of each SFA.
5. Use the TN-LC-NRUX basket subassembly lifting fixture to place the loaded TN-LC-NRUX basket subassembly into the TN-LC-NRUX basket.
6. Install the TN-LC-NRUX basket subassembly top tube cap.
7. Repeat steps 4 through 6, for the second TN-LC-NRUX basket subassembly.

Following completion of above listed steps, the TN-LC-NRUX basket wet loading is continued in step 15, Section 7.1.2 of Chapter 7.

7.7.1.2 TN-LC-NRUX Basket Dry Loading

The starting condition for the TN-LC-NRUX basket dry loading following steps assumes completion of the cask preparation steps in Section 7.1.1 and steps 1-4 of Section 7.1.3 of Chapter 7.

The dry loading procedure described in this section is applicable when using the TN-LC cask for loading NRU and/or NRX fuel from a hot cell (or other dry storage location) into the TN-LC cask with TN-LC-NRUX basket which is accessible from the hot cell.

The procedure described below assumes that each of the two TN-LC-NRUX basket subassemblies is loaded and staged prior to placement into the TN-LC cask. Alternately, the subassemblies may be pre-placed in the TN-LC cask and loaded in situ.

Prior to the loading, verify that the TN-LC-NRUX basket is in place and that the basket spacer plate has been bolted to the TN-LC lid.

1. Stage the empty TN-LC-NRUX basket subassemblies.
2. The potential for fuel misloading is essentially eliminated through the implementation of procedural and administrative controls. The controls instituted to ensure that acceptable SFAs are placed into the TN-LC cask will typically consist of the following:
 - A cask loading plan is developed to verify that the candidate intact SFAs meet the fuel qualification requirements of the applicable sections as listed in step 12 of Section 7.1.1.
 - The loading plan is independently verified and approved before fuel load.
 - A fuel movement schedule is then written, verified, and approved based upon the loading plan. All fuel movements from any rack location are performed under strict compliance with the fuel movement schedule.
3. Prior to loading an SFA into a TN-LC-NRUX basket subassembly, the identity of the assembly is to be verified by two individuals using a video camera or other means. Read and record the identification number from the SFA and check this identification number against the site loading plan which indicates which SFAs are acceptable for transport.
4. Position the SFA for insertion into the selected TN-LC-NRUX basket subassembly compartment and load the SFA. Repeat steps 2 and 3 for each SFA to be transported in the specific TN-LC package shipment. Record the compartment position of each SFA.
5. Use the TN-LC-NRUX basket tube assembly lifting fixture to place the loaded TN-LC-NRUX basket tube assembly into the TN-LC-NRUX basket.
6. Install the TN-LC-NRUX basket tube assembly top tube cap.
7. Repeat steps 4 through 6, for the second TN-LC-NRUX basket tube assembly.

Following completion of the above listed steps, the TN-LC-NRUX dry loading is continued in step 5, Section 7.1.3 of Chapter 7.

7.7.1.3 TN-LC-NRUX Basket Wet Unloading

The starting condition for the following steps assumes completion of the cask unloading preparation steps in Section 7.2.1 and steps 1-12 of Section 7.2.2.1 of Chapter 7.

The NRUX SFAs may be unloaded directly from the TN-LC cask, or the TN-LC-NRUX basket tube assembly may be removed from the cask, staged, and unloaded away from the cask. The sequence below assumes that the SFAs are unloaded directly from the cask.

1. Remove the TN-LC-NRUX basket tube assembly top tube cap.
2. Unload the SFAs using the appropriate grapple or handling system.
3. Replace the TN-LC-NRUX basket tube assembly top tube cap.
4. Repeat steps 1 through 3 above for the second TN-LC-NRUX basket tube assembly.

Following completion of the above steps, the TN-LC-NRUX basket wet unloading is continued in step 13, Section 7.2.2.1 of Chapter 7.

7.7.1.4 TN-LC-NRUX Basket Dry Unloading

The starting condition for the following steps assumes completion of the cask unloading preparation steps in Section 7.2.1 and steps 1-6 of Section 7.2.2.2 of Chapter 7.

The loaded TN-LC-NRUX basket tube assembly is unloaded directly from the TN-LC cask, using a dry shielded transfer system.

1. Lower the transfer system radiation shield over the TN-LC cask.
2. Access the TN-LC cask cavity by removing the lid, if necessary.
3. Using the transfer system lifting mechanism, lift a loaded TN-LC-NRUX basket tube assembly from the basket and transfer it to the staging pit.
4. After disengaging from the basket subassembly, repeat step 3 to remove the second loaded basket subassembly from the basket.
5. Return the cask to its prescribed empty configuration (this may include reinstalling the empty basket subassemblies and installing the TN-LC cask lid).

Following completion of the above listed steps, the TN-LC-NRUX basket dry unloading is continued in step 7, Section 7.2.2.2 of Chapter 7.

Appendix 7.7.2
TN-LC-MTR Basket Wet and Dry Loading and Unloading

TABLE OF CONTENTS

7.7.2.1	TN-LC-MTR Basket Wet Loading.....	7.7.2-1
7.7.2.2	TN-LC-MTR Basket Dry Loading	7.7.2-3
7.7.2.3	TN-LC-MTR Basket Wet Unloading	7.7.2-4
7.7.2.4	TN-LC-MTR Basket Dry Unloading.....	7.7.2-5

Appendix 7.7.2 TN-LC-MTR Basket Wet and Dry Loading and Unloading

NOTE: References in this Chapter are shown as [1], [2], etc., and refer to the reference list in Section 7.5. A glossary of terms used in this Chapter is provided in Chapter 7, Section 7.6.

Site-specific conditions and requirements may require the use of different equipment and ordering of steps than those described below to accomplish the same objectives or to meet acceptance criteria to ensure the integrity of the package.

7.7.2.1 TN-LC-MTR Basket Wet Loading

The starting condition for the following steps assumes completion of the preparation steps in Section 7.1.1 and steps 1-14 of Section 7.1.2 of Chapter 7.

The wet loading procedure described in this section is applicable only when using the TN-LC cask for loading MTR spent fuel elements (SFE) from a fuel pool into the TN-LC cask with TN-LC-MTR basket, which is submerged in a fuel pool.

Each TN-LC-MTR basket is comprised of a basket structure with three slots which are each filled with a stack (column) of up to six fuel buckets. The procedure described below assumes that each of the fuel buckets is staged and loaded prior to placement into the TN-LC cask. Alternately empty fuel buckets may be placed in the TN-LC cask and loaded in situ.

1. Stage the empty TN-LC-MTR fuel buckets.
2. The potential for fuel misloading is essentially eliminated through the implementation of procedural and administrative controls. The controls instituted to ensure that acceptable SFEs are placed into the TN-LC cask will typically consist of the following:
 - A package loading plan is developed to verify that the candidate intact SFEs meet the fuel qualification requirements of the applicable sections as listed in step 12 of Section 7.1.1.
 - The loading plan is independently verified and approved before fuel load.
 - A fuel movement schedule is then written, verified, and approved based upon the loading plan. All fuel movements from any rack location are performed under strict compliance with the fuel movement schedule.
3. Prior to loading an SFE into a TN-LC-MTR fuel bucket, the identity of the SFE is to be verified by two individuals using a video camera or other means. Read and record the identification number from the SFE and check this identification number against the site loading plan which indicates which SFEs are acceptable for transport.
4. Position the SFE for insertion into the selected TN-LC-MTR fuel bucket compartment and load the SFE. Repeat step 3 for each SFE to be loaded in the specific TN-LC-MTR fuel bucket. After the fuel bucket has been fully loaded, check and record the identity of each of the SFEs.

5. Use the TN-LC-MTR fuel bucket lifting fixture to place a loaded TN-LC-MTR fuel bucket into the TN-LC cask.
6. Repeat steps 3, 4 and 5 to load one complete stack of TN-LC-MTR fuel buckets. After the uppermost fuel bucket in a stack has been loaded, install the appropriate top tube cap.
7. Repeat steps 3, 4, 5 and 6 as required, for the remaining two fuel bucket stacks.

Following completion of above listed steps, the TN-LC-MTR basket wet loading is continued in step 15, Section 7.1.2 of Chapter 7.

7.7.2.2 TN-LC-MTR Basket Dry Loading

The starting condition for the following steps assumes completion of the preparation steps in Section 7.1.1 and steps 1-4 of Section 7.1.3 of Chapter 7.

The dry loading procedure described in this section is applicable only when loading MTR spent fuel elements (SFEs) from a hot cell (or other dry storage location) into the TN-LC cask with TN-LC-MTR basket.

Each TN-LC-MTR basket is comprised of a basket structure with three slots which are each filled with a stack (column) of up to six fuel buckets. The procedure described below assumes that each of the fuel buckets is staged and loaded prior to placement into the TN-LC cask. Alternately empty buckets may be placed in the TN-LC cask and loaded in situ.

1. Stage the empty TN-LC-MTR fuel buckets.
2. The potential for fuel misloading is essentially eliminated through the implementation of procedural and administrative controls. The controls instituted to ensure that acceptable SFEs are placed into the TN-LC cask will typically consist of the following:
 - A loading plan is developed to verify that the candidate intact SFEs meet the fuel qualification requirements of the applicable sections as listed in step 12 of Section 7.1.1.
 - The loading plan is independently verified and approved before fuel load.
 - A fuel movement schedule is then written, verified, and approved based upon the loading plan. All fuel movements from any rack location are performed under strict compliance with the fuel movement schedule.
3. Prior to loading an SFE into a TN-LC-MTR fuel bucket, the identity of the assembly is to be verified by two individuals using a video camera or other means. Read and record the identification number from the SFE and check this identification number against the site loading plan which indicates which SFEs are acceptable for transport.
4. Position the SFE for insertion into the selected TN-LC-MTR fuel bucket compartment and load the SFE. Repeat step 3 for each SFE to be loaded in the specific TN-LC-MTR fuel bucket. After the fuel bucket has been fully loaded, check and record the identity of each of the SFEs.
5. Use the TN-LC-MTR fuel bucket lifting fixture to place a loaded TN-LC-MTR fuel bucket into the TN-LC cask.
6. Repeat steps 3, 4 and 5 to load one complete stack of TN-LC-MTR fuel buckets. After the uppermost bucket in a stack has been loaded, install the appropriate top tube cap.
7. Repeat steps 3, 4, 5 and 6 as required, for the remaining two fuel bucket stacks.

Following completion of the above listed steps, the TN-LC-MTR basket dry loading is continued in step 5, Section 7.1.3 of Chapter 7.

7.7.2.3 TN-LC-MTR Basket Wet Unloading

The starting condition for the following steps assumes completion of the unloading preparation steps in Section 7.2.1 and steps 1-12 of Section 7.2.2.1 of Chapter 7.

The MTR SFEs may be unloaded directly from the cask or the TN-LC-MTR fuel buckets may be removed from the cask, staged, and unloaded away from the cask. The sequence below assumes that the SFEs are unloaded directly from the cask.

1. Remove the TN-LC-MTR fuel bucket top tube cap.
2. Unload the SFEs using the appropriate grapple or handling system. Use the TN-LC-MTR fuel bucket handling fixture to remove the empty fuel bucket.
3. Alternately, use the TN-LC-MTR fuel bucket handling fixture to remove the loaded TN-LC-MTR fuel bucket from the cask, secure the fuel bucket, and unload the SFEs from the bucket.
4. Stage the unloaded TN-LC-MTR fuel buckets.
5. When a complete column of fuel buckets is unloaded, stack the empty TN-LC-MTR fuel buckets and top tube cap in the cask, if appropriate.
6. Repeat steps 1 through 5 for each of the remaining stacks to complete the unloading.

Following completion of the above steps, the TN-LC-MTR basket wet unloading is continued in step 13, Section 7.2.2.1 of Chapter 7.

7.7.2.4 TN-LC-MTR Basket Dry Unloading

The starting condition for the following steps assumes completion of the unloading preparation steps in Section 7.2.1 and steps 1-6 of Section 7.2.2.2 of Chapter 7.

The MTR SFEs are unloaded directly from the TN-LC cask using a dry shielded transfer system.

1. Lower the transfer system radiation shield over the TN-LC cask.
2. Access the TN-LC cask cavity by removing the lid, if necessary.
3. Using the transfer system lifting mechanism, lift a loaded TN-LC-MTR fuel bucket from the basket and transfer it to the staging pit.
4. After disengaging from the basket subassembly, repeat step 3 as necessary to remove all of the loaded fuel buckets from the basket.
5. Return the cask to its prescribed empty configuration (this may include reinstalling the empty fuel buckets and installing the TN-LC cask lid).
6. Remove the transfer system radiation shield.

Following completion of the above listed steps, the TN-LC-MTR basket dry unloading is continued in step 7, Section 7.2.2.2 of Chapter 7.

Appendix 7.7.3
TN-LC-TRIGA Basket Wet and Dry Loading and Unloading

TABLE OF CONTENTS

7.7.3.1	TN-LC-TRIGA Basket Wet Loading	7.7.3-1
7.7.3.2	TN-LC-TRIGA Basket Dry Loading.....	7.7.3-3
7.7.3.3	TN-LC-TRIGA Basket Wet Unloading.....	7.7.3-4
7.7.3.4	TN-LC-TRIGA Basket Dry Unloading	7.7.3-5

Appendix 7.7.3 TN-LC-TRIGA Basket Wet and Dry Loading and Unloading

NOTE: References in this Chapter are shown as [1], [2], etc., and refer to the reference list in Section 7.5. A glossary of terms used in this Chapter is provided in Chapter 7, Section 7.6.

Site specific conditions and requirements may require the use of different equipment and ordering of steps than those described below to accomplish the same objectives or to meet acceptance criteria to ensure the integrity of the package.

Each TN-LC package containing a TN-LC-TRIGA basket is comprised of a basket structure which is a stack (column) of up to five TN-LC-TRIGA basket subassemblies. Each TN-LC-TRIGA basket has a three by three array of fuel compartments with each compartment capable of accommodating four TRIGA SFAs.

7.7.3.1 TN-LC-TRIGA Basket Wet Loading

The starting condition for the following steps assumes completion of the preparation steps in Section 7.1.1 and steps 1-14 of Section 7.1.2 of Chapter 7.

The wet loading procedure described in this section is applicable only when loading TRIGA spent fuel assemblies (SFA) from a hot cell (or other dry storage location) or fuel pool into the TN-LC cask containing a TN-LC-TRIGA basket which is submerged in a fuel pool.

The procedure described below assumes that each of the TN-LC-TRIGA baskets is staged and loaded prior to placement into the TN-LC cask. Alternately, empty baskets may be placed in the TN-LC cask and loaded in situ, sequentially.

1. Stage an empty TN-LC-TRIGA basket consisting of a stack of five basket subassemblies.
2. The potential for fuel misloading is essentially eliminated through the implementation of procedural and administrative controls. The controls instituted to ensure that acceptable fuel assemblies are placed into the TN-LC cask will typically consist of the following:
 - A package loading plan is developed to verify that the candidate intact SFAs meet the fuel qualification requirements of the applicable sections as listed in step 12 of Section 7.1.1.
 - The loading plan is independently verified and approved before fuel load.
 - A fuel movement schedule is then written, verified, and approved based upon the loading plan. All fuel movements from any rack location are performed under strict compliance with the fuel movement schedule.
3. Prior to loading of an SFA into a TN-LC-TRIGA basket, the identity of the assembly is to be verified by two individuals using a video camera or other means. Read and record the identification number from the fuel assembly and check this identification number against the site loading plan which indicates which SFAs are acceptable for transport.

4. Position the SFA for insertion into the selected TN-LC-TRIGA basket compartment and load the SFA.
5. Repeat steps 3 and 4 for each SFA to be transported in the specific TN-LC package shipment. After the TN-LC-TRIGA basket has been fully loaded, check and record the identity of each of the SFAs.
6. Install the TN-LC-TRIGA basket top spacer.
7. Use the TN-LC-TRIGA basket lifting lugs to place the loaded basket into the TN-LC cask.
8. Following completion of above listed steps, the TN-LC cask is ready for draining as described in step 15, Section 7.1.2 of Chapter 7.

7.7.3.2 TN-LC-TRIGA Basket Dry Loading

The starting condition for the TN-LC-TRIGA basket dry loading assumes completion of the preparation steps in Section 7.1.1 and steps 1-4 of Section 7.1.3 of Chapter 7.

The dry loading procedure described in this section is applicable only when loading TRIGA spent fuel assemblies (SFA) from a hot cell (or other dry storage location) into the TN-LC cask containing a TN-LC-TRIGA basket.

The procedure described below assumes that each of the TN-LC-TRIGA baskets is staged and loaded prior to placement into the TN-LC cask. Alternately, empty baskets may be placed in the TN-LC cask and loaded in situ, sequentially.

1. Stage an empty TN-LC-TRIGA basket consisting of a stack of five basket subassemblies.
2. The potential for fuel misloading is essentially eliminated through the implementation of procedural and administrative controls. The controls instituted to ensure that acceptable SFAs are placed into the TN-LC cask will typically consist of the following:
 - A package loading plan is developed to verify that the candidate intact SFAs meet the fuel qualification requirements of the applicable sections as listed in step 12 of Section 7.1.1.
 - The loading plan is independently verified and approved before fuel load.
 - A fuel movement schedule is then written, verified, and approved based upon the loading plan. All fuel movements from any rack location are performed under strict compliance with the fuel movement schedule.
3. Prior to loading of a SFA into a TN-LC-TRIGA basket, the identity of the assembly is to be verified by two individuals using a video camera or other means. Read and record the identification number from the SFA and check this identification number against the site loading plan which indicates which SFAs are acceptable for transport.
4. Position the fuel assembly for insertion into the selected TN-LC-TRIGA basket compartment and load the SFA.
5. Repeat steps 3 and 4 for each SFA to be transported in the specific TN-LC package shipment. After the TN-LC-TRIGA basket has been fully loaded, check and record the identity of each of the SFAs.
6. Install the TN-LC-TRIGA basket top spacer.
7. Use the TN-LC-TRIGA basket lifting fixture to place the loaded basket into the TN-LC cask.

Following completion of the above listed steps, the TN-LC-TRIGA basket dry loading is continued in step 5, Section 7.1.3 of Chapter 7.

7.7.3.3 TN-LC-TRIGA Basket Wet Unloading

The starting condition for the following steps assumes completion of the package unloading preparation steps in Section 7.2.1 and steps 1-12 of Section 7.2.2.1 of Chapter 7.

The TRIGA SFAs may be unloaded directly from the cask or the TN-LC-TRIGA baskets may be removed from the cask, staged, and unloaded away from the cask. The sequence below assumes that the SFAs are unloaded directly from the cask.

1. Remove the TN-LC-TRIGA basket top spacer.
2. Unload all SFAs from the basket using the appropriate grapple or handling system. Use the TN-LC-TRIGA basket handling fixture to remove the empty fuel basket.
3. Repeat Step 2 until all TN-LC-TRIGA baskets have been emptied and removed from the TN-LC cask.
4. Stage the unloaded TN-LC-TRIGA baskets.

Following completion of the above steps, the TN-LC-TRIGA basket wet unloading is continued in step 13, Section 7.2.2.1 of Chapter 7.

7.7.3.4 TN-LC-TRIGA Basket Dry Unloading

The starting condition for the following steps assumes completion of the cask unloading preparation steps in Section 7.2.1 and steps 1-6 of Section 7.2.2.2 of Chapter 7.

The TRIGA SFAs may be unloaded directly from the cask, or the TN-LC-TRIGA basket subassemblies may be removed from the cask, staged, and unloaded away from the cask. The sequence below assumes that the SFAs are unloaded directly from the cask.

1. Remove the TN-LC-TRIGA basket top spacer.
2. Unload all SFAs from the basket using the appropriate grapple or handling system. Use the TN-LC-TRIGA basket handling fixture to remove the empty fuel basket.
3. Repeat Step 2 until all TN-LC-TRIGA baskets have been emptied and removed from the TN-LC cask.
4. Stage the unloaded TN-LC-TRIGA baskets.
5. Following completion of the above listed steps, the TN-LC-TRIGA basket dry unloading is continued in step 7, Section 7.2.2.2 of Chapter 7.

Appendix 7.7.4
TN-LC-1FA Basket Wet and Dry Loading and Unloading

TABLE OF CONTENTS

7.7.4.1	TN-LC-1FA Basket Wet Loading	7.7.4-1
7.7.4.2	TN-LC-1FA Basket Dry Loading.....	7.7.4-3
7.7.4.3	TN-LC-1FA Basket Wet Unloading.....	7.7.4-5
7.7.4.4	TN-LC-1FA Basket Dry Unloading	7.7.4-6

Appendix 7.7.4

TN-LC-1FA Basket Wet and Dry Loading and Unloading

NOTE: References in this chapter are shown as [1], [2], etc., and refer to the reference list in Section 7.5. A glossary of terms used in this chapter is provided in Chapter 7, Section 7.6.

Site-specific conditions and requirements may require the use of different equipment and ordering of steps than those described below to accomplish the same objectives or to meet acceptance criteria to ensure the integrity of the package.

7.7.4.1 TN-LC-1FA Basket Wet Loading

The starting condition for the following steps assumes completion of the preparation steps in Section 7.1.1 and steps 1-14 of Section 7.1.2 of Chapter 7.

The wet loading procedure described in this section is applicable only when using the TN-LC cask for loading LWR spent fuel assemblies (SFA) or fuel rods from a fuel pool into the TN-LC cask with TN-LC-1FA basket, which is submerged in a fuel pool.

A TN-LC cask with a TN-LC-1FA basket may be configured in one of three configurations:

- A TN-LC-1FA basket for transporting a PWR SFA,
- A BWR sleeve and hold-down ring placed inside the TN-LC-1FA basket when transporting a BWR SFA, or
- A TN-LC-1FA 25 pin can placed inside the BWR sleeve when transporting individual LWR fuel rods.

Spacers may be required for shorter SFAs/rods. The TN-LC-1FA 25 pin can may be loaded prior to placement in the cask or loaded while in the cask.

1. Verify that the TN-LC-1FA basket is configured appropriately for one of the three payloads as listed above.
2. The potential for fuel misloading is essentially eliminated through the implementation of procedural and administrative controls. The controls instituted to ensure that acceptable SFAs or rods are placed into the TN-LC cask consist of the following:
 - A package loading plan is developed to verify that candidate SFAs or rods meet the fuel qualification requirements of the applicable sections as listed in step 12 of Section 7.1.1.
 - The loading plan is independently verified and approved before fuel load.
 - A fuel movement schedule is then written, verified, and approved based upon the loading plan. All fuel movements from any rack location are performed under strict compliance with the fuel movement schedule.

3. Prior to loading SFAs or fuel rods into a TN-LC-1FA basket, the identity of the spent fuel is to be verified by two individuals using a video camera or other means. Read and record the identification number from the SFA/fuel rods, if applicable, and check this identification number against the site loading plan which indicates which SFAs/fuel rods are acceptable for transport.
4. Position the SFA or fuel rod for insertion into the TN-LC-1FA basket compartment:
 - If loading an SFA,
 - Load the PWR or BWR SFA as applicable into the TN-LC-1FA basket.
 - Record the identity of the SFA.
 - If loading fuel rods,
 - Load the fuel rods to be transported into the TN-LC-1FA 25 pin can.
 - After the TN-LC-1FA 25 pin can has been loaded, check and record the identity of the fuel rods.
 - Place a fuel can spacer as required.
 - Install the pin can lid.

Following completion of above listed steps, the TN-LC cask is ready for draining as described in step 15, Section 7.1.2 of Chapter 7.

7.7.4.2 TN-LC-1FA Basket Dry Loading

The starting condition for the TN-LC-1FA basket assumes completion of the preparation steps in Section 7.1 and steps 1-4 of Chapter 7, Section 7.1.3.

A TN-LC cask with a TN-LC-1FA basket may be configured in one of three configurations:

- A TN-LC-1FA basket for transporting a PWR SFA,
- A BWR sleeve and hold-down ring placed inside the TN-LC-1FA basket when transporting a BWR SFA, or
- A TN-LC-1FA 25 pin can placed inside the BWR sleeve when transporting individual LWR fuel rods.

Dry loading of a PWR/BWR fuel assembly must be conducted in a helium environment. Spacers may be required for shorter SFAs/rods. The TN-LC-1FA 25 pin can may be loaded prior to placement in the cask or loaded while in the cask. This procedure assumes the TN-LC-1FA 25 pin can is loaded with fuel rods prior to loading the can into the TN-LC cask.

1. Verify that the TN-LC-1FA basket is configured appropriately for one of the three payloads as listed above.
2. The potential for fuel misloading is essentially eliminated through the implementation of procedural and administrative controls. The controls instituted to ensure that acceptable SFAs or rods are placed into the TN-LC cask consist of the following:
 - A package loading plan is developed to verify that candidate SFAs or rods meet the fuel qualification requirements of the applicable sections as listed in step 12 of Section 7.1.1.
 - The loading plan is independently verified and approved before fuel load.
 - A fuel movement schedule is then written, verified, and approved based upon the loading plan. All fuel movements from any rack location are performed under strict compliance with the fuel movement schedule.
3. Prior to loading SFA or fuel rods into a TN-LC-1FA basket, the identity of the spent fuel is to be verified by two individuals using a video camera or other means. Read and record the identification number from the SFA/fuel rods, if applicable, and check this identification number against the site loading plan which indicates which SFAs/fuel rods are acceptable for transport.
4. Position the SFA or TN-LC-1FA 25 pin can for insertion into the TN-LC-1FA basket compartment:
 - If loading an SFA,

- Load the PWR or BWR SFA as applicable into the TN-LC-1FA basket.
- Record the identity of the SFA.
- If loading a TN-LC-1FA 25 pin can,
 - Load the fuel rods to be transported into the TN-LC-1FA 25 pin can.
 - After the TN-LC-1FA 25 pin can has been fully loaded, check and record the identity of the fuel rods.
 - Place a fuel can spacer as required.
 - Install the pin can lid.
 - Position the TN-LC-1FA 25 pin can for insertion into the TN-LC cask. Note that this step is done with the TN-LC cask oriented horizontally.
 - The TN-LC-1FA 25 pin can is inserted into the cask cavity using site transfer equipment.
 - Assemble the loaded TN-LC cask as required prior to upending.
 - Upend the TN-LC cask.

Following completion of the above listed steps, the TN-LC-1FA basket dry loading is continued in step 5, Section 7.1.3 of Chapter 7.

7.7.4.3 TN-LC-1FA Basket Wet Unloading

The starting condition for the following steps assumes completion of the unloading preparation steps in Section 7.2.1 and steps 1-12 of Section 7.2.2.1 of Chapter 7.

The TN-LC-1FA contents may be unloaded directly from the cask or the TN-LC-1FA basket may be removed from the cask, staged, and unloaded away from the cask. The sequence below assumes that the contents are unloaded directly from the cask.

1. If unloading BWR or PWR SFAs:
 - If necessary, remove fuel spacer.
 - Remove TN-LC-1FA BWR hold-down ring if unloading a BWR SFA.
 - Unload the PWR or BWR SFA as applicable using the appropriate grapple.
 - Place the SFA in the appropriate location in the pool.
 - Replace the BWR hold-down ring, if necessary.

2. If unloading fuel rods:
 - Remove TN-LC-1FA BWR hold-down ring if necessary to gain access to the TN-LC-1FA 25 pin can lid.
 - Remove the TN-LC-1FA 25 pin can lid.
 - Unload the fuel rods from the TN-LC-1FA 25 pin can using the appropriate handling tool.
 - After all fuel rods have been removed, replace the TN-LC-1FA 25 pin can lid.
 - Replace the TN-LC-1FA BWR hold-ring if necessary.

Following completion of the above steps, the TN-LC-1FA basket wet unloading is continued in step 13, Section 7.2.2.1 of Chapter 7.

7.7.4.4 TN-LC-1FA Basket Dry Unloading

The starting condition for the following steps assumes completion of the unloading preparation steps in Section 7.2.1 and steps 1-6 of Section 7.2.2.2 or Section 7.2.2.3 of Chapter 7 for SFA or fuel rod unloading, respectively.

1. If unloading BWR or PWR SFAs:

- If necessary, remove fuel spacer.
- Remove the TN-LC-1FA BWR hold-down ring if unloading a BWR SFA.
- Unload the PWR or BWR SFA as applicable using the appropriate grapple.
- Place the SFA in the appropriate location in the hot cell.
- Replace the BWR hold-down ring, if necessary.

Following completion of the above listed steps, the TN-LC-1FA dry unloading is continued in step 7, Section 7.2.2.2 of Chapter 7.

2. If unloading fuel rods from the TN-LC-1FA 25 pin can:

Note that the TN-LC-1FA 25 pin is unloaded while the TN-LC cask is horizontal.

- Install temporary shielding around the bottom plug and remove the bottom plug.
- Attach the transfer system ram to the base of the TN-LC-1FA 25 pin can and push the TN-LC-1FA 25 pin can out of the TN-LC cask.
- Stage the TN-LC-1FA 25 pin can as required for removal of the fuel rods.
- Retract the TN-LC-1FA 25 pin can back into the TN-LC cask. Alternately, the ram may be disconnected, and the TN-LC-1FA 25 pin can may be left in the hot cell work area.
- Remove the transfer system ram as necessary to allow reattachment of the bottom plug.
- Reattach the bottom plug.

Following completion of the above listed steps, the TN-LC-1FA dry unloading is continued in step 7 Section 7.2.2.3 of Chapter 7.

Chapter 8 Acceptance Tests and Maintenance Program

TABLE OF CONTENTS

8.1	Acceptance Tests	8-1
8.1.1	Visual Inspection and Measurements	8-1
8.1.2	Weld Examinations.....	8-1
8.1.3	Structural and Pressure Tests.....	8-2
8.1.4	Containment Boundary Leakage Tests.....	8-2
8.1.5	TN-LC Cask Component and Material Tests	8-3
8.1.6	Shielding Tests.....	8-4
8.1.7	Neutron Absorber Tests	8-6
8.1.8	Thermal Tests.....	8-13
8.2	Maintenance Program	8-14
8.2.1	Structural and Pressure Tests.....	8-14
8.2.2	Leakage Tests.....	8-14
8.2.3	Component and Material Tests	8-14
8.2.4	Periodic Thermal Tests	8-15
8.2.5	Miscellaneous Tests	8-16
8.3	References.....	8-17

Chapter 8 Acceptance Tests and Maintenance Program

NOTE: References in this Chapter are shown as [1], [2], etc. and refer to the reference list in Section 8.3.

8.1 Acceptance Tests

The following reviews, inspections, and tests shall be performed on the TN-LC packaging prior to initial transport. Many of these tests will be performed at the fabricator's facility prior to delivery of the TN-LC cask for use. Tests will be performed in accordance with written procedures.

8.1.1 Visual Inspection and Measurements

Visual inspections are performed at the fabricator's facility to ensure that the packaging conforms to the drawings and specifications. The visual inspections include:

- cleanliness inspections,
- visual weld inspections as required by ASME Boiler and Pressure Vessel (BP&V) Code [1],
- inspection of sealing surface finish, and
- dimensional inspections for conformance with the drawings included in Chapter 1, Appendix 1.4.1.

8.1.2 Weld Examinations

The structural analyses performed on the packaging are presented in Chapter 2. To ensure that the packaging can perform its design function, the structural materials are chemically and physically tested to confirm that the required properties are met.

To the maximum extent practical, all welding is performed using qualified processes and qualified personnel according to the ASME BP&V Code. Base materials and welds are examined in accordance with the ASME BP&V Code requirements. NDE requirements for welds are specified on the drawings provided in Appendix 1.4.1. All NDE is performed in accordance with written procedures. The inspection personnel are qualified in accordance with SNT-TC-1A [2].

The containment welds of the TN-LC cask are designed, fabricated, tested and inspected in accordance with ASME B&PV Code Subsection NB [1]. Welds of the noncontainment cask structure are inspected as per the NDE acceptance criteria of ASME B&PV Code, Subsection NF [1].

The TN-LC cask baskets are designed, fabricated, and inspected in accordance with the ASME B&PV Code Subsection NG [1].

Alternatives to the Code are described in Chapter 2, Section 2.1.4 and Appendix 2.13.13.

8.1.3 Structural and Pressure Tests

8.1.3.1 Load Tests

One set of trunnions is provided for the TN-LC transport package lifting. The trunnions have a single shoulder (single failure proof). The trunnions are fabricated and tested in accordance with ANSI N14.6 [3]. A load test of 3.0 times the design lift load (for single failure proof trunnions) is applied to the trunnions for a period of ten minutes to ensure that the trunnions can perform satisfactorily.

A force equal to 1.5 times the impact limiter weight will be applied to the hoist rings of each impact limiter for a period of ten minutes. At the conclusion of the test, the impact limiter hoist rings will be examined visually for defects and permanent deformation.

8.1.3.2 Pressure Tests

A pressure test is performed on the TN-LC cask at a pressure between 45.0 and 50.0 psig. This is well above 1.5 times the maximum normal operating pressure of 16.9 psig (Chapter 3, Table 3-8). The test pressure is held for a minimum of ten minutes. The test is performed in accordance with ASME B&PV Code, Section III, Subsection NB, Paragraph NB-6200 or NB-6300. All visible joints and surfaces are examined visually for possible leakage after application of the pressure.

In addition, a bubble leakage test is performed on the neutron shield enclosure. The purpose of this test is to identify any potential leakage paths in the enclosure welds.

8.1.4 Containment Boundary Leakage Tests

8.1.4.1 TN-LC Cask Leakage Tests

Leakage tests are performed on the TN-LC cask containment boundary prior to first use, typically at the fabricator's facility. The fabrication verification leakage test can be separated into the following five tests: 1) cask leakage integrity, 2) vent port plug seal integrity, 3) drain port plug seal integrity, 4) lid seal integrity, and 5) bottom plug (Option 1 or 2) seal integrity. These tests are usually performed using the helium mass spectrometer method. Alternative methods are acceptable provided that the required sensitivity is achieved. The leakage test is performed in accordance with ANSI N14.5 [4] or ISO-12807 [5]. The personnel performing the leakage test are qualified in accordance with SNT-TC-1A [2].

8.1.4.1.1 Cask Leakage Integrity Test

Prior to lead pour and final machining of the inner shell, the containment boundary, including containment boundary base metal and welds, will be leakage tested in accordance with the requirements of ANSI N14.5 or ISO-12807 using temporary closures and seals, as necessary, for the bottom plug and lid. As the inner shell will not be accessible for leakage testing after lead is poured, leakage testing will be performed during the fabrication process as permitted by ANSI N14.5 Table 1. As one means of performing a portion of this test, the interior of the cask cavity may be flooded with a helium atmosphere while a vacuum is drawn on the lead cavity to

determine the leakage rate. If a leak is discovered, the source will be determined and repaired, and the shell will be retested to ensure that the measured leakage rate is less than 1×10^{-7} ref cm^3/s .

Similarly, the lid forging will not be accessible for leakage testing after lead is poured into the forging or after a machined lead piece is installed and captured with the gamma shielding cap. The lid forging will be leak tested using temporary closures and seals. If leakage is found, the leak will be repaired and the forging retested, as described above for the inner shell, prior to lid gamma shielding installation.

The leakage tests will be performed in conjunction with the non-destructive examination of the inner shell welds in accordance with ASME B&PVC Code, Section III, Subsection NB. Liquid penetrant examination of all final machined weld surfaces of the inner shell will be performed per the Code.

8.1.4.1.2 Fabrication Verification Leakage Tests

The fabrication verification leakage tests include the following:

- Cask vent port plug seal integrity
- Cask drain port plug seal integrity
- Cask lid seal integrity
- Bottom Plug (Option 1 or 2) seal integrity

The tests will be performed as described in Chapter 7, Section 7.4.1, in accordance with the ANSI N14.5 or ISO-12807. The acceptance criterion requires each component to be individually leak tight, that is, the leakage rate must be less than 1×10^{-7} ref cm^3/s .

8.1.5 TN-LC Cask Component and Material Tests

8.1.5.1 Valves, Rupture Discs, and Fluid Transport Devices

There are no valves, rupture discs, or couplings in the containment of the TN-LC packaging.

8.1.5.2 Gaskets

The lid and all the other containment penetrations are sealed using O-ring seals. Leakage testing of the seals is described in Section 8.1.4.1.

8.1.5.3 Impact Limiter Leakage Test

Prior to initial use, after all the wood blocks have been installed and the seal welds have been completed, the following test will be performed on the impact limiter to verify that the impact limiter wood is completely enclosed, thereby preventing any moisture exchange with the ambient environment.

Each impact limiter container will be pressurized to a pressure between 2.0 and 3.0 psig. All the weld seams and penetrations will be tested for leakage using a soap bubble test. If bubbles are detected, the weld will be repaired and the test re-performed.

8.1.5.4 Functional Tests

The following functional tests will be performed prior to the first use of the TN-LC package. Generally these tests will be performed at the fabrication facility.

- (a) Installation and removal of the lid, bottom plug, vent and drain port plugs, and other fittings will be observed. Each component will be checked for difficulties in installation and removal. After removal, each component will be visually examined for damage. Any defects will be corrected prior to the acceptance of the cask.
- (b) Each TN-LC-1FA basket as well as each TN-LC-MTR, TN-LC-TRIGA and TN-LC-NRUX fuel assembly/element compartment will be checked by gauge to demonstrate that the fuel assemblies or elements, as applicable, will fit in the basket.

8.1.6 Shielding Tests

Chapter 5 presents the analyses performed to ensure that the TN-LC package shielding design is adequate.

8.1.6.1 Gamma Shield Test

The TN-LC cask poured lead gamma shielding shall be inspected via gamma scanning at the intersections of a grid no larger than 6 x 6 inches on the outside of the shell prior to installation of the neutron shield.

The acceptance criterion for the gamma scan is based on dose rate measurements of a test block constructed to replicate the layers of stainless steel, lead, and stainless steel in the TN-LC cask. The thickness of each stainless steel layer in the test block shall be no less than the minimum specified thickness of the corresponding cask shell, and the thickness of the lead layer in the test block shall be no less than 95% of the nominal thickness of lead specified for the cask. The dose rate measured using the test block shall be the maximum acceptable reading for the inspected cask.

The source/detector distance used in the cask inspection shall be the same as that used in establishing the maximum dose rate limit. Inspection results which exceed this limit will be evaluated to ensure that the regulatory dose rate limits will not be exceeded.

8.1.6.2 Neutron Shield

The radial neutron shield is protected from damage or loss by the aluminum tubes and steel enclosure. The neutron shield material, VYAL B, is a proprietary vinyl ester resin mixed with alumina hydrate and zinc borate, which are added for their fire retardant properties. Alternately, Resin F, a borated reinforced polymer may be used for neutron shield material.

The primary function of the resin is to shield against neutrons, which is performed primarily by the hydrogen content in the resin. The sole function of the boron is to suppress n- γ reactions with hydrogen. The resin also provides some gamma shielding, which is a function of the overall resin density, and is not sensitive to composition.

The following are acceptance values for density and chemical composition for the VYAL B resin. The reference values bounded by those used in the shielding calculations of Chapter 5 are included for comparison.

Reference values		Acceptance Testing Values		
Element	Minimum wt %	Element	Wt %	Acceptance range (wt %)
H	4.59	H	5.0	± 8
B	0.82	B	0.9	± 10

The minimum VYAL B resin density in acceptance testing is 1.75 g/cm³. Each VYAL B resin batch is tested for acceptable density. This test is performed to ensure all resin placed into the cavities has consistent density and will provide uniform shielding. Resin composition or density test results which fall outside of this range will be evaluated to ensure that the shielding regulatory dose limits are not exceeded.

The proprietary process for the VYAL B mixing and installation is described in the SAR Chapter 5, Section 5.3.3.

The following are acceptance values for density and chemical composition for the alternate Resin F shielding material. The values used in the shielding calculations of Chapter 5 are included for comparison. From a shielding standpoint, Resin F bounds VYAL B.

Chapter 5 values		Acceptance Testing Values		
Element	Minimum wt %	Element	wt %	Acceptance range (wt %)
H	4.44	H	5.05	-10 / +20
B	0.82	B	1.05	± 20

The minimum Resin F density in acceptance testing is 1.76 g/cm³. Resin F composition or density test results which fall outside of this range will be evaluated to ensure that the shielding regulatory dose limits are not exceeded.

Density testing will be performed on every mixed batch of Resin F. Chemical analysis will be made on the first batch mixed with a given set of components and each time a new lot of one of the major components is introduced. Major components are aluminum oxide, zinc borate and the polyester resin, which combined make up 92% of Resin F by weight.

The individual aluminum tubes containing the resin are then installed around the outside of the cask as shown in TN-LC SAR drawing (Chapter 1, Appendix 1.4.1). The installation of the tubes into the annulus between the cask outer shell and the neutron shield shell is controlled to maximize the tube-to-tube contact, thus minimizing gaps between adjacent tubes.

Tests are performed at loading to ensure that the radiation dose limits are not exceeded for each TN-LC package.

8.1.7 Neutron Absorber Tests

The neutron absorber used for criticality control in the TN-LC cask baskets may consist of any of the following types of material:

- (a) Borated aluminum
- (b) Boron carbide/Aluminum metal matrix composite (MMC)
- (c) Boral[®]

The TN-LC package safety analyses do not rely upon the tensile strength of these materials. The radiation and temperature environment in the TN-LC package is not sufficiently severe to damage these metallic/ceramic materials. To assure performance of the neutron absorber's design function only the presence of B10 and the uniformity of its distribution need to be verified, with testing requirements specific to each material. The boron content of these three types of materials is given in Appendix 1.4 for each basket type.

References to metal matrix composites throughout this Chapter are not intended to refer to Boral[®], which is described later in this section.

8.1.7.1 Borated Aluminum

The material is produced by direct chill (DC) or permanent mold casting with boron precipitating primarily as a uniform fine dispersion of discrete AlB_2 or TiB_2 particles in the matrix of aluminum or aluminum alloy (other boron compounds, such as AlB_{12} , can also occur). For extruded products, the TiB_2 form of the alloy shall be used. For rolled products, AlB_2 , TiB_2 , or a hybrid may be used.

Boron is added to the aluminum in the quantity necessary to provide the specified minimum B10 areal density in the final product, with sufficient margin to minimize rejection, typically 10 % excess. The amount required to achieve the specified minimum B10 areal density will depend on whether boron with the natural isotopic distribution of the isotopes B10 and B11, or boron enriched in B10 is used. In no case shall the boron content in the aluminum or aluminum alloy exceed 5% by weight.

The criticality calculations take credit for 90% of the minimum specified B10 areal density of borated aluminum. The basis for this credit is the B10 areal density acceptance testing, which shall be as specified in Section 8.1.7.7. The specified acceptance testing assures that at any location in the material, the minimum specified areal density of B10 will be found with 95% probability and 95% confidence.

8.1.7.2 Boron Carbide/Aluminum Metal Matrix Composites (MMC)

The material is a composite of fine boron carbide particles in an aluminum or aluminum alloy matrix. The material shall be produced by direct chill casting, permanent mold casting, powder metallurgy, or thermal spray techniques. It is a low-porosity product with a metallurgically bonded matrix. The boron carbide content shall not exceed 40% by volume. The boron carbide content for MMCs with an integral aluminum cladding shall not exceed 50% by volume.

The final MMC product shall have density greater than 98% of theoretical density demonstrated by qualification testing, with no more than 0.5 volume % interconnected porosity. For MMC with an integral cladding, the final density of the core shall be greater than 97% of theoretical density demonstrated by qualification testing, with no more than 0.5 volume % interconnected porosity of the core and cladding as a unit of the final product.

At least 50% by weight of the B₄C particles in MMCs shall be smaller than 40 microns. No more than 10% of the particles shall be over 60 microns.

Prior to use in the TN-LC baskets, MMCs shall pass the qualification testing specified in Section 8.1.7.8 and shall subsequently be subject to the process controls specified in Section 8.1.7.9.

The criticality calculations take credit for 90% of the minimum specified B10 areal density of MMCs. The basis for this credit is the B10 areal density acceptance testing, which is specified in Section 8.1.7.7. The specified acceptance testing assures that at any location in the final product, the minimum specified areal density of B10 will be found with 95% probability and 95% confidence.

8.1.7.3 BORAL[®]

This material consists of a core of aluminum and boron carbide powders between two outer layers of aluminum, mechanically bonded by hot-rolling an “ingot” consisting of an aluminum box filled with blended boron carbide and aluminum powders. The core, which is exposed at the edges of the sheet, is slightly porous. Before rolling, at least 80% by weight of the B₄C particles in Boral[®] shall be smaller than 200 microns. The nominal boron carbide content shall be limited to 65% (+ 2% tolerance limit) of the core by weight.

The criticality calculations take credit for 75% of the minimum specified B10 areal density of Boral[®]. B10 areal density will be verified by chemical analysis and by certification of the B10 isotopic fraction for the boron carbide powder, or by neutron transmission testing. Areal density testing is performed on a coupon taken from the sheet produced from each ingot. If the measured areal density is below that specified, all the material produced from that ingot will be either

rejected, or accepted only on the basis of alternate verification of B10 areal density for each of the final pieces produced from that ingot.

8.1.7.4 Visual Inspections of Neutron Absorbers

Neutron absorbers shall be 100% visually inspected in accordance with the Certificate Holder's QA procedures. Material that does not meet the following acceptance criteria shall be reworked, repaired, or scrapped. Blisters shall be treated as non-conforming. Inspection of MMCs with an integral aluminum cladding shall also include verification that the matrix is not exposed through the faces of the aluminum cladding and that solid aluminum is not present at the edges. For Boral, visual inspection shall verify that there are no cracks through the cladding, exposed core on the face of the sheet, or solid aluminum at the edge of the sheet.

8.1.7.5 Other Visual Inspections Criteria

For borated aluminum and MMCs, visual inspections shall follow the recommendations in Aluminum Standards and Data, Chapter 4 "Quality Control, Visual Inspection of Aluminum Mill Products" [6]. Local or cosmetic conditions such as scratches, nicks, die lines, inclusions, abrasion, isolated pores, or discoloration are acceptable.

8.1.7.6 Thermal Conductivity Testing

Testing shall conform to ASTM E1225 [8], ASTM E1461 [9], or equivalent method, performed at room temperature on coupons taken from the rolled or extruded production material. Previous testing of borated aluminum and metal matrix composite shows that thermal conductivity increases slightly with temperature. Initial sampling shall be one test per lot, defined by the heat or ingot, and may be reduced if the first five tests meet the specified minimum thermal conductivity.

If a thermal conductivity test result is below the specified minimum, at least four additional tests shall be performed on the material from that lot. If the mean value of those tests, including the original test, falls below the specified minimum, the associated lot shall be rejected.

After twenty five tests of a single type of material, with the same aluminum alloy matrix, the same boron content, and the same primary boron phase, e.g., B₄C, TiB₂, or AlB₂, if the mean value of all the test results less two standard deviations meets the specified thermal conductivity, no further testing of that material is required. This exemption may also be applied to the same type of material if the matrix of the material changes to a more thermally conductive alloy (e.g., from 6000 to 1000 series aluminum), or if the boron content is reduced without changing the boron phase. The measured thermal conductivity values shall satisfy the minimum required conductivities as specified in SAR Chapter 3, Section 3.2.2.2. In cases where the specified thickness of the neutron absorber may vary, the equations introduced in Section 3.2.2.2 shall be used to determine the minimum required effective thermal conductivity.

The thermal conductivity test requirement does not apply to aluminum that is paired with the neutron absorber.

8.1.7.7 Specification for Acceptance Testing of Neutron Absorbers by Neutron Transmission

a) Neutron Transmission acceptance testing procedures shall be subject to approval by the Certificate Holder. Test coupons shall be removed from the rolled or extruded production material at locations that are systematically or probabilistically distributed throughout the lot. Test coupons shall not exhibit physical defects that would not be acceptable in the finished product, or that would preclude an accurate measurement of the coupon's physical thickness.

A lot is defined as all the pieces produced from a single ingot or heat or from a group of billets from the same heat. If this definition results in lot size too small to provide a meaningful statistical analysis of results, an alternate larger lot definition may be used, so long as it results in accumulating material that is uniform for sampling purposes.

The sampling rate for neutron transmission measurements shall be such that there is at least one neutron transmission measurement for each 2000 in² of final product in each lot.

The B10 areal density is measured using a collimated thermal neutron beam up to 1 inch diameter.

The neutron transmission through the test coupons is converted to B10 areal density by comparison with transmission through calibrated standards. These standards are composed of a homogeneous boron compound without other significant neutron absorbers. For example, boron carbide, zirconium diboride or titanium diboride sheets are acceptable standards. These standards are paired with aluminum shims sized to match the effect of neutron scattering by aluminum in the test coupons. Uniform but non-homogeneous materials such as metal matrix composites may be used for standards, provided that testing shows them to provide neutron attenuation equivalent to a homogeneous standard.

Standards will be calibrated, traceable to nationally recognized standards, or by attenuation of a monoenergetic neutron beam correlated to the known cross section of B10 at that energy.

Alternatively, digital image analysis may be used to compare neutron radioscopic images of the test coupon to images of the standards. The area of image analysis shall be no more than 0.75 in².

The minimum areal density specified shall be verified for each lot at the 95% probability, 95% confidence level or better. If a goodness-of-fit test demonstrates that the sample comes from a normal population, the one-sided tolerance limit for a normal distribution may be used for this purpose. Otherwise, a non-parametric (distribution-free) method of determining the one-sided tolerance limit may be used. Demonstration of the one-sided tolerance limit shall be evaluated for acceptance in accordance with the Certificate Holder's QA procedures.

b) The following illustrates one acceptable method and is intended to be utilized as an example. The acceptance criterion for individual plates is determined from a statistical analysis of the test results for their lot. The B10 areal densities determined by neutron transmission are converted to volume density, i.e., the B10 areal density is divided by the thickness at the location of the neutron transmission measurement or the maximum thickness of the coupon. The lower tolerance limit of B10 volume density is then determined, defined as the mean value of B10

volume density for the sample, less K times the standard deviation, where K is the one-sided tolerance limit factor with 95% probability and 95% confidence [7].

Finally, the minimum specified value of B10 areal density is divided by the lower tolerance limit of B10 volume density to arrive at the minimum plate thickness which provides the specified B10 areal density.

Any plate which is thinner than the statistically derived minimum thickness or the minimum from 8.1.7.7.a or the minimum design thickness, whichever is greater, shall be treated as non-conforming, with the following exception: local depressions are acceptable, so long as they total no more than 0.5% of the area on any given plate, and the thickness at their location is not less than 90% of the minimum design thickness. Edge effects due to manufacturing operations such as shearing, deburring, and chamfering, need not be included in this determination.

Non-conforming material shall be evaluated for acceptance in accordance with the Certificate Holder's QA procedures.

8.1.7.8 Specification for Qualification Testing of Metal Matrix Composites

8.1.7.8.1 Applicability and Scope

MMCs acceptable for use in the TN-LC cask baskets are described in Section 8.1.7.2.

Prior to initial use in a spent fuel transport system, such MMCs shall be subjected to qualification testing that will verify that the product satisfies the design function. Key process controls shall be identified per Section 8.1.7.9 so that the production material is equivalent to or better than the qualification test material. Changes to key processes shall be subject to qualification before use of such material in a spent fuel dry storage or transport system.

ASTM test methods and practices are referenced below for guidance. Alternative methods may be used with the approval of the Certificate Holder.

8.1.7.8.2 Design Requirements

In order to perform its design functions, the product must have, at a minimum, sufficient strength and ductility for manufacturing and for both normal and accident conditions of the transport system. This is demonstrated by the tests in Section 8.1.7.8.4. It must have a uniform distribution of boron carbide. This is demonstrated by the tests in Section 8.1.7.8.5.

8.1.7.8.3 Durability

There is no need to include accelerated radiation damage testing in the qualification. Such testing has already been performed on MMCs, and the results confirm what would be expected of materials that fall within the limits of applicability cited above. Metals and ceramics do not experience measurable changes in mechanical properties due to fast neutron fluences typical over the lifetime of spent fuel transport, about 10^{15} neutrons/cm².

Thermal damage and corrosion (hydrogen generation) testing shall be performed unless such

tests on materials of the same chemical composition have already been performed and found acceptable. The following paragraphs illustrate two cases where such testing is not required.

Thermal damage testing is not required for unclad MMCs consisting only of boron carbide in an aluminum 1100 matrix because there is no reaction between aluminum and boron carbide below 842°F, well above the basket temperature under normal conditions of transport [10].

Corrosion testing is not required for MMCs (clad or unclad) consisting only of boron carbide in an aluminum 1100 matrix, because testing on one such material has already been performed by Transnuclear [11].

8.1.7.8.3.1 Delamination Testing of Clad MMC

Clad MMCs shall be subjected to thermal damage testing following water immersion to ensure that delamination does not occur under normal conditions of storage.

8.1.7.8.4 Required Qualification Tests and Examinations to Demonstrate Mechanical Integrity

At least three samples, one each from approximately the two ends and middle of the qualification material run shall be subject to:

(a) room temperature tensile testing (ASTM- B557) [12] demonstrating that the material has the following tensile properties:

- Minimum yield strength, 0.2% offset: 1.5 ksi
- Minimum ultimate strength: 5 ksi
- Minimum elongation in 2 inches: 0.5%

As an alternative to the elongation requirement, ductility may be demonstrated by bend testing per ASTM E290 [13]. The radius of the pin or mandrel shall be no greater than three times the material thickness, and the material shall be bent at least 90 degrees without complete fracture.

(b) Testing to verify more than 98% of theoretical density for non-clad MMCs and 97% for the matrix of clad MMCs. Testing or examination for interconnected porosity on the faces and edges of unclad MMC, and on the edges of clad MMC shall be performed by a means to be approved by the Certificate Holder. The maximum interconnected porosity is 0.5 volume %.

And for at least one sample,

(c) for MMCs with an integral aluminum cladding, thermal durability testing demonstrating that after a minimum 24 hour soak in either pure or borated water, then insertion into a preheated oven at approximately 825°F for a minimum of 24 hours, the specimens are free of blisters and delamination and pass the mechanical testing requirements described in test 'a' of this section.

8.1.7.8.5 Required Tests and Examinations to Demonstrate B10 Uniformity

Uniformity of the boron distribution shall be verified either by:

- (a) Neutron radioscopy or radiography (ASTM E94[14], E142[15], and E545[16]) of material from the ends and middle of the test material production run, verifying no more than 10% difference between the minimum and maximum B10 areal density, or
- (b) Quantitative testing for the B10 areal density, B10 density, or the boron carbide weight fraction, on locations distributed over the test material production run, verifying that one standard deviation in the sample is less than 10% of the sample mean. Testing may be performed by a neutron transmission method similar to that specified in Section 8.1.7.7 or by chemical analysis for boron carbide content in the composite.

8.1.7.8.6 Approval of Procedures

Qualification procedures shall be subject to approval by the Certificate Holder.

8.1.7.9 Specification for Process Controls for Metal Matrix Composites

8.1.7.9.1 Applicability and Scope

Key processing changes shall be subject to qualification prior to use of the material produced by the revised process. The Certificate Holder shall determine whether a complete or partial re-qualification program per Section 8.1.7.8 is required, depending on the characteristics of the material that could be affected by the process change.

8.1.7.9.2 Definition of Key Process Changes

Key process changes are those which could adversely affect the uniform distribution of the boron carbide in the aluminum, reduce density, reduce corrosion resistance, reduce the mechanical strength or ductility of the MMC.

8.1.7.9.3 Identification and Control of Key Process Changes

The manufacturer shall provide the Certificate Holder with a description of materials and process controls used in producing the MMC. The Certificate Holder and manufacturer shall identify key process changes as defined in Section 8.1.7.9.2.

An increase in nominal boron carbide content over that previously qualified shall always be regarded as a key process change. The following are examples of other changes that are established as key process changes as determined by the Certificate Holder's review of the specific applications and production processes:

- (a) Changes in the boron carbide particle size specification that increase the average particle size by more than 5 microns or that increase the amount of particles larger than 60 microns from the previously qualified material by more than 5% of the total distribution but less than the 10% limit,

- (b) Change of the billet production process, e.g., from vacuum hot pressing to cold isostatic pressing followed by vacuum sintering,
- (c) Change in the nominal matrix alloy,
- (d) Changes in mechanical processing that could result in reduced density of the final product, e.g., for PM or thermal spray MMCs that were qualified with extruded material, a change to direct rolling from the billet,
- (e) For MMCs using a magnesium-alloyed aluminum matrix, changes in the billet formation process that could increase the likelihood of magnesium reaction with the boron carbide, such as an increase in the maximum temperature or time at maximum temperature,
- (f) Changes in powder blending or melt stirring processes that could result in less uniform distribution of boron carbide, e.g., change in duration of powder blending, and
- (g) For MMCs with an integral aluminum cladding, a change greater than 25% in the ratio of the nominal aluminum cladding thickness (sum of two sides of cladding) and the nominal matrix thickness could result in changes in the mechanical properties of the final product.

In no case shall process changes be accepted if they result in a product outside the limits established in Sections 8.1.7.8.1 and 8.1.7.8.4.

8.1.8 Thermal Tests

The thermal evaluation of the TN-LC package described in Chapter 3 is performed using very conservative and bounding assumptions. Gaps between the components are modeled in the thermal analysis to account for possible gaps expected during fabrication. Gaps are assumed to be present during NCT and HAC post-fire cases when calculating heat flow out of the cask, and gaps are assumed closed when calculating heat flow into the cask (i.e., during the HAC fire). The calculated cladding temperatures are much lower than the cladding temperature limit, assuring a large margin of safety.

For these reasons, thermal acceptance testing is not required for the TN-LC package.

8.2 Maintenance Program

8.2.1 Structural and Pressure Tests

Within 14 months prior to any lift of a TN-LC package, the trunnions shall be subject to either of the following:

- A test load equal to 300% of the maximum service load per ANSI N14.6 [3], paragraph 7.3.1(a) for single failure proof trunnions.
- Dimensional testing, visual inspection and nondestructive examination of accessible critical areas of the trunnions including the bearing surfaces in accordance with Paragraph 6.3.1(b) of ANSI N14.6 [3].

8.2.2 Leakage Tests

The following containment boundary components shall be subject to periodic maintenance, and preshipment leakage testing in accordance with ANSI N14.5 [4] or ISO-12807 [5]:

- Lid and seals
- Bottom Plug (Option 1 and 2) and seals
- Vent Port Plug Seal
- Drain Port Plug Seal

Test	Frequency	Acceptance Criteria	Typical Method (ANSI N14.5 TABLE A.1 [4])
Periodic	Within 12 months prior to shipment	Each component individually $\leq 1 \times 10^{-7}$ ref cm ³ /s	(He) A.5.3 A.5.4
Pre-shipment	Before each shipment, after the contents are loaded and the package is closed	No detected leakage, sensitivity of 10^{-3} ref cm ³ /s or better, unless seal is replaced.	A.5.1 A.5.2 A.5.8 A.5.9
Maintenance	After maintenance, repair, or replacement of containment components, including inner seals	Each component individually $\leq 1 \times 10^{-7}$ ref cm ³ /s	(He) A.5.3 A.5.4

No leakage tests are required prior to shipment of an empty TN-LC packaging.

8.2.3 Component and Material Tests

8.2.3.1 Fasteners

All threaded fasteners and port plugs shall be inspected at the time of use for deformed or stripped threads. Damaged parts shall be evaluated for continued use and replaced as required.

At a minimum, the TN-LC lid and bottom plug bolts shall be replaced at least every 75 shipments (round trip) to ensure adequate fatigue strength is maintained.

8.2.3.2 Impact Limiters

A visual examination of the impact limiters before each shipment will be performed to ensure that the impact limiters have not degraded. If there is no evidence of weld cracking or other damage which could result in water in-leakage, the wood performance is assured. If there is visual damage, the impact limiter will be removed from service, repaired, if possible, and inspected for degradation of the wood. Impact limiters will be leakage tested once every five years to ensure that water has not entered the impact limiters. If the leakage test indicates that the impact limiters have a leak, a humidity test will be performed to verify that there is no free water in the impact limiters.

8.2.3.3 Valves, Rupture Discs, and Gaskets on Containment Vessel

If the bottom plug or the lid is removed, the seals are replaced prior to transport of a loaded TN-LC package. The seals will be leakage tested after retorquing the bolts in accordance with Chapter 7, Section 7.4.

O-ring seals may be reused for transport of an empty TN-LC packaging.

There are no valves, rupture discs, or couplings on the containment of the TN-LC packaging.

8.2.3.4 Shielding

There are no periodic tests or inspections required for the TN-LC gamma or neutron shielding. As described in Chapter 7, radiation surveys will be performed on the package exterior to ensure that the limits specified in 10CFR71.47 are met prior to each shipment.

The material composition of the VYAL B or Resin F neutron shielding resin employed in the shielding calculations is based on minimum guaranteed values that are determined by extensive tests under various (including extreme) environmental conditions. These tests indicate that the neutron shielding resin does not degrade under normal conditions and is durable over extended periods of time. The shielding calculations employed are based on conservative models and design basis source terms and demonstrate that the dose rate criteria are satisfied with sufficient margin. The comparisons of calculated and measured dose rate have indicated that the calculated dose rates are highly conservative. The 10CFR71 dose rate compliance measurements serve to indicate the shielding effectiveness of the package. Therefore, periodic tests for the neutron shielding resin are not necessary.

8.2.4 Periodic Thermal Tests

There are no periodic tests or inspections required for the TN-LC package heat transfer components.

8.2.5 Miscellaneous Tests

There are no additional maintenance tests required for the TN-LC package.

8.3 References

1. ASME Boiler and Pressure Vessel Code, Section III and Appendices, 2004 Edition including 2006 addenda.
2. SNT-TC-1A, "American Society for Nondestructive Testing, Personnel Qualification and Certification in Nondestructive Testing."
3. ANSI N14.6-1993, "American National Standard for Special Lifting Devices for Shipping Containers Weighing 10,000 Pounds or More for Nuclear Materials."
4. ANSI N14.5-1997, "American National Standard for Leakage Tests on Packages for Shipment of Radioactive Materials."
5. ISO-12807, "Safe transport of radioactive material - Leakage testing on packages," First Edition, 1996.
6. "Aluminum Standards and Data, 2003," The Aluminum Association.
7. Natrella, "Experimental Statistics," Dover, 2005.
8. ASTM E1225, "Thermal Conductivity of Solids by Means of the Guarded-Comparative-Longitudinal Heat Flow Technique."
9. ASTM E1461, "Thermal Diffusivity of Solids by the Flash Method."
10. Sung, C., "Microstructural Observation of Thermally Aged and Irradiated Aluminum/Boron Carbide (B4C) Metal Matrix Composite by Transmission and Scanning Electron Microscope," 1998.
11. Boralyn testing submitted to the NRC under docket 71-1027, 1998.
12. ASTM B557, "Standard Test Methods of Tension Testing Wrought and Cast Aluminum and Magnesium-Alloy Products."
13. ASTM E290, "Standard Methods for Bend Testing of Materials for Ductility."
14. ASTM E94, Recommended Practice for Radiographic Testing
15. ASTM E142, Controlling Quality of Radiographic Testing
16. ASTM E545, Standard Method for Determining Image Quality in Thermal Neutron Radiographic Testing